HYDROGEL BASED WOUND DRESSING MATERIAL USING FISH BASED COLLAGEN AND SILVER NANOWIRES AS ANTIMICROBIAL AGENT
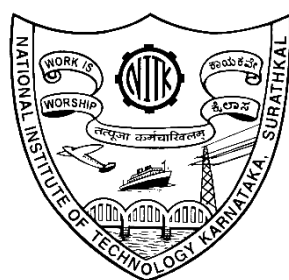
Thesis

Submitted in partial fulfillment of the requirements for the degree of

DOCTOR OF PHILOSOPHY

By

DIKSHA SHARMA

Register Number: 165048CH16F01

DEPARTMENT OF CHEMICAL ENGINEERING

NATIONAL INSTITUTE OF TECHNOLOGY KARNATAKA,

SURATHKAL, MANGALORE - 575025

December 2021

D E C L A R A T I O N

I hereby *declare* that the Research Thesis entitled **"HYDROGEL BASED WOUND DRESSING MATERIAL USING FISH BASED COLLAGEN AND SILVER NANOWIRES AS ANTIMICROBIAL AGENT"** which is being submitted to the **National Institute of Technology Karnataka, Surathkal** in partial fulfillment of the requirements for the award of the Degree of **Doctor of Philosophy** in the **Department of Chemical Engineering**, is a *bonafide report of the research work carried out by me*. The material contained in this Research Thesis has not been submitted to any University or Institution for the award of any degree.

DIKSHA SHARMA

Register number: 165048CH16F01

Department of Chemical Engineering

Place: NITK, Surathkal

Date: 23-12-2021

C E R T I F I C A T E

This is to certify that the Research Thesis entitled **"HYDROGEL BASED WOUND DRESSING MATERIAL USING FISH BASED COLLAGEN AND SILVER NANOWIRES AS ANTIMICROBIAL AGENT"** submitted by **Mrs. Diksha Sharma (Register Number: 165048CH16F01)** as the record of the research work carried out by her, is *accepted as the Research Thesis submission* in partial fulfillment of the requirements for the award of degree of **Doctor of Philosophy**.

Research Guide
Dr. P. E. JagadeeshBabu
Associate Professor
Dept. of Chemical Engineering
NITK, Surathkal

Research Co-Guide
Dr. Raj Mohan B
Professor
Dept. of Chemical Engineering
NITK, Surathkal

Chairman - DRPC
Dr. P. E. JagadeeshBabu
Associate Professor
Dept. of Chemical Engineering
NITK, Surathkal

ACKNOWLEDGEMENT

The present thesis is the result of a research work carried out at Department of Chemical Engineering of National Institute of Technology Surathkal, Mangalore, India. I am thankful to each person who was linked directly or indirectly in completion of this work.

It is my ultimate duty, and privilege to express my deep appreciations and sincere gratitude to my research guide **Dr. P. E. JagadeeshBabu**, Associate Professor, Department of Chemical Engineering, NITK, Surathkal and my co-guide **Dr. Raj Mohan B**, Professor, Department of Chemical Engineering, NITK, Surathkal, who have guided me during the course on this study. Without their invaluable guidance, round the clock support and encouragement, it was impossible to complete this research work. It was a life time experience to work under the supervision and guidance of such knowledgeable persons.

I am extremely thankful to the RPAC committee members, **Dr. Udaya Kumar Dalimba** and **Dr. Keyur Raval** for their critical comments during my progress seminars, which enabled me to notice the flaws in my research work and make the necessary improvements according to their reviews and comments. They have provided valuable insights into the relevance of this study.

I humbly express my sincere gratitude to **The Director**, NITK, Surathkal for rendering all help during the time period of thesis. With my all heart, I would like to express my deep gratitude to **Dr. P. E. JagadeeshBabu**, Associate Professor and Head, Department of Chemical Engineering, NITK, Surathkal and the former HODs **Dr. Raj Mohan B**, **Dr. Hari Mahalingam**, and **Dr. Prasanna B. D.**, Department of Chemical Engineering, NITK, Surathkal for providing me necessary facilities, funding, and support during the phase of my research work. I would also like to thank all the faculty members of the **Department of Chemical Engineering**, NITK, Surathkal for their valuable support and encouragement.

I take this opportunity to express my sincere thanks to **Mr. Sadashiva**, **Mrs. Thrithila Shetty**, **Mrs. Shashikala Mohan**, **Mrs. Bhavyashree**, **Mrs. Vijetha**, **Mr. Mahadeva**,

ABSTRACT

Chronic wounds fail to heal naturally and do not proceed through the sequential wound healing stages within an expected time frame. These wounds are characterized by extended inflammatory phase, excessive exudate and high alkaline pH (8.9), followed by elevated inflammatory cytokines, high levels of matrix metalloproteinases (MMPs) and obstinate bacterial infections. This disrupts the natural healing process leading to impaired wound healing. The prime objective of this research work was to develop a pH-sensitive smart wound dressing material which can maintain an optimal exudate based on the wound pH, through which MMPs activity can be controlled to achieve better healing and also reduce bacterial infection.

In this work, a pH-responsive hydrogel composed of poly(aspartic acid) (PAsp), poly(vinyl alcohol) (PVA) along with collagen and silver nanowires (Ag NWs) was prepared via free radical polymerization method. Collagen used in the wound dressing material was successfully extracted from marine waste i.e., Sole fish skin that can enhance the wound healing process. The extraction process was optimized using Response Surface Methodology (RSM) with Box-Behnken Design (BBD) for achieving maximum yield. The optimal conditions to obtain highest collagen yield was determined to be, an acetic acid concentration of 0.54 M, NaCl concentration of 1.90 M, solvent/solid ratio of 8.97 mL/g and time of 32.32 hrs. The maximum collagen yield of 19.27 ± 0.05 mg/g of fish skin was achieved under the optimal conditions. The analysis of variance (ANOVA) and contour plots exhibited a significant interaction of all the selected variables over collagen extraction process. SDS-PAGE (Sodium dodecyl sulfate-polyacrylamide gel electrophoresis) analysis suggested that the extracted collagen contained three α-chains i.e. $(\alpha 1)_2$, $\alpha 2$ (M.W. 118, 116 kDa) and one β chain (M.W. 200 kDa) which was similar to commercially available calf skin type I collagen. Ag NWs used in the wound dressing material act as an antibacterial agent and were synthesized using hydrothermal method by reducing silver nitrate ($AgNO_3$) using fructose in the presence of poly(vinylpyrrolidone) (PVP). Scanning electron microscopy (SEM) analysis showed that ultra-long, uniform and thin silver nanowires were obtained under optimized conditions; 0.02 M $AgNO_3$, 0.016 g/mL of fructose, 0.16 g/mL of PVP at 160 °C within

22 hrs. The dynamic light scattering (DLS) analysis revealed that the silver nanowires obtained had an average diameter of 77 nm possessing high level of crystallinity with face centered cubic (FCC) phase that was evident from the X-ray diffraction (XRD) patterns peaked at (111), (200), (220), (311) and (222) planes. A pH-sensitive hydrogel based wound dressing material i.e., PAsp/PVA/Collagen hydrogel loaded with Ag NWs was synthesized and optimized by altering the components namely concentration of PAsp (50mg-200 mg), PVA (4%-10%), collagen (0.5 mg/mL-3 mg/mL), Ag NWs (2.5 mg, 5 mg and 10 mg), ammonium persulfate (APS) (75 mg-150 mg) and ethylene glycol di-methacrylate (EGDMA) (0.25 mM-1 mM) based on the properties like swelling characteristics, physical strength and stability of the hydrogel. A maximum swelling ratio of 1511% have been achieved at the optimised condition in the presence of collagen at pH 10 whereas 1286% was achieved in the absence of collagen. However, the swelling ratio of PAsp/PVA/Collagen hydrogel (1511%) slightly decreased with the addition of Ag NWs and achieved swelling ratio of 1405% at pH 10 when hydrogel loaded with 5 mg Ag NWs. The prepared dressing material had good pH-sensitivity to alkaline environment and exhibited maximum swelling at pH 10 and minimum at pH 3. Through this mechanism, developed wound dressing material can maintain pH by removing excess exudate on wound bed and can retain required moist environment for better healing process. Antibacterial activity of hydrogel loaded with 5 mg Ag NWs exhibited 99.92% reduction in viable *E. coli* colonies. The hydrogel was assessed for its cytotoxicity on L929 cells by Sulforhodamine B (SRB) assay and it was revealed that hydrogel had not shown any toxicity and promoted cell proliferation. *In-vivo* wound healing studies showed that PAsp/PVA/Collagen impregnated with 5 mg Ag NWs improves the healing process and exhibited re-epithelization within 12 days with no scar formation, which is also confirmed by assessing histological parameters. Histological evaluation revealed good dermal layer formation with a high healing score. Comprehensively, the results suggested that PAsp/PVA/Collagen hydrogel impregnated with 5 mg silver nanowires can be a novel wound dressing material for chronic wounds.

CONTENTS

Chapter – 1

INTRODUCTION

Chapter – 2

LITERATURE REVIEW

Chapter – 3

MATERIALS AND METHODS

Chapter – 4

EXTRACTION, OPTIMIZATION AND CHARACTERIZATION OF COLLAGEN FROM SOLE FISH SKIN

Chapter – 5

SYNTHESIS OF SILVER NANOWIRES USING FRUCTOSE AS A REDUCING AGENT AND ITS ANTIBACTERIAL AND ANTIOXIDANT ANALYSIS

Chapter – 6

SYNTHESIS AND CHARACTERIZATION OF pH-SENSITIVE HYDROGEL BASED ON COLLAGEN CROSS-LINKED POLY(ASPARTIC ACID)/POLY(VINYL ALCOHOL)

Chapter – 7

SYNTHESIS, CHARACTERIZATION AND *IN-VIVO* EVALUATION OF SMART WOUND DRESSING MATERIAL WITH ENHANCED HEALING PROPERTIES FOR CHRONIC WOUNDS

Chapter – 8

SUMMARY AND CONCLUSIONS

LIST OF FIGURES

LIST OF TABLES

LIST OF ABBREVIATIONS

Abbreviation	Description
1D	One dimensional
3D	Three dimensional
AAS	Atomic absorption spectroscopy
$AgNO_3$	Silver nitrate
Ag NWs	Silver nanowires
ANOVA	Analysis of variance
APS	Ammonium persulfate
ATR-FTIR	Attenuated total reflection-Fourier transform infrared spectroscopy
BBD	Box-Behnken design
CFU	Colony forming unit
CO_2	Carbon dioxide
CPCSEA	Committee for the Purpose of Control and Supervision of Experiments on Animals
DI	Deionized water
DLS	Dynamic light scattering
DMEM	Dulbecco's modified Eagle's medium
DPPH	2,2-diphenyl-1- picrylhydrazyl
DSC	Differential scanning calorimetry
ECM	Extracellular matrix
EDAX	Energy dispersive X-ray analysis
EDTA	Ethylenediaminetetraacetic acid

Abbreviation	Description
EGDMA	Ethylene glycol di-methacrylate
EGF	Epidermal growth factor
FBS	Fetal Bovine Serum
FCC	Face centered cubic
FESEM	Field emission scanning electron microscope
FGF	Fibroblast growth factor
FTIR	Fourier-transform infrared spectroscopy
HCl	Hydrochloric acid
H&E	Hematoxylin & Eosin
IC_{50}	Half maximal inhibitory concentration
KBr	Potassium bromide
L929	Mouse fibroblast cell line
LB	Luria Bertani
MIC	Minimum inhibitory concentration
MMPs	Matrix metalloproteinases
MW	Molecular weight
NaCl	Sodium chloride
NaOH	Sodium hydroxide
NC	Negative control
NCCS	National Centre for Cell Science
NPs	Nanoparticles
OD	Optical density

Abbreviation	Description
OVAT	One variable at a time
PBS	Phosphate buffer saline
P2VP	Poly(2-vinylpyridine)
P4VP	Poly(4-vinylpyridine)
PAA	Poly(acrylic acid)
PAsp	Poly(aspartic acid)
PC	Positive control
PDEAEMA	Poly(N,N-diethylamino ethyl methacrylate)
PDMAEMA	Poly(N,N-dimethylamino ethyl methacrylate)
PEG	Poly(ethylene glycol)
PHEMA	Poly(2-hydroxyethyl methacrylate)
PMAA	Poly(methacrylic) acid
PVA	Poly(vinyl alcohol)
PVP	Poly(vinyl pyrrolidone)
PSI	Poly(succinimide)
ROS	Reactive oxygen species
RPM	Revolutions per minute
RSM	Response surface methodology
SD	Standard deviation
SD rat	Sprague-Dawley rat
SDS-PAGE	Sodium dodecyl sulfate-polyacrylamide electrophoresis
SEM	Scanning electron microscope

Abbreviation	Description
SR	Swelling ratio
SRB	Sulforhodamine B
TCA	Trichloroacetic acid
TEMED	Tetramethylethylenediamine
TGA	Thermogravimetric analysis
UV	Ultra-violet
w.r.t	With respect to
XRD	X-ray diffraction

NOMENCLATURE

Symbol	Description
°C	Degree Celsius
%	Percentage
±	Plus or minus
<	Less than
>	Greater than
θ	Angle
α	Alpha
β	Beta
λ	Lambda
μg	Microgram
μL	Microliter
μm	Micrometer
Å	Angstrom
$A_{control}$	Absorbance of control
A_o	Area of initial wound at 0th day
$A_{treated}$	Absorbance of treated cells
A_{sample}	Absorbance of sample
A_t	Area of wound on the day of changing dressing
cm	Centimeter
g	Gram
hrs	Hours

Symbol	Description
kDa	Kilo Dalton
keV	Kiloelectron volt
kg	Kilogram
kV	Kilo volt
mA	Milliampere
mg	Milligram
mins	Minutes
mL	Milliliter
mM	Millimolar
nm	Nanometer
R^2	Correlation coefficient
t	Time
W	Watt
w/v	Weight per volume
w/w	Weight by weight
W_o	Dry weight of hydrogel
W_o	Initial weight of dry hydrogel before degradation
W_t	Wet weight of hydrogel at time t
W_t	Dry weight of hydrogel at time t after degradation

CHAPTER 1

INTRODUCTION

1.1 Background of the research and motivation

Globally, chronic wounds have become a more challenging medical issue which affects mostly ageing population and in particular patients suffering from type-2 diabetes and obesity (Sen 2019). As per the Wound Healing Society (US), wound is termed as the breakage or injury in the normal anatomical structure and function of the skin (Boateng et al. 2008). Wounds are mainly categorized as acute or chronic wounds based on the duration and their healing propensity. Acute wound heals normally within an expected time frame and proceed through the sequential healing stages like hemostasis, inflammation, proliferation and remodeling whereas chronic wounds fail to heal naturally within a specific time period and do not follow the routine healing phases (Koehler et al. 2018; Rieger et al. 2013). Irrespective of wound type, in the inflammation phase, the wound healing process is influenced by excessive exudate, its pH, followed by bacterial infections and tissue necrosis. During the inflammation phase, macrophages and neutrophils will be attracted towards the wound bed, and further secretion of inflammatory cytokines will boost the production of matrix metalloproteinases (MMPs). Chronic wounds are generally in an alkaline state (8.9), and because of this the activity of MMPs increases. Excessive MMPs will degrade the extracellular matrix, affect the growth factors, and block the cell migration and cell proliferation. This condition disrupts the general healing process, and handling this condition has become a serious medical issue.

Across the world, millions of people are suffering from chronic wounds and acute wounds every year (Shi et al. 2019). In US alone, most of the population is significantly affected with chronic wounds and it is assumed that around 6.5-8.2 million population has suffered from chronic wounds (Hurd et al. 2021). Chronic wounds such as diabetic foot ulcer, pressure injuries, venous leg ulcers and arterial ulcers are accompanied with the followings; excessive exudate production, high risk of bacterial infection, damage of blood vessels and nerves that eventually lead to amputation of affected organs and

limbs (Pinto et al. 2020). The demand for wound care products has been increasing significantly which has resulted in increment of healthcare costs. This further has imposed a great economic burden on patients and entire health care system. The situation of patients suffering from chronic wounds is also adverse throughout the world. In this milieu, there is a requirement for the development of more effective and affordable wound dressing material which should have properties like retain required moisture, non-sticky in nature, remove excess exudate, biodegradable, biocompatible, antimicrobial, reduce bacterial infection to enhance the wound healing process and no scar formation at the end of healing process (Moura et al. 2013; Rezvani Ghomi et al. 2019).

Traditionally, wound dressing materials such as cotton wool, natural or synthetic bandages, gauze, lint, tulle were used as primary or secondary dressing materials for management of wounds. Their primary function was to maintain dry wound bed by absorbing excess exudates and thus prevent wound infection (Mir et al. 2018). Although, these wound dressing materials are cheap; yet they have some disadvantages such as regular replacement of dressings due to their dampness and fail to provide moist environment to wound (Rieger et al. 2013; Qu et al. 2018). These traditional dressing materials adhere to the wound surface which results in bleeding and pain upon removing it and it leads to infection, prolonged healing and scar formation. To overcome these major problems in wound management, modern dressing materials like hydrogels, foams, films, alginates and hydrocolloids have been developed to maintain moist wound environment that can promote faster healing process (Sweeney et al. 2012; Powers et al. 2016). Among all the modern wound dressing materials, hydrogels have been reported to be an ideal wound dressing material because it meets all requirements for wound healing. Hydrogels can control the amount of fluid in the wound and maintain the moist environment in the wound area. Hydrogels possess soft tissue like structure as they hold high content of water and also inhibits the bacterial invasion (Kamoun et al. 2017).

The first hydrogel was synthesized using cross-linked poly(2-hydroxyethyl methacrylate) (PHEMA) by Wichterle and Lim in 1960. It is interesting to note that hydrogels were the first biomaterials designed for human system. Hydrogels are

polymeric material with 3D polymeric cross-linked networks comprising of hydrophilic segments that are capable of acquiring a large amount of water, biological fluid or drug within them under physiological conditions without dissolution (Chai et al. 2017; Maheswari et al. 2014). The 3D cross-linked network of the hydrogels are formed via chemical or physical cross-linking. The absorption capacity of the hydrogel depends on the presence of hydrophilic pendant moieties such as $-SO_3H$, $-OH$, $-CONH_2$, $-COOH$, $-CONH$ in the polymeric backbone (Pinar et al. 2017; Bajpai et al. 2008). Further, these hydrogels are categorized into several types based on the origin, composition, physical structure, morphology, response to environmental stimuli (chemical, physical or biological), ionic charges, nature of cross-linking, etc. (Qiu and Park 2001; Susana et al. 2012). Hydrogels are synthesized by various polymerization methods such as suspension, solution and bulk polymerization by chemical and physical cross-linking routes (Maitra and Shukla 2014; Ahmed 2015). Chemically cross-linked hydrogels are extensively considered due to their excellent mechanical strength. The hydrogels synthesized in this study were prepared by using a chemical method i.e., free radical polymerization. There is a broad range of commercially available hydrogel-based wound dressing materials such as DermaGuaze™, Neoheal® Hydrogel, AquaDerm™, etc. which help to maintain an optimal wound moisture due to their water retaining capacity (Aswathy et al. 2020). However, these hydrogel-based wound dressing materials do not respond to wound external pH, and if there is excess production of wound exudate and if its pH is alkaline, it will enhance the MMPs activity.

Over the last decades, stimuli-responsive hydrogels have received substantial attention among researchers due to its vast applications in many areas like tissue engineering, drug delivery, wound healing and biosensors (Liu et al. 1993; Kim and Park 1998; Chen and Chang 2014). Hydrogels change their structure/chemical properties in response to external stimuli such as temperature, pH, solvent composition, electric field, and ionic strength and hence they are also called as stimuli-responsive hydrogels or smart polymers as shown in Figure 1.1 (Kaith et al. 2010; Mah and Ghosh 2013; Fu et al. 2019).
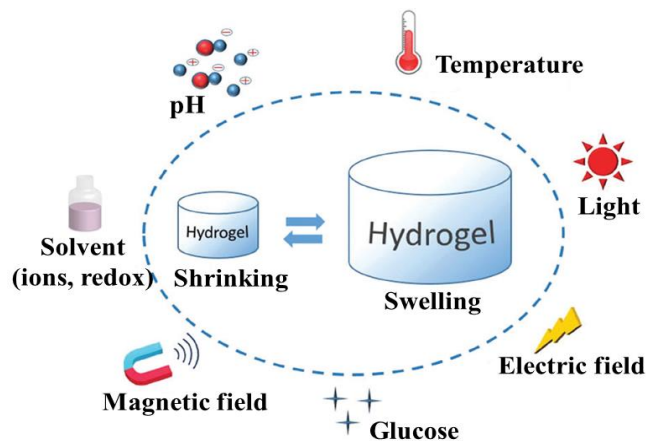
Figure 1.1 Hydrogel swell/de-swell in response to external stimuli (Fu et al. 2019)

The stimuli-responsive polymers can swell and de-swell according to the external environmental conditions and this behavior makes them suitable for the synthesis of intelligent biomaterials and biomimetic materials (Sood et al. 2016). Particularly, intelligent/smart material like pH-sensitive hydrogels are of specific interest in wound healing applications because of their swelling behavior based on the external pH and through this, pH sensitive hydrogels can retain liquid in its 3D network. The pH-sensitive hydrogel's behavior is due to the presence of ionizable pendant acidic or basic group in its polymeric backbone. Depending upon these pendant moieties, pH-sensitive hydrogels are categorized as anionic hydrogels (acidic group) and cationic hydrogels (basic group) as shown in Figure 1.2. At alkaline pH, the pendent acidic groups will be ionized and will be in negative charge, which will create an electrostatic repulsive force between them, and as the pH reduces, it will reach unionized state and vice-versa. This behavior results in the pH-dependent swelling/deswelling of the hydrogel network (Mallikarjun et al. 2021). Henceforth, it is well understood that these smart pH-sensitive hydrogels can maintain an optimal exudate based on the pH of the wound, through which MMPs activity can be controlled to achieve better healing. Some common anionic/cationic pH-sensitive polymers are poly(acrylic acid) (PAA), poly(methacrylic) acid (PMAA), poly(4-vinylpyridine) (P4VP), poly(2-vinylpyridine) (P2VP), poly(N,N-diethylamino ethyl methacrylate) (PDEAEMA) and poly(N,N-dimethylamino ethyl methacrylate) (PDMAEMA) (Gupta et al. 2002; Jabbari and Nozari 1999; Fei et al. 2002).
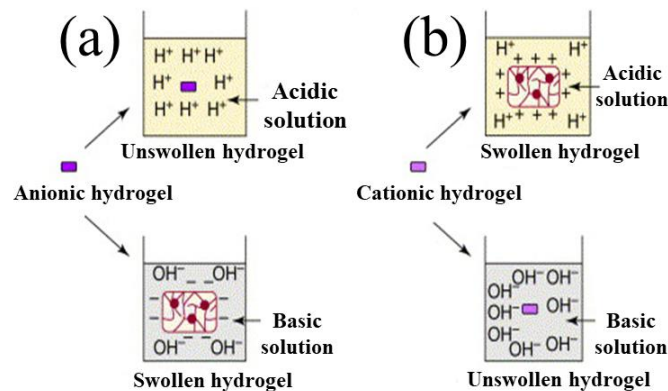
Figure 1.2 Swelling behavior of (a) anionic hydrogel (b) cationic hydrogel
(Mallikarjun et al. 2021)

Nowadays, poly(amino acids) like poly(aspartic acid) (PAsp) are in great demand to synthesize pH sensitive hydrogels because of their high water absorption capacity, biocompatibility and biodegradability (Montesano et al. 2015). PAsp is a poly-anion, biodegradable and water-soluble polymer that swells at alkaline pH due to the presence of free carboxyl group in its structure (Liu et al. 2013). Therefore, it is considered as a suitable pH-sensitive polymer for the development of wound dressing material which absorb excess exudate in response to wound pH and maintain optimal moist wound environment for better healing (Sharma et al. 2017). PAsp based hydrogels are widely used for various applications in many fields like diaper industry, agriculture, wound dressings, tissue engineering, drug delivery, etc. (Kumar et al. 2012).

Recently, natural biopolymers such as collagen, chitosan, hyaluronic acid, alginate, silk, keratin are mainly focused by researchers to use them for the synthesis of hydrogel based wound dressing because of their properties similar to extracellular matrix, biodegradability, biocompatibility, ability to repair damage tissues (Pandey et al. 2017). However, these hydrogels show some disadvantages like poor mechanical strength and rapid biodegradation. In order to improve their mechanical properties and prolong the degradation time during healing process, it is required to blend natural polymers with synthetic polymers like poly(vinyl alcohol) (PVA), polyurethane, poly(acrylic acid), poly(methyl methacrylate), poly(ethylene glycol) (PEG), poly(vinyl pyrrolidone) (PVP), etc. for the development of hydrogel based wound dressing materials (Zine and

Sinha 2017). PVA blends with other natural polymers have been used since long time because of its ability to form films. PVA is a hydrophilic polymer and provides adequate mechanical strength to the hydrogel.

Collagen, being a well-known natural biopolymer that can aid in fast recovery of wound as it possesses chemotactic properties which can attract fibroblasts on wound bed and encourage fibroblasts to produce granulation tissue and deposition of newly formed collagen (Kleinman et al. 1978; Postlethwaite et al. 1978). Collagen is an abundant protein available in the extracellular matrix of all animals. Collagen molecules are rich in proline and hydroxyproline (20% of total amino acids), as well as glycine and alanine (over 50% of total amino acids) and it is the main constituent of animal skin, bone, and connective tissue (Vallejos et al. 2014). Nearly 27 types of collagen have been identified till now but the most common types are: Collagen type I, II, III, IV and V. However, 90% of the collagen available in living organisms is of Type I followed by Type II and III (Silvipriya et al. 2015). Type I collagen is present in various parts of animal body like skin, bones, dermis, tendon, ligaments and cornea (Krishnamoorthi et al. 2017). Collagen is commercially extracted from porcine and bovine which are the major sources of collagen. Due to transmission of diseases and some religious issues, these sources are banned by several communities and in some regions (Sadowska and Turk 2010). Therefore, it is important to search new sources of collagen i.e., marine species which has become promising alternative source for collagen extraction. In coastal region, fish-processing industries generate huge quantity of fish wastes in the form of skin, scales, bones which are rich in collagen (Normah and Nur-Hani Suryati 2015). However, fish skin has high content of collagen which can be used as potential source for collagen extraction and can be used in the wound dressing material to enhance the wound healing process. Hence, the utilization of fish wastes for the extraction of high value-added products would not only increase the profit of fish industries, but also reduce environmental pollution (Rodríguez et al. 2017).

Studies have reported that pH sensitive hydrogels do not have inherent bacteriostatic or antibacterial activity (Fan et al. 2014). In order to avoid wound infection caused by bacteria, antibacterial agents must be incorporated into these hydrogels. Among various antimicrobial agents, silver is the most common and well-studied agent due to its broad

6

antimicrobial spectrum (Rath et al. 2015). In order to develop long-term antibacterial effect against gram-positive and gram-negative bacteria, silver in the form of nanowires can be used in wound dressings owing to its larger surface area to volume ratio leading to improvement in wound healing efficacy (Li et al. 2020). Silver nanowires (Ag NWs) are 1D nanostructures having diameters of approximately 300 nm and lengths of approximately 100μm (Zhang et al. 2017). They are used in several fields like catalysis, bio-sensing, photo-electrochemistry and medicine due to their optical, mechanical, electromagnetic, catalytic and biochemical properties (Flores-Gonalez et al. 2018). In the past few decades, silver has been used for wide range of applications like wounds and burn treatment (Parikh et al. 2005; Ulkur et al. 2005), disinfection in water treatment (Russell and Hugo 1994; Chou et al. 2005), removal of microorganisms on textile fabrics (Jeong et al. 2005; Lee et al. 2007), inhibition of bacterial biofilm on catheter (Samuel and Guggenbichler 2007), etc. Due to increased number of applications, low-cost silver nanomaterials are in demand. There are different methods to synthesize Ag NWs like; photodetection technique (Zhou et al. 1999), hydrothermal method (Xu et al. 2006; Yang et al. 2010), electrochemical technique (Mazur 2004), ultraviolet irradiation method (Zou et al. 2004), chemical synthesis (Slistan-Grijalva et al. 2005), porous materials template (Kong et al. 2003), DNA template (Braun et al. 1998), polyol process (Lei et al. 2017) and coaxial electro-spinning (Gebeyehu et al. 2016). Among all the available methods, hydrothermal method is widely preferred due to its advantages like simple, low cost and high yield (Coskun et al. 2011). From the perspective of green chemistry, hydrothermal method is favourable as no organic solvents and non-hazardous substances were used. Generally, a variety of reducing agents like ethylene glycol (Coskun et al. 2011), methenamine (Xu et al. 2006), sodium citrate (Yang et al. 2010), etc have been used in the hydrothermal synthesis of silver nanowires. These reducing agents are costly and potentially hazardous to the environment which results in numerous biological risks. Thus, fructose was used to synthesize silver nanowires as it is an eco-friendly, cheap and easily available reducing agent.

In the present work, collagen was extracted from marine waste i.e., Sole fish skin and process variables like acetic acid concentration (M), concentration of NaCl (M), solvent/solid ratio (mL/g) and time (hrs) were optimized by using Response Surface Methodology (RSM) combined with Box-Behnken Design (BBD) in order to achieve

maximum yield of collagen. Then, hydrothermal route was used to synthesize Ag NWs using silver nitrate (AgNO$_3$) as precursor, poly(vinyl pyrrolidone) (PVP) as capping and stabilizing agent and fructose as an eco-friendly reducing agent. The influence of operating parameters like temperature, AgNO$_3$ molarity, fructose and PVP concentration on the morphology of Ag NWs were examined. The antioxidant activity of synthesized Ag NWs was also performed by 2,2-diphenyl-1- picrylhydrazyl (DPPH) method. Further, a pH-sensitive hydrogel based on PAsp/PVA and collagen was synthesized by free radical polymerization using APS (ammonium persulfate) as initiator and ethylene glycol di-methacrylate (EGDMA) as crosslinker. The process was optimized by varying PAsp/PVA concentration, collagen concentration, APS and EGDMA concentration. The pH responsiveness of the hydrogel was assessed by varying the pH of the buffer solution. The optimized PAsp/PVA/Collagen hydrogel was incorporated with Ag NWs, where Ag NWs act as antibacterial agent. Antibacterial analysis of synthesized Ag NWs and developed pH-sensitive hydrogel based wound dressing material i.e., PAsp/PVA/Collagen impregnated with Ag NWs were evaluated against *E. coli* bacterium. The synthesized hydrogel was characterised by FTIR, SEM, EDAX, TGA, DSC and XRD. *In-vitro* release study of silver ions from hydrogel matrix was performed. Cytotoxic studies of the developed wound dressing material were performed on L929 fibroblast cell lines. *In-vivo* wound healing potential of pH-sensitive PAsp/PVA/Collagen hydrogel impregnated with Ag NWs was assessed in a full-thickness excisional wound model in Sprague-Dawley (SD) rats. Histological examination was done to identify changes in the dermis and epidermis during the healing process.

CHAPTER 2

LITERATURE REVIEW

2.1 Introduction

This chapter presents a comprehensive review of available literature on research related to development of wound dressings for chronic wounds with special emphasis on pH-responsive hydrogels with silver nanomaterials as antimicrobial agents. The chapter begins with basics pertaining to different layers of human skin. This is followed by a brief historical background on methods adopted for wound healing and types of wound. Considering the present scenario, much focus is emphasized on chronic wounds. Major factors that cause impaired wound healing are also briefed. The natural wound healing process is schematically explained. Different types of wound dressings such as traditional dressings, modern dressings, biological dressings and their merits and demerits are also discussed. Emphasis is given to hydrogel-based dressing materials covering historical background of hydrogels, classifications of hydrogel and their applications. Further, stimuli-responsive hydrogels, especially pH-sensitive hydrogels mechanism responsible for swelling/deswelling of hydrogels are described. The key findings from the literature on pH-responsive hydrogels as wound dressings have been tabulated. A critical assessment has been performed on various sources of fish collagen, extraction method, collagen type and yield obtained. A detailed review of wound dressings based on collagen blended with other polymers, their preparation method, *in-vitro* and *in-vivo* studies have been tabulated. Moreover, wound dressings containing silver nanomaterials as antimicrobial agents and their mode of action have been critically examined. Research gaps have been listed and scope of the succeeding chapters is also highlighted.

2.2 Skin

Skin is the outermost covering of the human body which provides protection to underlying body organs from external environment. It is the largest organ and works as barrier against harmful UV rays, microbial infection and maintains the body

temperature. Further, it has other important functions like water loss prevention, reservoir for vitamin D synthesis, sensation for heat, cold, pain and immunological surveillance (Simões et al. 2018; Rezvani Ghomi et al. 2019). Skin comprised of three different layers named as epidermis, dermis and hypodermis.

Epidermis: The outer layer of skin is waterproof and mostly composed of keratinocytes which is responsible for providing protection to internal organs against outside environment (Chaudhari et al. 2016). The occurrence of stem cells makes this layer regenerative which subsequently play an important role in wound repair process.

Dermis: This layer is present just below the epidermis and consists of blood vessels, connective tissue, glands, nerves, and hair follicles. The main function of dermis is to provide flexibility, structural support to the skin and sensation of touch and heat (Paul and Sharma 2004). Fibroblasts are the main cells which secretes the protein molecules like collagen, elastin and fibronectin and form the part of extracellular matrix. Collagen is a fibrous protein which plays an important role in wound healing (Hassiba et al. 2016).

Hypodermis: It is the deepest layer of the skin also called as subcutaneous fat tissue lies underneath the dermis. This helps in providing thermal insulation and protection to the internal organs from injury. Figure 2.1 depicts the structure of normal human skin and its three layers (Kamoun et al. 2017).
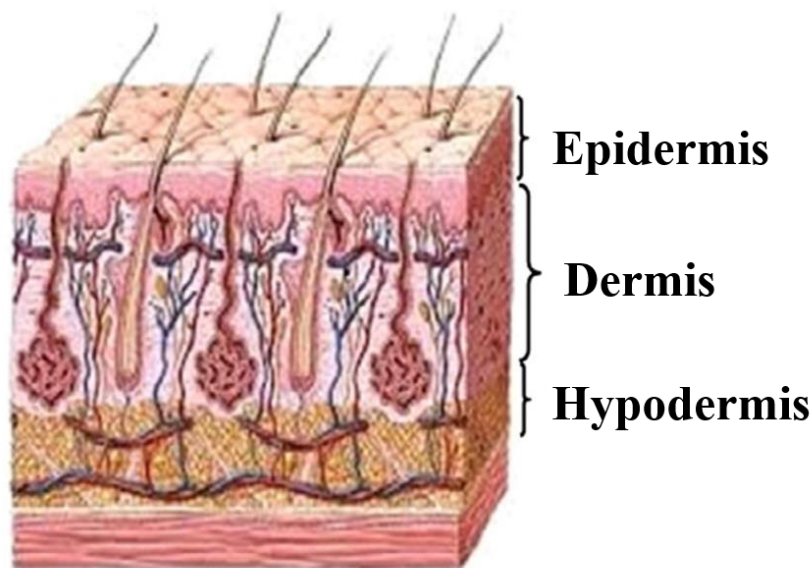
Figure 2.1 Structure of normal human skin (Kamoun et al. 2017)

In spite of the above-mentioned functions, our skin is so delicate which can be easily damaged by various external factors. This promotes bacterial infection in wound area, leading to delay in wound healing and sometimes causing death (Li et al. 2021).

2.3 Wound

Wound is described as the disruption encounters in the surface of skin because of various causes like heat, radiations, chemicals, electric current, friction, surgery or internally occurring physiological and medical illness (Boateng et al. 2008; Mir et al. 2018; Chaudhari et al. 2016). The quick repair of homeostatic biological conditions is required for complete healing of the wound so that the injured skin attains its original anatomy and function within a significant amount of time. If wound repair process delays, this will cause various problems like skin diseases, loss of hair and skin, origin of bacterial infection and in extreme conditions, dead tissue (Boateng and Catanzano 2015).

2.4 Historical development in wound healing

In Mesopotamia (2200 BC), the "three healing gestures" described as cleaning the wound, making wound plasters and wrapping the bandage around the wound were recorded on a clay tablet in science of wound healing. The plasters used for wound healing by Sumerians containing mixture of components like plants, mud, herbs, beer and oil as reported by Shah (2011). In Ayurveda, wound healing was defined in their medical terms as the *Sushruta Samhita* and *Charaka Samhita*. During this period, wound was healed by applying medicinal plants on the surface of skin but leaves a scar after healing (Bhishagratna 1963; Biswas and Mukherjee 2003). The Egyptians (1500 BC) were the first who used honey, grease obtained from animal fat and linen based textile gauze to prevent wound infection. Copper was also used by Egyptians for preventing bacterial infection. Around 460-377 BC, Hippocrates inscribed a statement about wound healing: "For an obstinate ulcer, sweet wine and a lot of patience should be enough." Romans named the four Basic Symbols of Inflammation like Rubor as redness, Tumor as swelling, Calor as warmth and Dolor as pain (Forrest 1982). During 120-201 AD, Galen who was a Greek surgeon and served Roman warriors. Initially, he suggested the usage of silk thread as stitching material for the complete wound closure

and maintain wound site moisture but later he reported carbolized catgut thread as stitching material. For the first time, the difference between chronic wound and acute wound was given by the Greeks. Galen also recommended that wash the wound with vinegar, boiled water and wine and treat the wound antiseptically. Later, there had been a substantial improvement in this field. Textile fibers were employed extensively as conventional (traditional) wound dressings in the 19th century owing to their availability in number of forms like wool, silk and cotton and especially in structural form such as nonwoven, knitted and composite. In France, Lumerie developed a wound dressing material made up of cotton gauze impregnated with paraffin (Cavendish 2007). In mid of 19th century, both Joseph Lister and Louis Pasteur were the first able to recognize the origin for management of infection by detecting the cause and developed the methods to prevent the infection (Cohen 1998). Lister developed antiseptic technique subsequently the aseptic technique to control the start of bacterial infection. During 1870s, Robert Wood Johnson produced gauze and introduced the antibiotics like iodine in wound dressing materials which was a big achievement in the field of wound care. 1n 1960s, Winter demonstrated that epithelization rate was much faster in moist wounds as compared to dry wounds when experiment done on pigs (Winter 1962; Winter and Scales1963). The era of modern wound dressings came in the 20th century. One of the significant criteria of modern wound dressings is to assure adequate moisture and the second is to provide moist wound healing environment.

2.5 Classification of Wounds

Wounds can be classified on different basis such as integrity of skin, number of skin layers affected, time and nature of healing process and degree of contamination as shown in Figure 2.2. The most common type of wounds is acute and chronic wounds. The different types of wounds are described in brief as below:

2.5.1 Integrity of skin

According to the integrity of skin, wounds are described as open and closed wounds. **Open wounds** are those where the layers of skin have been injured and the underlying tissue is being exposed to external environment. e.g. abrasion, puncture, avulsion and laceration (Velnar et al. 2009). These wounds are not always severe and can be treated at home.
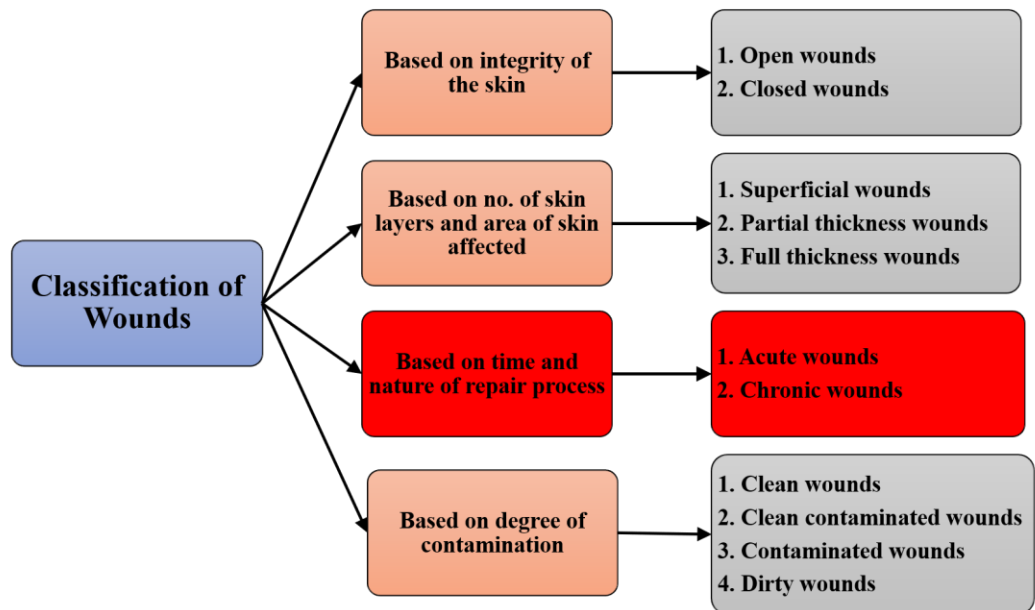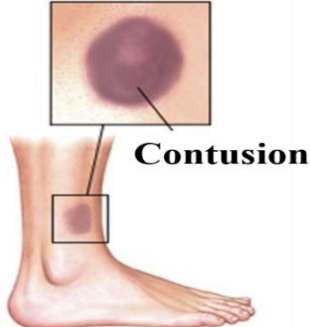
Figure 2.2 Classification of wounds
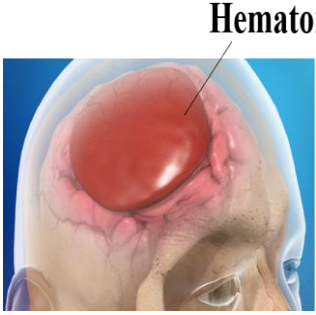
Closed wounds are defined as injuries in which skin remains intact and internal tissues have been damaged and bleeds but does not come in direct contact to the outside environment. The main examples of closed wounds are contusions, hematomas and crush injuries (Degreef 1998; Velnar et al. 2009). The examples of open and closed wounds are discussed in Table 2.1.

Table 2.1 Illustration of examples of open and closed wounds (Enoch and Leaper 2008; Kumar and Leaper 2008)

Types of wound	Examples	Description	Illustration
Open wounds	Abrasion	occurs when the skin is rubbed against rough surface	

	Puncture	occurs when sharp objects like nails, needles create small hole in the tissues of skin	
	Avulsion	tearing of skin and internal tissues due to accidents, explosions, animal bites	
	Laceration	deep cuts caused by sharp object like knives	
Closed wounds	Contusions	where underlying blood vessels, capillaries, tissues, organs, bone get damaged by blunt trauma	

| | Hematomas | blood vessels and capillaries have been injured due to trauma which results in oozing of blood from them and collected in small area inside the body | |
| | Crush Injuries | high pressure or force occurs on the body part that presses them between two objects | |

2.5.2 Number of skin layers and area of skin affected

On the basis of depth of the wound, it can be categorized into three types: superficial wounds, partial thickness wounds and full-thickness wounds. Table 2.2 presents wound classification based on wound depth.

Table 2.2 Types of wound according to depth of wound (Torres et al. 2013; Percival 2002; Boateng et al. 2008)

Types of wound	Description	Healing time
Superficial	Wounds in which injury only affects the outer layer of skin i.e., epidermis	These wounds will heal within 10 days by regeneration of the epithelial cells with no scar formation.

Partial thickness	Injury involves the loss of epidermis along with dermis layer like sweat glands, hair follicles and blood vessels	This type of wound may require 10-21 days to heal with scar formation.
Full-thickness	Wounds which affect the underlying subcutaneous fat layer besides to epidermis and dermis layers.	Full thickness wounds heal by the combination of re-epithelization and wound contraction and requires > 21 days to heal with significant scarring.

2.5.3 Time and nature of repair process

Based on the time taken to heal and nature of wound healing process, wounds are mainly classified as acute and chronic wounds.

Acute wounds are the tissue injuries that heal themselves with minimal scarring within the expected time frame. Generally, these wounds heal within 8-12 weeks (Velnar et al. 2009; Hassiba et al. 2016). The main causes of acute wounds include mechanical damage because of some external factors like abrasion, stabbing by hard objects, incision, penetration wounds by knife or gunshots. There are some another causes of acute wounds such as corrosive chemicals, radiations, electrical shock and exposure to intense heat (Zahedi et al. 2010).

Chronic wounds are the wounds that initially start as acute wound and turn out to be chronic when it fails to proceed through the normal stages of wound healing in an orderly and timely manner. On average, a chronic wound is classified as one that fails to heal beyond 12 weeks and often recur (Dunnill et al. 2017). Chronic wounds are arrested prolonged in the inflammatory phase of healing which causes the higher levels of neutrophils, pro-inflammatory cytokines, biofilm phenotype bacteria and protein-digesting enzymes (matrix metalloproteinases). When MMPs are present in the right balance, wound healing can be endorsed by promoting cell migration, remodelling and the breaking down of damaged extracellular matrix. But when they are present at elevated levels for a prolonged period of time it will result in increased break down of

cellular components and healthy extracellular matrix (ECM) which is associated with impaired wound healing. The factors which delays the healing process of chronic wounds include diabetes, persistent infection, excessive exudate, tissue hypoxia, necrosis, high levels of inflammatory cytokines and reactive oxygen species (ROS), poor primary treatment and other patient related factors like age, smoking, poor nutrition, obesity as shown in Figure 2.3 (Guo and DiPietro 2010). This leads to the disruption of the normal phases of wound healing process.
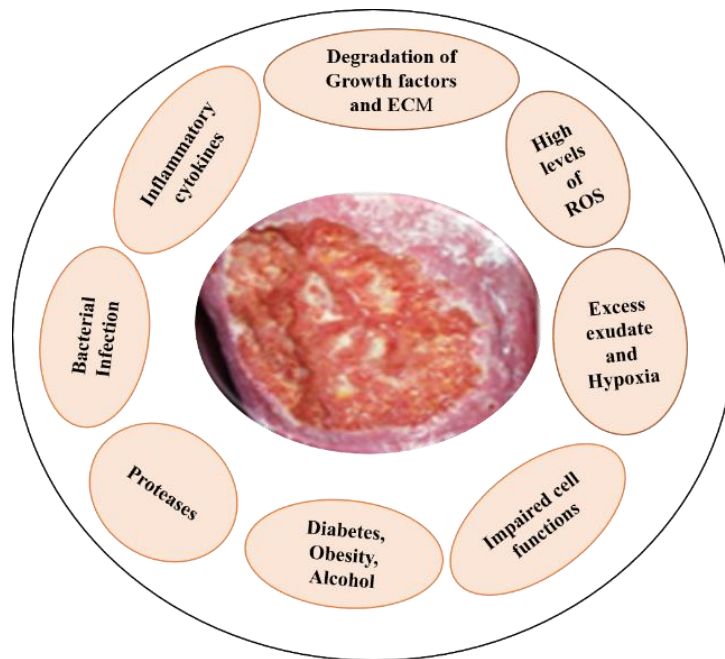
Figure 2.3 Factors affecting the healing of chronic wounds

The common examples of chronic wounds are diabetic foot ulcers, venous leg ulcers, arterial ulcer, pressure ulcers, deep wounds as shown in Figure 2.4 (Sweeney et al. 2012; Abrigo et al. 2014; Larouche et al. 2018).

The fundamental differences between acute and chronic wounds based on the immune response is highlighted in Figure 2.5. It may be observed that healing of acute wound progress through a cascade of events that are divided into four overlapping stages such as hemostasis, inflammation, proliferation and remodeling. The immune cells such as T cells, neutrophils, macrophages and platelets play an important role in conciliating this process. In acute wound healing, low levels of inflammatory cytokines and MMPs are present. Angiogenesis promotes re-epithelization, migration of fibroblasts and

deposition of collagen. But chronic wounds fail to proceed beyond inflammation stage due to the persistent bacterial infection and imbalance between pro and anti-inflammatory signals which hinders the wound healing process. Elevated inflammatory cells and MMPS lead to the degradation of growth factors and ECM, impaired angiogenesis, fibroblast senescence and prevents macrophage phenotype conversion (Wang et al. 2020).

Figure 2.4 Examples of chronic wounds: (a) Venous leg ulcer (b) Arterial ulcer (c) Diabetic foot ulcer (d) Pressure sore (Larouche et al. 2018)
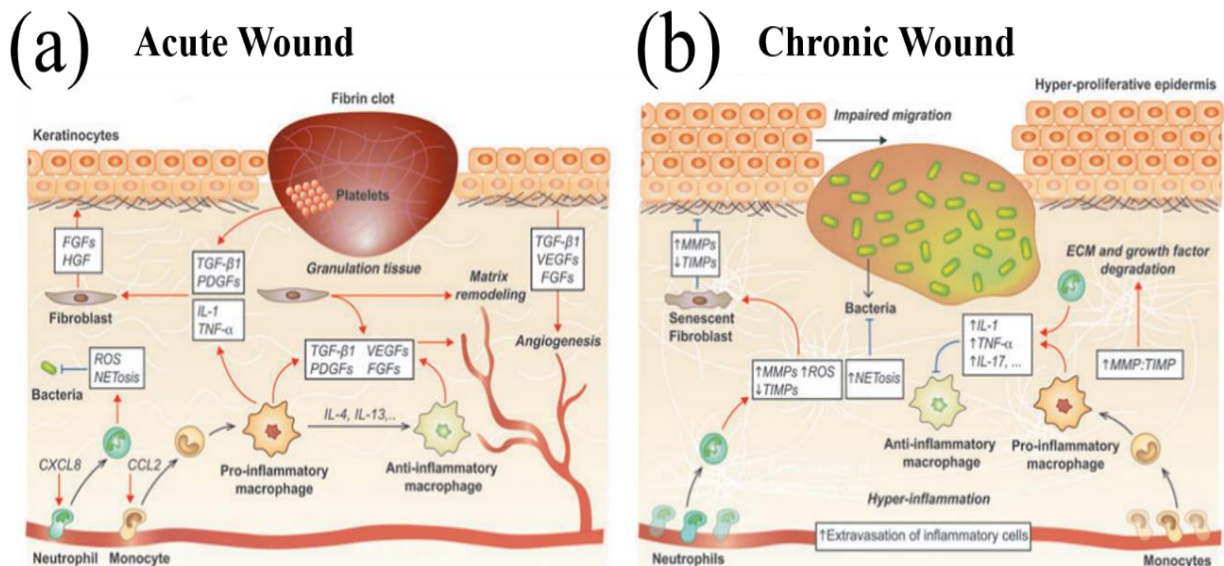
Figure 2.5 An illustration of natural phenomenon of immune response in acute and chronic wounds. Red arrows represent induction, black arrows represent differentiation and blue arrows show inhibition (Larouche et al. 2018)

2.5.4 Degree of microbial contamination

In 1964, National Research Council system, USA, has classified the into wound four types on the basis of contamination: clean, clean-contaminated, contaminated and dirty. The brief description of these wounds is discussed in Table 2.3.

Table 2.3 Wounds classification based on degree of microbial contamination
(Onyekwelu et al. 2017; Gottrup et al. 2005)

Types of wound	Description
Clean wounds	These wounds occur through elective surgery that are uninfected, uninflamed and do not enter the respiratory, alimentary, genital, or urinary tracts. They are operative incisional wounds, non-traumatic and mostly closed. If drainage is required then closed drainage method is necessary Eye surgery, mastectomy and herniorrhaphy are its examples.
Clean-contaminated	Wounds that occurred during emergency surgery otherwise they are clean. They are reopened for drainage or other surgical reasons and also enter the respiratory, alimentary, genital, or urinary tracts under controlled conditions without unusual contamination. They develop high risk of infection after operation e.g., ear surgery, appendix, nasal, thoracic, etc.
Contaminated	These are open, fresh and accidental wounds that involves operation with major break in sterile technique or discharge from gastrointestinal contents to the wound. Incisions involve acute or non-purulent inflammation are considered in this category.

	These are old traumatic wounds with retained devitalized tissue and cause postoperative infection because of the microorganisms were already present in the operation field before the operation. Purulent inflammation involved in this category.
Dirty	

2.6 Natural wound healing process

Wound healing is a complex biological process that begins immediately in response to any skin or tissue injury. It stays for months to years based on the type of injury. In case of normal wound repair, it undergoes through a series of overlapping and associated integrated phases which results in the restoration of normal tissue with its native tensile strength and replacement of devitalized tissue as well as missing tissue (Sundaramurthi et al. 2014; Hassiba et al. 2016).
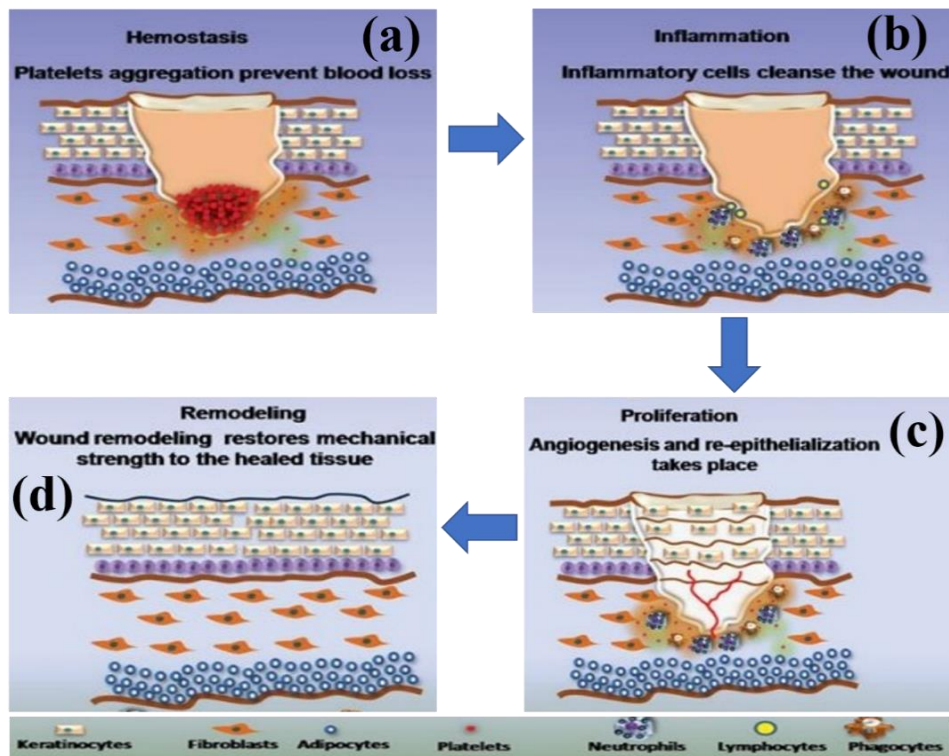
Figure 2.6 Representation of sequential stages in natural wound healing process (a) Hemostasis (b) Inflammation (c) Proliferation (d) Remodeling (Sundaramurthi et al. 2014)

There are four stages of natural wound healing process which are named as hemostasis, inflammation, proliferation and remodeling as depicted in Figure 2.6.

Hemostasis: It occurs instantaneously when there is any skin injury. At that time, platelets play a crucial role in the clot creation. The injured blood vessels constrict to prevent the blood flow to the injured site. Platelets aggregate to the wound site and release different proteins such as fibronectin (formation of fibrin network), fibrinogen (clotting of exudate), chemokines, cytokines. With the help of other proteins such as thrombospondin and vitronectin as well as combination of both these proteins, platelets produce the clot to stop further bleeding in the wound. Chemokines secreted by the platelets attract inflammatory cells such as macrophages, neutrophils and lymphocytes towards the wound bed and initiate the inflammation process (Zahedi et al. 2010).

Inflammation: This stage continues for 6 days. Mast cells produce histamine and serotonin activates vasodilatation and increased capillary permeability which allow the entry of inflammatory cells to wound site. Neutrophils secrete growth factors and help to remove foreign material and bacteria by the process of phagocytosis. Later, monocytes differentiate into macrophages, which assists in removing necrotic tissue, microbes and release various growth factors to stimulate collagen production that influences re-epithelization.

Proliferation: In this stage, epithelial cells and fibroblasts migrate from wound edge region to centre until the whole wound surface is covered by newly formed epithelial cells. Granulation tissue is formed by a process called angiogenesis (formation of new blood vessels) and secretion of matrix proteins i.e., collagen by fibroblasts. Production of collagen and its cross-linking offer mechanical strength to the restored tissue. Proliferation of fibroblasts and collagen production process lasts upto 3 weeks.

Remodeling: This is the final step in wound healing process. Wound contraction occurs by moving wound edges towards centre to cover the wound area. Myofibroblasts play an important role in wound closure by producing actin. Remodeling or maturation process is inscribed by rearrangement of disorganised collagen fibrils. Type III collagen is substituted by type I collagen and then collagen fibrils are remodeled into strong fibres. Granulation tissue is replaced by completely newly formed healthier ECM and

excess collagen is degraded by MMPs. The maturation stage begins around week 3 and continues for several months to attain scarless skin (Boateng et al. 2008).

In a nutshell, when an average healthy person suffers from any tissue injury, the wound healing process should follow normal stages in a systematic manner to repair wound within expected time frame. However, if a wound does not proceed through normal process of wound healing and is stalled in one of the stages, then it falls under consideration of chronic non-healing wounds. Various reasons that delay wound healing process are mentioned above in Figure 2.3. Amongst all factors, microbial infection is the most common and significant factor which may result from inappropriate wound dressings leading to a delay in wound healing process. Moreover, delayed wound healing also causes an excessive production of exudates that leads to maceration of healthy tissue around the wound. So, it is very important to choose the most appropriate wound dressing for successful wound healing.

2.7 Wound dressings

Globally, every year, a large number of people suffer from various types of skin injuries such as accidents, burns by boiling water or oil, fire etc. Moreover, due to very expensive medical care and related treatments for repair of such kind of skin damages render common people impoverished (Kamoun et al. 2017). Owing to these particular reasons, a need for the development of ideal wound dressing material has become an issue of research interest. The selection of suitable wound dressing for rapid and effective healing should be based on wound type, depth of the wound, volume of wound exudate and bacterial infection. An ideal or desired wound dressing material should possess important characteristics during the time of its selection such as (a) non-adherent to wound bed, (b) maintain moist wound environment, (c) remove excess exudate, (d) impermeable to bacteria, (e) cost effective, (f) mechanically stable, (g) exchange of gases, (h) easily changed and removed, (i) non-toxic, biocompatible and biodegradable as depicted in Figure 2.7 (Vijayakumar et al. 2019). The wound care is dependent on wound dressing material as it creates a physical obstruction between surroundings and the wound itself. In addition to this, wound dressings also boost wound healing process by reducing bacterial infection, promote collagen synthesis, re-epithelization and decreasing pH of the wound bed (Zhang and Zhao 2020).
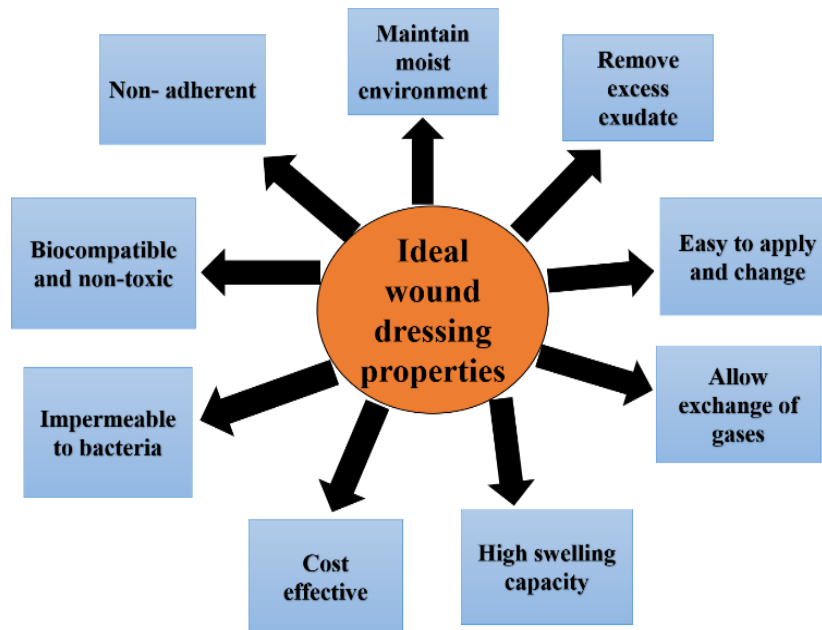
Figure 2.7 Characteristics of ideal wound healing material

Historically, various materials such as animal fat, honey, plant leaves and mud have been used to heal wounds as reported by Forrest (1982). Subsequently, wet-to-dry dressings were widely used but Winter demonstrated a moist wound healing model. He revealed that wet or moist dressings are able to heal wound faster as compared to dry dressing as shown in Figure 2.8.
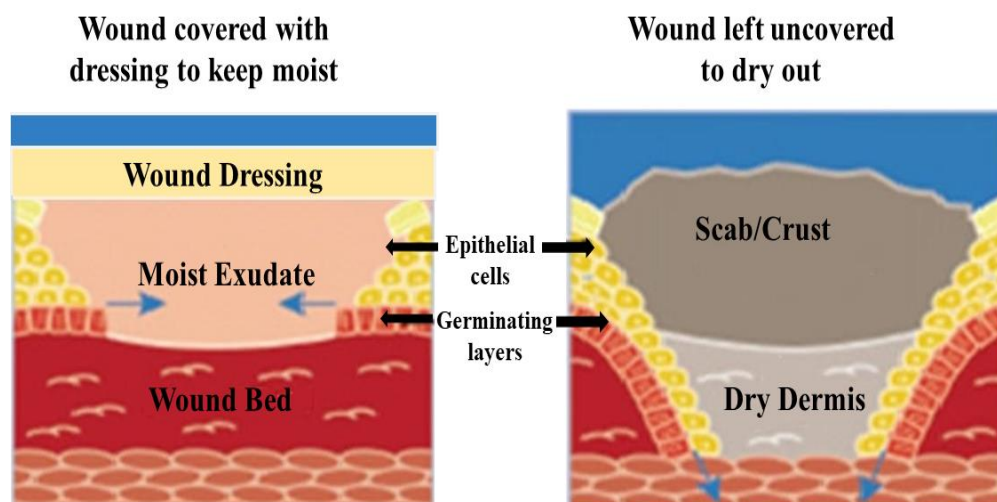
Figure 2.8 Wound healing model in moist environment versus dry condition (Uzun 2018)

The fact is attributed to newly formed epithelial cells migrate faster in moist environment from wound edge to the injury site than in dry condition. Furthermore, wound heals faster without any scab formation in moist condition whereas in dry condition scab is formed which impedes the migration of epithelial cells. Therefore, wet dressings were regarded as appropriate candidates for tissue repair and wound dressing (Winter 1962). Due to the requirement of moist wound environment for rapid healing, there is a great demand of modern wound dressings referred as advanced wound dressing materials or occasionally ideal wound dressing materials depending upon the context thereof. Virtue of employing advanced dressings is therefore to achieve an improvement on particular properties of wound dressing material so that a close proximity to ''ideal wound dressing material'' is attained. Related to this argument is an assessment of characteristics of wound and to develop an understanding on selection of accessible products which are assumed to be ideal dressings. The first modern wound dressing was introduced in mid 1980s. Further, these dressings were expanded in different forms as films, hydrogels, foam, hydrocolloids, alginates as described by Stashak et al. (2004). Based on different aspects of dressings, these are mainly classified as passive, interactive and biological or bioactive dressings. Passive dressings include gauze which are used only to cover the wound area to repair by itself. Interactive products such as hydrogels, foam, films are occlusive and allow transmission of gases and barrier against bacteria. Bioactive dressing materials like collagen, chitosan, alginate, hyaluronic acid are biocompatible, biodegradable and have significant role in wound healing (Hassiba et al. 2016).

2.7.1 Traditional dressings

In the past years, Boateng et al. (2008) reported that cotton wool, natural or synthetic bandages, gauze, lint, tulle are used as traditional dressings for wound management. They were used as primary and secondary dressings to prevent the entry of harmful bacteria into wound and keep wound dry by absorbing exudate. These are suitable for minimal exuding wounds, clean, minor and superficial wounds. Apart from being less cost effective, these dressings required frequent changing as they became moistened and strongly adhered to the wound resulting in pain and necrosis of renewed epithelial cells during their removal. Subsequently, these dressings are not able to provide moist

environment to wound so advanced modern dressings are designed to overcome these drawbacks as mentioned by Dhivya et al. (2015).

2.7.2 Modern wound dressings

To improve the traditional dressing materials, a wide range of modern wound care products have been developed to create and maintain moist wound environment for facilitating faster healing. These dressings are fabricated from synthetic polymers and act as carrier for delivery of entrapped therapeutic agents at the wound site in the form of films, foams, hydrogels, hydrocolloids and alginate as summarised in Table 2.4.

Table 2.4 Classification of modern dressings along their advantages and disadvantages (Sweeney et al. 2012; Zahedi et al. 2010; Powers et al. 2016)

Polymeric dressing type	Composition	Suitable for	Advantages	Drawbacks	Commercially available products
Films	Polyurethane or other polymers	Superficial and dry wounds	These are thin, and transparent so that wound can be easily monitored. They have good permeability for gases.	These dressing stick to wound bed and its removal damage the renewed epithelium. They are poor in absorbing excess exudate and in bacterial invasion.	Tegaderm, Blister film, Poly skin II, Silon-TSR
Foams	Polyethylene glycol bounded with polyurethane or silicone	Burns, chronic wounds	These dressings have high capacity to absorb excess exudate and maintain moist wound environment.	They are not applicable for dry wounds and have less stability. They form opaque layer and semi-permeable for exchange of gases.	Flexzan, Lyofoam, Crafoams, Biatain
Hydrogel	Crosslinking of hydrophilic polymers such	Dry and necrotic wounds	Hydrogels retain significant amount of water, so they are	They are used for moderately exuding wounds and also leads to	Nu-gel, Tegagel, Flexigel, Hypergel

	as PVA, PEG, PVP		highly absorbent and have cooling and soothing effect. They are non-adherent and easy to remove.	maceration of skin tissue because of their water retention capacity. Their mechanical strength is poor.	
Alginate	Polysaccharides such as alginate crosslinked with salt solutions of Na, Ca, Zn	Surgical, highly exuding wounds and thickness burns	They are highly absorbent and non-adherent dressings. They have good mechanical strength and better bacterial invasion.	These are not suitable for dry wounds and if wounds are too dry, cause pain while removing. Dressings are frequently changed to avoid dampness.	Algisite, Sorbsan, Omiderm, Algiderm
Hydrocolloids	Carboxymethyl cellulose, pectin and gelatin (gel forming materials) combined with	Minor burns, pressure sores and traumatic injuries	Hydrocolloids can apply to both moist and dry wounds. Though, they are impermeable to water but while absorbing exudate these will lead to formation	These dressings are not used for heavily exuding wounds.	Duoderm, Hydrocol, Nuderm, Tegasorb

	elastomers and adhesives		of gel and can be easily removed without causing pain.		

In relation of the available basic understanding on literature of merits and demerits of all class of modern wound dressing materials, it is inferred that hydrogel are the best choice for designing as per desired wound dressing material. Hydrogels as a dressing material for chronic wounds satisfy all the needs required during wound healing in the shortest time period because of the following reasons:

(i) Hydrogel contains high water content (around 90 wt.%) and only 10 wt.% of polymers whether natural or synthetic. Due to this property, hydrogel-based dressings are used for necrotic and dry wounds (Madaghiele et al. 2014).

(ii) These dressings provide cooling effect to patients as well as low adherence to wound bed for reduction of pain (Sood et al. 2014).

(iii) Hydrogel maintain the moist environment in the wound area because of their ability to absorb and hold the wound exudate which in turn enhances proliferation of fibroblast and migration of epithelial cells (Sahiner et al. 2016).

(iv) Hydrogels possess mesh like structure which is similar to ECM, allow to entrap bioactive molecules and cells. These molecules are released to the wound site in a controlled manner while absorbing exudate by hydrogels. In addition, hydrogel structures are permeable for gaseous exchange and prohibits the entry of bacteria to wound site (Chen et al. 2016b).

2.7.3 Biological wound dressings

There has been enormous development in the methods required for enhancement of functions of wound dressing materials. These involve inclusion of compounds having bioactive nature such as synthetic drugs, peptides, growth factors, naturally occurring compounds or plant extracts into wound dressing material to develop biological or medicated dressings. These dressings are developed from biomaterials or bioactive polymers which have therapeutic effects on stages of wound healing process. The commonly used bioactive polymers include collagen, chitosan, hyaluronic acid and alginate are biocompatible, biodegradable and derived from natural tissues (Moura et al. 2013). Bioactive polymers can be used alone or combined with other polymers based on wound type. Furthermore, bioactive dressings are entrapped with antimicrobial agents and growth factors to boost wound healing process. Collagen is a fibrous structural protein and present in extracellular matrix. It promotes wound healing

process by stimulating fibroblasts cells to synthesize new collagen fibres and accelerate the migration of epithelial and endothelial cells when come in contact with wound tissue (Silva et al. 2014). Hyaluronic acid is natural polymer present in connective tissues and also a part of ECM which enhances the wound healing by monitoring inflammatory mediators (Supp and Boyce 2005). Chitosan is naturally occurring polysaccharide and plays an active role in wound healing by the formation of granulation tissue in proliferative phase of healing process (Ueno 2001). Till now, biological dressings have been reported the most demanding dressings as compared to other dressing materials.

2.8 Necessity of engaging dressing materials based on hydrogels

A critical assessment of the archival literature pertaining to merits and demerits of traditional wound dressing materials dating back to 19th century inferred existence of basic issues such as regular change of dressing is required because of their dampness. These dressings stick to wound which results in pain and peeling off newly formed epithelial cells. Also, they do not provide moist wound environment. Therefore, an urge for the development of modern wound dressing materials that would be implied as ideal dressings of the futuristic wound care applications has arrived in the present scenario.
 Keeping in view of the past achievements, and the recently reported studies, a shift towards bioactive wound dressings have become an area of interest to arrive at prominent solutions for issues to be addressed appropriately for wound care management. Therefore, hydrogels and their various combinations to obtain optimized solutions for mechanical stability and related attributes desired for fast healing process are currently the most explored materials in terms of their capability for advanced wound care applications.

2.9 Historical background of hydrogels

The term hydrogel was introduced for the first time in literature in 1894 (Bemmelen 1894). Hydrogels of present era were basically colloidal gels made of inorganic salts. In 1949, hydrogel material was first used based on poly(vinyl alcohol) and crosslinked with formaldehyde was reported as biomedical implant (Kirschner and Anseth 2013). Subsequently, PVA based hydrogels were prepared by Danno (1958) using gamma radiation for crosslinking. In 1960, Wichterle and Lim were the first researchers who

prepared hydrogel based on crosslinked poly(2-hydroxyethyl methacrylate) (pHEMA) polymer and used in contact lens. It was only after the advent of this application of hydrogel that revolutionized research and development of hydrogel materials for biomedical field (Wichterle and Lim 1960). pHEMA hydrogels showed properties similar to modern hydrogels such as ability to absorb high amount of water and maintain their structure. Hydrogels gained more attention for biomedical applications since 1970s particularly in the field of stimuli responsive hydrogels thereafter also referred as smart hydrogels. In 1971, Kopecek reported synthesis of first pH sensitive hydrogel, which was obtained by addition of some inorganic groups on the backbone of pHEMA and examined the permeability of NaCl is controlled by pHEMA membranes in response to pH (Kopecek 2009). Buwalda et al. (2014) classified hydrogels on the basis of historical background into three generations:

(i)   The primary purpose of first-generation hydrogel was to prepare crosslinked hydrogels with remarkably good mechanical stability and high swelling. This generation started from 1960s onwards.

(ii)   The second-generation began from start of 1970s and comprised of stimuli responsive hydrogels i.e., response to various external stimuli like change in pH, concentration of particular molecules, temperature, etc.

(iii)   Third generation of hydrogel were interested in the evolution of stereo complexed materials such as PEG-PLA hydrogel physically crosslinked by cyclodextrin. With this advancement, interest has been increasing in the development of existing stimuli responsive or smart hydrogels with tunable properties. These smart hydrogels can be utilized to prepare advanced medical devices.

Lim and Sun (1980) investigated calcium alginate for the preparation of microcapsules and used for the encapsulation of cell. Afterwards, Yannas et al. (1981) fabricated hydrogels comprised of collagen and shark fish cartilage to attain dressing material for healing wounds and burns. Nowadays, hydrogels have gained more attention by biomaterial scientists and researchers to utilize them for their biomedical applications such as tissue engineering, wound dressings, drug delivery, etc.

2.9.1 Hydrogels-An overview

Hydrogels are considered as novel polymers that are used for the development of new materials. Hydrogels are defined as 3D cross-linked polymeric networks comprising of hydrophilic polymers which have the ability to absorb a large amount of water (Havanur and Farheenand 2019). They have water retaining capacity because hydrophilic pendant groups like -CONH, -OH, -COOH,- $CONH_2$, -SO_3H, etc., are present in the polymeric backbone and also maintains their 3D structure under swollen state by either physical or chemical crosslinking (Hennink and Nostrum 2012; Kamath and Park 1993). Hydrogels which are chemically crosslinked will have covalent bonds between the polymer chains whereas physically cross-linked hydrogels are stabilized by physical forces such as hydrophobic, hydrogen bonding or ionic interactions and chain entanglement (Jen et al. 1996). Owing to cross-linking between polymer networks, hydrogels attain mechanical strength as well as physical stability in their structure. Also, crosslinking prevents hydrogel from dissolution in water in spite of absorbing significant amount of water or biological fluids through osmotic pressure and capillary action (Hoare and Kohane 2008; Varaprasad et al. 2017). These forces get balanced to reach in equilibrium condition and further causes the expansion of polymer chains. The swelling process of hydrogel i.e., diffusion of water molecules in hydrogel matrix is expanded by Gibas and Janik (2010) into three steps:

(i) The first step involves the interaction of water molecules to hydrophillic group present in hydrogel, this intreacted water is termed as primary bound water (Ullah et al. 2015).

(ii) In the second stage, water molecules bind with hydrophobic groups existing in polymer chains, this bound water is called as secondary boundary water. Both these primary and secondary bound water form total bound water.

(iii) In the third step, physical or chemical cross-linking resist the osmotic pressure of hydrogel towards dilution, thus additional water is absorbed. Free water or bulk water is referred as water imbibed at equilibrium state and fills the void spaces in the centre of large pores of hydrogel and between polymeric chains.

Therefore, hydrogel is 3D crosslinked polymer networks which is generally described as mesh as shown in Figure 2.9.
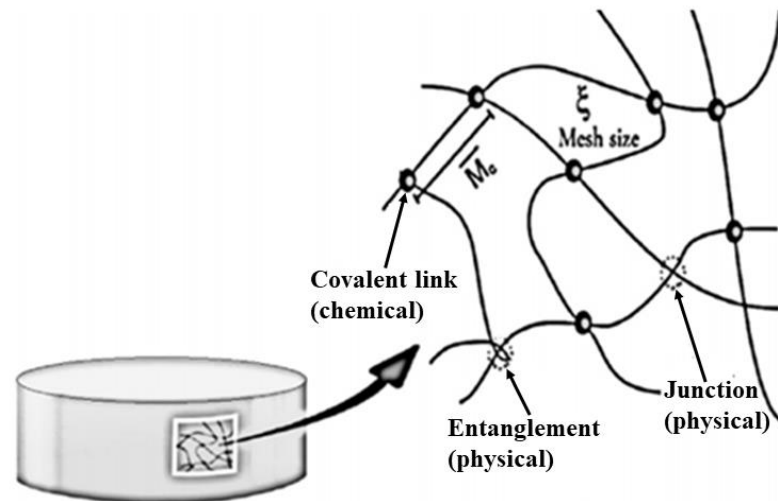
Figure 2.9 Physically and chemically cross-linked hydrogel network (Ullah et al. 2015)

These meshy structures retain the water or biological fluid, and an elastic force is developed because of expansion and contraction of hydrogel and in turn maintains the strength of hydrogel. Hydrogels have some unique properties such as soft nature, porous structure and high-water content which make them too closely mimic the extracellular matrix present in living tissue. Swelling degree depends upon density of crosslinking and polymer concentration. Higher the crosslinking density, lesser will be swelling and brittleness in hydrogel increases (Okay 2009).

2.9.2 Classification and application of hydrogels

The worldwide research on hydrogels has directed to their extensive development leading to a large variety. Therefore, depending upon the attributes obtained or related to these materials such as nature of response to external stimulus, method of preparation, ionic charge, cross-linking type, biodegradability and source hydrogels are classified. Hydrogels are prepared in various forms (microparticles, coatings, sheets or membranes, solid molded and liquids) have broad range of applications like targeted drug delivery vector material (Hoffman 2012; Sosnik and Seremeta 2017), as wound dressing (Ngadaonye et al. 2013; Mir et al. 2018), as implants or catheters (Netti et al.

1993; Ullah et al. 2015), as transdermal drug delivery (Caló and Khutoryanskiy 2015) as contact lenses (Sosnik and Seremeta 2017) and in tissue engineering (Kondiah et al. 2016), etc. The classification of hydrogels and their corresponding applications are listed in Table 2.5.

Table 2.5 Classification of hydrogels on the basis of various aspects and their applications

Basis of Classification	Hydrogels		Applications	Reference
	Type	Polymers		
Based on Composition (method of preparation)	Homopolymer	Poly(2-hydroxyethyl methacrylate) (pHEMA), Poly(ethylene glycol) (PEG), Poly(vinyl alcohol) (PVA), Poly(vinyl pyrrolidine) (PVP), Poly(acrylic acid) (PAA)	Drug delivery, contact lenses, wound healing, regeneration of cells of spinal cord and bone marrow, producing artificial cartilage and scaffolds for cell attachment.	Peppas et al. 1999; Benamer et al. 2006; Syková et al. 2006; Bavaresco et al. 2008; Kubinová et al. 2010
	Co-polymer	Poly(lactic-co-glycolic acid) PLGA-PEG-PLGA, PEG-poly(ε-caprolactone)-PEG, Methacrylic acid (MAA)-PEG-PEGMA, PVP-PEG, PVP-CMC (carboxymethyl cellulose), Acrylamide-acrylic acid, γ-benzyl L-glutamate (BLG) and poloxamer	Tissue repair, drug delivery, cell encapsulation, scaffolds for tissue engineering, wound dressing material.	Lugão et al. 2002; Kim and Peppas 2003; Qiao et al. 2005; Wang et al. 2007; Gong et al. 2009

	Interpenetrating (IPN)	Chitosan-PNIPAM, Polyethylene glycol diacrylate (PEGDA)-chitosan, Polyurethane (PU)-PAA, Calcium alginate/dextran-hydroxyethyl methacrylate (dex-HEMA)	Oral drug delivery, bio-separation, wound dressing material, artificial muscles, sensors, pharmaceutics, 2D and 3D scaffolds for vascular cells regeneration and tissue engineering.	Abraham et al. 2001; Alvarez-Lorenzo et al. 2005; Liu and Chan-Park 2009; Pescosolido et al. 2011
	Semi-interpenetrating	Linear cationic polyallylammonium chloride entrapped in acrylamide-acrylic acid, PVP-PAA, Alginate-poly(N-isopropylacrylamide) (PNIPAAm), Gum arabic-pHEMA, chitosan-PEO, Guar gum-poly (MAA), PVP-CMC	Controlled drug delivery, tissue engineering, waste water treatment.	Ju et al. 2002; Zhang et al. 2005; Gils et al. 2010; Lu et al. 2010
Based on Source	Natural	Collagen, Chitosan, Gelatin, Alginate, Cellulose, etc.	Wound healing, tissue engineering, repair nerves for spinal cord,	Patravale and Mandawgade 2008;

	Synthetic	PVA, PEG, PEO, PAA, PNIPAAm, PLA, etc.	cellular response improvement, and recover functions of sensory motor, food packaging, cosmetics and agriculture industry.	Jamnongkan and Kaewpirom 2010; Gorrasi et al. 2012; Valderruten et al. 2014; Kong et al. 2017
	Semi-Synthetic	Cellulose derivatives, Gelatin methacrylate		
Based on Configuration	Amorphous	Poly(methyl methacrylate) (PMMA)	Dental implants and bone cements as filling material, injectable gels, shape memory hydrogels, wound care	Osada and Gong 1993; Varvarenko et al. 2010; Verné et al. 2015; Okay 2018
	Crystalline	Polypropylene		
	Semi-crystalline	Acrylic acid and n-octadecyl acrylate, N,N-dimethylacrylamide and n-octadecyl acrylate		
Based on Cross-linking	Chemical cross-linking	Acrylic acid-gelatin (free radical polymerization and crosslinker ethylene glycol dimethacrylate)	Healing of skin ulcers, drug delivery	Bukhari et al. 2015; Croitoru et al. 2020

		PVA-kappa carrageenan (freeze thaw method)		
	Physical cross-linking			
Based on Ionic Charge	Anionic	CMC, Poly(aspartic acid) (swelling in basic pH)	Drug delivery, wound healing	Schmaljohann 2006; Colo et al. 2007; Du et al. 2015
	Cationic	Chitosan-poly(ethylene imine) (swelling in acidic medium)		
	Neutral	N-carboxymethyl chitosan (anionic constituent) and N-trimethyl chitosan (cationic constituent)		
Based on Degradability	Biodegradable	PLGA-PEG-PLGA, Poly(L-aspartic acid-citric acid)	Injectable hydrogels for drug delivery, wound dressings, dental implants	Qiao et al. 2005; Kumar et al. 2012; Takeda et al. 2015
	Non-biodegradable	Poly(HEMA)		

Based on Response to external stimuli	Physical	Temperature	Poly(acrylic acid-co- acrylamide), Poly(NIPAM-co-acrylamide), Poly(NIPAM-co-2-hydroxyethyl methacrylate), Poly(N-isopropylacrylamide), Poly(N,N-diethylacrylamide) (PDEAM)	Controlled drug release, self-healing material, gene delivery, bioconjugation, biomimetic actuators, bio separation, drug delivery in colon, wound dressing materials, biosensors	Schmaljohann 2006; JagadeeshBabu et al. 2011
		Light	2,6-bis(benzoxal-2-yl) pyridine and Poly(trimethylenium iminium trifluorosulfonimide) blend		Alvarez-Lorenzo et al. 2009
		Pressure	PDEAM (Poly(N,N-diethylacrylamide)), PNIPAM (Poly(N-isopropylacrylamide))		Pan et al. 2014
		Magnetic field	Poly(acrylamide) hydrogel blended with Fe_3O_4 nanoparticles		Namdeo et al. 2009
		Electric field	Polypyrrole, Polythiophene		Jeong and Gutowska 2002

	Chemical	pH	Poly(L-lysine), Poly(aspartic acid), Poly(acrylic acid), Poly(methacrylic acid (PMAA), Poly(ethylene imine), Poly(N,N-dimethyl aminoethyl methacrylamide), Poly(lactic acid), Guar-gum, Chitosan, Alginate		Park et al. 2003; Cao et al. 2009; Wang et al. 2012
		Glucose	PNIPAAm and glucose sensing moiety 3-acrylamidophenylboronic acid (AAPBA)		Matsumoto et al. 2004
		Redox	Polypyrrole, Polyaniline		Greene et al. 2017
		Ionic strength	Poly(acrylic acid)-kappa(carrageenan)		Rasool et al. 2010
	Biological	Enzyme	Poly(acrylic acid)-glycidyl methacrylate dextran (GMD)		Kim and Oh 2005
		DNA	Single stranded (ss) DNA conjugated with polyacrylamide		Murakami and Maeda 2005

		Antigen	Antigen-antibody complex entrapped in N-succinimidylacrylate hydrogel		Miyata et al. 2002

2.9.3 Stimuli-sensitive hydrogels

Stimuli-sensitive hydrogels are also called as smart hydrogels that respond to external stimuli and undergo volume phase transition and swell or shrink accordingly (Das 2013; Koetting et al. 2015). Environmental stimuli such as physical i.e., temperature, light, magnetic field, electric field and chemical i.e., pH, ionic strength, glucose, CO_2, redox and biological i.e., enzyme, antigen, DNA define the primary class of stimuli-sensitive hydrogels. Another class of hydrogels called as dual responsive hydrogels have been delevoped to combine two stimuli-responsive mechanisms into one polymeric system, for example, polyacrylic acid-co-polyvinyl sulfonic acid is a glucose sensitive hydrogel that also respond to change in pH (Kang and Bae 2003). Over the years, smart hydrogels have gained more attention due to their unique responsive nature to external stimuli. Stimuli-responsive swelling behavior of hydrogels is shown in Figure 2.10 and their mechanisms in response to stimuli is illustrated in Figure 2.11.
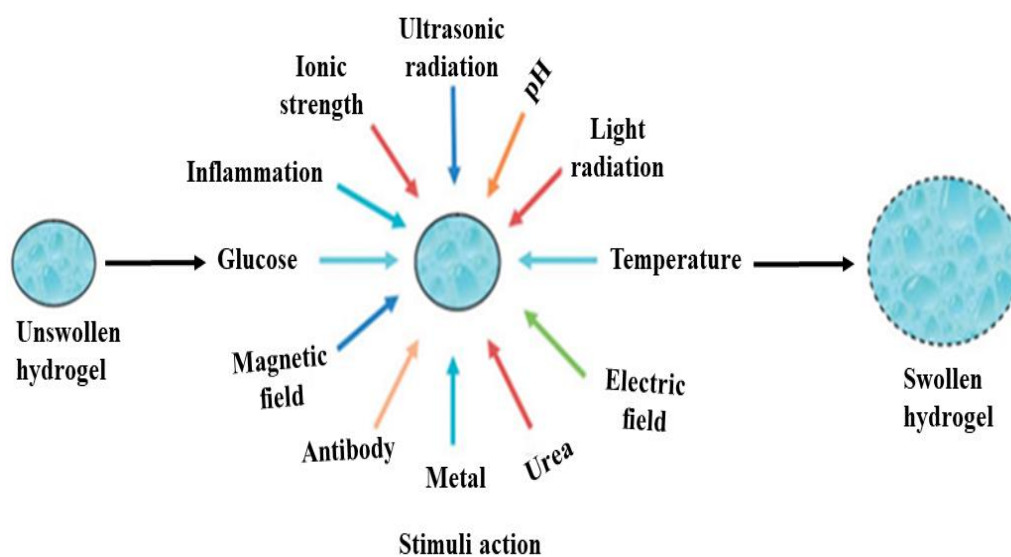
Figure 2.10 Stimuli responsive swelling behavior of hydrogel (Sood et al. 2016)

Among these smart hydrogels, pH sensitive hydrogels have shown a great importance because of their potential applications in pharmaceutical and biomedical fields such as wound healing, drug delivery, tissue engineering and biosensors.
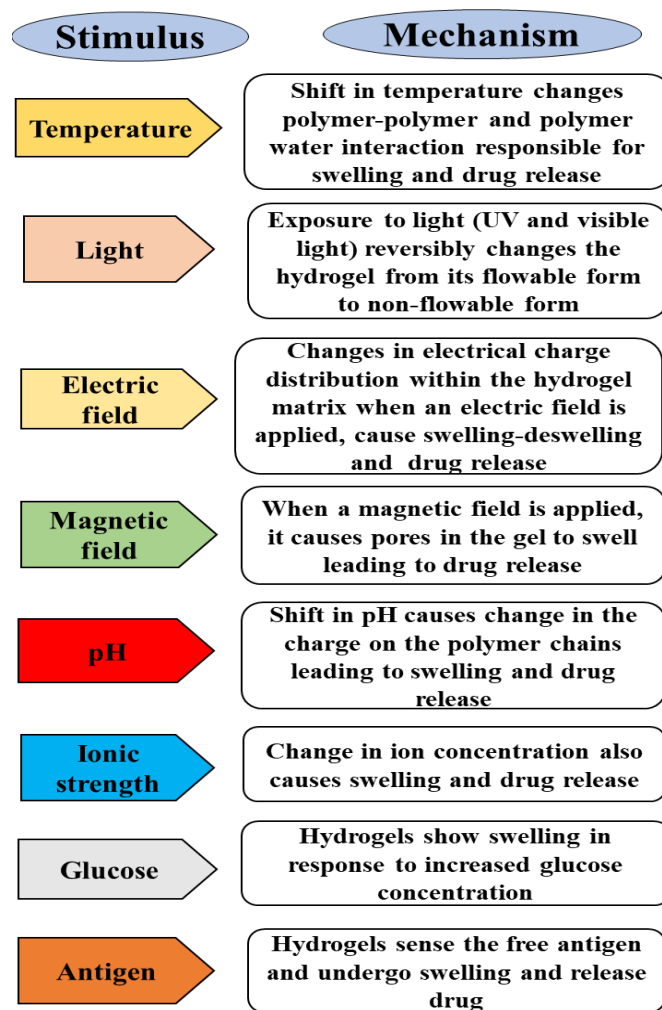
Figure 2.11 Mechanism of stimulus responsive hydrogels (Rizwan et al. 2017)

2.9.4 pH-sensitive hydrogels

pH-sensitive hydrogels are a class of stimuli responsive hydrogels that can respond to change in environmental pH and undergo abrupt volume transition or shape. These hydrogels comprise of pH-sensitive polymers having ionizable pendant groups such as acidic and basic functional groups that can donate or accept protons due to pH variation in surrounding environment (Qiu and Park 2001; Jeong and Gutowska 2002). The degree of ionization (pK_a or pK_b) is drastically changed at a particular pH in these hydrogels (Ullah et al. 2015). Owing to this, pendant groups become ionized that results in rapid change in volume of hydrogel. The electrostatic repulsive or attractive forces are generated between these ionized pendant groups which in turn produces osmotic swelling/deswelling pressure on hydrogel matrix (Peppas and Langer 1994). Based on

pendant groups present in polymer, these hydrogels are categorized as cationic hydrogels and anionic hydrogels. Hydrogels consist of cationic polymers are also known as polycations having ionizable pendant basic groups (amine groups). The ionization of these pendant groups takes place when pH of medium is less than pK_b which in turn enhances the swelling capacity of hydrogel because of electrostatic repulsion between the polymer chains. e.g. poly(4-vinylpyridine), poly(2-vinylpyridine), poly(N,N-diethylamino ethyl methacrylate) (PDEAEMA) and poly(N,N-dimethylamino ethyl methacrylate) (PDMAEMA) (Gupta et al. 2002). At low pH, basic groups present in cationic hydrogels accept protons and show swelling in acidic medium due to protonation of amine groups. Alternatively, hydrogels having anionic polymers are known as polyanions like poly(acrylic acid) (PAA), poly(methacrylic) acid (PMAA), poly(aspartic acid) (PAsp), etc. They contain pendant acidic groups (carboxylic acid and sulphonic acid) which loose protons at higher pH and show swelling in alkaline medium. When the pH of medium is greater that pK_a value, ionization of acidic pendant groups takes place leading to the swelling of hydrogel network due to electrostatic repulsion between the negative charges present in polymer chains (Jabbari and Nozari 1999; Fei et al. 2002).

2.9.4.1 Swelling/deswelling mechanism of pH-responsive hydrogels

The swelling of pH-responsive hydrogels mainly depends upon two factors (a) polymer properties like hydrophilicity, cross-linking density, ionic charge, concentration, hydrophobicity, pK_a or pK_b value of acidic and basic pendant group respectively (b) swelling medium properties like pH, counter ion and ionic strength (Ullah et al. 2015). The pH-sensitive behavior of the hydrogel network is due to the presence of ionizable pendant moieties in the polymer backbone. Due to the protonation of these pendant moieties, they form hydrogen bonds within the polymer network, as a result hydrogel stays in a collapsed state and it can retain any entrapped therapeutic payload within the polymeric matrix. When these hydrogels are exposed to an aqueous environment of an appropriate pH, ionization of these pendant groups will occur and fixed charges present on the polymer back-bone will create an electrostatic repulsive force between them. This results in the pH-dependent swelling/deswelling of the hydrogel network as the water is absorbed/expelled (Steichen et al. 2016). Small shift in pH results in desirable

change in mesh size of hydrogel matrix. Pendant acidic groups of anionic hydrogels are ionized above pK_a value of polymer matrix and un-ionized below pK_a value. This leads to swelling of hydrogel at $pH > pK_a$ due to osmotic pressure created by ions present on polymer chains. Cationic hydrogels show reverse mechanism and swell at low pH. The swelling behavior of cationic and anionic hydrogels has been described in detail in the previous section and has been summarized by Rizwan et al. (2017) as shown in Figure 2.12
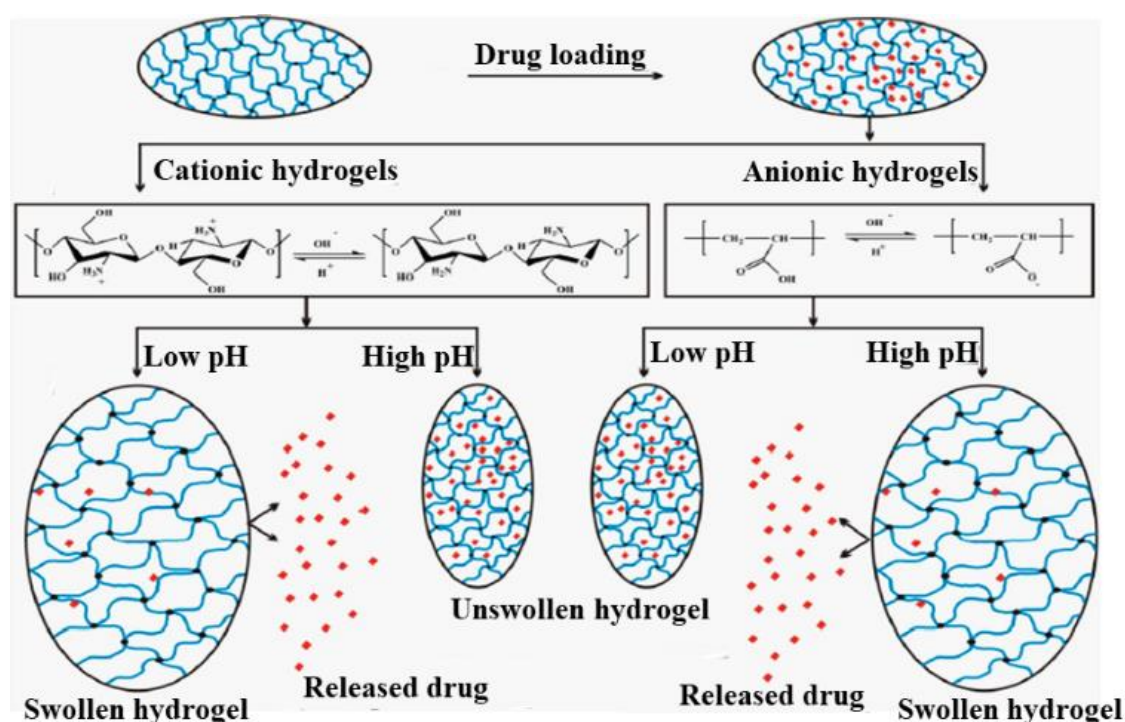
Figure 2.12 Swelling/deswelling behavior of cationic and anionic hydrogels in response to pH and released drug (Rizwan et al. 2017)

2.9.4.2 Need of pH-responsive polymer-based hydrogels as wound dressings

pH is one of the major factors which has an important role to play in the wound healing cascade. Schneider et al. (2007) demonstrated that every phase of healing process required different pH ranges. Several studies have been reported that a small variation in pH of the wound affects many factors during healing process such as angiogenesis, MMPs activity, fibroblast proliferation, bacterial toxicity and wound closure (Gethin 2007). The pH of the intact skin is 5.5 but chronic wounds have alkaline pH that lies in the range of 7.5-8. It has been reported by Robert at al. (1997) that wounds having high

alkaline pH exhibited slower healing rate as compared to wounds having pH near to neutral. Similarly, when wound proceeds towards healing process, pH of the wound surface changes from alkaline to neutral and eventually become acidic (Kaufman et al. 1985). Many efforts have contributed to reduce the pH of wound surface using topical agents such as acetic acid; but it cannot be used for longer period as it reduces pH only for one hour and does not have antimicrobial effect (Milner 1992). Recently, the use of honey has been started in dressings to change wound surface pH. It was reported that after treatment with honey significantly reduced the surface pH which in turn reduce MMPs activity, increase fibroblast proliferation and promoting wound healing (Gethin et al. 2008). In view of this, special class of stimuli sensitive hydrogels i.e., pH responsive hydrogels as wound dressings came into existence. These hydrogels have a propensity to exhibit pH-sensitive swelling behavior because of the presence of ionizable groups. Hydrogels having anionic acidic groups, such as carboxylic groups show less ionization and reduced swelling at low pH. When the pH of the medium is increased above the pK_a value, the anionic groups become more ionized leading to charge repulsion and increased swelling capacity of hydrogel (Yoshida et al. 2013). In case of chronic wounds, excess of exudate is produced because of bacterial infection and pH of wound surface shifts to alkaline. Therefore, to absorb more exudate and reduce wound surface pH; a new class of polymers are used to synthesize pH-responsive hydrogels that are known as superabsorbent polymers (SAP) (Zhao et al. 2005). Most of the commercially available SAPs prepared from petroleum derived monomers lack biocompatibility and biodegradability (Montesano et al. 2015).To overcome this, poly(amino acids) like poly(aspartic acid) PAsp, poly(lysine) and poly(glutamic acid) are used for hydrogel synthesis because of its structural similarity with protein. PAsp is a polyanion, biodegradable and water-soluble polymer that shows high swelling at alkaline pH and less swelling at acidic pH (Sharma et al. 2016). Since the polymer absorb more fluid at high pH, it causes lowering of pH in wound bed to evoke a better healing response (Sharma et al. 2017). Due to their higher absorption property, it has found applications in many fields like diaper industry, agriculture, wound dressings, tissue engineering, drug delivery, etc. (Yegappan et al. 2018; Fu et al. 2018). At present, most of the research is underway on the use of pH-responsive hydrogels as wound dressings which is mentioned in Table 2.6.

Table 2.6 List of some pH-responsive polymers-based hydrogels as wound dressings

Author (year)	pH-responsive hydrogel	Preparation method	Swelling studies	Released component	*In-vitro* studies (Antimicrobial and cytotoxicity assay)	*In-vivo* studies (Animal wound model and healing time)
Gann et al. (2009)	PVA/poly(acrylic acid)/aspirin composite	Freeze thawing (physical crosslinking)	Higher swelling in alkaline conditions	Aspirin	-	-
Tomic et al. (2010)	Poly(HEMA)/itaconic acid)	γ-irradiation	Higher swelling in pH 7.4	-	Cytotoxicity assay on L929 fibroblast cells. Antimicrobial activity against *E. coli* and *Staphylococcus aureus*	-
Tsao et al. (2011)	Chitosan/poly(γ-glutamic acid) polyelectrolyte complex	Complex formation between polymers	Swelling ratio of 959%	-	-	Full thickness excision wound model in ICR

			achieved in pH 7.4			mice. Healing time-14 days
Banerjee et al. (2012)	Poly(N-isopropylacrylamide-co-acrylic acid)	Free radical polymerization	Higher swelling in pH 7.9	BSA, EGF and VEGF	Cytotoxicity assay on human keratinocyte cells (HaCat cell).	Full thickness excision wound model in murine. Healing time-28 days
Vuković et al. (2015)	2-hydroxyethyl acrylate and itaconic acid/copper	Free radical polymerization	Maximum swelling achieved in pH 6.80	Copper	Antimicrobial activity against *E. coli*, *Staphylococcus aureus* and *Candida albicans*	-
Shi et al. (2015)	Poly(γ-glutamic acid)/silk sericin/naproxen	Mixing of polymers and crosslinked with ethylene glycol diglycidyl ether	Maximum swelling achieved in pH 7.4	Naproxen	Cytotoxicity assay on L929 mouse fibroblast cells	Full thickness excision wound model in SD rats. Healing time-15 days
Ninan et al. (2016)	Tannic acid-Carboxylated	Physical cross-linking	Higher swelling	Tannic acid	Cytotoxicity assay on NIH/3T3 mouse	-

	Agarose/Zn salts Composite		exhibited in acidic conditions		fibroblast cells. Antibacterial activity against *E. coli*	
Pamfil et al. (2017)	2-hydroxyethyl methacrylate/citr aconic anhydride-modified collagen/ciproflo xacin	Free radical polymerization	Swelling ratio of 200% achieved in pH 7.4	Ciprofloxacin	Antibacterial activity against *Staphylococcus aureus*	-
Omidi et al. (2017)	Carbon dots/chitosan	Solvent casting	-	-	Cytotoxicity assay on L929 mouse fibroblast cells. Antibacterial activity against *Staphylococcus aureus*	Full thickness excision wound model in rats. Healing time-18 days
Zhang et al. (2018b)	Chitosan/heparin /poly (γ-glutamic acid)/superoxide dismutase	Electrostatic interactions	Good swelling achieved in pH 7.4	Superoxide dismutase	Cytotoxicity assay on NIH/3T3 mouse fibroblast cells	Full thickness excision wound model in diabetic SD

						rats. Healing time-21 days with 89.8% wound closure
Qu et al. (2018)	Quaternized chitosan (QCS) and benzaldehyde-terminated Pluronic*F127	Schiff base reaction	Higher swelling achieved in pH 6	Curcumin	Cytotoxicity assay on L929 mouse fibroblast cells. Antibacterial activity against *E. coli* and *Staphylococcus aureus*	Full thickness excision wound model in female Kunming mice. Healing time-15 days
Rasool et al. (2019)	Chitosan/PVP/poly(acrylic acid)	Blending of polymers	Maximum swelling achieved in distilled water	Silver-sulfadiazine	Antibacterial activity against *E. coli*	-

Sharma et al. (2019b)	Poly(aspartic acid)/polyacrylic acid /GHK-Cu	Free radical polymerization	Higher swelling exhibited in alkaline conditions	GHK-Cu	-	Full thickness excision burn model in Wistar rats. Healing time-15 days with 84.61% wound closure
Shi et al. (2019)	Alginate/CaCO$_3$ microparticles	Microfluidic technique	Good swelling achieved in pH 7.4	Rifamycin and bFGF	Cytotoxicity assay on NIH/3T3 mouse fibroblast cells. Antibacterial activity against *Staphylococcus aureus*	Full thickness excision wound model in SD rats. Healing time-21 days

Ding et al. (2020)	Collagen/chitosan injectable hydrogel	Mixing of polymers and crosslinked with dialdehyde-terminated PEG	-	-	Antibacterial activity against *E. coli* and *Staphylococcus aureus*	Full thickness excision wound model in SD mice. Healing time-21 days with 93.1% wound closure
Ma et al. (2020)	Hydroxypropyl chitin/tannic acid/ferric ion (HPCH/TA/Fe) injectable hydrogel	Mixing of polymers in aqueous solutions	Good swelling achieved in pH 5.5 and pH 9	Tannic acid	Cytotoxicity assay on NIH/3T3 mouse fibroblast cells. Antibacterial activity against *E. coli* and *Staphylococcus aureus*	Full thickness excision wound model in female BALB/c mice and also infected with *Staphylococcus aureus*. Healing time-12days

					Cytotoxicity assay on NIH/3T3 mouse fibroblast cells. Antibacterial activity against *E. coli* and *Staphylococcus aureus*	Full thickness excision wound model in rats. Healing time- 16 days
Ren et al. (2020)	Tannic acid/keratin/graphene oxide quantum dots	Simple mixing and crosslinked with citric acid	Higher swelling achieved in pH 10	-	Cytotoxicity assay on NIH/3T3 mouse fibroblast cells. Antibacterial activity against *E. coli* and *Staphylococcus aureus*	Full thickness excision wound model in rats. Healing time- 16 days
Rezaei et al. (2021)	Silk fibroin-sodium alginate nanoparticles (SF-SANPs) embedded in PNIPAM	Desolvation method for SF-SANPs	Swelling ratio of 759.23% achieved in pH 7.4	Vancomycin and EGF	Cytotoxicity assay on L929 mouse fibroblast cells. Antibacterial activity against *Staphylococcus aureus*	Full thickness excision burn model in Wistar albino rats and also infected with MRSA. Healing time- 21 days with 91% wound closure

2.10 Natural polymers-based dressings for wound healing

Recently, naturally derived biopolymers based hydrogels have attracted researchers interest to use them for various biomedical applications due to their similarity to the extracellular matrix, non-toxicity, biodegradability, biocompatibility, ability to repair damaged tissues (Subhan et al. 2015; Pandey et al. 2017). The commonly used natural polymers (derived from animal or plant source) for the development of hydrogel as wound dressings such as collagen, chitosan, hyaluronic acid, alginate, silk, and keratin (Moura et al. 2013). The hydrogels obtained from natural polymers exhibit some limitations such as rapid biodegradation and weak mechanical strength. To overcome these limitations, many efforts have focused for the development of a new class of biomaterials named as bioartificial polymeric materials; based on combination of both natural and synthetic polymers (Giusti et al. 1994). In general, synthetic polymers such as PVA, polyurethane, poly(acrylic acid), poly(methyl methacrylate), PEG, PVP, etc. have been used for the preparation of dressing material owing to their good mechanical properties (Zine and Sinha 2017). Nevertheless, they are less biocompatible and biodegradable which limits their use in living tissues. Both these natural and synthetic polymers have their merits and demerits. Therefore, it is required to chemically modify natural polymers and blend with synthetic polymers in order to improve properties like mechanical properties, biocompatibility and prolong degradation time during healing process (Cumpstey 2013).

At present, poly(vinyl alcohol) (PVA) is one of the oldest synthetic and most frequently used polymers as in pharmaceutical industry and in biomedical engineering because of its capability to crosslink and form films without incorporation of toxic additives. The polymer is hydrophilic in nature and exhibits excellent water holding property (Pal et al. 2007). It provides adequate mechanical properties, good biocompatibility, better adhering with surrounding tissue and resist wear and fatigue. Owing to these properties, it has been applied in various biomedical applications like drug delivery systems, artificial heart surgery and wound dressings (Marin et al. 2018; Kamoun et al. 2015). While, PVA based hydrogels limit their use alone as wound dressing material because of having inadequate stiffness and elasticity. Thus, hydrogels based on PVA blended

with natural polymers such as collagen, chitosan, gelatin, hyaluronic acid, etc. are more attractive due to their good compatibility, easy for chemical modification and abundance of these polymers (Coviello et al. 2007). Amongst the known natural biopolymers, collagen represent the most promising candidate for the development of biomaterial and wound dressing materials which mimics the human skin.

2.10.1 Collagen

In 1881, the use of collagen started as a modern biomaterial when Joseph Lister and his student William Macewen stated the advantages of a biodegradable suture named as "catgut;" collagen-based biomaterial developed from small intestine of sheep (Chattopadhyay and Raines 2014). Collagen is a fibrous structural protein and it is a major component of extracellular matrix of living organisms (Marousek et al. 2015). It plays a vital role in maintaining the integrity of the biological structure, functions of various tissues (Gelse et al. 2003; Schmidt et al. 2016) and it constitutes about 25-30% of total proteins. It has a wide range of applications in many industries like leather industries, film industries, cosmetics, pharmaceuticals, biomedical and food industries (Silva et al. 2014; Singh et al. 2011; Sujithra et al. 2013). It exhibits significant properties such as high tensile strength, low antigenicity and good biocompatibility. Collagen induces coagulation of blood platelets, affects cell differentiation and contributes to wound healing (Leitinger and Hohenester 2007; Dang et al. 2017).

A total of 27 types of collagen have been identified so far and these are classified on the basis of their distribution in tissues, functions, organization and supramolecular structures (Silvipriya et al. 2015). However, the most abundant form of collagen is the type I collagen, which has triple helix structure containing three polypeptide α-chains (α1-α1-α2) of about 1000 residues and molecular weight around 300 kDa. Each α-chain composes of repeated sequence of triple (Gly-X-Y)n, where X and Y are often proline (Pro) and hydroxyproline (Hyp) as shown in Figure 2.13 (Addad et al. 2011; Yang et al. 2014). Type I collagen is found in various parts of living organisms like tissues, skin, bones, dermis, tendon, ligaments and cornea (Krishnamoorthi et al. 2017).

2.10.2 Sources

As far as the sources of collagen are concerned, mammalian collagens such as bovine and pig are the major sources of collagen for industrial applications. Since these

collagens are associated with many problems like an outbreak of bovine spongiform encephalopathy (BSE), foot-and-mouth disease (FMD) and restriction based on religion (Duan et al. 2009; Liang et al. 2014; Zhao and Chi 2009), identification of new source is highly essential.
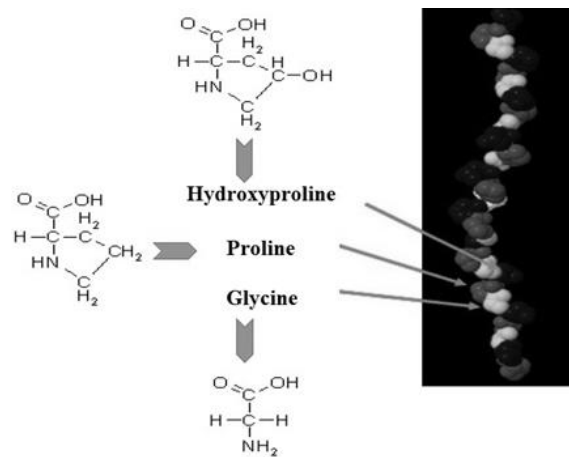
Figure 2.13 Structure of collagen (Silvipriya et al. 2015)

Marine species can be used as an alternate and safe source for the extraction of collagen, where different types of marine species have been identified like eel fish, cuttlefish, seaweed pipe fish, squid, catfish, ocellate puffer fish (Khan et al. 2009; Kołodziejska et al. 1999; Nagai et al. 2002; Shanmugam, 2012; Veeruraj et al. 2013; Zhang et al. 2009). Also, marine species have high content of collagen, less toxic and immunogenic as compared to mammalian collagens. The most important sources of collagen are skin, scales, bones and fins of fresh water and marine fish species.

Moreover, fishing industries generate about 30% of fish processing wastes comprises of skin, scale and bone which have high content of collagen and have received increasing attention as collagen sources (Wang et al. 2008a). Generally, fish skin contains a large amount of collagen which can be extracted and used (Liu et al. 2007). Eco-friendly utilization of these wastes for the extraction of collagen could be the best options for efficient waste management and production of value-added products increase the profit of fishing industries (Kittiphattanabawon et al. 2005). Nevertheless, fish collagen has several disadvantages such as poor mechanical strength, low content of amino acids, rapidly biodegradation and melting point (Subhan et al. 2015). These

problems can be overcome by combining fish collagen with other synthetic or natural polymer and by functional modification.

2.10.3 Extraction methods for collagen

The extraction of collagen from any source whether it is terrestrial or marine involves two steps: (i) pre-treatment (ii) collagen extraction. There are different methods used for extraction of collagen; depending upon the methods collagen is categorized as ASC (acid soluble collagen), PSC (pepsin soluble collagen), SSC (salt soluble collagen) and UAC (ultrasound assisted collagen). The properties and yield of extracted collagen are varied on the basis of extraction method type and source of raw material. Many researchers have reported various sources of fish collagen such as carp (*Cyprinus carpio*) (Duan et al. 2009), catla *(Catla catla)* (Pati et al. 2010), brownbanded bamboo shark (*Chiloscyllium punctatum*) (Kittiphattanabawon et al. 2010), baltic cod (*Gadus morhua*) (Sadowska and Turk 2010), amur sturgeon (*Acipenser schrenckii*) (Liang et al. 2014; Wang et al. 2014b), black carp *(Mylopharyngdon piceus)* (Wu et al. 2014), tilapia (*Oreochromis niloticus*) (Chen et al. 2016a), African catfish (*Clarias gariepinus*) and salmon *(Salmo salar)* (Tylingo et al. 2016), jelly fish (*Acromitus hardenbergi*) (Khong et al. 2017), cuttlefish (*Sepia pharaonis*) (Krishnamoorthi et al. 2017), rohu (*Labeo rohita)* and bluefin tuna (*Thunnus orientalis*) (Tanaka et al. 2018), golden carp (*Probarbus jullieni)* (Muhammed et al. 2018) and yellowfin tuna (*Thunnus albacares*) (Nurilmala et al. 2019) along with their extraction method and yield as summarized in Table 2.7.

2.10.4 Importance of collagen-based dressings for wound healing

Collagen plays an essential role in wound repair as it is key component of extracellular matrix. It provides an appropriate environment for proliferation of fibroblast that aids in wound repair process. Furthermore, collagen activates inflammatory cells to promote angiogenesis process and also binds with platelets to produce thrombin during hemostasis phase of wound healing (Vermylen et al. 1986; Sweeney et al. 2003). Usually, MMPs are important to break down the unhealthy ECM but when their levels are elevated, they degrade the native collagen leading to impaired healing process (Brett 2008). Thus, collagen in dressings act as substrate for MMPs to degrade and spared the ECM destruction (Chattopadhyay and Raines 2014). These collagen fragments are

chemotactic for migration of fibroblasts and keratinocyte cells which helps in the formation of granulation tissue and collagen synthesis (Fleck and Simman 2010). In addition, collagen-based dressings absorb excessive wound exudate and maintain moist wound environment (Brett 2008).

Table 2.7 Various fish collagen sources, extraction method, collagen type and yield obtained

Collagen extraction method	Sources	Raw material used	Yield	Type of collagen
Acid solubilization	Carp (*Cyprinus carpio*)	Skin Scales Bones	41.3% 1.35% 1.06%	Type I collagen
	Jelly fish (*Acromitus hardenbergi*)	Bell	0.09%	Type III collagen
	Cuttlefish (*Sepia pharaonis*)	Skin	1.66%	Type I collagen
	Tilapia (*Oreochromis niloticus*)	Skin Scale	27.2% 3.2%	Type I collagen
	African catfish (*Clarias gariepinus*) Salmon *(Salmo salar)* Baltic cod (*Gadus morhua*)	Skin	-	Type I collagen
	Rohu (*Labeo rohita*) Catla *(Catla catla)*	Scales	5 wt.%	Type I collagen
	Brownbanded bamboo shark (*Chiloscyllium punctatum*)	Skin	9.38% (wet wt.)	Type I collagen
	Bluefin tuna (*Thunnus orientalis*)	Skin	5.4%	Type I collagen
Salt solubilization	Amur sturgeon (*Acipenser schrenckii*)	Cartilage Muscle	2.18% 3.08%	Type I collagen
Pepsin solubilization	Rohu (*Labeo rohita*)	Swim bladder	465.2g/kg	Type I collagen
	Yellowfin tuna (*Thunnus albacares*)	Skin	22.79%	Type I collagen
	Baltic cod (*Gadus morhua*)	Backbone	-	Type I collagen
	Golden carp (*Progarbus jullieni)*	Skin	79.27%	Type I collagen
	Amur sturgeon (*Acipenser schrenckii*)	Cartilage Muscle	58.49% 55.92%	Type I collagen
	Black carp (*Mylopharyngdon piceus*)	Skin	45.7%	Type I collagen
Ultrasound assisted (with pepsin solubilization)	Golden carp (*Progarbus jullieni*)	Skin	94.88%	Type I collagen
Extrusion-hydro-extraction	Tilapia (*Oreochromis niloticus*)	Scale	49.2%	Type I collagen

There are several collagen-based wound dressings obtained from bovine animals and porcine that are commercially available such as Biobrane^{TM}, Integra^{TM}, Permacol^{TM}, Alloderm^{TM}, etc. (Shevchenko et al. 2009). Because of transmission of diseases and some religious conflicts; search for safe sources of collagen i.e., marine species are highly focused. Recently, several studies have reported to show the potential of collagen dressings for wound healing applications as represented in Table 2.8.

Table 2.8 List of collagen-based dressing materials and their application in wound healing

Author (year)	Collagen dressings		Preparation method	Biodegradation/ Swelling studies	*In-vitro* studies (Antimicrobial and cytotoxicity assay)	*In-vivo* studies (Animal wound model and healing time)
	Components of dressing	Collagen source				
Chen et al. (2008)	Collagen/cellulose nanofibrous membrane	Collagen type I from porcine tendon	Electrospinning	-	Cytotoxicity assay on NIH/3T3 mouse fibroblast cells.	Full thickness excision wound model in male SD rats. Healing time-21 days
Duman et al. (2014)	Collagen/polycapro lactone nanofibrous scaffold	Collagen type I from rat tail	Electrospinning	-	Cytotoxicity assay on HS2 human dermal keratinocyte cells	-
Song et al. (2015)	Collagen/histidine/ Ag NPs scaffold	Collagen type I (atelocollagen) from porcine	*In situ* hybridization	Completely degrade within 70 hrs	Cytotoxicity assay on L929 fibroblast cells. Antibacterial activity against *P. aeruginosa* and	Full thickness excision burn model in male SD rats and also infected with *P. aeruginosa.* Healing time-21days

					Staphylococcus aureus	
Amal et al. (2015)	Collagen/chitosan/starch/ membrane loaded with *Punica granatum* pericarp extract	Collagen type I from cobia fish skin	Casting	-	Antibacterial activity against *P. aeruginosa*	Excision wound model in Guinea pig. Healing time-25 days with 98.3% wound closure
Pal et al. (2016)	Collagen sponge	Collagen type I from mrigal fish scales	Freeze drying	Completely degrade within 18 days. Swelling ratio of 410% achieved in pH 7.4	Cytotoxicity assay on human foreskin keratinocytes and fibroblasts cells	Full thickness excision wound model in male Wistar rats. Healing time-15 days with scar
Zhou et al. (2016)	Collagen nanofibers and sponge	Collagen type I from tilapia fish skin	Electrospinning	-	Cytotoxicity assay on HaCaTs human keratinocyte cells	Full thickness incision wound model in male SD rats. Healing time-14 days with scar

					Cytotoxicity assay on NIH/3T3 mouse fibroblast cells. Antibacterial activity against *E. coli*, *P. aeruginosa* and *Staphylococcus aureus*	Full thickness excision burn model in male SD rats and also infected with *P. aeruginosa*. Healing time-21days with scar
Guo et al. (2017)	Collagen/cellulose/ curcumin/gelatin scaffold	Collagen type I from bovine tendon	Freeze drying	-		
Kandhasamy et al. (2017)	Collagen/polyhydr oxybutyrate/gelatin /ostholamide nanofibrous scaffold	Collagen type I from tail of Wistar rats	Electrospinning	Degradation of 82.4% within 24 hrs. Maximum swelling of 300% achieved in pH 7.4	Cytotoxicity assay on NIH 3T3 mouse fibroblast cells. Antibacterial activity against *E. coli*, *P. aeruginosa*, *Staphylococcus*	Full thickness incision wound model in male Wistar rats. Healing time-15 days

					aureus, *Staphylococcus epidermidis*, *Bacillus subtilis*, *Bacillus cereus*, *Micrococcus luteus* and fungal strains	
Pamfil et al. (2017)	2-hydroxyethyl methacrylate/citraconic anhydride-modified collagen/ciprofloxacin	Collagen type I and III from bovine skin	Free radical polymerization	15.31% of degradation within 72 hrs. Swelling ratio of 200% achieved in pH 7.4	Antibacterial activity against *Staphylococcus aureus*	-
Zhou et al. (2017)	Collagen/bioactive glass nanofibers	Collagen type I tilapia fish from skin	Electrospinning	-	Cytotoxicity assay on HaCaTs human keratinocyte cells, HDFs (Human	Full thickness incision wound model in male SD rats. Healing time- 14 days with scar

				dermal fibroblasts) and HUVECs (human umbilical vein endothelial cells). Antibacterial activity against *Staphylococcus aureus*	
Ge et al. (2018)	Collagen/dialdehyde xanthan gum/Ag NPs composite	Collagen type I from bovine tendon	Periodate oxidation and lyophilization	Swelling ratio of 3700% achieved in distilled water	Cytotoxicity assay on L929 mouse fibroblast cells. Antibacterial activity against *E. coli*, *P. aeruginosa* and *Staphylococcus aureus*	Full thickness incision burn model in rabbits and infected with *P. aeruginosa*. Healing time-18 days

Marin et al. (2018)	Collagen/PVA/indo methacin sponge	Collagen type I from bovine skin	Chemical crosslinking and lyophilization	Collagen:PVA (75:25) was most stable matrix while other samples degraded within 72 hrs	-	Full thickness excision burn model in female Wistar rats. Healing time-14 days
Pathan et al. (2019)	Collagen/hydroxyp ropyl methyl cellulose/curcumin nanogel	Collagen type I from catla fish scales	Nanoemulsion	-	-	Full thickness excision wound model in male Wistar albino rats. Healing time-20 days
Lukáč et al. (2019)	Collagen/gentamici n sponge	Collagen type I from *Cyprinus carpio* fish skin	Lyophilization	36% of degradation within 168 hrs. Swelling ratio of 3000% achieved in pH 7.4	Antibacterial activity against *P. aeruginosa*	Full thickness incision wound model in male Wistar rats and infected with *P. aeruginosa*. Wound healing studies were not reported; release of gentamicin from

					sponge was investigated to control infections.
Rana et al. (2020)	Amnion/collagen hydrogel + collagen/chitosan membrane	Collagen from rabbit skin	Blending of polymers and solvent evaporation	Swelling ratio ranged from 1.26-2.59	Cytotoxicity assay on brine shrimp	Full thickness excision burn model in female Wistar rats. Healing time-16 days with 72% wound closure

2.11 Wound dressings impregnated with antimicrobial agents

Wound infections happen immediately when bacteria adhere to the wound surface. Bacterial biofilm formation and high microbial burden induces excessive exudate production, which are the main causes in delaying wound healing in chronic wounds (Bowler et al. 2001; Levine et al. 1976). In early phases of chronic wound formation, *Staphylococcus aureus* (gram-positive bacteria) is major infection causing bacteria whereas in later phases, gram-negative organisms such as *P. aeruginosa and E. coli* have tendency to enter in deep layers of skin which results in tissue damage (Cardona and Wilson 2015). In past, traditional dressings such as cotton, gauze and bandages functionalized with topical antiseptic agents like povidone iodine, hydrogen peroxide, acetic acid and sodium hypochlorite solutions were used to reduce bacterial infections (White et al. 2001). These agents have broad antimicrobial spectrum but they can be detrimental to healthy tissues and ECM cell components like fibroblasts, keratinocytes which are important for wound healing (White et al. 2006). Furthermore, the usage of antibiotic drugs such as streptomycin, neomycin, ciprofloxacin, etc., in wound dressings has become popular to kill microorganisms (Pawar et al. 2013; Sinha et al. 2013). They are non-toxic and act on specific cell target but they are more prone to loss of activity due to the development of antibiotic-resistant bacteria (Lipsky and Hoey 2009). To overcome this problem, several researchers have developed polymeric antimicrobial dressings to control microbial invasion. Recently, biopolymers containing antimicrobial agents such as Ag NPs, ZnO NPs, Fe_3O_4 NPs, TiO_2 NPs, etc., have been utilized in wound dressings (Simões et al. 2018). Amongst the available nanoparticles, Ag NPs have gained significant attention due to their broad inhibitory action towards approximately 650 species of microorganisms and against antibiotic resistant strains of microbes (Zewde et al. 2016).

With the aid of nanotechnology, silver at nano scale possess significantly larger surface area to volume ratio, leading to enhanced antimicrobial activity and subsequently promote wound healing efficacy (Rath et al. 2015). Silver is used in different forms such as metal, salt, nanomaterials. Although they exhibited excellent antimicrobial efficiency however there are some reasons which limits their use in wound dressing

material. Ag NPs when incorporated within the hydrogel matrix resulted in an uncontrollable release of NPs on the wound bed which cause various toxic effects such as oxidative stress, cell apoptosis, DNA damage and also cause toxicity to human epidermal keratinocytes. But as compared to these forms, the highly anisotropic Ag NWs have the advantages in forming a percolated network when fabricated as a film or applied to a matrix. This results in the phenomenon of suppressed release of Ag NWs on wound bed but acted as barrier inside the hydrogel matrix for the entry of microbes due to sustained release of silver ions. Moreover, Ag NWs are known to be safe for humans and exhibit long-term antibacterial effect against gram positive and gram-negative bacteria. The use of Ag NWs in polymeric coatings may open a new opportunity to reduce the microorganisms infection (Jiang and Teng 2017).

2.11.1 Antimicrobial activity of silver nanomaterials impregnated dressings for wound healing applications

Silver metal and its compounds work against microbes in a number of ways and act as an efficient antimicrobial agent. Silver NPs also perform their antibacterial effect by anchoring to cell wall and generate reactive oxygen species (ROS) and toxic metal ions. Under physiological conditions, silver metal changes to silver ion and interact with negatively charged groups present in surface of bacterial cells; thereby altering permeability functions of cell wall. There is formation of pores on bacterial cell surface which leads to its disruption and also loss of inner membrane components (Sondi and Salopek-Sondi 2004). Simultaneously, silver nanoparticles can also enter the cell wall and affect metabolic pathways by inducing the production of ROS (Kim et al. 2007). Moreover, NPs interacts with phosphorus and sulphur groups of DNA, respiratory enzymes, ribosomes; thus inhibiting DNA replication, protein deactivation and ultimately cell death (Wang et al. 2017). Thus, silver metal and its compound are effective antibacterial agents and help to prevent infection of the wound. The antimicrobial action of silver nanomaterials on bacteria is depicted in Figure 2.14.

Nowadays, silver nanomaterials-based dressing materials have gained more attention in wound healing applications due to their physicochemical and antimicrobial properties against both gram-positive and gram-negative bacteria (Madhumathi et al. 2010) and also inhibit fungal infections (Gunasekaran et al. 2011). These dressings

when applied at the wound site, the Ag nanomaterials come in contact with wound exudate and become ionised. The released silver ions enter bacterial cell and damage membrane and DNA which leads to death of microorganisms (Chowdhury and Al-Jumaily 2016). Table 2.9 summarizes the different types of wound dressing materials containing silver nanomaterials as antimicrobial agents.
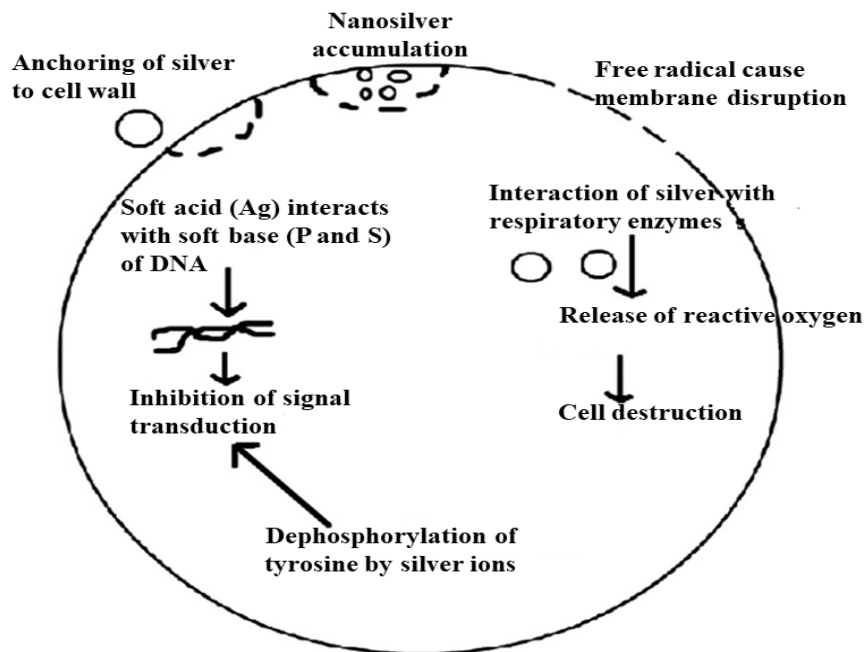
Figure 2.14 Antimicrobial action of silver nanomaterials on bacteria (Prabhu and Poulose 2012)

69

Table 2.9 List of wound dressings containing silver nanomaterials as antimicrobial agents

Author (year)	Components of dressing	Preparation method		Reducing agent for silver	Biodegradation/ Swelling studies	*In-vitro* studies (Antimicrobial and cytotoxicity assay)	*In-vivo* studies (Animal wound model and healing time)
		Wound dressing preparation	Silver nanomaterial synthesis				
Madhumathi et al. (2010)	Chitin/nanosilver composite	Lyophilization	Turkevich method	Sodium citrate	-	Cytotoxicity assay on L929 mouse fibroblast cells. Antibacterial activity against *E. coli* and *Staphylococcus aureus*	-
Anisha et al. (2013)	Chitosan/hyaluronic acid/nanosilver composite	Freeze drying	Chemical reduction	Glucose	Degradation of 30% within 336 hrs. Maximum swelling achieved in pH 7.4	Cytotoxicity assay on human dermal fibroblast (HDF) cells. Antibacterial activity against *S. aureus*, MRSA, *E. coli, K. pneumoniae* and *P. aeruginosa*	-

Boonkaew et al. (2014)	2-acrylamido-2-methylpropane sulfonic acid (AMPS)/silver nanoparticles hydrogel	Free radical polymerization	UV irradiation (Ag NPs synthesized in hydrogel)	-	Swelling ratio of 5000% achieved in pH 7.4	Cytotoxicity assay on human dermal fibroblasts (NHDF) cells and L929 mouse fibroblast cells. Antibacterial activity against *P. aeruginosa, Staphylococcus aureus* and MRSA	-
Fan et al. (2014)	Acrylic acid/graphene/Ag hydrogel	*In situ* polymerization	Chemical reduction	Glucose	Swelling ratio of 1456% achieved in pH 7.4	Cytotoxicity assay on L929 mouse fibroblast cells. Antibacterial activity against *S. epidermidis* and *E. coli*	Full thickness excision wound model in male SD rats. Healing time-15 days
Lin et al. (2016)	Commercially available silver dressings such as Aquacel® Ag (hydrofibres with ionic	-	-	-	-	Antibacterial activity against *P. aeruginosa*	Full thickness excision wound model in male SD rats and also

	silver), KoCarbonAg® (activated carbon with Ag NPs) and Acticoat 7 (rayon and silver coated polyethylene film)						infected with *P. aeruginosa.* Healing time-12 days in case of KoCarbonAg® dressing
Hashmi et al. (2017)	Chitosan/silver nanocolloids hydrogel	Blending of polymers	Biosynthesis	*Aerva javanica* plant extract	-	Cytotoxicity assay on cancerous cell lines; MCF-7, Huh-7, and HeLa cells and normal cell line; HCEC cells. Antibacterial activity against MRSA *and P. aeruginosa*	Partial thickness burn wound model in Balb/c mice infected with *P. aeruginosa* and MRSA. Healing time- 19 days
Zhang et al. (2018a)	Collagen/alginate/Ag NPs composite	Blending of polymers	Chemical reduction	NaBH$_4$	-	Cytotoxicity assay on NIH/3T3 mouse fibroblast cells. Antibacterial activity	-

					against *P. aeruginosa* and *Staphylococcus aureus*	
Goetten de Lima et al. (2018)	CMC/PVP/Agar/Ag NPs hydrogel	γ-irradiation	γ-irradiation (Ag NPs synthesized in hydrogel)	-	Swelling ratio of 400% achieved in pH 7	Cytotoxicity assay on L929 mouse fibroblast cells.	Subcutaneous incision wound model in rabbits. Healing time- 21 days
Tao et al. (2019)	Sericin/PVA/Ag NPs hydrogel	Freeze thawing	Light irradiation (Ag NPs synthesized in hydrogel)	Reduction of Ag$^+$ to Ag NPs using tyrosine residues of sericin protein	Swelling ratio of 800-850% achieved in pH 7.4	Cytotoxicity assay on NIH/3T3 mouse fibroblast cells and HEK-293 human embryonic kidney cells. Antibacterial activity against *E. coli*, *P. aeruginosa* and *Staphylococcus aureus*	Full thickness excision wound model in Wistar rats. Healing time-14 days with scar

Masood et al. (2019)	Chitosan/PEG/Ag NPs hydrogel	Blending of polymers	Chemical reduction (Ag NPs synthesized in hydrogel)	PEG	Swelling ratio of 4g/g achieved in pH 7.4	Antibacterial activity against *P. aeruginosa*, *S. aureus*, *E. coli* and B. *subtilis*	Full thickness excision wound model in diabetic rabbits. Healing time-12 days
Diniz et al. (2020)	Gelatin/alginate/Ag NPs hydrogel	Blending of polymers	Biosynthesis (Ag NPs synthesized in hydrogel)	Reduction by using gelatin and alginate	-	Cytotoxicity assay on L929 mouse fibroblast cells. Antibacterial activity against *P. aeruginosa* and *S. aureus*	Full thickness excision wound model in female Wistar rats. Healing time-14 days
Li et al. (2020)	Thiolate chitosan/Ag NWs hydrogel	Evaporation induced self-assembly	Polyol method	Glycerol	-	Cytotoxicity assay on L02 cells. Antibacterial activity against *E. coli* and *S. aureus*	Superficial skin wound model in pregnant rabbits. Healing time-14 days

Lee et al. (2021)	Chitosan/PVA/EGF/Ag$^+$ hydrogel	Emulsification and freeze thawing	Chemical reduction (Ag$^+$ synthesized in hydrogel)	-	Swelling ratio of 90% achieved in pH 7.4	Cytotoxicity assay on NIH/3T3 mouse fibroblast cells and human keratinocytes (KERTr) cells. Antibacterial activity against *S. epidermidis* and *S. aureus*	Full thickness excision wound model in diabetic SD rats. Healing time-14 days

2.12 Scope and objectives of the research work

Based on the detailed literature survey, it is clear that there is a huge need for the development of smart wound dressing material for chronic wounds to enhance wound healing process. A major portion of research work based on the potential of modern wound dressing materials that respond to pH levels is still pending and therefore will evolve as a thrust area in years ahead. Maintaining an appropriate level of wound moisture and simultaneously to reduce microbial infection in chronic wounds are the major clinical challenges in wound care management. Though, literature shows that, a lot of research is going on the development of hydrogel-based wound dressing materials that can retain the wound moisture irrespective of the wound condition. However, if the wound exudate is more and if its pH is alkaline due to bacterial infection, then the hydrogel-based wound dressing material are not successful to reduce the wound pH which enhances the MMPs activity leading to delay in wound healing process. Moreover, diabetic foot ulcers that are characterized as chronic i.e., non-healing wounds are promoted due to diabetes mellitus and leading to wound repair complications thus representing an important challenge in medical field for the development of efficient but cost-effective wound dressings. Several researchers have discussed about the applications of pH-sensitive hydrogels in drug delivery and tissue engineering. Though, there has been a dearth in literature on the development of pH-sensitive hydrogels as smart wound dressings that can respond to change in wound environment such as pH under basic or acidic conditions and results in uptake of fluid which is the main factor for regeneration of tissue.

Nevertheless, a lot of literature is available that has discussed about marine sources for collagen extraction and importance of marine collagen in non-biomedical and biomedical applications. However, only few literatures have thrown light on fish collagen-based dressings and their application in wound healing. Also, wound dressings containing nanoparticles (silver) as an antimicrobial agent are largely discussed but the use of Ag NWs in wound dressings is not studied. Keeping this research gap in mind, a pH-responsive smart wound dressing material is developed for chronic wounds to maintain an optimal exudate in response to wound pH, through which MMPs activity can be controlled and also reduce bacterial infection to achieve better healing. The aim

of the present study is to synthesize pH-sensitive hydrogel using PAsp/PVA blended with collagen and Ag NWs to enhance the wound healing process that results in scarless skin. Collagen used in this study is extracted from marine waste which can enhance healing process whereas Ag NWs act as antibacterial agent. Further, *in-vitro* studies and *in-vivo* evaluation of wound healing efficacy of smart wound dressing material in animal excision wound model are also aimed. To achieve the above-described hypothesis, following objectives are framed and executed.

1. Identification of a marine source for the extraction of collagen
   - Selection of specific marine source.
   - Extraction of collagen and its optimization.
   - Purification and characterization of collagen using SDS-PAGE, FTIR, SEM, DSC.
2. Synthesis of silver nanowires
   - Optimization of synthesis of silver nanowires.
   - Characterization of silver nanowires using SEM, DLS, XRD, FTIR.
   - Antimicrobial activity of synthesized silver nanowires.
3. Synthesis of pH-sensitive hydrogel
   - Optimization of synthesis of pH-sensitive hydrogel.
   - Characterization of hydrogel using SEM, DSC, FTIR, TGA.
4. Synthesis and characterization of wound dressing material comprising of pH sensitive hydrogel, collagen and silver nanowires
   - Optimization of wound dressing material.
   - Characterization of wound dressing material using SEM, XRD, EDAX.
5. *In-vivo* studies of synthesized wound dressing material.

2.13 Organization of the thesis

The research work carried out in this thesis is organized and divided into following chapters:

Chapter 1 presents the introduction of the thesis. This chapter deals with the background of research, the need for the study and the importance of the present study. It starts with a brief introduction about chronic wounds, hydrogels with special emphasis on pH-sensitive hydrogels, collagen and its role in wound healing and silver nanowires as an antimicrobial agent.

Chapter 2 presents an extensive review of the literature. This chapter summarizes the detailed literature review on development of wound dressings for chronic wounds with special emphasis on pH-responsive hydrogels as wound dressings with silver nanomaterials as antimicrobial agent. The research gaps are highlighted in the existing literature reports. Based on the literature review, the scope and objectives of the work are planned and presented at the end of this chapter.

Chapter 3 describes materials and methods employed for the research work as per the stated objectives of the work. The experimental procedures such as collagen extraction, silver nanowire synthesis, synthesis of smart hydrogel-based wound dressing material, animal studies are also explained in detail in this chapter.

Chapter 4 covers the results and discussion on optimization of extraction of collagen from Sole fish skin using RSM with BBD and its characterization.

Chapter 5 discusses the synthesis of silver nanowires using hydrothermal method and its characterization, the effect of process parameters on the morphology of synthesized silver nanowires. Ag NWs were also evaluated for their antibacterial and antioxidant activity.

Chapter 6 presents the results on synthesis of a pH sensitive hydrogel based on poly(aspartic acid) (PAsp), poly(vinyl alcohol) (PVA) along with collagen by free radical polymerization, the effect of operating parameters on the swelling characteristics and physical stability of the hydrogel and its characterization. The pH responsive behavior of hydrogel was also studied by varying the pH of buffer solution.

Chapter 7 describes the synthesis and characterization of pH-responsive hydrogel-based wound dressing material i.e., PAsp/PVA/Collagen hydrogel impregnated with Ag NWs and the effect of Ag NWs on the swelling characteristics and physical stability of the hydrogel. The *in-vitro* evaluation of the hydrogel was carried out by cellular toxicity test, and degradation for long-term usage. The release study of silver ions from dressing material and antibacterial activity of hydrogel loaded with Ag NWs against *E. coli* were also performed. *In-vivo* wound healing studies was assessed in full thickness excisional wound model in rats. Results were presented in the form of tables and figures wherever necessary. Detailed discussion on the results with proper justification and literature support is also presented in this chapter.

Chapter 8 summarizes the overall work outcomes and propose scope for future work in this direction.

CHAPTER 3

MATERIALS AND METHODS

3.1 Materials

Sole fish skin waste was collected from Surathkal fish market, Mangalore, Karnataka, India (12°58′50.5″N, 74°48′12.2″E). Sodium hydroxide (NaOH), sodium chloride (NaCl), butanol (99%, purity), silver nitrate (AgNO$_3$), fructose (C$_6$H$_{12}$O$_6$), L-Aspartic acid (98.5%), orthophosphoric acid (85%) were procured from Loba Chemie Pvt. Ltd., Mumbai, India and acetic acid was purchased from Merck India Ltd. Acrylamide, bis-acrylamide, Tris-HCl, SDS (sodium dodecyl sulphate), APS (ammonium persulfate, 98%), TEMED (tetramethylethylenediamine, 99%), glycerol, β-mercaptoethanol, bromophenol blue, Coomassie R-250 and poly(vinyl alcohol) (PVA) were purchased from HiMedia Laboratories Pvt. Ltd., India. Calf skin type-I collagen, pre-stained protein marker, poly(vinyl pyrrolidone) (PVP) powder (MW~40,000), DPPH (2,2-diphenyl-1-picrylhydrazyl) and cross-linker-ethylene glycol dimethacrylate (EGDMA, 98%) were purchased from Sigma-Aldrich, India. Milli-Q water was used throughout the experimentation.

3.2 Methods

The overall methodology and experimental program to achieve specific objectives within work frame of pH-sensitive hydrogel-based wound dressing material using fish-based collagen and Ag NWs as antimicrobial agent is summarized in the form of flowchart as shown in Figure 3.1.

3.3 Pre-treatment of Sole fish skin

The Sole fish skin was treated with 0.3 M NaOH in the ratio of 1/10 (w/v) to remove non-collagenous proteins. The mixture was continuously stirred for 4 hrs and NaOH solution was changed for every 60 mins. After 4 hrs of treatment, the solution was removed using cheesecloth. The treated skins were then washed with distilled water until neutral pH was attained and then the skin was defatted for 30 hrs by keeping it in a 20% butanol solvent in the ratio of 1 g in 10 mL and for every 10 hrs the butanol

solution was changed. The defatted skins were washed with distilled water until it reached neutral pH.
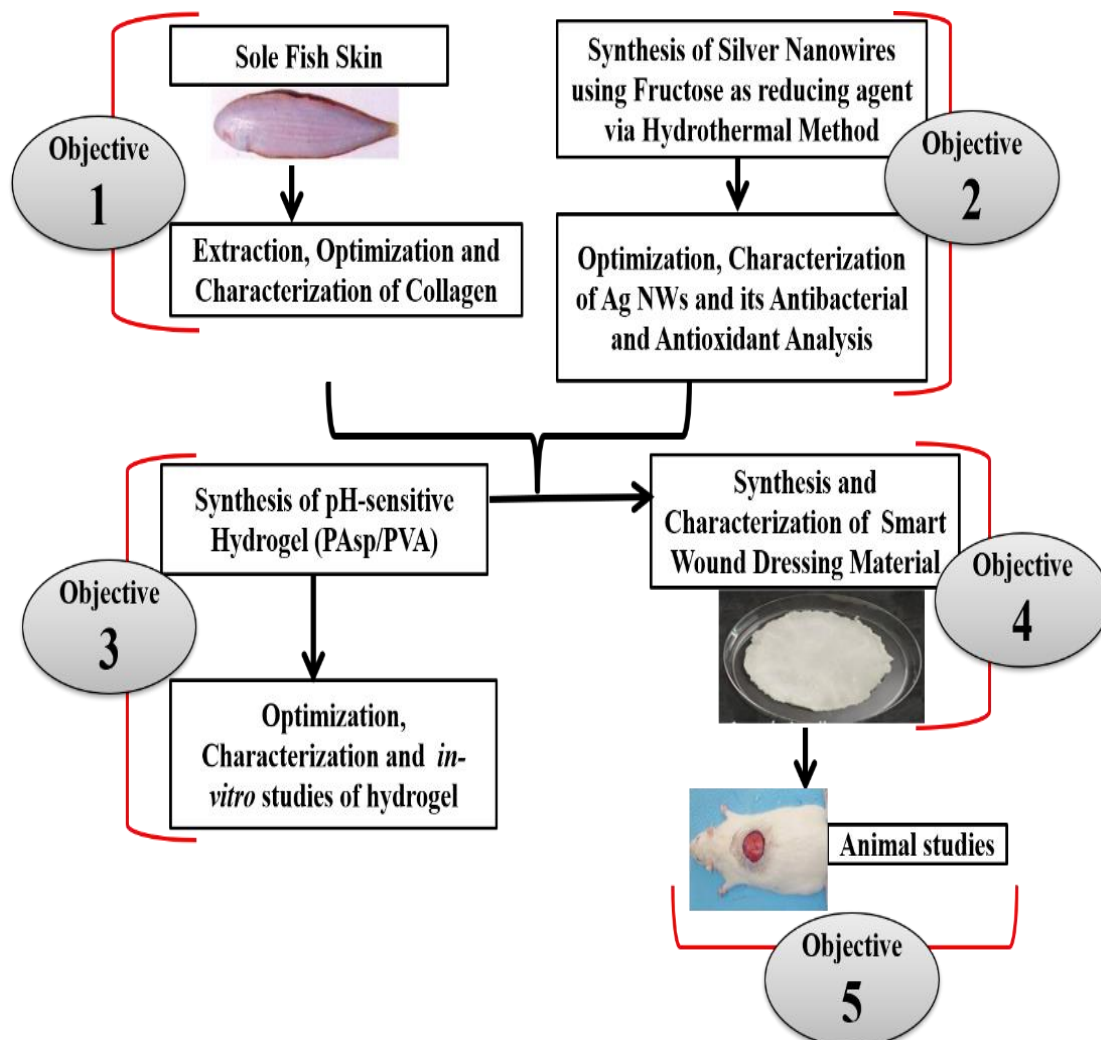
Figure 3.1 Flowchart depicting overall methodology and experimental programme

3.3.1 Extraction procedure of collagen

After the pre-treatment process, the sample was transferred to flask containing different concentrations of acetic acid. The acetic acid treated samples were filtered through four-layer cheesecloth. The filtrate was then precipitated by adding 0.05 M tris-HCl and appropriate quantity of NaCl to obtain different concentrations (0.5 M, 1.0 M, 1.5 M, 2.0 M and 2.5 M) of NaCl in the solution and the pH was adjusted using 5 M NaOH until the filtrate reached faintly basic pH. The precipitate thus obtained was centrifuged at 13,000 rpm for 40 mins. The supernatant was discarded and the pellet was collected and dissolved in a 5 mL of acetic acid solution and dialyzed against 1 litre of 0.1 M

acetic acid for 24 hrs. The samples were further dialyzed in distilled water for another 24 hrs. All these steps were performed at 10 °C (Nagai and Suzuki 2000; Nagai and Suzuki 2002; Muyonga et al. 2004; Skierka and Sadowska 2007). Schematic representation and process is depicted in the form of flowchart as shown in Figure 3.2a and Figure 3.2b.
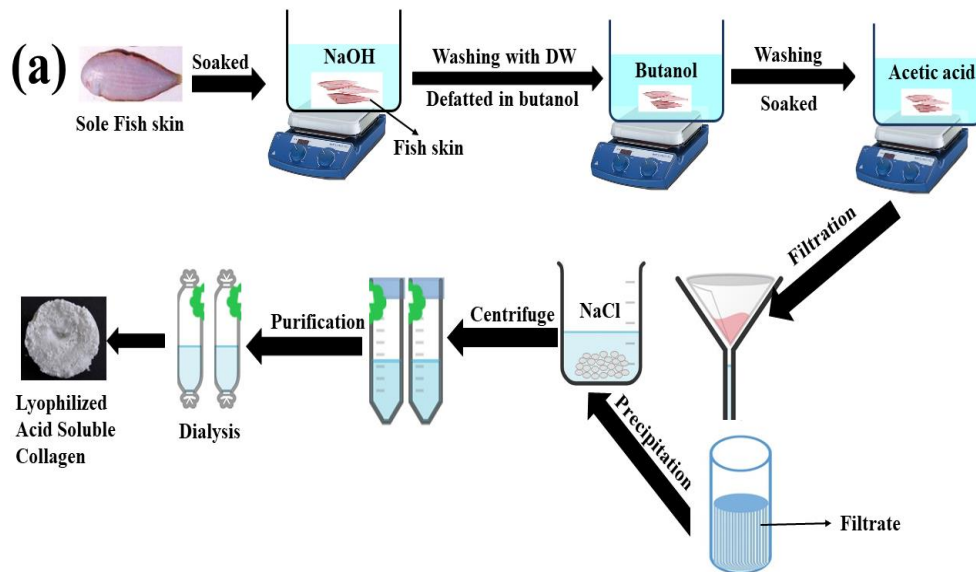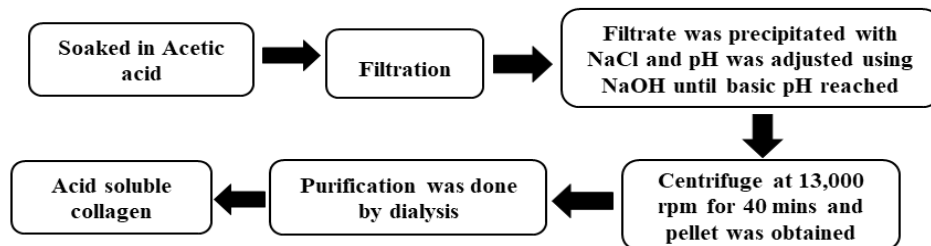
Figure 3.2 Extraction of collagen from Sole fish skin (a) Schematic representation (b) Flowchart of the process

3.3.2 Experimental study

The variables used for optimization of collagen extraction using OVAT method were acetic acid (0.2-1.0 M), NaCl (0.5-2.5 M), solvent/solid ratio (8-16 mL/g) and time (12-60 hrs). A total number of 20 single-factor experiments were performed in triplicates to determine the effect of the selected operating variables on collagen extraction. Details of reaction parameters for collagen extraction are tabulated in Appendix AI.1-4.

3.3.2.1 Response Surface Methodology

Best optimal conditions for the extraction of collagen from sole fish skin was determined by using Response Surface Methodology (RSM). RSM is a statistical tool used to build an empirical model and to find the best set of variables for the desirable response. In this work, Box Behnken Design (BBD) was employed by varying four variables at three levels (-1, 0, +1), where (0) was considered as the central point, (-1) as low level (below central point) and (+1) as high level (above central point). Independent variables and its levels are shown in the Table 3.1.

Table 3.1 Coded values and independent variables used for optimization

Independent variables	Symbols	Coded levels		
		-1	0	1
Acetic acid (M)	A	0.4	0.6	0.8
NaCl (M)	B	1.5	2.0	2.5
Solvent/solid (mL/g)	C	8	10	12
Time (hrs)	D	24	36	48

Range of these variables were decided based on the initial experiments. To evaluate the effect of independent variables i.e., A (Acetic acid), B (NaCl), C (Solvent/solid), D (Time) on collagen extraction, a design matrix of 29 runs was obtained using Box Behnken Design. Following full quadratic model expression was used to predict the optimal point.

$$Y = \beta_0 + \sum_{i=1}^{4} \beta_i x_i + \sum_{i=1}^{4} \beta_{ii} x_i^2 + \sum_{i<j}^{4} \beta_{ij} x_i x_j$$

where, Y represents the response variables, β_0 is a constant, β_i, β_{ii} and β_{ij} are the linear, quadratic and cross-product coefficients, respectively. X_i and X_j are the levels of the independent variables. The efficiency of the model was analysed using F-test and the R-test was used to determine its statistical significance. The effect of individual variables was identified by performing the detailed analysis of variance (ANOVA) on the coded level of variables. The RSM and design of experiments were done by using Design-Expert version 10.0.6.0 (Stat-Ease, Inc., Minneapolis, MN).

3.3.3 Protein estimation

Based on the modified Lowry's method, collagen yield was quantified using UV-VIS-spectrophotometer (Ultraviolet-Visible spectroscopy, Hitachi) at 650 nm (Kiew and Don, 2013). Calibration curve for pure collagen is given in Appendix AII.1. The following equation was used to calculate collagen yield:

$$\text{Yield} \left(\frac{\text{mg}}{\text{g}} \right) = \frac{\text{Concentration} \left(\frac{\text{mg}}{\text{mL}} \right) * \text{Final extracted volume (mL)}}{\text{Weight of dried skin (g)}} \qquad (3.1)$$

3.3.4 Electrophoretic analysis

4% stacking gel was prepared using 30:0.8% acrylamide: bis-acrylamide, Tris-HCl (pH 6.8), 20% SDS, 10% ammonium persulfate and TEMED. 8% separating gel was prepared using 30:0.8% acrylamide: bis-acrylamide, Tris-HCl (pH 8.8), 20% SDS, 10% ammonium persulfate and TEMED. Sample loading dye contains 25% glycine, 20% SDS, 5% β-mercaptoethanol, 0.1% bromophenol blue. After the completion of electrophoresis, gel was analysed after staining the gel in Coomassie Brilliant Blue R-250 solution. The gel was visualized with the help of Mini-PROTEAN electrophoretic system.

3.4 Hydrothermal synthesis of silver nanowires

The synthesis of Ag NWs was done by an effective and simple hydrothermal method. In this procedure, $AgNO_3$ (0.02 M, 15 mL), fructose (0.08 g, 5 mL), NaCl (0.04 M, 15 mL) and PVP (0.8 g, 5 mL) were prepared using deionized water (DI). PVP was dissolved in water which was maintained at 65 °C and the remaining solutions were prepared at room temperature. Fructose and $AgNO_3$ solutions were mixed under continuous stirring for 10 mins followed by the addition of PVP solution and then kept

under stirring for 15 to 20 mins. Then, NaCl solution was added drop-wise into the above solution under continuous stirring until it dissolved completely. The appearance of turbidity indicates the formation of the hydrosol, which is later poured into a Teflon-lining stainless-steel autoclave and placed in an oven at 160 °C for 22 hrs (Bari et al. 2016). The autoclave was allowed to air-cool and a fluffy grey white precipitate (final product) was separated from the mixture by centrifugation at 10,000 rpm for one hour. The precipitate was centrifugally washed for 3 to 4 times with deionized water/acetone at 10,000 rpm for 10 mins to remove the impurities. The final product was dried under vacuum at 60 °C and subjected for further characterization. A schematic representation and flowchart of hydrothermal synthesis of Ag NWs is shown in Figure 3.3a and Figure 3.3b. The effect of process parameters, such as temperature (120 °C-170 °C), AgNO$_3$ molarity (0.01-0.04 M), fructose concentration (0.008-0.032 g/mL), PVP concentration (0.08-0.2 g/mL) on the morphology of Ag NWs were studied and optimized using OVAT (one variable at a time) method. Ranges of variables that are optimized are tabulated in Appendix AI.5.

Hydrothermal Synthesis
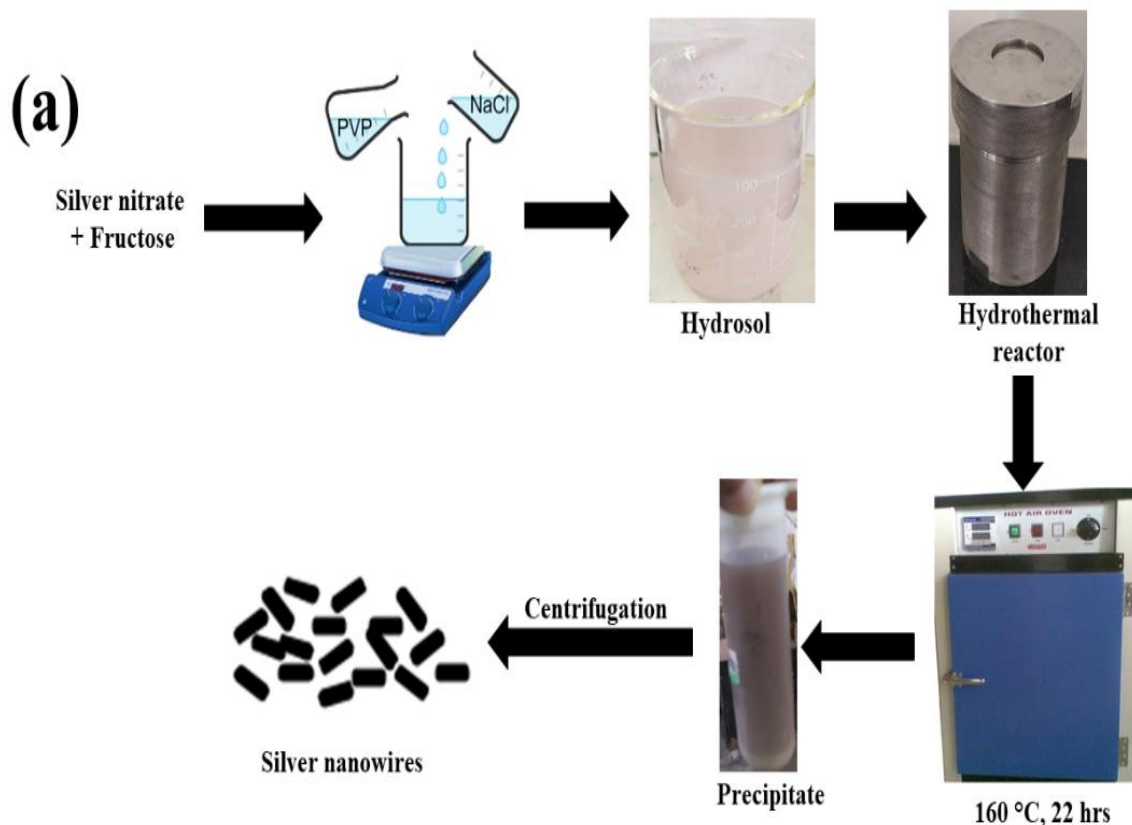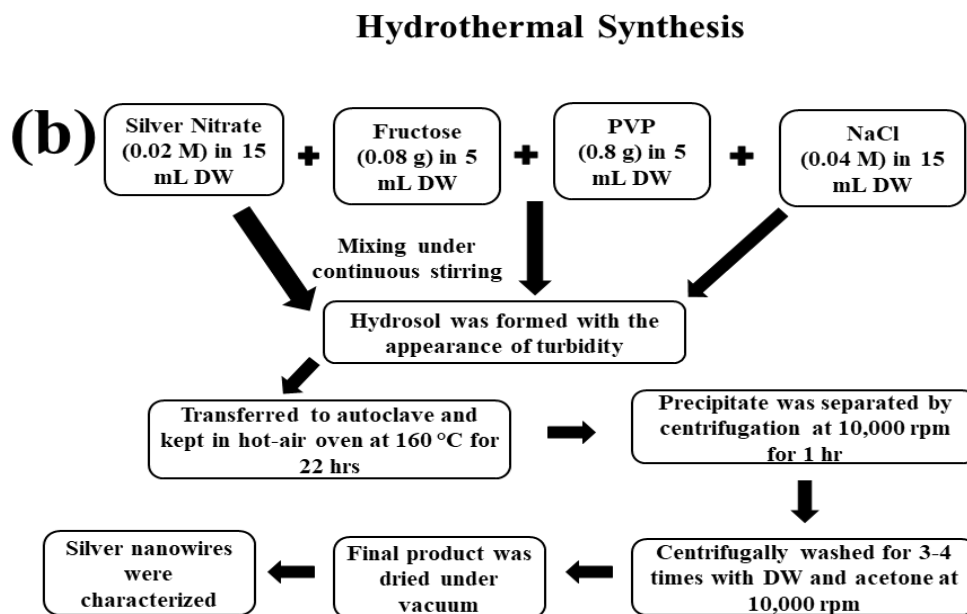
Figure 3.3 Hydrothermal synthesis of Ag NWs (a) Schematic representation (b) Flowchart of the process

3.4.1 Antibacterial analysis of silver nanowires

The antibacterial activity of the synthesized Ag NWs was estimated by minimum inhibitory concentration (MIC) method. MIC is the lowest concentration of an antibacterial agent such as Ag NWs used to inhibit the bacterial growth. Firstly, *E. coli* bacterial culture was grown by inoculating a colony of *E. coli* in Luria Bertani broth and kept at 37 °C in an incubator shaker for overnight at 150 rpm. 100 µL of overnight grown fresh bacterial culture of *E. coli* was then transferred to 5 different conical flasks containing 100 mL of sterile LB broth and various concentrations of Ag NWs (20, 40, 60, 80 and 100 µg/mL) were also added. All these flasks were kept in an incubator shaker at 37 °C for 12 hrs maintained at 150 rpm. The growth of *E. coli* was examined after 12 hrs by measuring the absorbance of the culture media at $\lambda_{max} = 600$ nm (Uddandarao and Balakrishnan 2017). Furthermore, the visible bacterial colony count approach was also used to confirm the antimicrobial activity of the Ag NWs by taking 100 mL of sterile LB broth and was inoculated with 100 µL of overnight grown fresh bacterial culture of *E. coli* and adding Ag NWs at a concentration of 80 µg/mL. A control flask without Ag NWs was also placed and these suspensions were kept for

incubation at 37 °C for 12 hrs on a rotary shaker with 150 rpm. 100 µL of bacterial suspension from the incubated flasks was serially diluted (10^{-1}, 10^{-2}, 10^{-3}, 10^{-4}, 10^{-5}, 10^{-6}, 10^{-7}, 10^{-8}) and then 50 µL of each diluted solution was spread on LB agar plate. These plates were incubated at 37 °C for 24 hrs and then no. of bacterial colonies were counted (Fellahi et al. 2013). The process flowchart of antibacterial analysis is given in Figure 3.4.
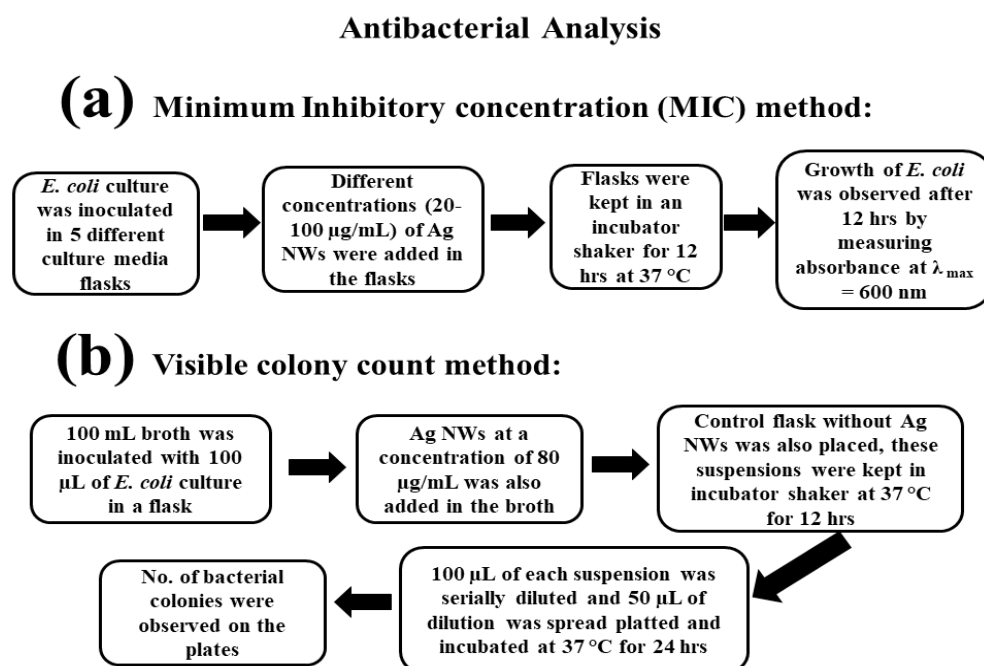
Figure 3.4 Flowchart of process of antibacterial analysis

3.4.2 Determination of Radical Scavenging Activity (DPPH)

The antioxidant activity of Ag NWs was determined using DPPH radical scavenging assay at various concentrations of Ag NWs (20, 40, 60, 80 and 100 µg/mL), which were dispersed in methanol. Then, 0.1 mM of DPPH (1 mL) was mixed with 1 mL of sample suspension followed by vigorous shaking and left in dark for 30 mins. The absorbance was measured at 517 nm using spectrophotometer and DPPH was used as a control (Murali et al. 2017). Figure 3.5 represents flowchart of antioxidant assay. The following equation was used to calculate the percentage inhibition:

$$\text{Inhibition (\%)} = \frac{A_{control} - A_{sample}}{A_{control}} \times 100 \qquad (3.2)$$

where $A_{control}$ is absorbance of control and A_{sample} is absorbance of sample.

DPPH radical scavenging assay:
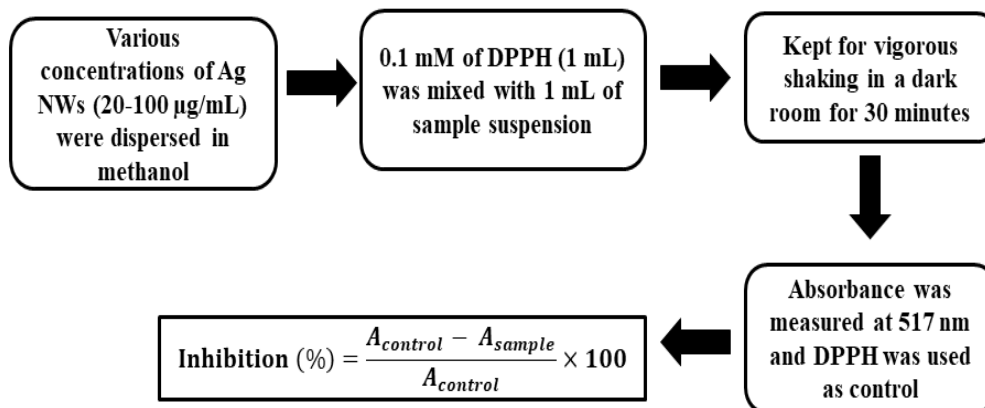
Figure 3.5 Flowchart of process of DPPH assay

$$\text{Inhibition} \ (\%) = \frac{A_{control} - A_{sample}}{A_{control}} \times 100$$

3.5 Synthesis of poly(aspartic acid) (PAsp)

PAsp was synthesized by polycondensation of aspartic acid. 5 g of L-Aspartic acid powder and 2.18 mL of o-phosphoric acid were taken in a beaker. The mixture was heated for 6 mins at 300 W microwave irradiation to obtain a yellow fluffy powder of poly(succinimide) (PSI). NaOH solution was added dropwise to hydrolyse poly(succinimide) under continuous stirring which was kept on an ice bath. The pH of reaction mixture was adjusted to 7 using 35% HCl solution. The reaction mixture was precipitated using saturated methanol and filtered using vacuum filtration (Sharma et al. 2017). The final product poly(aspartic acid) (PAsp) thus obtained was stored for further use and the schematic reaction is shown in Figure 3.6.
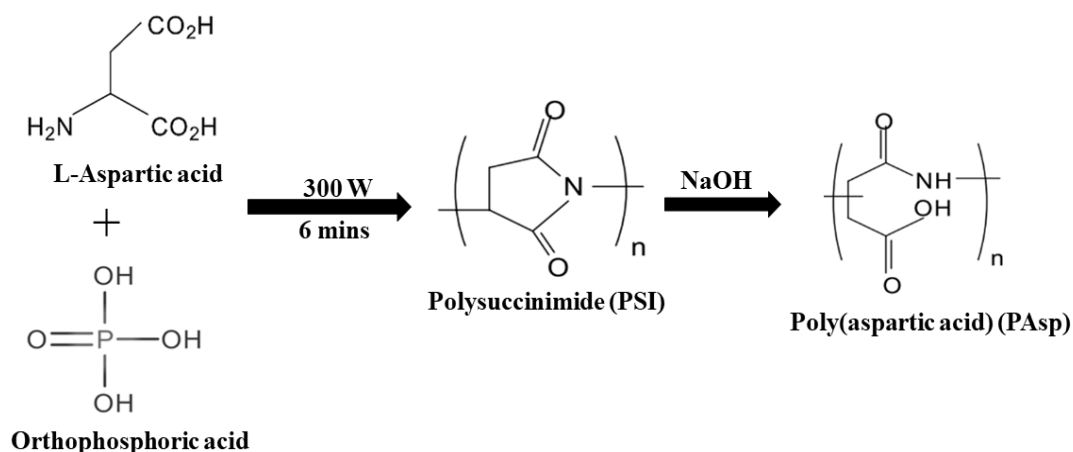
Figure 3.6 Synthesis of PAsp from L-Aspartic acid

3.6 Preparation of pH-sensitive poly(aspartic acid) (PAsp)/poly(vinyl alcohol) (PVA) hydrogel

The hydrogel was synthesized by free radical polymerization method. 100 mg PAsp was dissolved in 500 µL of water and then 2 mL of EGDMA (0.75mM) was added and stirred for 10 mins. 2 mL of PVA (8%) solution was added to the above mixture under continuous stirring. Further, 125 mg of APS (initiator) was added to the above-mentioned mixture. The reaction mixture was stirred constantly to get homogenous solution and then heated to 80 °C until the hydrogel was formed. At the end of the reaction, the synthesized hydrogels were washed with distilled water to remove the residual unreacted molecules until the neutral pH was reached. The prepared hydrogel was freeze dried and stored for further use (JagadeeshBabu et al. 2011). The effect of reaction parameters such as polymer concentration, crosslinker and initiator on hydrogel stability and swelling capacity were optimized using OVAT method which is tabulated in Appendix AI.6. The synthesized hydrogel was further analysed for its swelling behavior using gravimetric method as mentioned in section 3.9.

3.7 Preparation of PAsp/PVA/Collagen-based hydrogel

In order to obtain stable hydrogel sheet upon addition of collagen, components of optimised PAsp/PVA hydrogel (S1) were increased and further optimised on the basis of swelling studies and physical stability. PAsp (150mg) was dissolved in 750 µL of water and then 3 mL of EGDMA (0.75mM) was added under continuous stirring for 10 mins. 3 mL of PVA solution (8%) was added to the reaction mixture under constant stirring, followed by the addition of different concentrations of collagen solution (0.5 mg/mL, 1 mg/mL, 2 mg/mL, 3 mg/mL). Further, 188 mg of APS (initiator) was added to the reaction mixture and after complete mixing, the temperature of the reaction was raised to 80 °C and maintained for 30 mins. After completing the reaction, synthesized hydrogels were washed with distilled water until the water reached to neutral pH. The hydrogel was freeze dried and further analysed for its swelling behavior as given in section 3.9. The feed composition of the collagen-based hydrogel is tabulated in Appendix AI.7.

3.8 Synthesis of PAsp/PVA/Collagen impregnated with silver nanowires hydrogel-based smart wound dressing material

To prepare hydrogel sheet, PAsp (150mg) was dissolved in 750 µL of water and then 3 mL of EGDMA (0.75mM) was added under continuous stirring for 10 mins. 3 mL of PVA solution (8%) was added to the reaction mixture under constant stirring, followed by the addition of 4.5 mL of 1 mg/mL collagen solution. Further, different amounts of Ag NWs such as 2.5 mg, 5 mg and 10 mg were suspended in 500 µL of water and added to the reaction mixture. After that APS (188 mg) was added to the mixture to initiate the reaction and after complete mixing, the temperature of the reaction was raised to 80 °C and maintained for 30 mins. After completing the reaction, the synthesized hydrogels were washed with distilled water until the pH reached to neutral and then freeze dried. The schematic representation of synthesis procedure of smart wound dressing material is illustrated in Figure 3.7. Swelling behavior of hydrogel impregnated with Ag NWs was given in section 3.9. Further, hydrogel loaded with different amounts of Ag NWs were analysed for its antibacterial activity and also release study of Ag ions from hydrogel matrix which are described in section 3.8.1 and 3.8.2 respectively.
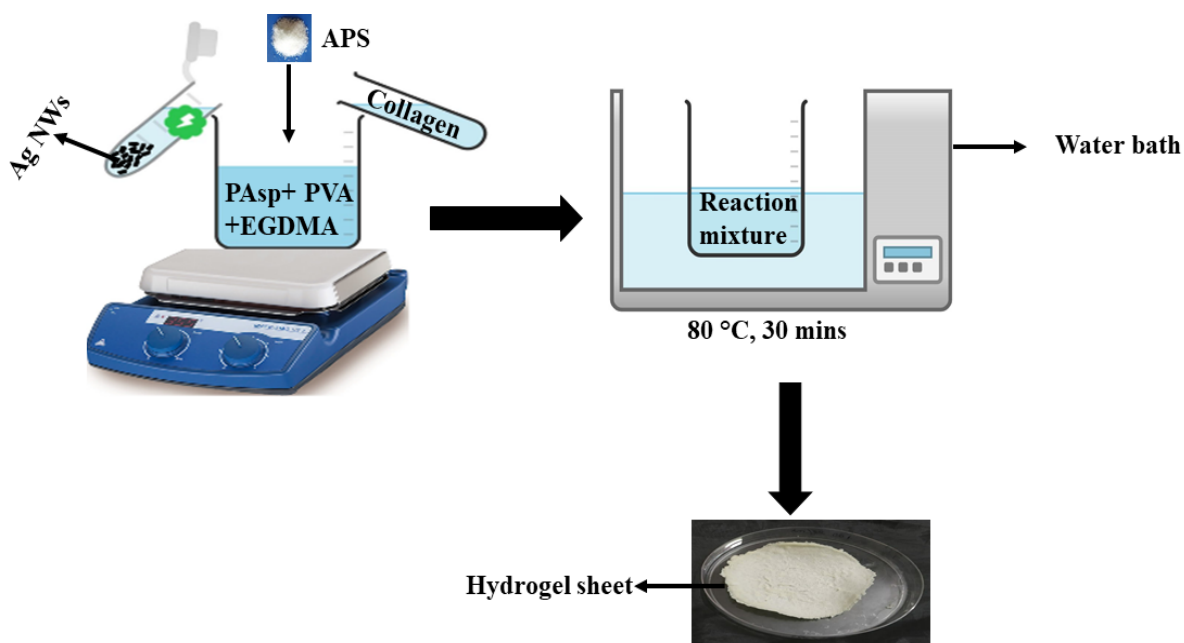
Figure 3.7 Schematic representation of preparation of PAsp/PVA/Collagen hydrogel impregnated with Ag NWs

3.8.1 Antibacterial studies of hydrogel loaded with silver nanowires

The antibacterial activity of PAsp/PVA/Collagen hydrogel (blank) and hydrogel impregnated with different amounts of Ag NWs such as 2.5 mg, 5 mg and 10 mg were evaluated against *E. coli* by colony count method. 500 µL of overnight grown fresh bacterial culture of *E. coli* was inoculated in five different conical flasks containing 25 mL of sterile Luria Bertani (LB) broth. These flasks were kept in an incubator shaker at 37 °C for 2 hrs at 150 rpm. *E. coli* growth in culture media was observed by measuring its optical density (O.D.) at 600 nm and colony forming unit per mL (CFU/mL) by colony count method (Sharma et al. 2019a). These readings were considered as initial reading before adding hydrogels. Further, blank hydrogel and hydrogel impregnated with 2.5 mg, 5 mg and 10 mg Ag NWs were UV sterilized and added in four different flasks. A control flask was placed containing untreated pure *E. coli* culture. All five flasks were incubated on a rotatory shaker for 15 hrs at 37 °C. The growth of *E. coli* was again monitored after 15 hrs with O.D. at 600 nm and CFU, which were considered as final readings. CFU was calculated using spread plate method (Masood et al. 2019). 0.1 mL aliquot of bacterial culture of each incubated flask was serially diluted (10^{-1}, 10^{-2}, 10^{-3}, 10^{-4}, 10^{-5}, 10^{-6}) and then 50 µL of each diluted solution was spread on LB agar plate (Boonkaew et al. 2014). The plates were incubated at 37 °C for 24 hrs to determine colony forming units. Difference between these initial and final readings give the actual bacteria reduction count. The following equation was used to calculate the percentage reduction in bacterial number:

$$\% \text{ bacterial reduction} = \frac{Initial\ viable\ count - Final\ viable\ count}{Initial\ viable\ count} \times 100 \qquad (3.3)$$

where initial viable count is no. of bacterial CFU before addition of hydrogel and final viable count is no. of bacterial CFU after 15 hrs incubation with hydrogel.

3.8.2 *In-vitro* release of silver ions from hydrogel

The concentration of Ag ions released from hydrogel matrix was analysed by atomic absorption spectroscopy (AAS). Hydrogel loaded with 2.5 mg, 5 mg and 10 mg Ag NWs were immersed in 15 mL of distilled water (pH 7) for 7 days or 168 hrs at 37 °C. 5 mL of immersion solution was collected after every 24 hrs and investigated for release of Ag ions from hydrogel network in distilled water. Afterwards, 5 mL of immersion

solution was replaced with fresh distilled water (Rath et al. 2015; Hiep et al. 2016; Mekkawy et al. 2017). A calibration curve was obtained by dissolving different concentrations of $AgNO_3$ solution as given in Appendix AII.2. The Ag ions content released from hydrogel was calculated from the calibration curve of $AgNO_3$ solution.

3.9 Swelling studies in different pH solutions

pH-dependent swelling behavior of the hydrogel was determined by immersing pre-weighed dry hydrogel samples (0.1 g) loaded with and without different amounts of Ag NWs (2.5 mg, 5 mg and 10 mg) in different buffer solution with different pH values ranging from 3-10. The pH of buffer solution was adjusted using 0.1 M NaOH and 0.1 M HCl solution. At predetermined time intervals, swollen hydrogels were removed and the excess water on the surface was wiped with a wet filter paper and then weighed using a weighing balance. The swelling ratio (SR) was measured at every 30 mins interval and was calculated using the following equation:

$$\text{SR (\%)} = \frac{W_t - W_o}{W_o} \times 100 \tag{3.4}$$

where W_t is the wet weight of hydrogel at time t and W_o is the dry weight of hydrogel.

3.10 *In-vitro* degradation study of hydrogel

Degradation study of prepared pH- sensitive hydrogel based wound dressing material was done to check its stability at the wound site. The degradation rate of hydrogel was determined by immersing the pre-weighed dry hydrogel samples (0.18 g) in 15 mL of phosphate buffered saline (1X PBS, pH 7.4) for 6 weeks or 42 days at 37 °C. The samples were withdrawn after definite time intervals and PBS was refreshed every week (Yang et al. 2017). Hydrogel samples were washed with distilled water, lyophilized to remove excess water and then weighed again using weighing balance. The degradation rate of hydrogel samples was estimated by gravimetric method through weight loss and was calculated as follows:

$$\text{Degradation (\%)} = \frac{W_0 - W_t}{W_o} \times 100 \tag{3.5}$$

where W_o is the initial weight of dry hydrogel before degradation and W_t is the dry weight of hydrogel at time t after degradation.

3.11 Characterization techniques

The X-ray diffraction (XRD) patterns of synthesized Ag NWs and hydrogel impregnated with Ag NWs were investigated using a X'Pert Pro X-ray Diffractometer (Rigaku mini-flex 600) operated at a current and voltage of 30 mA and 40 kV respectively with Cu Kα radiation (λ=1.5418 Å) in the range of 30°-90° (2θ). The morphological characterization of the synthesized Ag NWs and extracted collagen was done using JEOL JSM-638OLA scanning electron microscope (SEM), whereas the surface morphology of the hydrogel and hydrogel loaded with Ag NWs were analysed by field emission scanning electron microscope (FESEM; ZEISS Gemini). The samples were coated with gold film before visualization. Differential scanning calorimetry (DSC) analysis of collagen, PAsp, PVA and hydrogel samples were performed using TA instruments, Model Q150. 10 mg of sample was sealed in aluminium pans and heated at 10 °C min^{-1} from 30 °C to 600 °C and the flow rate of nitrogen was maintained at 50 mL/min. The thermal properties of collagen, PAsp, PVA and dried hydrogels were evaluated with thermogravimetric analyzer (TGA, Hitachi-6300) under the nitrogen atmosphere at a flow rate of 50 mL min^{-1}.The temperature was raised from room temperature to 600 °C at a heating rate of 10 °C min^{-1}. The particle size of aqueous dispersed Ag NWs was measured using dynamic light scattering (DLS) instrument (Horiba SZ-100) equipped with laser diode at a scattering angle of 90° in an ambience of 25 °C temperature. FTIR (Fourier transform infrared spectroscopy) was used to analyse the functional groups and the interactions between the bonds of the extracted collagen, Ag NWs, PAsp, PVA and hydrogel samples. The samples of collagen and Ag NWs were prepared using KBr (potassium bromide) pellet method and scanned between 650 and 4000 cm^{-1} wavenumbers, using FTIR instrument (Jasco FTIR-4200, Japan). While PAsp, PVA and hydrogel samples were analysed using attenuated total reflectance-Fourier transform infrared spectroscopy (ATR-FTIR; IRPrestige-21, Shimadzu). The release of Ag ions from the hydrogel matrix was monitored by atomic absorption spectroscopy (AAS-GBC 932 plus). Collagen yield was quantified using UV-VIS-spectrophotometer (Hitachi, U-2900). Energy dispersive X-ray analysis (EDAX; ZEISS Gemini) was carried out to identify the elemental composition of hydrogel and hydrogel loaded with Ag NWs.

3.12 Culturing of Cell lines

Mouse fibroblast (L929) cell lines was procured form National Centre for Cell Science (NCCS), Pune, Maharashtra, India. These cells were cultured in T-25 flasks containing Dulbecco's Modified Eagle's Medium (DMEM, Sigma, Saint Louis, MO, USA) supplemented with 10% Fetal Bovine Serum (FBS, Hyclone, Logan, UT, USA), and 1% antibiotics (streptomycin/penicillin) purchased from HiMedia, India. The cell cultures were incubated at 37 °C in a humidified incubator with 5% CO_2. The cells were observed under inverted microscope to assess the degree of confluency. When 70-80% cell confluence was attained, they should be passaged. The media was removed from culture flask and adhered cells were washed with PBS. Now, the adhered cells were rinsed with 1-2 mL of 0.2% trypsin-0.02% disodium EDTA (ethylenediaminetetra-acetic acid) solution and remnants of medium were washed off and then discarded. Furthermore, about 2 to 3 drops of 0.2% trypsin-0.02% disodium EDTA was again added to cover the cell culture plate and placed in the CO_2 incubator for about 2-5 mins. When the cells start to detach from the surface of the flask and become round in shape, sufficient volume of medium was added to the flask to neutralize the trypsin activity and draw the cell suspension into a glass or plastic pipette. Cells were counted in haemocytometer and cell concentration was adjusted with growth medium to attain a suitable cell seed density.

3.12.1 *In-vitro* cytotoxicity study of hydrogel-based smart wound dressing material
The cytotoxicity studies of hydrogel samples such as PAsp/PVA hydrogel, PAsp/PVA/Collagen hydrogel, PAsp/PVA/Collagen hydrogel loaded with 2.5 mg Ag NWs, 5 mg Ag NWs and 10 mg Ag NWs were performed on L929 cells and evaluated by Sulforhodamine B (SRB) assay (Vichai and Kirtikara 2006; Martins et al. 2015). Further, the hydrogel samples were sterilized with 70% ethanol and then immersed in 4 mL of DMEM medium for 72 hrs. The extraction medium of hydrogel samples was collected and investigated for cytotoxicity study. Cells were seeded in 96-well plate (Eppendorf Pvt. Ltd.) at a seeding density of 5000 cells per well and incubated at 37 °C for 24 hrs for cell adhesion. Subsequently, medium was replaced with different concentrations of hydrogel samples (7.81 µg/mL, 15.62 µg/mL, 31.25 µg/mL, 62.6 µg/mL, 125 µg/mL, 250 µg/mL and 500 µg/mL) and again incubated at 37 °C in a

humidified atmosphere with 5% CO_2 for 48 hrs. After the completion of incubation period, the medium was removed and 100 µL of 10% TCA (trichloroacetic acid) was added to each well and incubated for an hour at 4°C for fixation. Further, TCA was removed and the plate was washed thrice with tap water and allowed for air drying at room temperature. 100 µL of 0.057% SRB dye (prepared in 1% acetic acid) was added to each well and incubated for 30 mins in the dark at room temperature. The wells were then washed thrice with 1% acetic acid and 200 µL of Tris base (10 mM, tris (hydroxymethyl) aminomethane) solution was added to the wells and placed on the shaker for 10 mins to dissolve the dye. Absorbance was measured at 540 nm using microplate reader. The cells in culture medium deprived of any treatment were considered as negative control. The percentage of cell viability was calculated from the following equation:

$$\text{Cell viability (\%)} = \frac{A_{treated}}{A_{control}} \times 100 \qquad (3.6)$$

where $A_{treated}$ is expressed as absorbance of cells treated with hydrogel samples and $A_{control}$ is absorbance of control cells without any treatment. The results of percentage of cell viability of cells treated with hydrogel samples were compared with control which was assumed as 100%.

3.13 *In-vivo* studies

3.13.1 Animals

Healthy, adult male Sprague-Dawley (SD) rats (250-300 g) were selected for *in-vivo* studies and purchased from central animal research facility of Manipal Academy of Higher Education, Manipal, Karnataka, India. They were housed under standard environmental conditions of temperature (25 °C ± 0.5 °C) and humidity (50 ± 5%) with 12 hrs light/dark cycle. The rats were fed a standard diet of pellets and water ad libitum. Animal studies were performed in the central animal house of Kasturba Medical College, Manipal, Karnataka, India. Mandating process of experimental protocol was approved by the Institutional Animals Ethics Committee (Ref. No: IAEC/KMC/41/2020) and animal studies have been carried out in accordance with the guidelines approved by the Committee for the Purpose of Control and Supervision of Experiments on Animals (CPCSEA).

3.13.2 Full-thickness excision animal wound model

Animal studies were carried out for 16 days. On the first day of study, the rats were anesthetized using ketamine (60mg/kg). The hairs from the dorsal region of rats were shaved off and implanted site was cleaned with 70% ethanol. A full thickness excision wound with diameter of 6 mm was created on back of each rat with biopsy punch. The rats were divided into six groups with six animals in each group to examine the wound healing effect of pH-sensitive hydrogel-based dressing materials as shown below:

Group I: Negative control (NC)- Uncovered wound without any dressing (Open wound)

Group II: Positive control (PC)- Wound treated with topically applied marketed silver nitrate gel (0.2%, w/w)

Group III: Wound treated with topically applied PAsp/PVA hydrogel

Group IV: Wound treated with topically applied PAsp/PVA/Collagen hydrogel

Group V: Wound treated with topically applied PAsp/PVA/Collagen hydrogel impregnated with 2.5 mg Ag NWs

Group VI: Wound treated with topically applied PAsp/PVA/Collagen hydrogel impregnated with 5 mg Ag NWs

The wounded area was covered with these dressings as aforesaid that were latter fixed with medical tape. The dressings were changed at a regular interval of every 4th day and photographs were taken with camera. Wound size reduction was checked on 4th day, 8th day, 12th day and 16th day after wound creation. The area of wounds was measured by Image J software. The percentage of wound closure was determined by the following formula:

$$\text{Wound closure (\%)} = \frac{A_0 - A_t}{A_0} \times 100 \tag{3.7}$$

where A_0 is expressed as area of initial wound at 0th day and A_t is area of wound on the day of changing dressing i.e., 4th day, 8th day, 12th day and 16th day. The flowchart of experimental design for animal studies is shown in Figure 3.8.

3.13.3 Histological analysis

On 4th day, 8th day and 16th day, animals from each group were randomly selected and euthanized. The skin tissues around the wound area were excised for histological analysis. The removed wound samples were fixed in 10% formalin solution and then dehydration was done with increasing concentrations (50%, 70%, 90% and 100%) of

97

alcohol. After dehydration, samples were dipped in xylene to remove alcohol and then embedded in paraffin wax. Thin transverse sections of 5 µm of tissue samples were prepared using microtome and kept on glass slides. Slides were heated on hot plate to remove wax from sectioned tissue and finally the slides were dipped in xylene to clear the section.

```
                    ┌─────────────────────────┐
                    │  Sprague-Dawley Rats    │
                    └─────────────────────────┘
                                │
                                ▼
                    ┌─────────────────────────┐
                    │ Infliction of Wound: Excision │
                    └─────────────────────────┘
                                │
                                ▼
                    ┌─────────────────────────┐
                    │    Treatment Groups     │
                    └─────────────────────────┘
```

| Negative Control (Untreated) | Positive Control (Silver nitrate gel) | PAsp/PVA | PAsp/PVA/ Collagen | PAsp/PVA/Collagen with 2.5 mg Ag NWs | PAsp/PVA/Collagen with 5 mg Ag NWs |

```
                    ┌─────────────────────────┐
                    │ Procurement of Skin Samples │
                    │      Day 4, 8 and 16    │
                    └─────────────────────────┘
                                │
                                ▼
                    ┌─────────────────────────┐
                    │    Histological study   │
                    └─────────────────────────┘
```
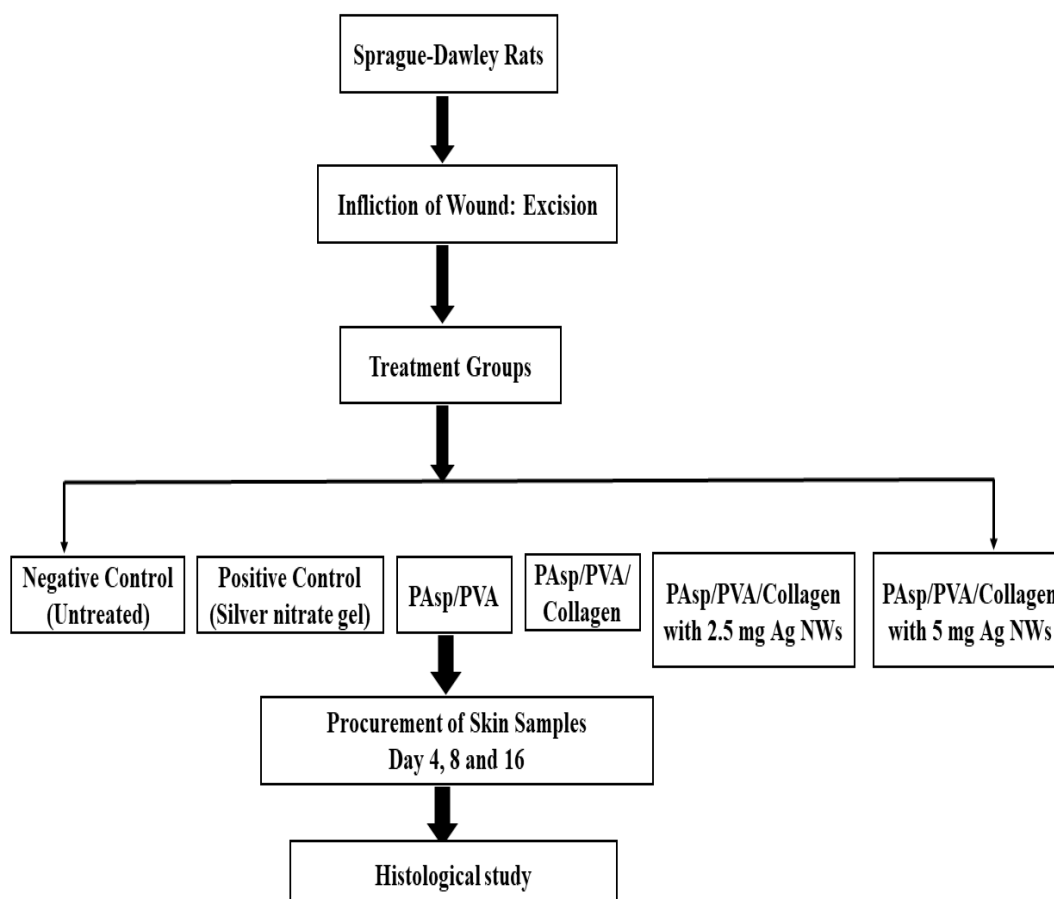
Figure 3.8 Flowchart of experimental design for *in-vivo* studies

To perform staining, the tissue sections were rehydrated using decreasing concentrations of alcohol (100%, 90%, 70% and 50%) and then dipped in water. After rehydration, sectioned tissues were stained with Hematoxylin & Eosin (H&E). Subsequently, the stained samples were examined under optical microscope for evaluating histopathological changes in dermal and epidermal regions. Histological parameters such as collagen fibre orientation, amount of granulation tissue formation, inflammation infiltration, pattern of collagen, amount of early and mature collagen were assessed while examining the tissue specimen microscopically. Healing score was

calculated by considering these histological parameters as shown in Table 3.2 (Bektas et al. 2020; Xia et al. 2020; Sultana et al. 1970).

Table 3.2 Histological parameters assessed to calculate healing score

S. No.	Histological Parameters
1.	Amount of granulation tissue (profound-1, moderate-2, scanty-3, absent-4)
2.	Inflammatory infiltrate (plenty-1, moderate-2, a few-3)
3.	Collagen fibre orientation (vertical-1, mixed-2, horizontal-3)
4.	Pattern of collagen (reticular-1, mixed-2, fascicle-3)
5.	Amount of early collagen (profound-1, moderate-2, minimal-3, absent-4)
6.	Amount of mature collagen (profound-1, moderate-2, minimal-3)

Grading of healing status:

1. Good- 16 to 19

2. Fair- 12 to 15

3. Poor- 8 to 11

3.14 Statistical analysis

The determination of wound contraction measurement; the difference between two groups were statistically analysed using GraphPad Prism software version 9.0.1.151 and two-way ANOVA and Tukey test were performed for determining significant variations in obtained results. The results were compared with negative control group and value of $P < 0.05$ was considered significant. The results were shown as mean ± SD (standard deviation).

CHAPTER 4

EXTRACTION, OPTIMIZATION AND CHARACTERIZATION OF COLLAGEN FROM SOLE FISH SKIN

4.1 Introduction

In this chapter, discussion on optimization of extraction of collagen from marine waste i.e., Sole fish skin, is presented. The extraction process was optimized by using One Variable at a Time (OVAT) approach and Response Surface Methodology (RSM) combined with Box-Behnken Design (BBD) in order to achieve maximum yield. The extracted collagen was characterized using SDS-PAGE, SEM, FTIR.

4.2 Optimization of process variables

The effect of operating variables like acetic acid (M), NaCl (M), solvent/solid ratio (mL/g) and time (hrs) on the extraction of collagen were studied by one variable at a time (OVAT) method. The detailed analysis is as follows: -

4.2.1 Effect of acetic acid on collagen extraction

The effect of acetic acid (0.2 to 1.0 M) on collagen extraction was determined while keeping the other three variables as constant (NaCl-1.0 M, solvent/solid ratio-12 mL/g, time-24 hrs). When acetic acid concentration was increased, the yield of collagen increased gradually and a maximum of 15.97 mg/g of fish skin at 0.6 M of acetic acid was obtained. Beyond 0.6 M, the collagen yield was found to reduce gradually (Wang et al. 2008b) from 0.8 M to 1.0 M because of denaturation of collagen structure which is indicated by the different collagen yield levels as shown in Figure 4.1.

4.2.2 Effect of NaCl on collagen extraction

The extraction process was carried out by salting-out method using various concentrations of NaCl ranging from 0.5 to 2.5 M. While optimising NaCl concentration, other variables like acetic acid (0.6 M), solvent/solid ratio (12 mL/g), time (24 hrs) were kept as constant. The highest yield of collagen, 17.68 mg/g of fish

skin was observed at a concentration of 2.0 M of NaCl and beyond 2.0 M, the yield of collagen decreased as shown in Figure 4.2.
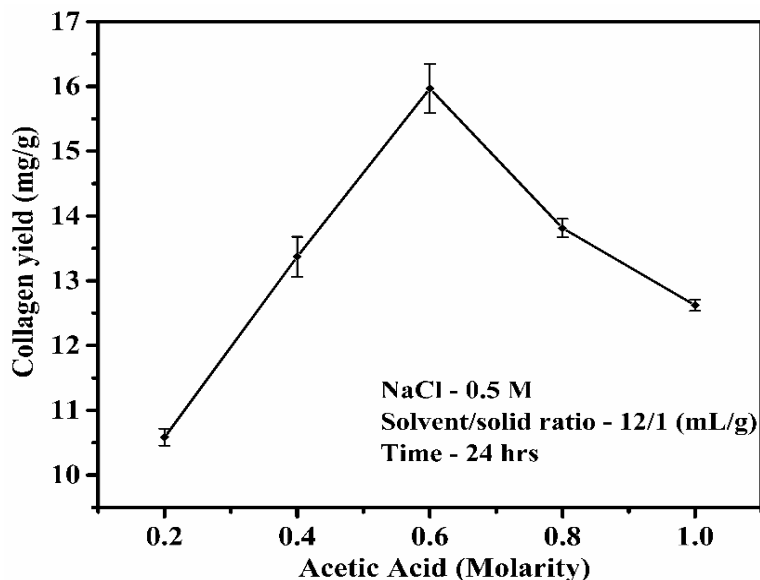
Figure 4.1 Effect of various acetic acid concentrations on collagen yield

The reduction in the yield of collagen might be due to enhanced hydrophobic-hydrophobic interaction between protein chains as a result of increased ionic strength. Thus, variation in the ionic strength would have decreased the release of collagen from skin tissues as stated by Veeruraj et al. 2013.
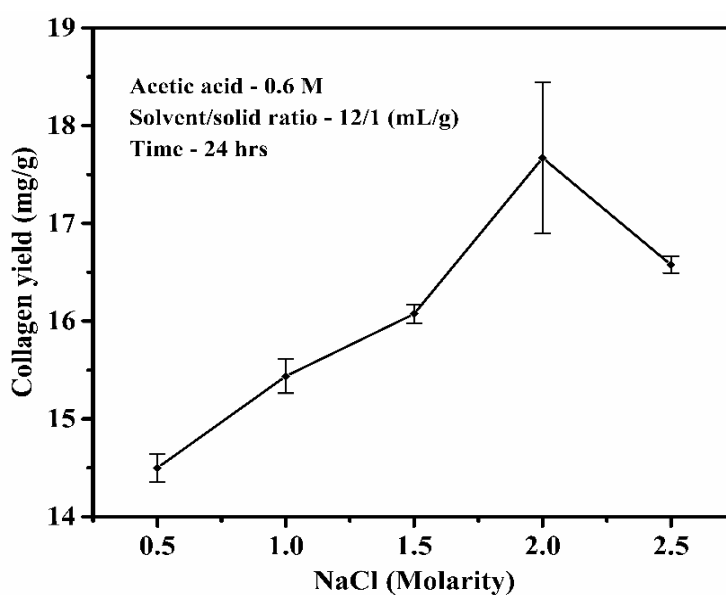
Figure 4.2 Effect of different concentrations of NaCl on collagen yield

4.2.3 Effect of solvent/solid ratio on collagen extraction

Solvent/solid ratio was optimized by performing collagen extraction process within the range of 4-12 mL/g of fish skin and keeping other variables as constant. Maximum collagen yield of 18.36 mg/g of fish skin was obtained at a solvent/solid ratio of 10 mL/g of fish skin (Kaewdang et al. 2014; Zhang et al. 2009). Figure 4.3 shows an increase in collagen yield with respect to solvent volume up to 10 mL and beyond this optimum value, the collagen yield decreased gradually due to increase in the acetic acid strength that has led to denaturation of collagen.
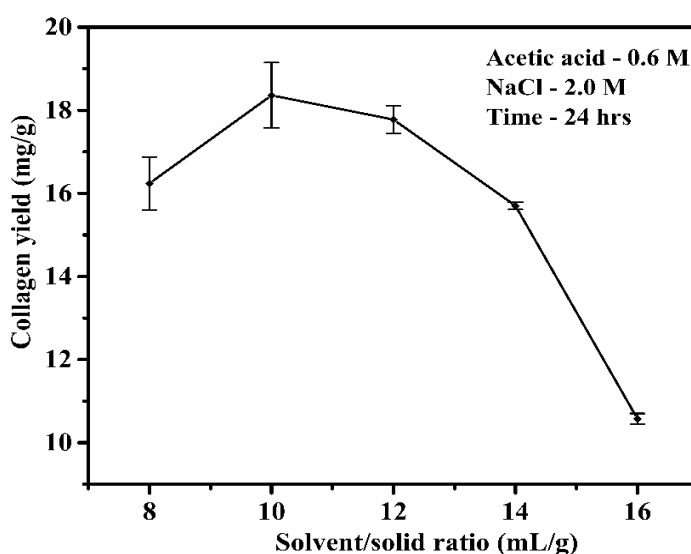
Figure 4.3 Effect of solvent/solid ratio on collagen yield (mL/g)

4.2.4 Effect of extraction time on collagen extraction

The optimization of extraction time was performed by extending the time of contact between optimum solvent and fish skin (solid) for 12 hrs to 60 hrs, keeping other variables constant (Wang et al. 2008b). The highest yield of 19.28 mg/g of fish skin was observed after 36 hrs, and beyond which a gradual decline in the collagen yield was observed due to slow degradation by acetic acid (Figure 4.4).

4.3 RSM model for collagen extraction process

A total of 29 runs and their responses using BBD experiment are shown in Table 4.1, where the collagen yield varied between 11.31 and 19.28 mg/g of fish skin. The regression model was obtained by fitting observed data using mathematical models having F-values of 2.2 (linear), 0.66 (2FI), 8.02 (cubic) and 726.66 (quadratic), where

quadratic model showed highest F-value amongst studied models. While other models showed higher p-values of 0.0899 (linear), 0.6789 (2FI), 0.0102 (cubic), the quadratic model showed a p value of < 0.0001 and it was considered as significant model.
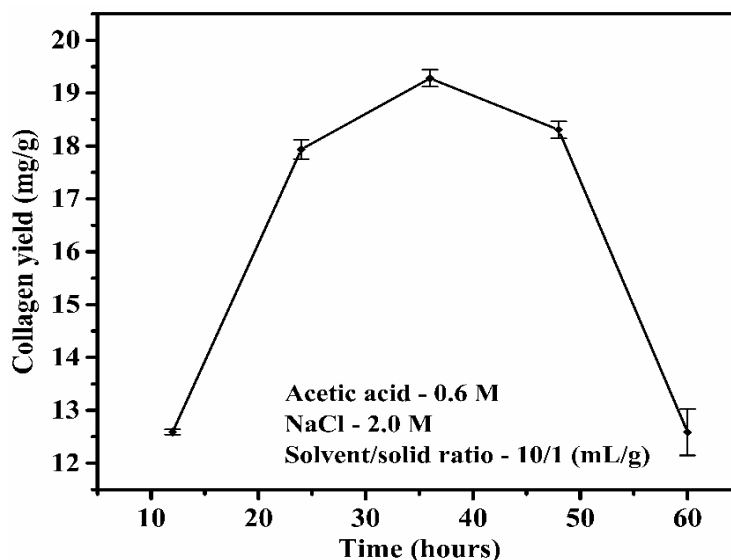
Figure 4.4 Effect of extraction time on collagen yield

Results indicate that quadratic model is the suitable model for chosen response and other models showed a significant lack of fit. The ANOVA result of quadratic model for collagen yield is provided in Table 4.2. The quadratic model has an F-value of 350.83, which indicates that the model was significant with only 0.01% chance that it could occur due to noise. In quadratic model, the significant model terms are A, B, C, D, AC, AD, BC, BD, CD, A^2, B^2, C^2, D^2. The F-value (lack of fit) of 5.84 implies that lack of fit is not significant. There is a 5.18% chance that a "Lack of Fit F-value" could be due to noise.

The equation in terms of coded factors could be used to make predictions about response for given levels of each factor. In the following equation, the levels are specified in their original units for each factor.

Coded factor

Collagen yield= +19.19 - 0.86*A + 0.21*B -1.04*C -1.20*D + 0.17*AB - 0.43*AC
           +1.03*AD - 0.57*BC + 1.71*BD - 0.48*CD - 1.87*A^2 - 1.95*B^2
           - 2.10*C^2 - 2.88*D^2

104

Table 4.1 Experimental observations of independent variable in Box-Behnken design

RUN NO.	Coded values				Collagen yield (mg/g) of fish skin	
	A	*B*	*C*	*D*	*Experimental value*	*Predicted value*
1	0.8	2.5	10	36	14.67	14.88
2	0.6	2.0	10	36	19.26	19.19
3	0.6	2.5	12	36	13.75	13.74
4	0.6	2.0	8	24	16.07	15.98
5	0.6	2.5	8	36	17.08	16.96
6	0.8	2.0	10	48	13.59	13.41
7	0.6	2.0	10	36	19.12	19.19
8	0.6	1.5	10	48	11.31	11.25
9	0.6	2.0	10	36	19.21	19.19
10	0.6	1.5	12	36	14.39	14.46
11	0.8	2.0	12	36	12.85	12.88
12	0.6	2.0	12	48	11.39	11.49
13	0.6	2.0	10	36	19.28	19.19
14	0.6	2.5	10	24	13.97	14.07
15	0.8	2.0	8	36	15.83	15.82
16	0.6	2.5	10	48	15.24	15.08
17	0.4	1.5	10	36	16.39	16.19
18	0.4	2.0	10	24	17.41	17.54
19	0.8	1.5	10	36	14.10	14.13
20	0.6	2.0	8	48	14.28	14.53
21	0.4	2.0	8	36	16.69	16.69
22	0.6	1.5	10	24	16.88	17.07
23	0.4	2.0	10	48	13.03	13.07
24	0.6	2.0	10	36	19.10	19.19
25	0.6	2.0	12	24	15.09	14.85
26	0.8	2.0	10	24	13.85	13.75
27	0.4	2.5	10	36	16.29	16.27

28	0.6	1.5	8	36	15.45	15.41
29	0.4	2.0	12	36	15.42	15.46

Table 4.2 ANOVA of response surface quadratic model

Source	Sum of Squares	Degrees of freedom	Mean Square	F Value	p-value Prob > F	Remark on significance
Model	144.04	14	10.29	350.83	< 0.0001	**Significant**
A-Acetic acid	8.91	1	8.91	303.80	< 0.0001	
B-NaCl	0.51	1	0.51	17.48	0.0009	
C-Solvent/solid	13.04	1	13.04	444.70	< 0.0001	
D-Time	17.35	1	17.35	591.68	< 0.0001	
AB	0.11	1	0.11	3.83	0.0707	
AC	0.73	1	0.73	24.93	0.0002	
AD	4.24	1	4.24	144.70	< 0.0001	
BC	1.29	1	1.29	43.93	< 0.0001	
BD	11.70	1	11.70	398.83	< 0.0001	
CD	0.91	1	0.91	31.10	< 0.0001	
A^2	22.79	1	22.79	777.16	< 0.0001	
B^2	24.65	1	24.65	840.60	< 0.0001	
C^2	28.69	1	28.69	978.42	< 0.0001	
D^2	53.64	1	53.64	1829.13	< 0.0001	
Residual	0.41	14	0.029			
Lack of Fit	0.38	10	0.038	5.84	0.0518	**Not significant**
Pure Error	0.026	4	$6.580 *10^{-3}$			
Corrected total	144.45	28				

4.3.1 Interaction of process variables

The interaction between independent variables was studied using contour plots which were drawn between two variables (A and B, A and C, A and D, B and C, B and D, and C and D), while the other variables were kept constant. All the variables used in this study showed both positive and negative effect in its quadratic terms. Figure 4.5a represents the collagen yield as a function of solvent/solid and acetic acid, while NaCl and time were kept as constant. The collagen yield first increased gradually to an optimal point of 19.19 mg/g (at solvent/solid-10 mL/g and acetic acid-0.6 M) and then decreases as both the variables were increased. A similar trend was observed in response surface plots (4.5b, 4.5c, 4.5d, 4.5e, 4.5f) drawn with the other variables.
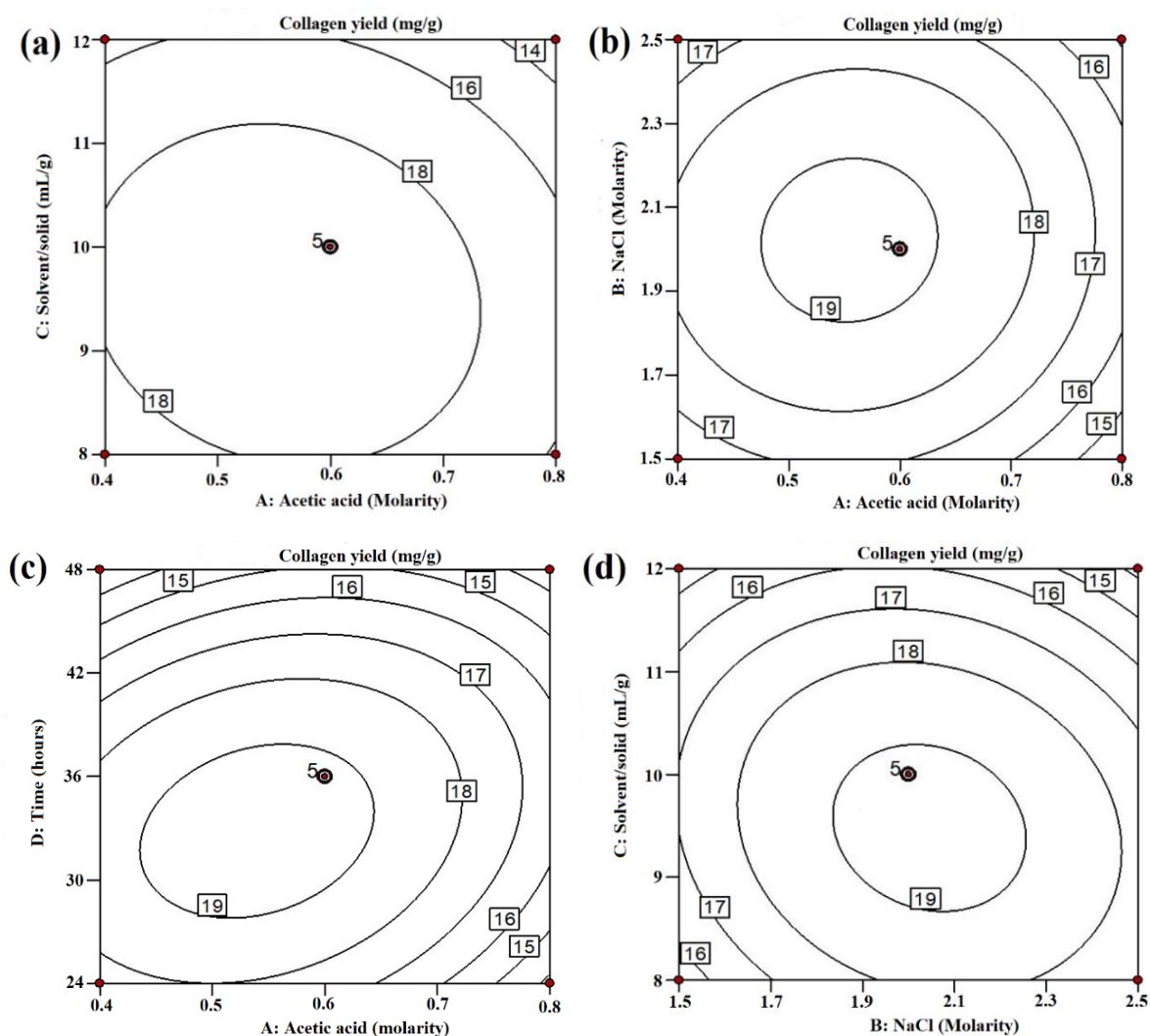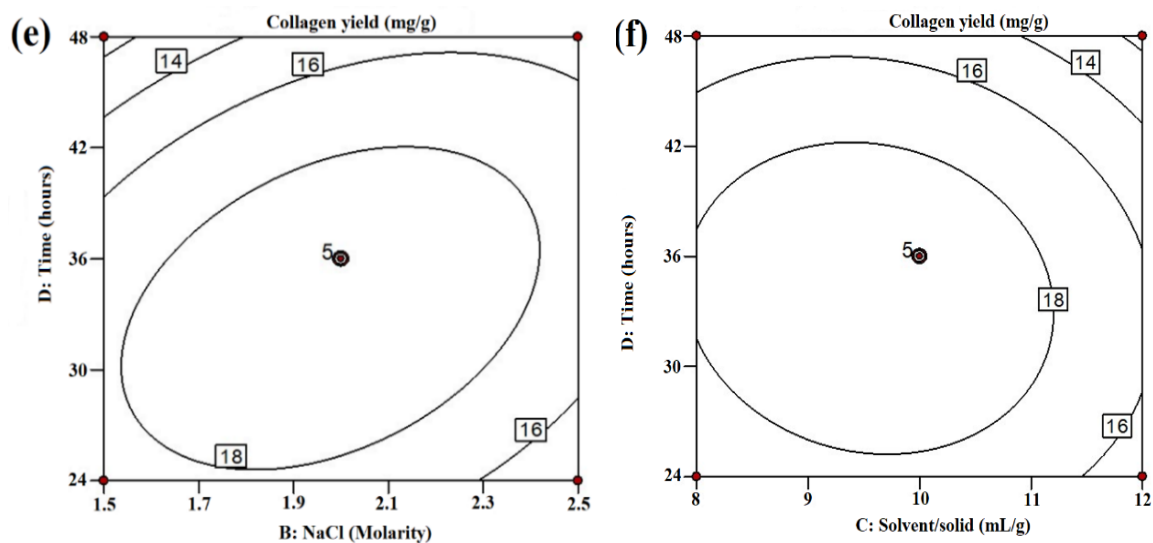
Figure 4.5 Contour plots of process variables: Influence of (a) Solvent/solid ratio and Acetic acid, (b) Acetic acid and NaCl, (c) Time and Acetic acid (d) Solvent/solid ratio and NaCl, (e) Time and NaCl and (f) Time and Solvent/solid ratio on collagen yield

The optimal yield of 19.19 mg/g was observed from contour plot at the following conditions; (1) NaCl-2.0 M & acetic acid-0.6 M (Figure 4.5b), (2) time-24 hrs & acetic acid-0.6 M (Figure 4.5c), (3) solvent/solid-10 mL/g & NaCl-2.0 M (Figure 4.5d), (4) time-24 hrs & NaCl-2.0 M (Figure 4.5e), (5) Time-24 hrs & solvent/solid-10 mL/g (Figure 4.5f).

4.3.2 Confirmatory studies for optimal conditions

RSM study was conducted to predict optimal values of acetic acid, NaCl, solvent/solid and time for the highest extraction of collagen from the Sole fish skin using lesser number of actual experiments. Based on confirmatory result as proposed by the design expert, experiments were performed using following data 0.54 M of acetic acid, 1.90 M of NaCl, 8.97 mL/g of solvent/solid and 32.32 hrs of time. A maximum yield of 19.27 ± 0.05 mg/g was achieved, using optimal response value, which is on par with the predicted yield of 19.24 mg/g.

4.4 Comparison of yield with other marine sources

As observed from Table 4.3, the yield of collagen from Sole fish skin was comparable to the yield of collagen from other marine fishes such as cuttlefish, yellow fin tuna,

Brama australis. From the table, it could be observed that from Sole fish skin we can extract highest amount of collagen next to Bigeye snapper, and Sole fish skin exhibited collagen yield similar to cuttlefish but in a relatively shorter period of time (32 hrs). In most of the cases, it can be seen that 0.5 M acetic acid and 2.0 M NaCl was used for extraction of collagen (Table 4.3). The optimum concentrations of acetic acid and NaCl used in the present study were found to be in line with literature findings for collagen extraction from other sources.

Table 4.3 Collagen extracted from various marine source with yield (%)

Sources	Part	Acetic acid (M)	NaCl (M)	Time (hrs)	Yield	Reference
Cuttlefish	Skin	0.5	0.8	72	2%	Nagai et al. 2001
Bigeye snapper	Skin	0.5	2.6	24	10.94%	Kittiphattanabawon et al. 2005
Yellowfin tuna	Swim bladder	0.5	2.6	48	1.07%	Kaewdang et al. 2014
Bramaaustralis	Skin	0.5	0.7	48	1.5%	Sionkowska et al. 2015
Sole fish	Skin	0.54	1.9	32	1.93%	Present work

4.5 Electrophoretic determination

Figure 4.6 demonstrates the result of electrophoretic analysis of Sole fish skin collagen and calf skin collagen. The lane M represents the pre-stained protein marker, while lane L1 consists of calf skin collagen and lane L2 consists of Sole fish skin collagen. α-chains in the range of 116-118 kDa and β-dimer at 200 kDa were observed on comparison of the bands of calf skin collagen and Sole fish skin collagen with the pre-stained protein marker, which were similar to the results reported by Zhang et al. (2009). From the electrophoretic analysis, the collagen present in Sole fish skin was identified as type I collagen (Skierka and Sadowska 2007; Liu et al. 2009).
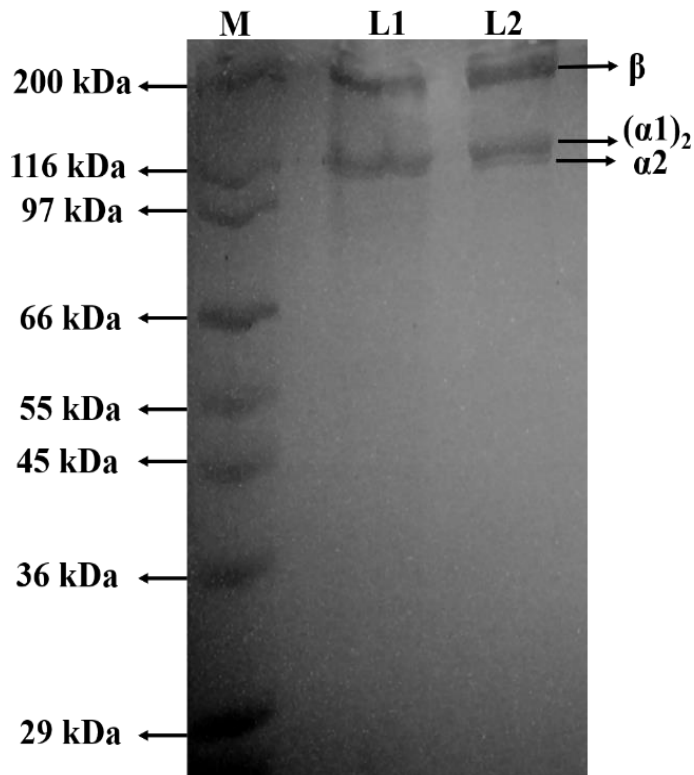
Figure 4.6 Electrophoretic comparative study pattern of collagen (M-Pre-Stained Protein Marker, L1-Type I Calf skin collagen, L2-Collagen extracted from Sole fish skin)

4.6 FTIR

The FTIR spectrum of extracted collagen from Sole fish skin is shown in Figure 4.7. Yan et al. (2008) has observed free N-H stretching vibration at 3328 cm^{-1}, but in our sample, N-H stretching vibration is shifted to 3310.21 cm^{-1} which means that hydrogen bond was shifted towards lower frequency (Duan et al. 2009; Li et al. 2004). Generally, the range of amide I band and amide II band is between 1625 and 1690 cm^{-1} and 1550-1600 cm^{-1} respectively. In this sample, the observed amide I band was around 1650.77 cm^{-1} and amide II band was shifted to a lower frequency of 1541.81 cm^{-1}, which supported the availability of hydrogen bond in the collagen. Amide III band was also present in our sample and it was observed at the wavenumber of 1238.08 cm^{-1} (Muyonga et al. 2004). The C-H stretching vibration, which usually occurs between 2854 and 1745 cm^{-1}, was observed at 2362.37 cm^{-1} (Abe and Krimm, 1972).
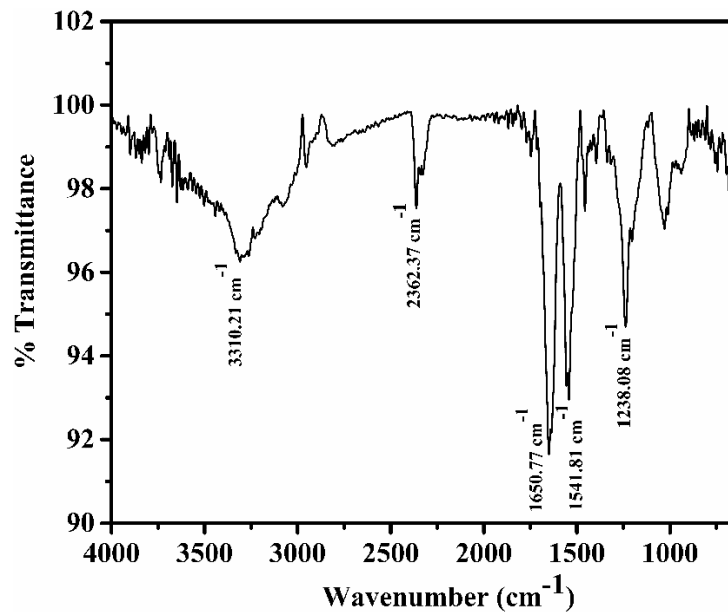
Figure 4.7 FTIR spectrum of collagen extracted from Sole fish skin

4.7 SEM

The synthesized collagen was observed under naked eye and SEM to analyze its morphology. Under naked eye (Figure 4.8a), the collagen appeared as a soft white sponge with pores on its surface. The electron micrograph (Figure 4.8b), showed random windings of coil-like structures which indicates the fibrous nature of the collagen. At higher magnification, the coil-like fibrils were found as a sheet interconnected to each other, as reported in the literature (Sankar et al. 2008; Wang et al. 2014a).
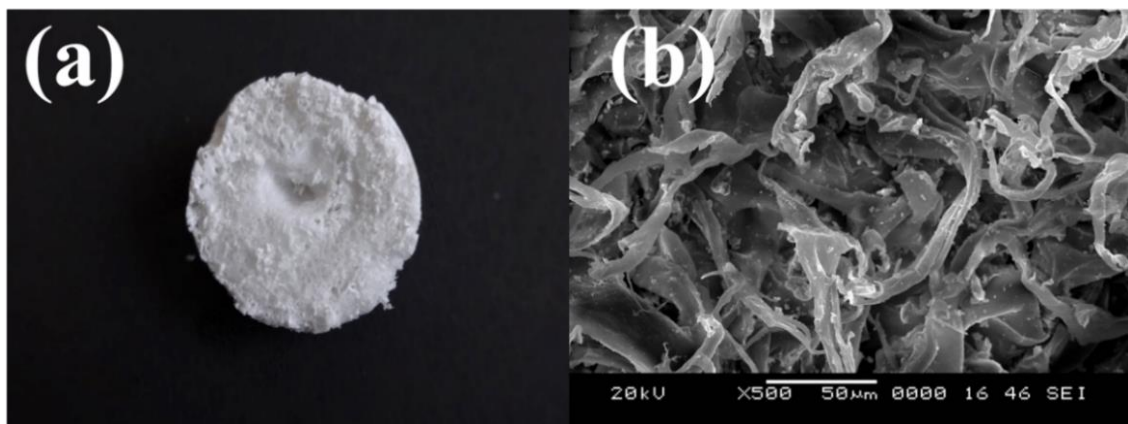
Figure 4.8 Lyophilized Sole fish skin collagen (a) as viewed in naked eye and (b) SEM micrograph

111

CHAPTER 5

SYNTHESIS OF SILVER NANOWIRES USING FRUCTOSE AS A REDUCING AGENT AND ITS ANTIBACTERIAL AND ANTIOXIDANT ANALYSIS

5.1 Introduction

In this chapter, silver nanowires were synthesized using hydrothermal method by reducing silver nitrate (AgNO$_3$) with fructose in the presence of poly(vinyl pyrrolidone) (PVP). PVP served as both capping and stabilizing agent along with sodium chloride (NaCl), which prevents the back reaction of silver ions to form precursor AgNO$_3$ and the fructose used is an eco-friendly reducing agent. The effect of parameters such as process temperature, AgNO$_3$ molarity, PVP and fructose (C$_6$H$_{12}$O$_6$) concentration on the synthesis of Ag NWs were investigated. The synthesized Ag NWs were characterised and analysed by using SEM, XRD, DLS and FTIR. Further, the antibacterial activity of Ag NWs was evaluated against *E. coli* bacterium and the antioxidant activity was also performed by DPPH method.

5.2 Optimization of the process parameters for silver nanowires synthesis

In order to optimize the process parameters one variable at a time (OVAT) method was used. The parameters used in experiments were silver nitrate concentrations, PVP, fructose and process temperature.

5.2.1 Effect of process temperature

Temperature is an important parameter in the synthesis of Ag NWs as it provides required thermal energy. SEM image (Figure 5.1) shows the effect of temperature ranging from 120 °C-170 °C on the morphology of synthesized Ag NWs. From the figure, it is found that at 120 °C, irregularly shaped silver nanoparticles (Ag NPs) were formed and this could be due to low reaction temperature which was insufficient enough to trigger selective faces for anisotropic growth of NWs. Dissolution of small Ag NPs and the diffusion of Ag atoms on the surface of Ag NWs require comparatively high temperature. As the reaction temperature was raised to 140 °C, nanoparticles start to

113

growth through a self-seeding mechanism and network like structures were formed. Increase in reaction temperature to 160 °C, enhanced formation of multiple twinned silver particles which implied production of uniform Ag NWs with high yield. Further, process temperature was increased to 170 °C which initiated number of multiple twinned nanoparticle formation in early stage of reaction because of the accessibility of excess thermal energy.
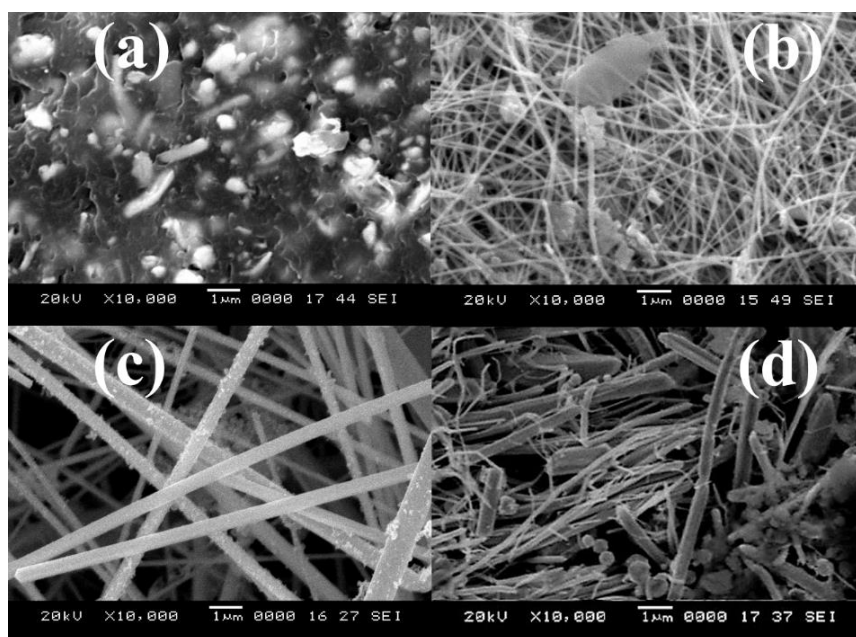
Figure 5.1 SEM images of Ag NWs grown through hydrothermal process conducted at different temperatures (a) 120 °C, (b) 140 °C, (c) 160 °C and (d) 170 °C (0.02 M $AgNO_3$, 0.016 g/mL fructose, 0.16 g/mL PVP, 0.04 M NaCl)

As a result, Ag NWs which were formed initially could able to grow up to 50 µm and later ones had low aspect ratios due to less availability of silver atoms in contrast to Ag NWs (Ostwald Ripening), similar observations were reported in the literature (Coskun et al. 2011). Thus, nanowires obtained at the optimum temperature of 160 °C was used for further analysis.

5.2.2 Effect of $AgNO_3$ concentration

$AgNO_3$ serves as a precursor and its concentration plays a vital role for the morphology and yield of Ag NWs. In this study, $AgNO_3$ concentration was varied (0.01 M, 0.02 M, 0.03 M, 0.04 M) while all the other process parameters remained constant. Figure 5.2 represents SEM images of the Ag NWs synthesized at various $AgNO_3$ concentrations.

114

From the figure it could be observed that at 0.04 M and 0.01 M AgNO$_3$ concentration, spherical shaped nanoparticles were obtained. At the lowest concentration of AgNO$_3$ i.e., (0.01 M) non-uniform Ag NWs along with nanoparticles and aggregates were observed. When 0.02 M AgNO$_3$ concentration was used, a uniform Ag NWs having small diameter with high aspect ratio were observed (Figure 5.2b). For 0.03 M AgNO$_3$ concentration a mixture of nanoparticles and Ag NWs having large diameter with low aspect ratio was observed (Figure 5.2c). Further increase in the concentration of AgNO$_3$ to 0.04 M has resulted in more nanoparticles rather than nanowires (Gebeyehu et al. 2017). It is evident from the results that 0.02 M AgNO$_3$ could produce perfect nanowires with smaller diameter and high aspect ratio. Thus, for further analysis 0.02 M AgNO$_3$ was used.
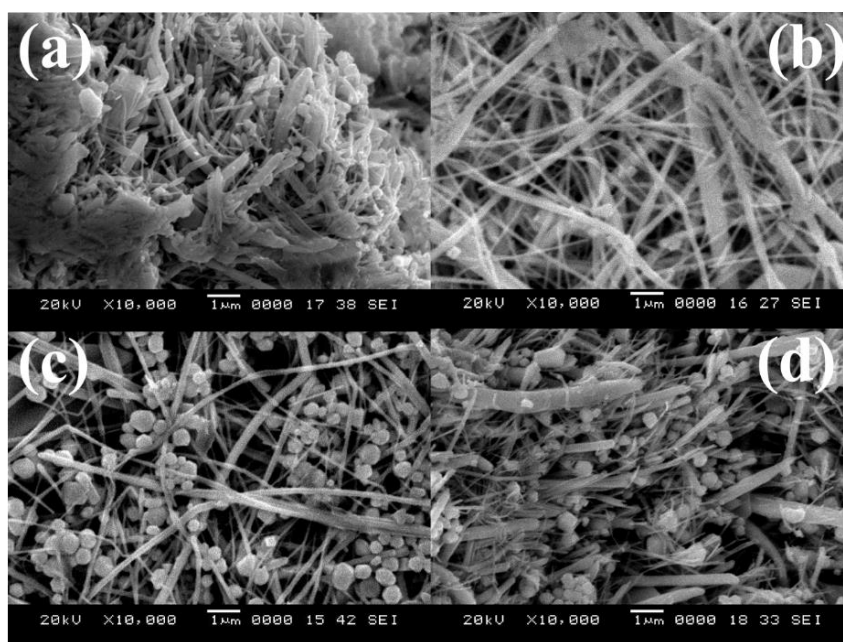
Figure 5.2 SEM images of Ag NWs synthesized at different molarities of AgNO$_3$ (a) 0.01 M, (b) 0.02 M, (c) 0.03 M and (d) 0.04 M (0.016 g/mL fructose, 0.16 g/mL PVP, 0.04 M NaCl, 160 °C temperature)

5.2.3 Effect of fructose concentration

Fructose is a soft reducing agent and plays an essential role in the formation of Ag NWs. In order to find optimum fructose concentration, different concentrations of fructose (0.008-0.032 g/mL) were used. Figure 5.3 displays SEM images of Ag NWs synthesized using different concentration of fructose. From SEM analysis, it was found

that uniform shaped Ag NWs were obtained at 0.016 g/mL fructose concentration. Increase in the fructose concentration has decreased average size of Ag NWs and this could be due to increase in rate of reaction which could have generated more nuclei and could have enhanced the lateral growth of wires in a relatively short period of time. Thus beyond 0.016 g/mL, in each silver NW lateral growth was observed on the surface of silver NW. However, lower concentrations of fructose have resulted in uneven thickness and shape of NWs (Figure 5.3a). Similarly, Wang et al. (2015) reported the formation of aggregates when low concentrations of glucose was used in the synthesis of Ag NWs.
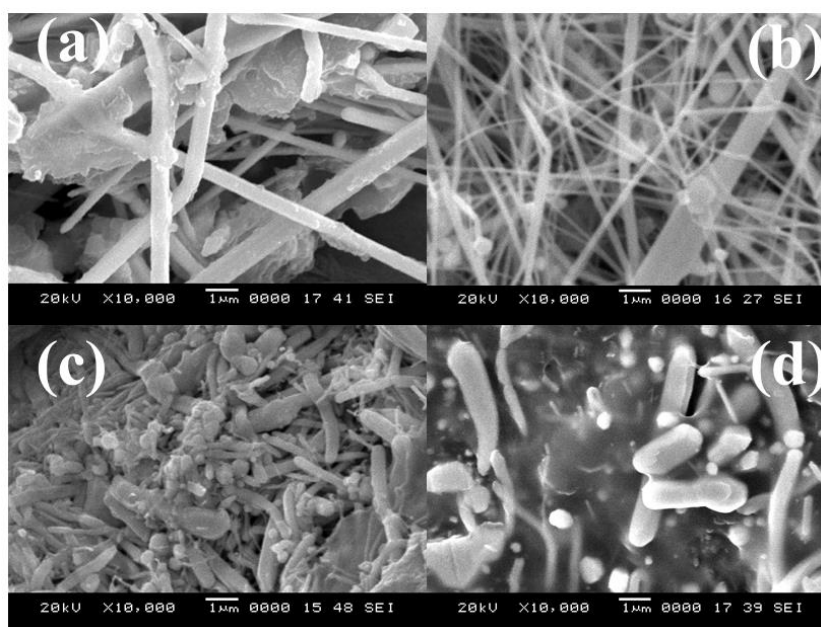
Figure 5.3 SEM images of Ag NWs synthesized at different fructose concentrations (a) 0.008 g/mL (b) 0.016 g/mL (c) 0.024 g/mL (d) 0.032 g/mL (0.02 M AgNO$_3$, 0.16 g/mL PVP, 0.04 M NaCl, 160 °C temperature)

5.2.4 Effect of PVP concentration

The morphology of Ag NWs depends on PVP concentration (0.08-0.2 g/mL). At lower PVP concentration, the prepared Ag NWs had non-uniform morphology with larger diameters. The multiple twin particles which were not able to grow into nanowires, lead to formation of micro-sized agglomerates in huge amounts. As PVP concentration increased to 0.16 g/mL, the diameter of nanowires decreased gradually and the

morphology was uniform with large aspect ratio of Ag NWs obtained as shown in Figure 5.4.
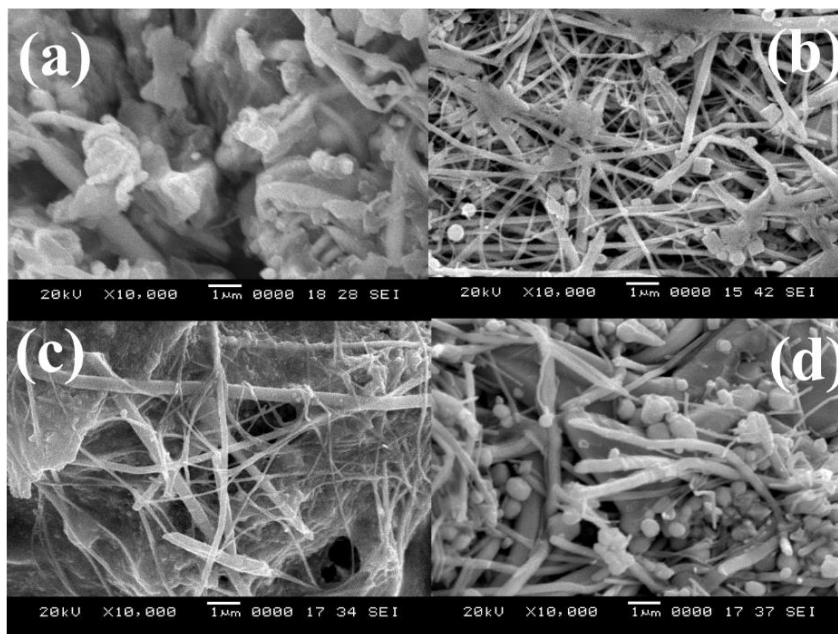
Figure 5.4 SEM images of Ag NWs synthesized at different PVP concentrations (a) 0.08 g/mL (b) 0.12 g/mL (c) 0.16 g/mL (d) 0.2 g/mL (0.02 M AgNO$_3$, 0.024 g/mL fructose, 0.04 M NaCl, 160 °C temperature)

Beyond 0.16 g/mL PVP concentration, more silver nanoparticles with very fewer Ag NWs were obtained. This could be due to excess use of PVP molecules that could have covered surface of all seeds of Ag nanoparticles which could have blocked the anisotropic growth (1D) of Ag NWs.

5.3 Characterization of silver nanowires

The crystal structure of synthesized Ag NWs was studied by X-ray diffraction analysis. The diffraction peaks at 38.2°, 44.36°, 64.5°, 77.4° and 81.65° correspond to (111), (200), (220), (311) and (222) planes of Ag, respectively. All diffraction peaks can be indexed to the planes of FCC structure of Ag indicating that crystalline Ag NWs of high purity were synthesized as depicted in Figure 5.5. The diffraction peaks are same as standard JCPDS database (No. 04-0783 for Ag NPs) for all reflections.
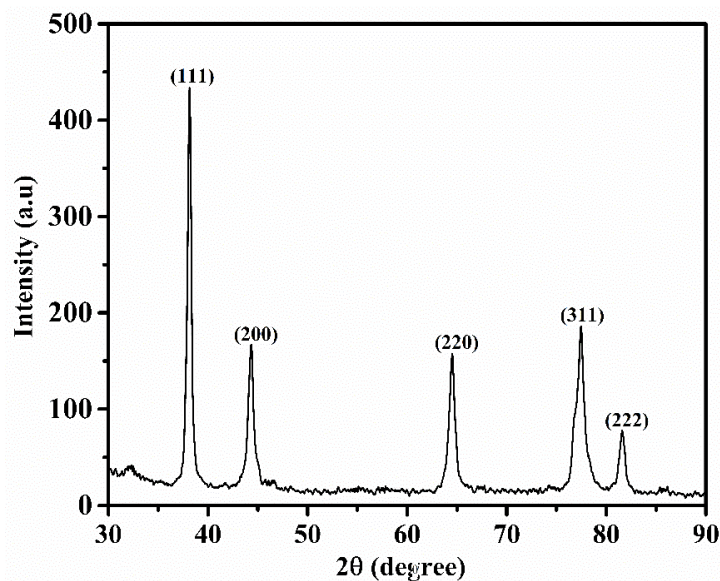
Figure 5.5 XRD pattern of synthesized Ag NWs (160 °C, 0.02 M AgNO$_3$, 0.016 g/mL fructose, 0.16 g/mL PVP)

The sample with optimized parameters (160 °C, 0.02 M AgNO$_3$, 0.016 g/mL fructose, 0.16 g/mL PVP) was subjected to dynamic light scattering analysis and DLS data indicates that the mean diameter of synthesized Ag NWs was around 77 nm as presented in Figure 5.6.
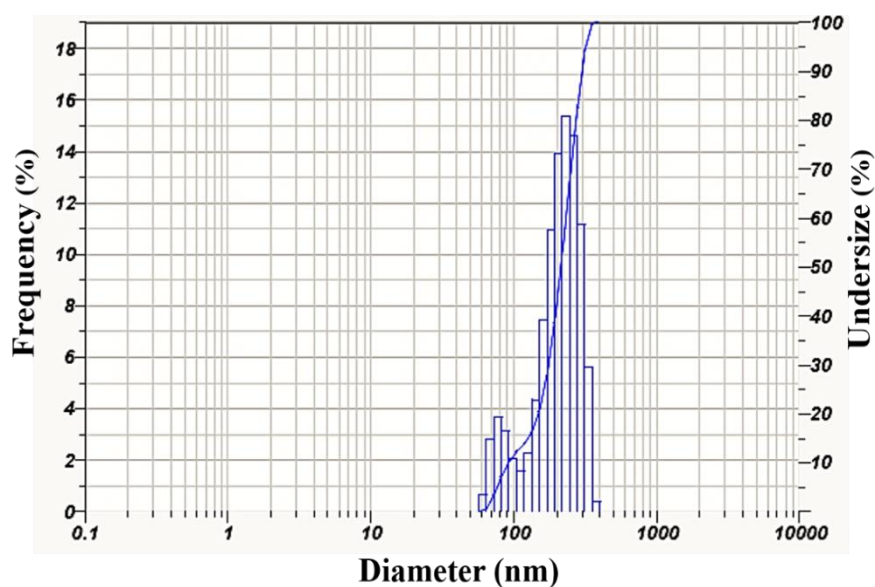
Figure 5.6 Size distribution of Ag NWs measured by the DLS technique (160 °C, 0.02 M AgNO$_3$, 0.016 g/mL fructose, 0.16 g/mL PVP)

FTIR was used to investigate surface chemical state of the synthesized Ag NWs and the possible interaction between silver and PVP. The FTIR spectrum of synthesized Ag NWs with optimized conditions (160 °C, 0.02 M AgNO$_3$, 0.016 g/mL fructose, 0.16 g/mL PVP) is shown in Figure 5.7. The absorption peak observed at 1,117 cm^{-1} could be due to -C-N- stretching vibration of amine group. The medium intense peaks observed at 1,403 cm^{-1} and 1,384 cm^{-1} are due to C=C stretching and -C-H bending vibrations respectively. The band observed at 1,561 cm^{-1} is due to N-H stretching vibrations. C=O absorption peak of Ag/PVP is shifted to 1,633 cm^{-1} but Kumar et al. (2015) observed this peak at 1,645 cm^{-1}, which meant that there is significant interaction between Ag NWs and carbonyl in PVP. This could be due to oxygen atoms of carbonyl group which allows adsorption of this polymer onto the surfaces of Ag particles.
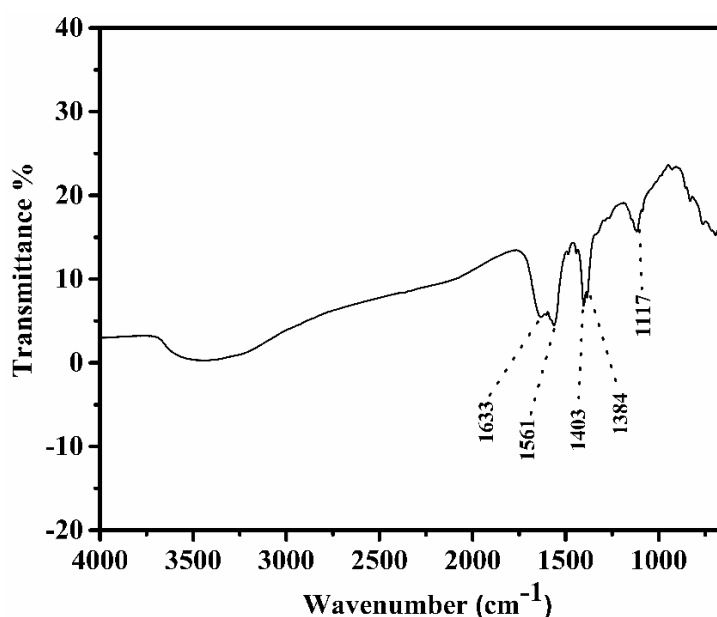
Figure 5.7 FTIR spectra of Ag NWs (160 °C, 0.02 M AgNO$_3$, 0.016 g/mL fructose, 0.16 g/mL PVP)

5.4 Estimation of antibacterial effectiveness using minimum inhibitory concentration method and visible colony count method

The susceptibility of bacteria was estimated by MIC method, which is described as minimum concentration of the metal nanowire at which no visible growth is observed and expressed as µg/mL. The antibacterial effectiveness of prepared Ag NWs on growth inhibition was obtained by measuring the OD$_{600}$ of bacteria grown at different

119

concentrations of Ag NWs (20-100 µg/mL). As concentration of nanowires was increased, bacterial growth got decreased (observation after 12 hrs) as shown in Figure 5.8. At 80 µg/mL of Ag NW concentration, a complete inhibition in the growth of *E. coli* was observed, which indicated MIC level of Ag NWs (Maiti et al. 2014).
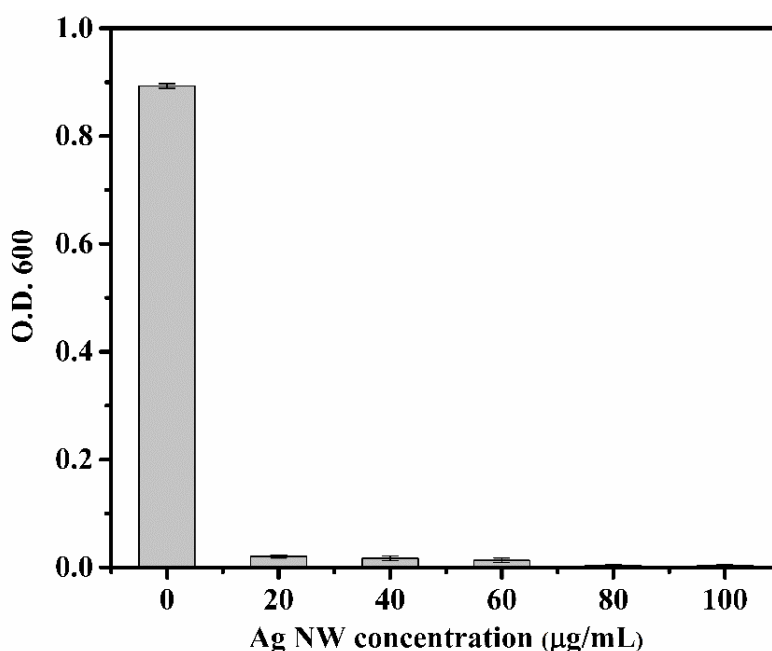
Figure 5.8 Optical density vs concentration of Ag NWs, MIC assay 80 µg/mL

Furthermore, antibacterial activity of Ag NWs was also studied by the visible colony count method against *E. coli* on LB agar plates. The results indicate that *E. coli* showed sensitivity towards Ag NWs, which was confirmed by the presence of very few colonies on Ag NWs treated bacterial culture plate and innumerable colonies were observed on control plate as shown in Figure 5.9. Thus, it can be concluded that synthesized Ag NWs are more effective against bacteria. Antibacterial activity of Ag NWs is due to direct contact of Ag NWs with bacterial cell wall resulting in pit formation in the cell wall which would have disrupted respiratory and permeability functions in bacterial cell. It was also proposed that Ag NPs not only anchor to the surface of a cell membrane and subsequently enter into bacteria where they interact with phosphorus and sulphur of the DNA, thus inhibiting DNA replication and ultimately cell death (Morones et al. 2005).
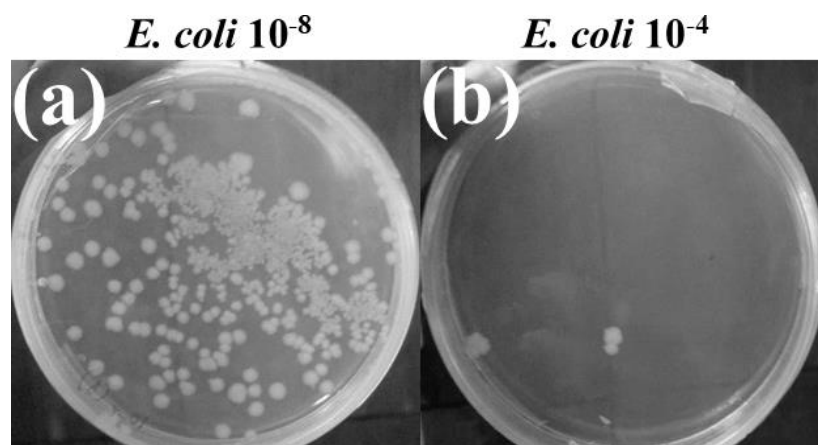
Figure 5.9 Photographs of bacterial colonies formed by *E. coli* (a) Untreated *E. coli* culture (control) (b) Treated *E. coli* culture with Ag NWs

5.5 Radical scavenging activity (DPPH assay)

The ability of Ag NWs to scavenge free radicals was evaluated using DPPH assay. The antioxidant activity of silver nanowires at different concentrations (20-100 µg/mL) were determined and it was observed that free radical scavenging activity increased with increasing concentration of Ag NWs. The results showed that Ag NWs exhibited 67.22% inhibition at a concentration of 100 µg/mL with an IC_{50} (half maximal inhibitory concentration) value of 17.36 µg/mL as shown in Figure 5.10.
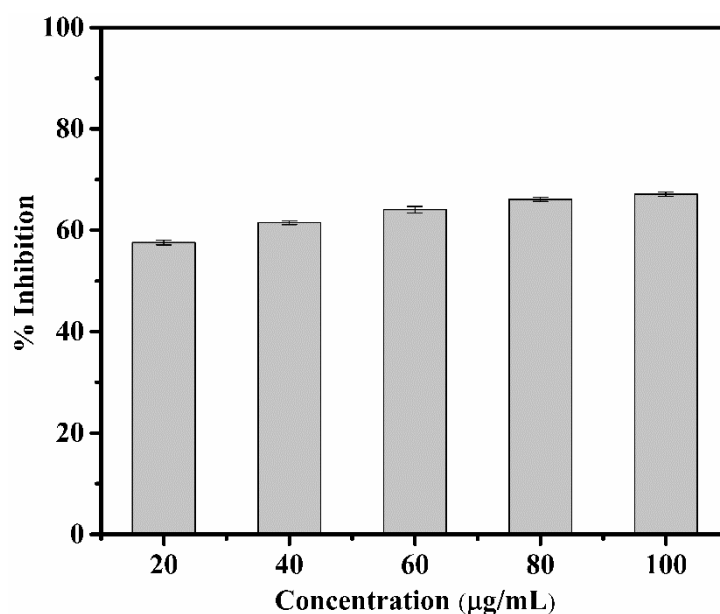
Figure 5.10 DPPH scavenging activity of synthesized Ag NWs

121

The IC_{50} value of synthesized Ag NWs showed best antioxidant activity when compared with other nanoparticles as shown in Table 5.1. Lower the IC_{50} values, higher will be the antioxidant activity of free radical scavengers.

Table 5.1 IC_{50} value of nanoparticles evaluated by DPPH assay

Nanoparticles	IC_{50} value (µg/mL)	Reference
Silver nanoparticles	30.60	Ajayi and Afolayan 2017
Silver nanoparticles	30.04	Mohanta et al. 2017
Silver nanoparticles	126.6	Kharat and Mendhulkar 2016
Silver nanoparticles	51.17	Ravichandran et al. 2016
Zinc oxide nanoparticles	95.09	Murali et al. 2017
Zinc oxide nanoparticles	2853	Suresh et al. 2015
Zinc oxide nanoparticles	46.62	Balaji and Kumar 2017
Copper oxide nanoparticles	38.00	Rehana et al. 2017
Silver nanowires	17.36	Present work

CHAPTER 6

SYNTHESIS AND CHARACTERIZATION OF pH-SENSITIVE HYDROGEL BASED ON COLLAGEN CROSS-LINKED POLY(ASPARTIC ACID)/POLY(VINYL ALCOHOL)

6.1 Introduction

This chapter focuses on the synthesis of a pH sensitive hydrogel based on poly(aspartic acid) (PAsp), poly(vinyl alcohol) (PVA) along with collagen by free radical polymerization using APS (ammonium persulfate) as initiator and ethylene glycol di-methacrylate (EGDMA) as crosslinker. The process variables like polymer concentration, crosslinker, initiator concentration and collagen concentration were optimised based on their effect on the properties like swelling characteristics and physical stability of the hydrogel. The pH responsiveness of the hydrogel was assessed by varying the pH of buffer solution. The synthesized PAsp/PVA/Collagen hydrogel was further characterized by using FTIR, TGA, DSC and SEM.

6.2 Effect of process parameters

The feed compositions were optimized in order to achieve physical stability and better swelling ratio of the hydrogel. The stability of the synthesized hydrogel was visually observed and swelling ratio was measured gravimetrically using buffer solutions at different pH. The composition of polymer (PAsp and PVA), cross-linker, initiator and collagen concentration were optimized by using OVAT method.

6.2.1 Effect of polymer (PAsp and PVA) concentration

The effect of polymer (PAsp) on the swelling capability of the hydrogel was analysed by varying the PAsp concentrations (50 mg, 100 mg, 150 mg and 200 mg) and keeping the other variables constant (PVA-8%; EGDMA-0.75 mM and APS-125 mg). It was visually observed that at 50 mg and 100 mg PAsp concentrations, the gels were mechanically stable under swollen state. Increase in the concentration of PAsp beyond 100 mg resulted in an unstable hydrogel and it started to disintegrate while washing with water as shown in Figure 6.1a. This is due to the formation of irregular

intermolecular crosslinked network and during washing or swelling measurement, the PAsp chains that are highly soluble in water could leach out slowly from hydrogel network (Maheswari et al. 2014; Lee et al. 2017). Hence, these two PAsp concentrations (150 mg and 200 mg) were not further considered for swelling studies.
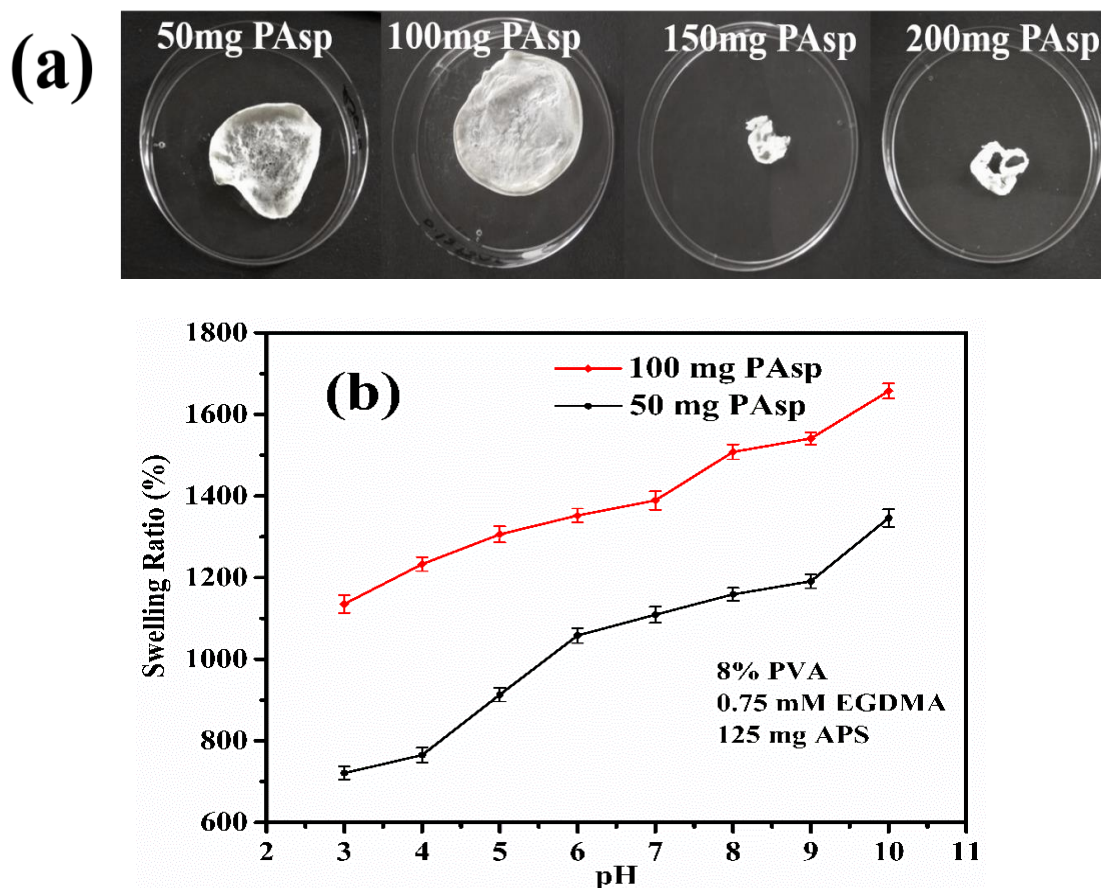
Figure 6.1 (a) Digital images of hydrogel (lyophilized) with different PAsp concentration (b) Effect of PAsp concentration on swelling capacity of hydrogel in different pH

Figure 6.1b depicts the effect of PAsp concentration on swelling capacity of the hydrogel. It is obvious from the figure that increase in PAsp concentration increases swelling ratio upto 100 mg and at higher PAsp concentration hydrogel losses its stability. The swelling study showed that PAsp concentration of 100 mg gave maximum swelling ratio of 1657% at pH 10 compared to 50 mg concentration. The change in the swelling behavior of hydrogel is due to hydrophilic groups present in the PAsp structure. As the PAsp concentration was increased the electrostatic repulsive force

between –COO⁻ groups enhanced and forced the polymer network to expand more which results in significant increase in the swelling ratio of the hydrogel (Liu et al. 2009).

PVA also plays an important role in hydrogel stability. The different percentage of PVA (4%, 6%, 8% and 10%) was used in the synthesis of hydrogel. From Figure 6.1c, it is observed that with increase in PVA percentage, the stability of hydrogel increased i.e., upto 8% PVA and beyond 8% PVA the stability of the hydrogel reduced (Gann et al. 2009; Chhatri et al. 2011). The increase in PVA has increased the hydrophilicity of the hydrogel due to which swelling ratio was enhanced as shown in Figure 6.1b. However, PVA exceeding 8% resulted in the formation of cross-linked (intermolecular bond) network and entanglement of polymer chains. This restricted the penetration of water molecules into the hydrogel and has decreased the water absorption capacity (Wang and Wang 2010). Thus, the optimum percentage of PVA used for the synthesis of hydrogel is 8%.
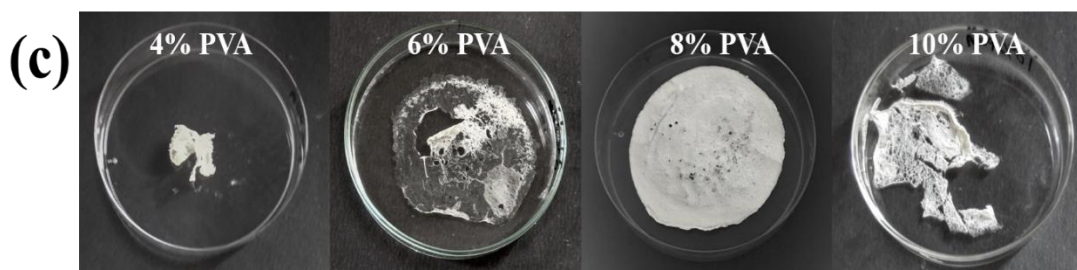
Figure 6.1 (c) Digital images of hydrogel with different PVA concentration

6.2.2 Effect of cross-linker

To synthesize a stable hydrogel, better cross-linking is required to prevent their dissolution in an aqueous environment. The concentration of EGDMA is varied from 0.25 mM to 1 mM to understand the effect of EGDMA content on the hydrogel stability. Hydrogels synthesized with crosslinker having concentration less than 0.75 mM were observed to be sticky and had poor network. Hydrogels prepared with 0.75 mM cross-linker was easy to handle and retained their structural stability as shown in Figure 6.2. As the concentration of EGDMA was increased, hydrogels showed the highest cross-linking points that resulted in increased crosslink density. Due to the strong cross linking, the porosity of the hydrogel could be decreased which would have diminished

interconnecting pore size and the capillary structure and hence, it confines the water absorption capacity (Chavda and Patel 2011). It can be concluded that optimum EGDMA concentration that can be used to prepare hydrogel with desired property is 0.75 mM.
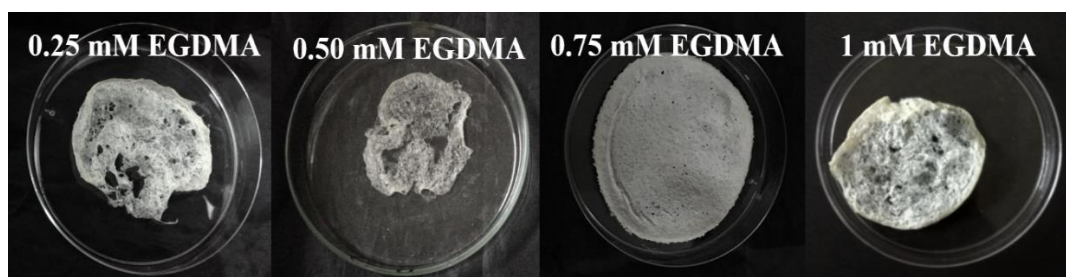
Figure 6.2 Effect of cross-linker on hydrogel stability

6.2.3 Effect of initiator (APS)

The effect of the initiator (75-150 mg) on hydrogel synthesis was determined while keeping other four variables constant (PAsp-100 mg; PVA-8% and EGDMA-0.75 mM). As the initiator concentration was increased, a significant improvement in the mechanical stability of the hydrogel was visually observed and Figure 6.3 shows the digital images of hydrogels using different concentrations of initiator.
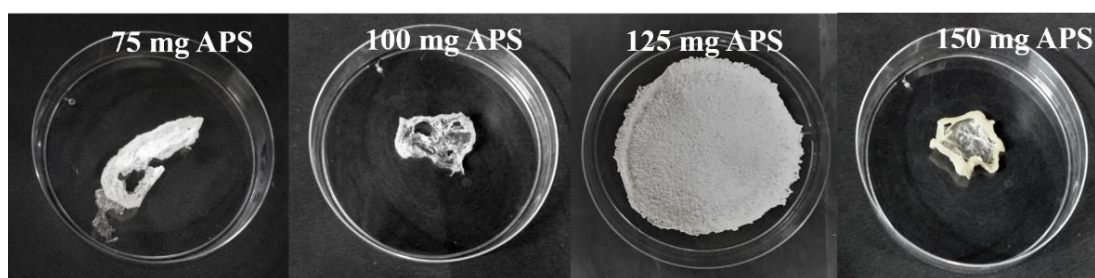
Figure 6.3 Effect of initiator on hydrogel stability

The initiator influences the crosslinking density of the hydrogel and also responsible for the inhomogeneity in the hydrogel system. From the figure, it is observed that when initiator concentration was below 125 mg, hydrogel is less stable and brittle in nature. At a concentration of 125 mg, hydrogel showed good strength and water uptake capacity of the hydrogel decreased with increase in initiator concentration. The maximum swelling was observed as 1657% at 125 mg of APS concentration as shown in Figure 6.1b. Increase in initiator concentration generates large number of free

radicals, which resulted in more crosslinking density in the network as reported by Pourjavadi et al. (2006).

6.3 pH and time dependent swelling studies

The swelling behavior of optimised PAsp/PVA hydrogel (S1) was investigated at different pH. The hydrogel was immersed in different buffer solutions ranging from pH 3-10 at different time intervals (30 min, 60 min, 90 min, 150 min and 180 min) at 37 °C. From Figure 6.4a, it was observed that there is an increment in the swelling ratio of the hydrogels as the pH were increased. This is due to the morphological change of the hydrogels and ionization of COOH group present in PAsp polymer network. The pK_a value of PAsp is about 2.09-3.86, and if ionization takes place beyond this value, the swelling ratio increases. Under acidic conditions, -COO⁻ groups are protonated and the polymeric network will collapse. Further increase in pH, COOH groups will get ionized and the electrostatic repulsion will occur between the carboxylate ions (-COO⁻) in PAsp polymer which leads to higher swelling ratio (Zhao et al. 2006; Liu et al. 2012). From the result, it can be concluded that the synthesized hydrogel is pH-sensitive in nature. Henceforth, it can be used as wound healing material.

It is also observed from Figure 6.4b that swelling ratio increases with time and level off after 60 mins for both acidic and alkaline pH. In addition, the swelling ratio of optimized hydrogel increases to 1434% at pH 10 in 30 mins and attains maximum swelling (1657%) in about 60 mins, while the swelling ratio at pH 3 increases to 1074% and achieves maximum swelling (1135%) within 60 mins. The swelling behavior of the hydrogel has increased at a particular time interval due to the increased concentration of COO⁻ groups in the hydrogel in alkaline pH and resulted in the electrostatic repulsion between ionic groups (-COO⁻) and higher osmotic pressure. This has led to faster water absorption capacity of the hydrogel. However, the charge screening effect by cations in buffer solution has led to decrease in the electrostatic forces and thus hydrogel has achieved the swelling equilibrium.
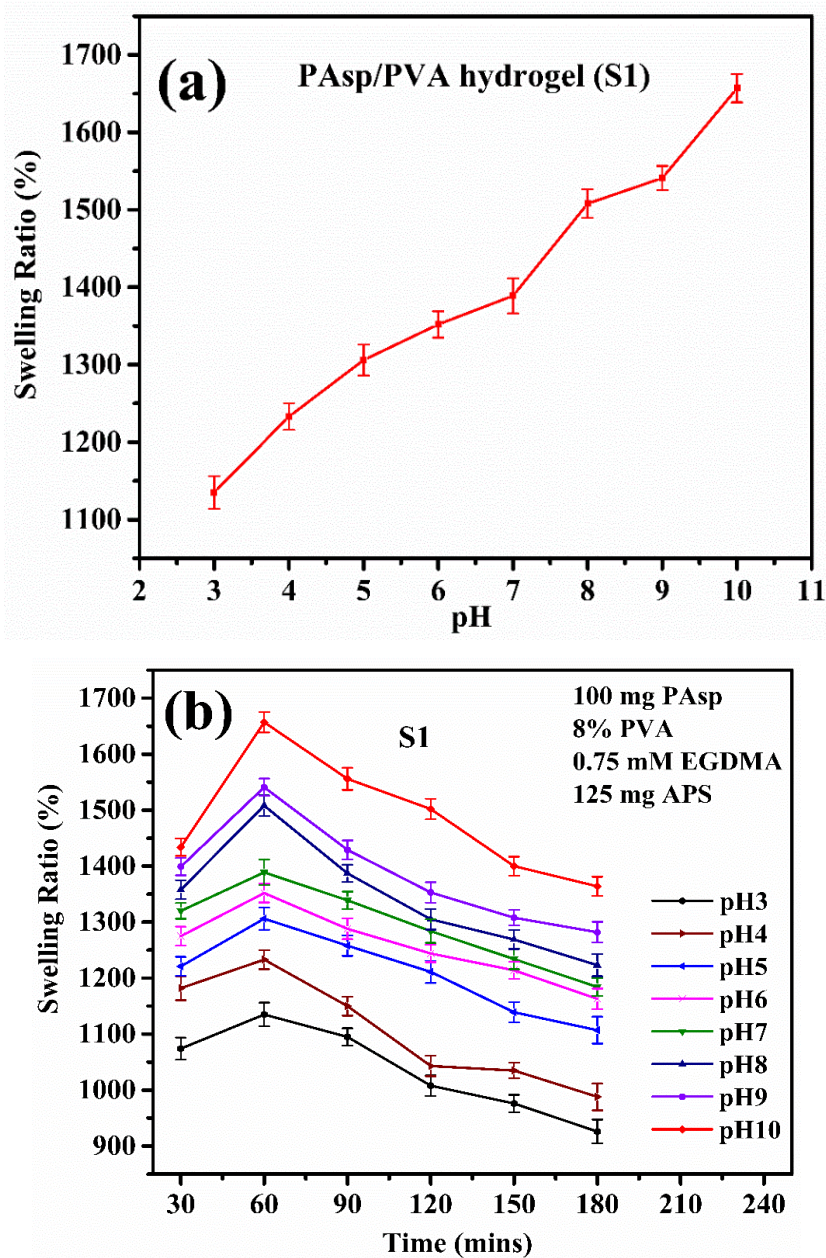
Figure 6.4 Swelling studies (a) pH dependent (b) Time dependent

6.4 Effect of collagen concentration on physical stability and swelling behavior of hydrogel

The optimized values of PAsp/PVA hydrogel (S1) were obtained as PAsp (100 mg), 2 mL of PVA (8%), 0.75 mM of EGDMA (2 mL) and APS (125 mg). To enhance the wound healing process, different concentrations of collagen (0.5 mg/mL, 1 mg/mL, 2 mg/mL and 3 mg/mL) were added to the optimised hydrogel and the effect of collagen

concentration on physical stability of hydrogel was also studied as shown in Figure 6.5a. Though, the optimised PAsp/PVA hydrogel (S1) has the highest swelling capacity, but while adding different concentrations of collagen, the hydrogels were relatively less stable and non-uniform. Upon addition of 0.5 mg/mL of collagen to the hydrogel, mechanically unstable hydrogel was obtained and it started to disintegrate while washing with water. So, the image of this hydrogel was not captured. When the collagen concentration was increased from 1 mg/mL to 3 mg/mL, the stability of hydrogel was decreased. Therefore, to improve stability and strength of hydrogel upon addition of collagen, feed composition of hydrogel (S1) was increased which is given in Table 6.1 The components of S1 hydrogel were further optimised on the basis of physical strength and swelling studies.

Table 6.1 Increment in feed composition of optimized PAsp/PVA hydrogel (S1)

Sample	PAsp (mg)	8% PVA (mL)	0.75 mM EGDMA (mL)	APS (mg)
S1	100	2	2	125
S2	150	3	3	188
S3	200	4	4	250
S4	250	5	5	313

It is clearly depicted from the Figure 6.5b, as the concentration of the components of the optimized hydrogel was increased, the density of hydrogel has increased and the porosity reduced, making the hydrogel thicker and stronger. The change in the gel density has decreased the swelling ratio, which could be due to the more entanglement in the gel network. Thus, the hydrogel S1 has the highest swelling ratio (1657%) as compared to other samples S2 (1286%), S3 (991%) and S4 (937%) at pH 10 as shown in Figure 6.5c. In spite of the highest swelling ratio obtained in case of S1 hydrogel, this hydrogel was not considered for further studies due to less stability on the addition of collagen. Henceforth, depending upon the physical stability of hydrogel and its corresponding maximum swelling ratio, S2 hydrogel was chosen that could fulfil these important two criterions.
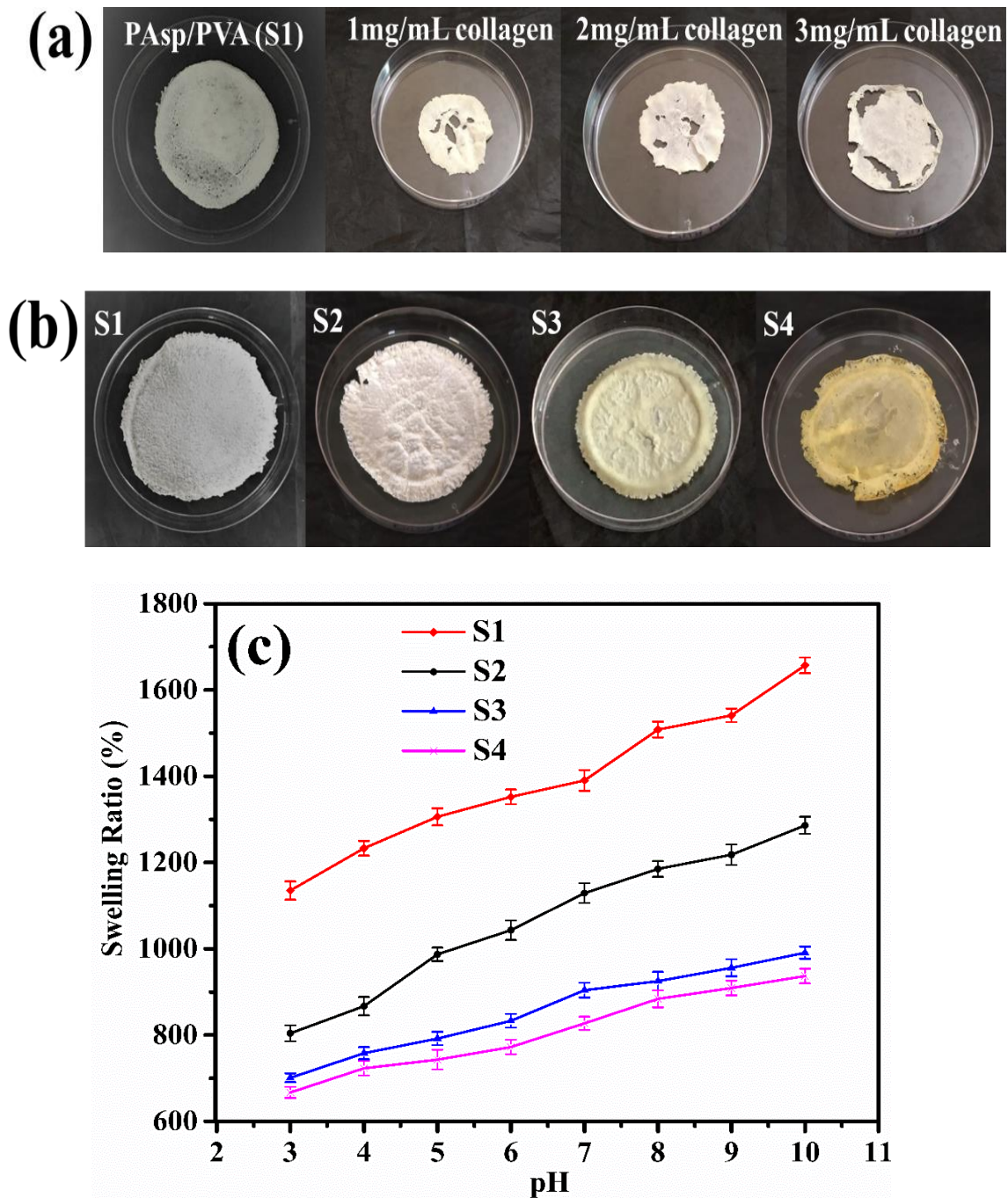
Figure 6.5 (a) Effect of collagen on physical stability of PAsp/PVA hydrogel (S1) (b) Digital images of hydrogel named as S1, S2, S3, S4 (c) pH dependent swelling studies of hydrogel

Collagen amount in the optimized hydrogel (i.e., S2) was optimized by varying the collagen concentration ranging from 0.5 mg/mL to 3 mg/mL. Figure 6.5d shows the effect of collagen on the stability of hydrogel (S2) and Figure 6.5e depicts the effect of

collagen on the swelling behavior of the hydrogel (S2) with respect to pH. From the figure, it was observed that the swelling ratios of PAsp/PVA hydrogel (S2) and hydrogel having different concentrations of collagen were decreased at low pH.
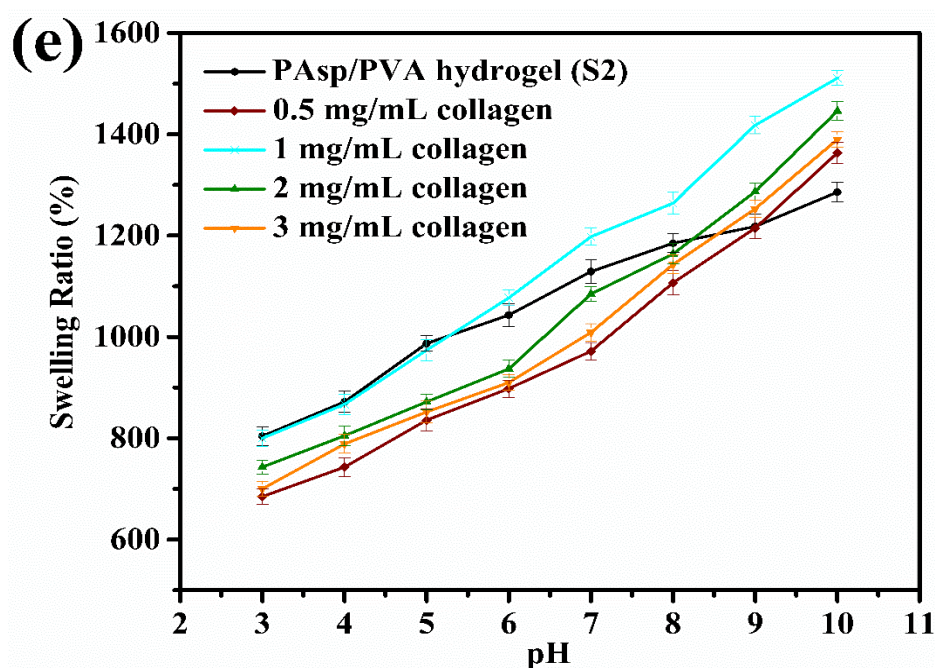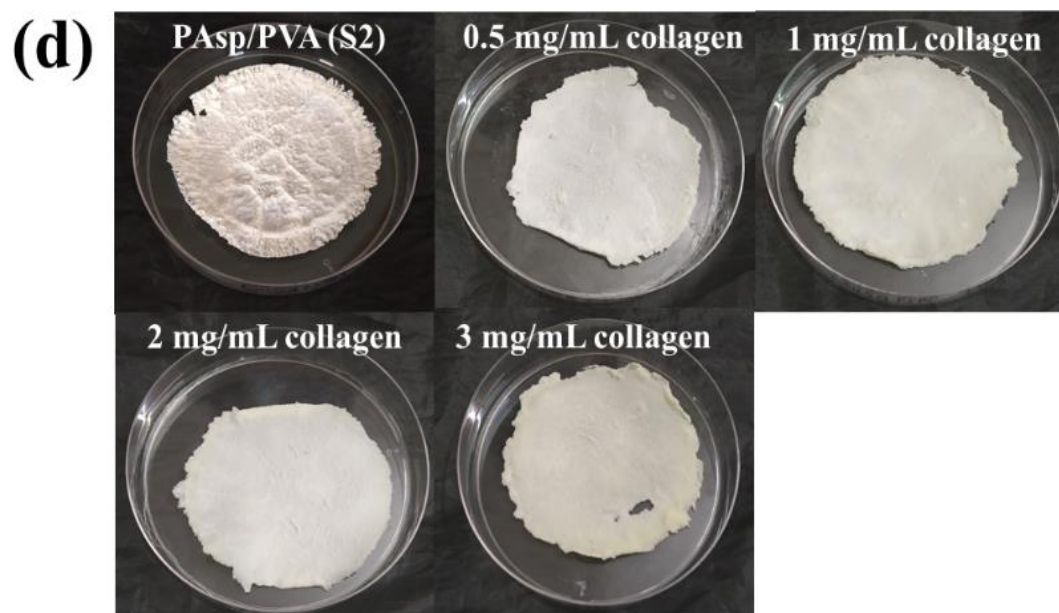
Figure 6.5 (d) Digital images of PAsp/PVA hydrogel (S2) with varying concentrations of collagen (e) Effect of collagen concentration on swelling ratio of hydrogel

PAsp/PVA hydrogel has swelling ratio of 804% whereas swelling ratio of hydrogel having different concentrations of collagen such as 0.5 mg/mL, 1 mg/mL, 2 mg/mL, 3 mg/mL was 685%, 800%, 743% and 700% respectively at pH 3. The decrease in swelling ratio could be due to the fact that at low pH, the carboxylate groups ($-COO^-$) present on hydrogel are in unionized state and gets protonated to form COOH group leading to the reduction of electrostatic repulsive forces generated between the $-COO^-$ ions and resulted in decreased swelling ratio of hydrogel (Peng et al. 2012; Liu et al. 2013). As the pH value of medium increases, swelling ratio of hydrogel also increased and hydrogel having 1 mg/mL collagen had the highest swelling ratio at pH 10. The swelling ratio was 1286% when no collagen was added in PAsp/PVA hydrogel and SR increased from 1286% to 1511% at pH 10 when collagen was present in the hydrogel. So, the addition of collagen has increased the swelling capacity of hydrogel in alkaline conditions as collagen also has -COOH, $-CONH_2$ and -CONH- groups in its structure. Moreover, when the concentration of collagen was increased from 0.5 mg/mL to 1 mg/mL, the swelling ratio has increased from 1363% to 1511% at pH 10. This could be explained by the fact that in alkaline medium the carboxylic group of collagen (-COOH) are deprotonated ($-COO^-$) which generates electrostatic repulsions between the $-COO^-$ ions. This has led to increase in the number of pores in the hydrogel network which resulted in increased absorption capacity (Pourjavadi et al. 2008). This result indicates that the PAsp/PVA/Collagen hydrogel had good pH-sensitivity in alkaline environments. Beyond 1 mg/mL of collagen concentration, the swelling ratio was found to reduce gradually from 1446% to 1390% at pH10. This could be because of the compact and dense structure of the hydrogel, which has resulted in the less diffusion of water molecules.

6.5 Characterization of hydrogel

SEM micrographs of internal structure of lyophilized hydrogels are shown in Figure 6.6 (a-j). From the figure, it can be noticed that PAsp/PVA hydrogel (Figure 6.6a) are devoid of pores when compared to other hydrogels like collagen-based hydrogel and hydrogels dipped in different buffer solution. Hydrogels dipped in higher pH solution has higher porosity and this has led to the formation of highly expanded network due to electrostatic repulsive forces among the carboxylate anions ($-COO^-$) present in PAsp

and collagen polymers. Higher electrostatic repulsive forces has generated several small pores in the polymeric network and this could have helped in easy diffusion of water molecules. Based on these interpretations, it may be inferred that upon incorporation of PAsp and collagen into the hydrogel can led to remarkable improvement in the swelling rate (Zhao et al. 2005; Sharma et al. 2017).
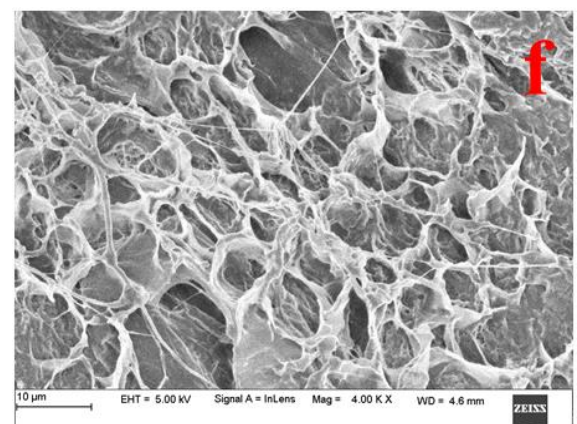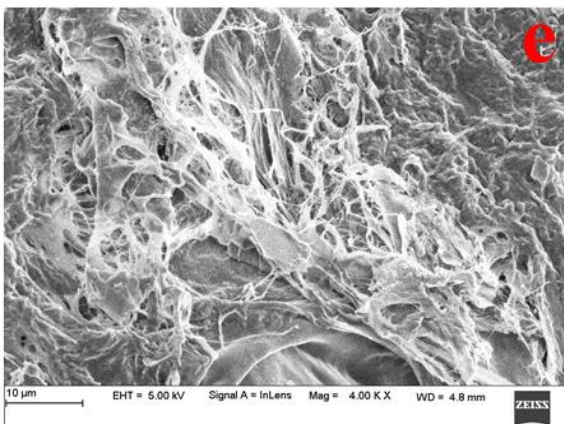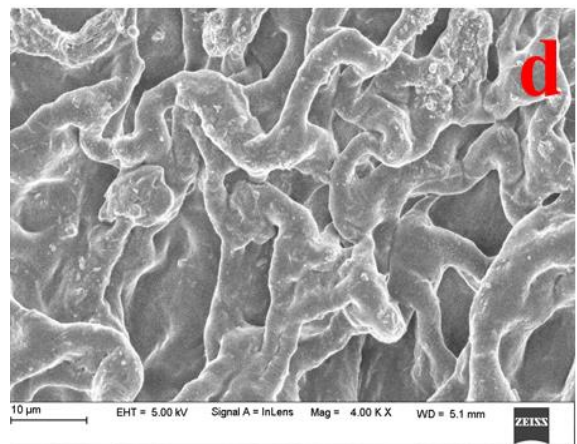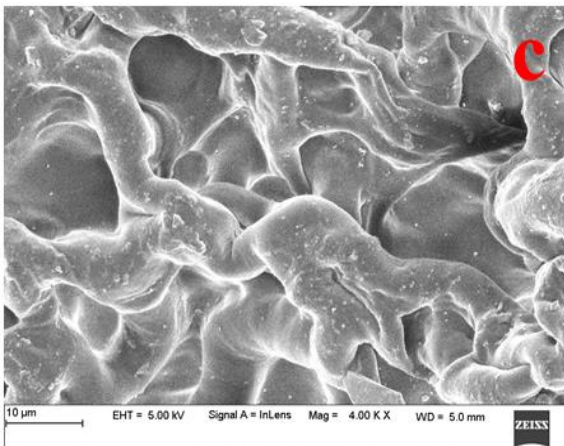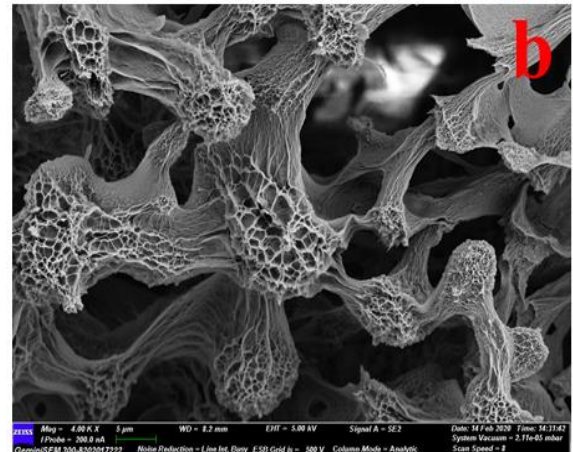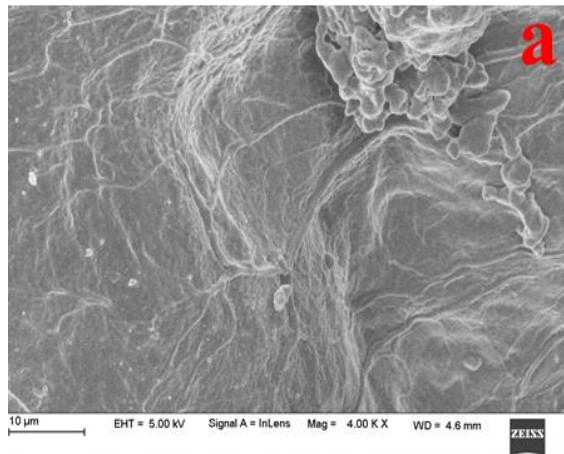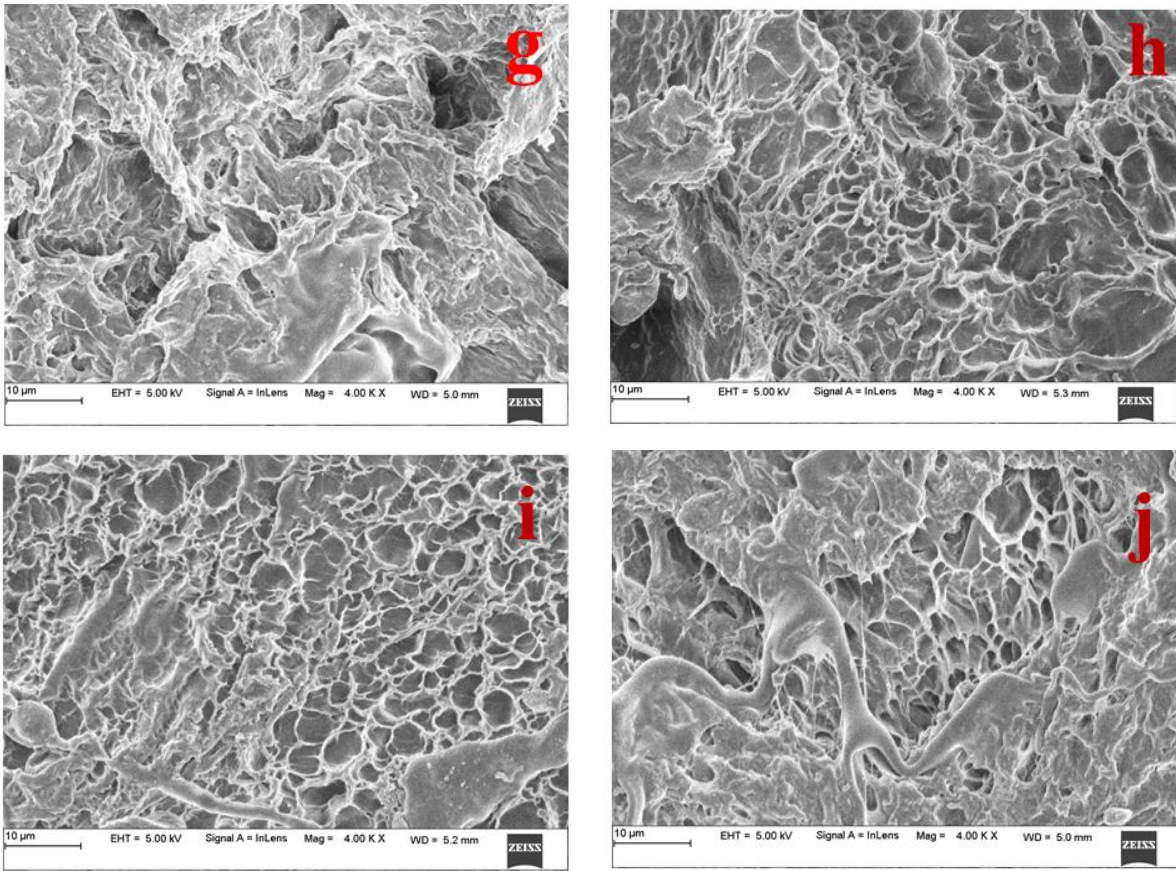
Figure 6.6 FESEM micrographs of hydrogels (a) PAsp/PVA hydrogel (S2) (b) PAsp/PVA/Collagen hydrogel (1 mg/mL collagen) (c) Hydrogel swollen in pH 3 (d) pH 4 (e) pH 5 (f) pH 6 (g) pH 7 (h) pH 8 (i) pH 9 (j) pH 10

Thermal behavior of the synthesized hydrogel was determined using DSC and TGA. Figure 6.7a depicts the DSC thermograms of pure PVA, PAsp, PAsp/PVA hydrogel. PVA exhibits a broad endothermic peak at 190 °C, which corresponds to the melting temperature of the PVA. PVA shows another sharp endothermic peak at 306 °C which is related to decomposition of the PVA (Mohsin et al. 2011). In addition, PAsp shows two endothermic peaks at 290 °C (melting) and 99 °C (water loss). The PAsp contained PVA hydrogel exhibits only one endothermic peak at 100 °C. No melting peak is observed in PAsp/PVA hydrogel due to the formation of intermolecular hydrogen bond between O-H group of PVA and COOH group of PAsp, which indicates that PAsp is well dispersed and blended well with PVA (Gann et al. 2009; Liu et al. 2012). Hence, it can be said that PAsp/PVA hydrogel has better thermal stability as compared to pure PAsp and PVA. In case of fish collagen, the endothermic peak observed at 140 °C could

be due to the loss of water and the appearance of another small peak around 343 °C could be the melting point of fish collagen due to the denaturation of helical structure of collagen (Sripriya and Kumar 2016). The hydrogel with collagen has exhibited an endothermic peak at 93 °C as shown in Figure 6.7b.
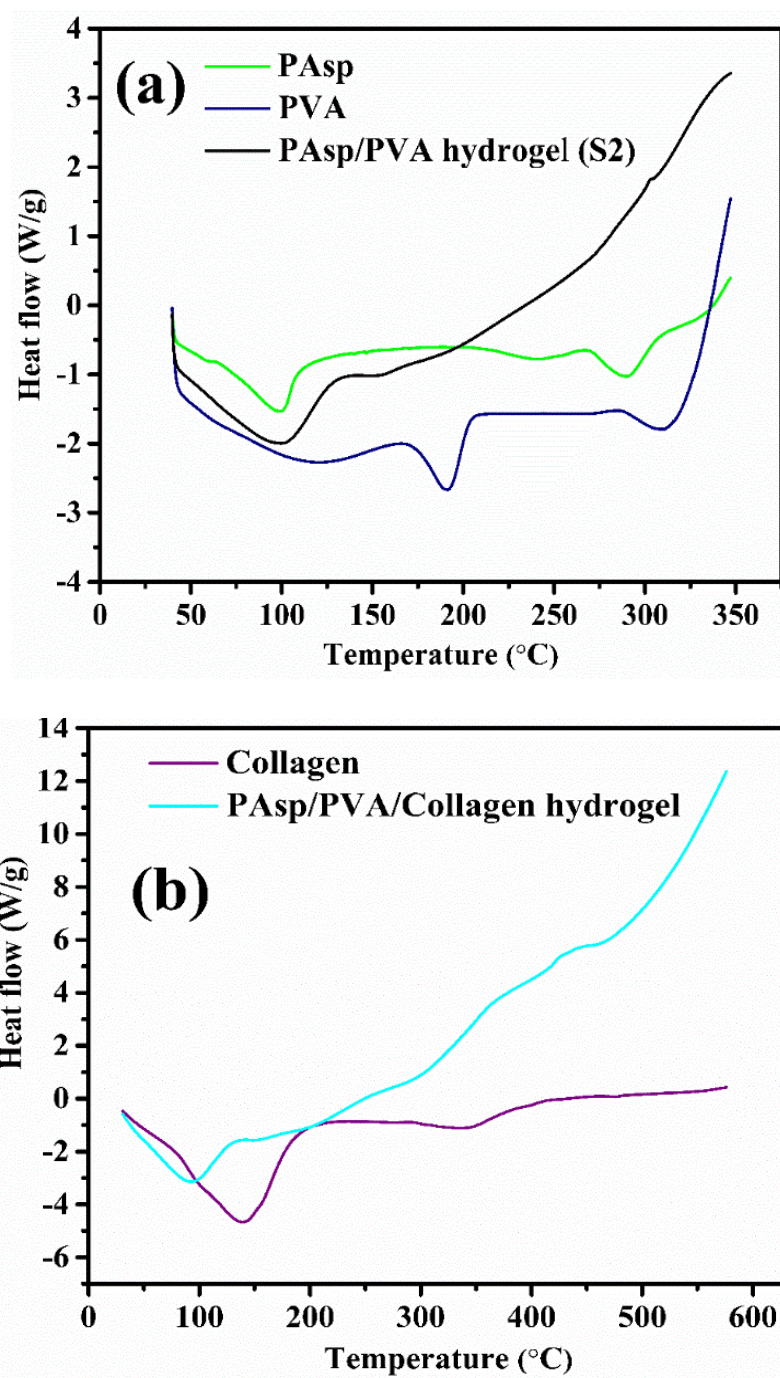
Figure 6.7 DSC thermograms (a) PAsp, PVA and PAsp/PVA hydrogel (S2) (b) Collagen and PAsp/PVA/Collagen hydrogel

135

The peak at 93 °C represents the loss of entrapped water but there is no melting peak observed. From this we can conclude that the PAsp/PVA/Collagen hydrogel can withstand a temperature upto 600 °C or higher as compared to the thermogram of pure fish collagen. This is due to the morphological changes in polymeric matrix and might be due to the intermolecular interaction between -C=O group and amino group (N-H) of collagen and PAsp. The intermolecular hydrogen bonds could have formed between the OH group of PVA and C=O group of PAsp and collagen and also between -C=O and amino group (N-H) of collagen and PAsp. Because of the strong cross linking between the polymers, the thermal stability of PAsp/PVA/Collagen hydrogel has increased which is confirmed from the TGA thermogram (Jayaramudu et al. 2017).

Thermogravimetric analysis of PAsp, PVA, PAsp/PVA hydrogel (S2), collagen and PAsp/PVA/Collagen hydrogel was performed as a function of temperature Vs weight loss (%) as given in Figure 6.8. The hydrogel showed a significant weight loss which was mainly due to the thermal breakdown of the polymer chain. A three-stage decomposition was found in PVA, PAsp/PVA and PAsp/PVA/Collagen hydrogels whereas two-stage decomposition had been observed in fish collagen and PAsp polymer. The initial weight losses in case of fish collagen and PAsp at temperature 120 °C were 32.20% and 6.57% respectively which is due to the elimination of water content and other volatile component. In case of fish collagen, the second weight loss of 73.69% was observed in the temperature range of 260-450 °C indicating the degradation of collagen helix structure (Ramanathan et al. 2014). The second weight loss of 39.92% for PAsp was observed in the temperature range of 200-510 °C, which is because of the decomposition of backbone polymer. The initial weight losses in PVA, PAsp/PVA hydrogel and PAsp/PVA/Collagen hydrogel were 5.41%, 5.47% and 13.69% at temperatures 120 °C, 80 °C and 95 °C respectively. In all these stages, the weight loss in the polymer (pure PVA) and hydrogels (PAsp/PVA and PAsp/PVA/Collagen) were mainly related to the water evaporation. The second stage weight losses in PVA, PAsp/PVA hydrogel and PAsp/PVA/Collagen hydrogel were 88.33%, 48.13% and 88.71% in the temperature range of 260-470 °C, 220-340 °C and 270-470 °C respectively. These weight losses could be due to the elimination of side

chains from the hydrogel and also degradation of amides and oxygenated functional groups from the polymer matrix (Sharma et al. 2015; Lee et al. 2017).
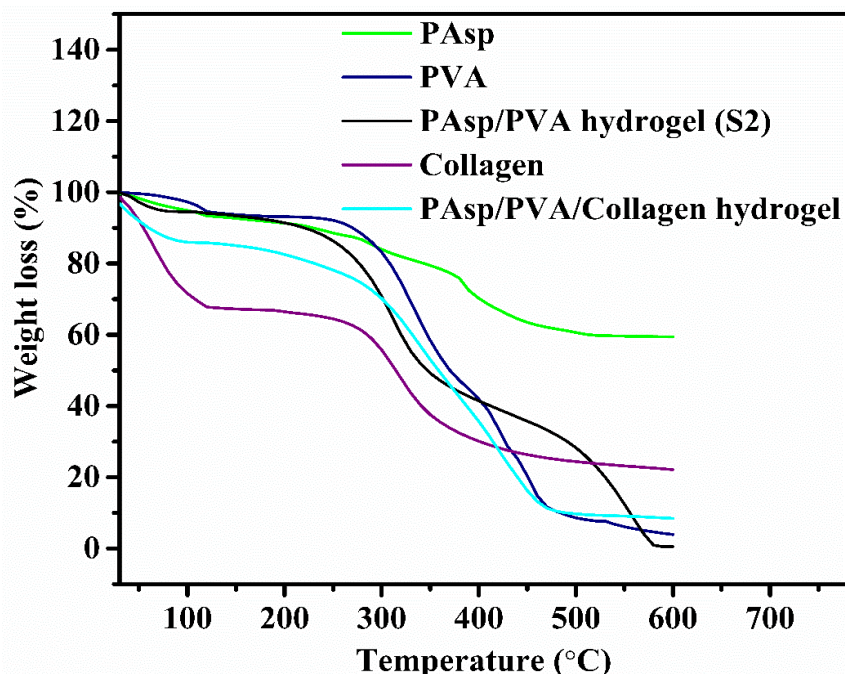
Figure 6.8 TGA thermograms of PAsp, PVA, PAsp/PVA hydrogel, Collagen and PAsp/PVA/Collagen hydrogel

The maximum decomposition of hydrogel was observed in the third stage because of the breakdown of crosslinked structure (Lim et al. 2016). The third stage weight loss in PVA, PAsp/PVA hydrogel and PAsp/PVA/Collagen hydrogel were found to be 96.02%, 99.02% and 91.52% in the temperature range of 470-600 °C, 340-580 °C and 470-600 °C respectively. The PAsp/PVA/Collagen hydrogel shows 50% of weight loss at 358 °C as compared to PAsp/PVA hydrogels (347 °C). Thus, it can be concluded that the thermal stability of PAsp/PVA/Collagen hydrogel was greatly improved by the addition of collagen into the PAsp/PVA hydrogels.

The molecular structure of PAsp, PVA, PAsp/PVA hydrogel (S2) and PAsp/PVA/Collagen hydrogel were investigated using ATR-FTIR as shown in Figures 4.9a and 4.9b. In the case of PAsp, the peaks at 943.19 cm^{-1}, 1074.35 cm^{-1} and 1398.39 cm^{-1} indicate the presence of C-O stretching of carboxyl (COOH) group, bending vibration of -CH_2- group, C-N stretching of acyl amide ($RCONH_2$) group and also C=O symmetric stretching of carboxylate anion. The bands observed at 1585.49 cm^{-1},

137

2368.59 cm^{-1} and 3257.77 cm^{-1} are related to N-H bending vibration of amide II (-CONH$_2$) group, C-H stretching vibration and N-H stretching vibration of amide group respectively (Figure 6.9a). Thus, it is confirmed that PAsp is successfully synthesized (Zhang et al. 2018c; Gao et al. 2010; Zhang et al. 2016). The spectrum of PVA shows characteristic peaks at 842.89 cm^{-1}, 949.30 cm^{-1}, 1089.78 cm^{-1}, 1240.23 cm^{-1}, 1373.32 cm^{-1}, 1427.32 cm^{-1}, 1720.50 cm^{-1}, 2910.58 cm^{-1}, 3305.99 cm^{-1} corresponds to C-C stretching vibration, CH$_2$ rocking vibration, C-O stretching of acetyl group present in the PVA back bone, C-H wagging vibration, CH$_2$ group wagging vibration, CH$_2$ group bending vibration, C=O in carbonyl group stretching, asymmetric stretching of CH$_2$ group and O-H stretching vibrations of hydroxyl groups of PVA accordingly (Khatuaa et al. 2015; Fonseca et al. 2006). The FTIR spectra of PAsp/PVA hydrogel (S2) showed similar character to those of PAsp and PVA. The characteristic peaks of pure PAsp and PVA at 943.19 cm^{-1} and 949.30 cm^{-1} are shifted towards higher wavenumber of 970.19 cm^{-1} (sample-S2), which confirmed the successful polymerization of polymer PAsp along with PVA (Tsao et al. 2011). Similarly, the wavenumber of other characteristic peaks of pure PVA and PAsp were also displaced in PAsp/PVA hydrogel spectrum with lesser intensity. Moreover, PAsp/PVA hydrogel has high content of PVA and thus the spectra of hydrogel showed higher number of absorption peaks of PVA as compared to PAsp.

From Figure 6.9b, it has been observed that the absorption spectrum of PAsp/PVA/Collagen hydrogel had a small shift in the wavenumber as compared to PAsp/PVA hydrogel, which indicates that the intermolecular interactions like hydrogen bond formation and electrostatic attraction occurred between collagen, PAsp and PVA polymers (Diniz et al. 2020). The bands observed at 3341.66 cm^{-1} and 2931.80 cm^{-1} for PAsp/PVA hydrogel samples were shifted to 3354.21 cm^{-1} and 2926.01 cm^{-1} in the case of PAsp/PVA/Collagen hydrogel sample, where there was no shift in the case of pure collagen (Krishnan et al. 2018). The peak at 3354.21 cm^{-1} is attributed to the amide A band associated with N-H stretching in case of collagen but in PAsp/PVA hydrogel, this band corresponds to O-H stretching vibrations due to the hydroxyl groups of PVA. Similarly, in collagen sample, peak at 2926.01 cm^{-1} ascribed to amide B band, which is related to CH$_2$ group stretching and in the case of PAsp/PVA hydrogel, this band is

attributed to same vibration i.e., asymmetric stretching of CH_2 group. Therefore, the other characteristic peaks of collagen such as amide I, amide II and amide III are difficult to distinguish in the spectra of PAsp/PVA/Collagen hydrogel, but they were observed at 1650.86 cm^{-1}, 1554.93 cm^{-1} and 1242.16 cm^{-1} as reported by Singh et al. (2011).
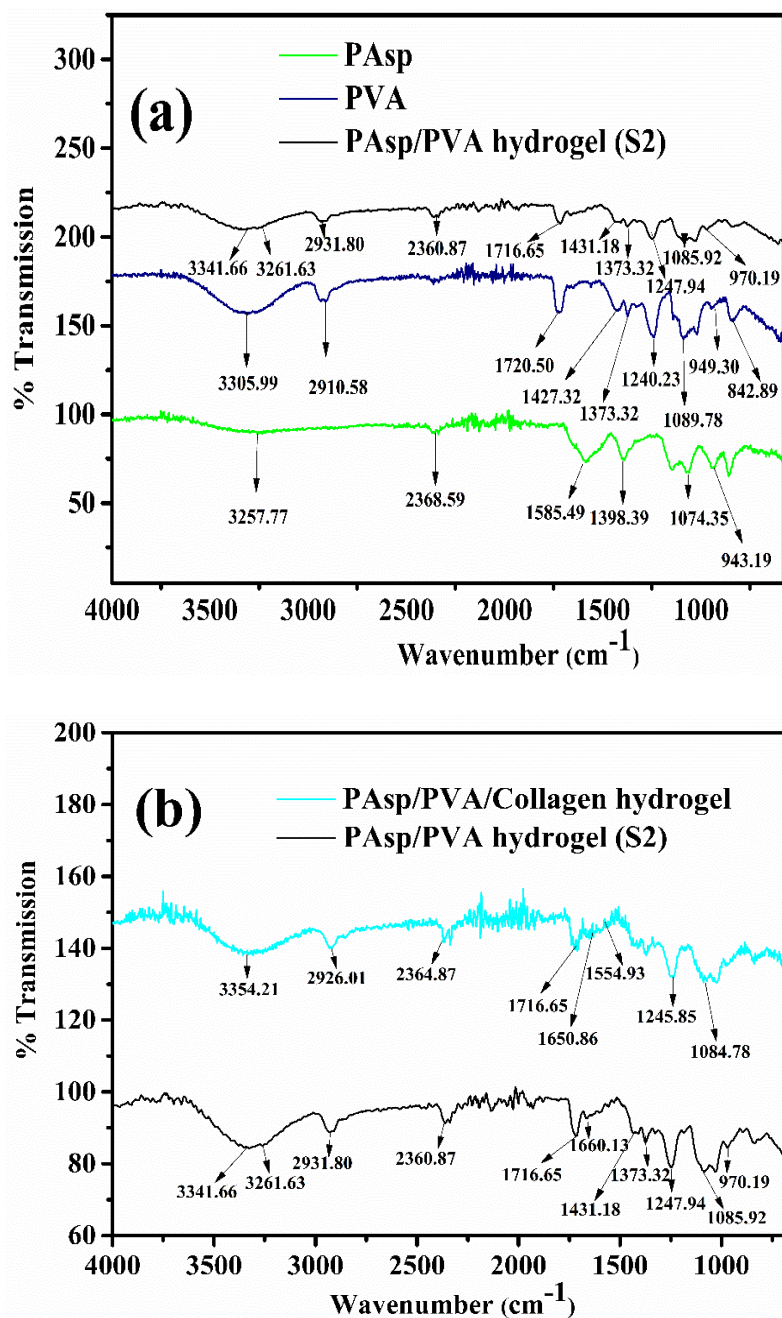
Figure 6.9 ATR-FTIR spectra (a) PAsp, PVA and PAsp/PVA hydrogel (b)
PAsp/PVA/Collagen hydrogel and PAsp/PVA hydrogel

This is because functional groups present in collagen such as COOH, NH_2, $CONH_2$ vibrates similarly like PAsp/PVA hydrogel, due to the presence of similar functional group in PAsp and PVA sample. Therefore, some of the peaks in PAsp/PVA/Collagen got overlapped and clear distinction between the peak is not possible in the samples (Marin et al. 2018).

6.6 Comparison of swelling ratio with other pH-sensitive hydrogels

In Table 6.2, swelling ratio (%) of the synthesized pH- sensitive PAsp/PVA/Collagen hydrogel is compared with other pH sensitive hydrogels which are reported in the literature. From the table, it is clear that PAsp/PVA/Collagen hydrogel shows better swelling in alkaline pH compared to other reported hydrogel. This could be due to the presence of PAsp and PVA along with collagen in right composition.

Table 6.2 Comparison of swelling ratio (%) of PAsp/PVA/Collagen hydrogel with other pH-sensitive hydrogels

Polymer	Method of preparation	Swelling Ratio (%)	Reference
Collagen/poly(vinyl alcohol)	Self -Assembly	1400	Marin et al. 2018
Chitosan-collagen peptide/oxidized konjac glucomannan	Schiff base reaction	265	Liu et al. 2018
Semi interpenetrated network of poly(N-isopropylacrylamide)/ poly(aspartic acid)	Free radical polymerization	200	Nistor et al. 2013

Kappa-carrageenan/poly (vinyl alcohol)	Polymer blending (Traditional mixing)	15.13	Hezaveh and Muhamad 2012
2-hydroxyethyl methacrylate/citraconic anhydride–modified collagen	Free radical polymerization	200	Pamfil et al. 2017
Interpenetrating network of poly(N-isopropylacrylamide)/poly(aspartic acid)	Free radical polymerization	1200	Liu et al. 2012
PAsp/PVA/Collagen	Free radical polymerization	1511	Present work

Thus, PAsp/PVA/Collagen hydrogel can be potentially used as wound dressing material due to the following reasons.

1. It can retain required moist environment for better healing process.
2. It can maintain pH by removing excess exudate on wound area.
3. It can enhance wound healing due to the presence of collagen, a tissue building material.

CHAPTER 7

SYNTHESIS, CHARACTERIZATION AND *IN-VIVO* EVALUATION OF SMART WOUND DRESSING MATERIAL WITH ENHANCED HEALING PROPERTIES FOR CHRONIC WOUNDS

7.1 Introduction

This chapter focuses on synthesis and characterization of pH-responsive hydrogel-based wound dressing material i.e., PAsp/PVA/Collagen hydrogel impregnated with Ag NWs by free radical polymerization using APS (ammonium persulfate) as initiator and ethylene glycol di-methacrylate (EGDMA) as crosslinker. The effect of concentration of Ag NWs on swelling behavior and structural stability of wound dressing material were also analysed. The synthesized Ag NWs impregnated PAsp/PVA/Collagen hydrogel was further characterized by using SEM, XRD and EDAX. *In-vitro* release study of silver ions from dressing material and antibacterial activity of hydrogel impregnated with Ag NWs against *E. coli* were also performed. The developed smart wound dressing material was evaluated for cytotoxicity study and *in-vivo* wound healing studies.

7.2 Mechanism of synthesized PAsp/PVA/Collagen hydrogel impregnated with silver nanowires

A smart hydrogel or pH-responsive hydrogel-based wound dressing material i.e., PAsp/PVA/Collagen impregnated with Ag NWs has been developed to achieve the following; absorb the excess exudate, control the wound surface pH, promote wound healing process and inhibit bacterial growth. Hydrogel was synthesized by free radical polymerization and the reaction mechanism is schematically illustrated in Figure 7.1. Here, PAsp and PVA solution was mixed and cross-linked with EGDMA. Collagen solution was added to the reaction mixture and then Ag NWs suspended in water were added. The first step initiates with the decomposition of APS (initiator) into free radicals (sulfate anion) by exposing it to heat at 80 °C. In the second step, these free radicals react with PAsp, PVA and collagen and undergo hydrogen abstraction from

one of the functional groups (COOH, NH$_2$ and OH) present in polymer to form macro-radicals (Pourjavadi et al. 2008). This process is repetitive, and these macro-radicals initiate the crosslinking reaction in the presence of EGDMA and a stable hydrogel sheet was formed. Ag NWs were embedded inside the pores of the hydrogel matrix as an antibacterial agent to control the bacterial infection in the wound bed. Therefore, PAsp/PVA/Collagen hydrogel impregnated with Ag NWs can be a novel wound dressing material for chronic wounds.
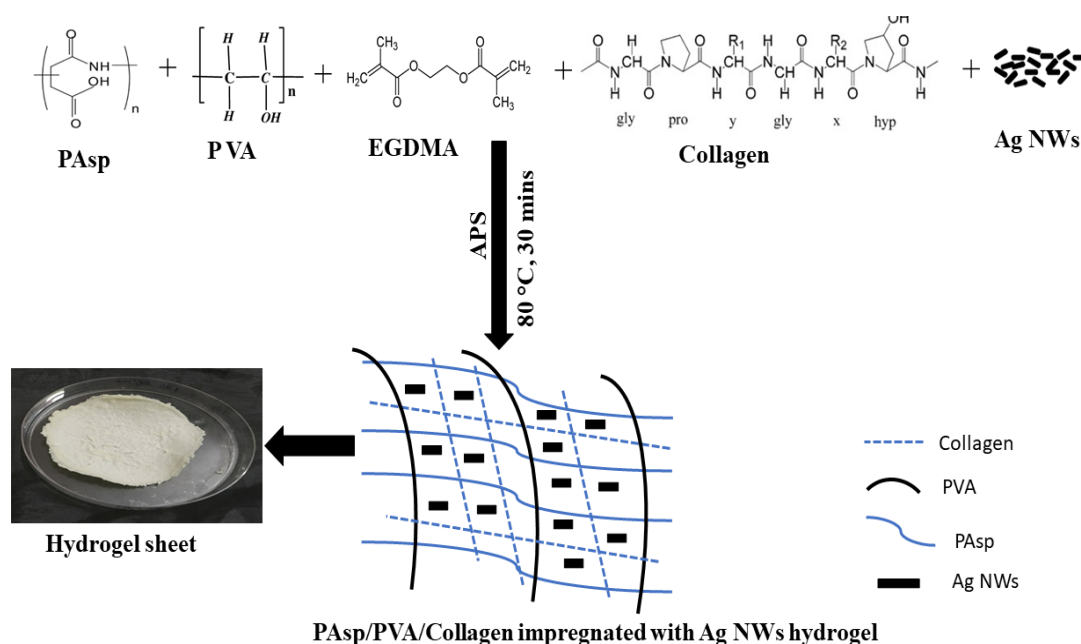
Figure 7.1 Reaction scheme of synthesis of PAsp/PVA/Collagen hydrogel impregnated with Ag NWs

7.3 Characterization

7.3.1 SEM

The effect of Ag NWs on the structural characteristics of porous PAsp/PVA/Collagen hydrogel could be discerned from relatively low-resolution and high-resolution SEM micrographs as shown in Figure 7.2 and Figure 7.3. PAsp/PVA/Collagen hydrogel incorporated with 2.5 mg, 5 mg and 10 mg Ag NWs are represented in Figures 7.2 and 7.3 (a-d) respectively. As Ag NWs are scaled at nanoscale, their actual existence in these micrographs is not revealed. Nevertheless, a strong interaction of Ag NWs leading to a reduced pore size is noticed within the hydrogel structure and this is validated using swelling ratio analysis (Basu et al. 2018; Hu et al. 2018).
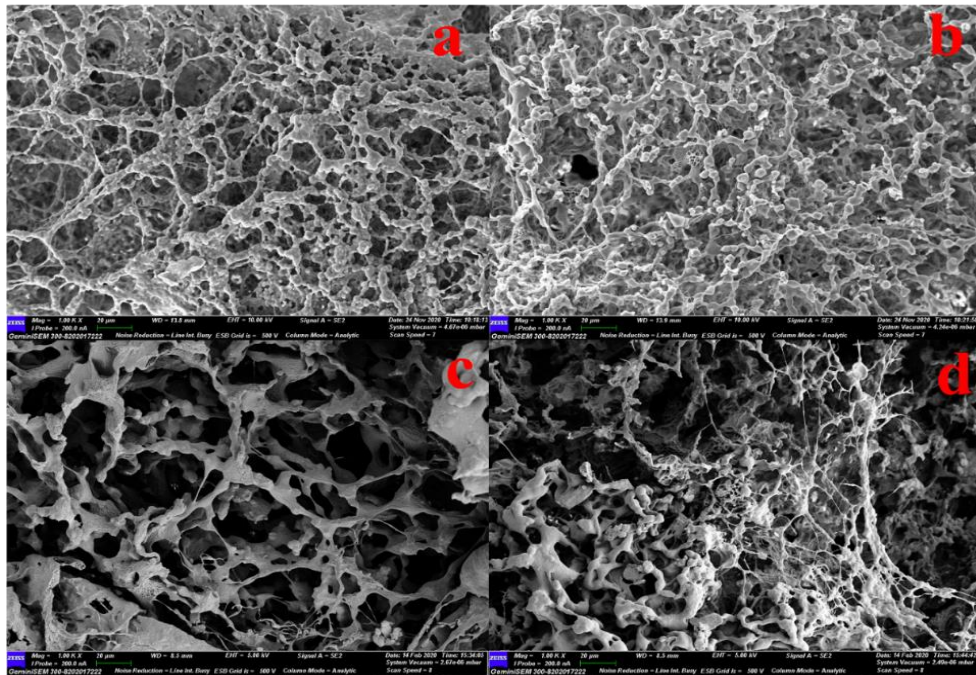
Figure 7.2 Low-resolution SEM micrographs of hydrogel (a) PAsp/PVA/Collagen hydrogel (b) Hydrogel impregnated with 2.5 mg Ag NWs (c) Hydrogel impregnated with 5mg Ag NWs (d) Hydrogel impregnated with 10 mg Ag NWs
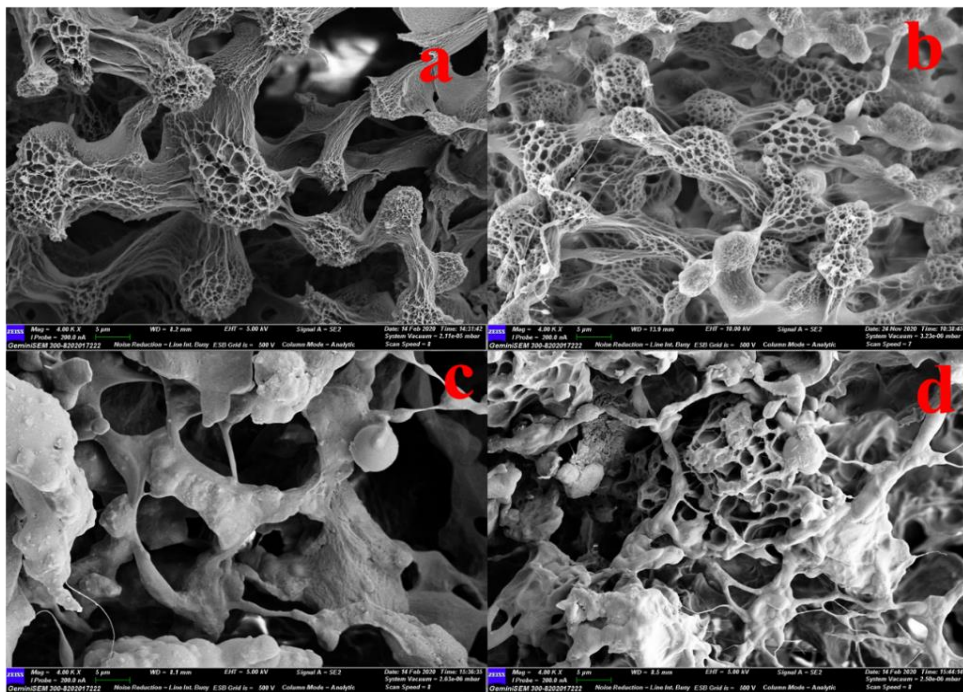
Figure 7.3 High-resolution SEM micrographs of hydrogel (a) PAsp/PVA/Collagen hydrogel (b) Hydrogel impregnated with 2.5 mg Ag NWs (c) Hydrogel impregnated with 5 mg Ag NWs (d) Hydrogel impregnated with 10 mg Ag NWs

Moreover, this effect could be due to the fact that Ag NWs block the void spaces inside the hydrogel matrix. The confirmation of presence of Ag NWs in PAsp/PVA/Collagen hydrogel has been carried out using area energy dispersive X-ray analysis (EDAX) as shown in Figure 7.4 (a-d).

7.3.2 Energy dispersive X-ray analysis (EDAX)

The existence of different amounts (2.5 mg, 5 mg and 10 mg) of Ag NWs in PAsp/PVA/Collagen hydrogel has been confirmed by energy dispersive X-ray analysis (EDAX) as depicted in Figure 7.4 (a-d). When compared to samples having 10 mg Ag NWs, the 2.5 mg and 5 mg samples having low amount of Ag NWs exhibited relatively low EDAX peaks as shown in Figures 7.4b and 7.4c. However, for sample having 10 mg Ag NWs, a strong peak at 3 keV was observed which confirmed the presence of silver in the hydrogel matrix (Patwadkar et al. 2015). The weight percentage of each element was also analysed and results revealed that amount of Ag NWs was more in case of PAsp/PVA/Collagen hydrogel loaded with 10 mg Ag NWs.

Element	Weight %	Atomic %
C (K)	64.15	71.94
O (K)	32.88	27.69

(a)

Element	Weight %	Atomic %
C (K)	64.15	71.94
O (K)	32.88	27.69
Ag (L)	2.96	0.37

(b)

Element	Weight %	Atomic %
C (K)	60.54	70.07
O (K)	33.58	29.17
Ag (L)	5.88	0.76

(c)

Element	Weight %	Atomic %
C (K)	33.63	57.06
O (K)	28.03	35.70
Ag (L)	38.34	7.24

(d)
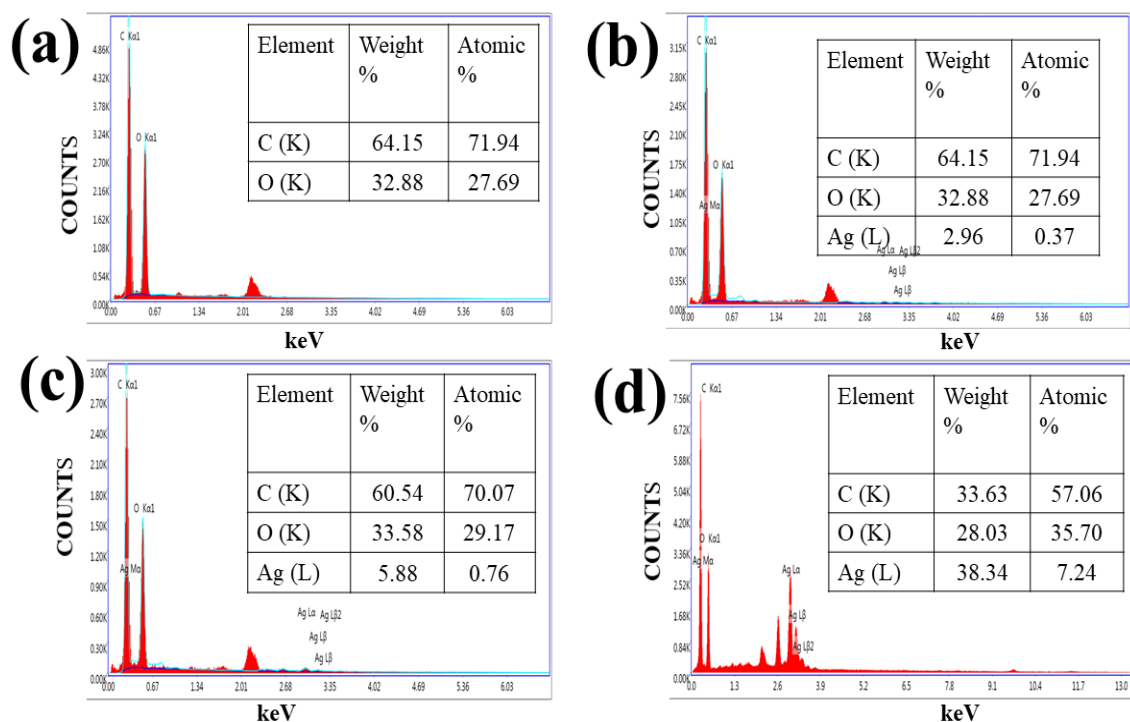
Figure 7.4 EDAX images of hydrogel (a) PAsp/PVA/Collagen hydrogel (b) Hydrogel impregnated with 2.5 mg Ag NWs (c) Hydrogel impregnated with 5mg Ag NWs (d) Hydrogel impregnated with 10 mg Ag NWs

7.3.3 XRD

The XRD patterns of PAsp/PVA/Collagen hydrogel and hydrogel loaded with different amounts of Ag NWs such as 2.5 mg, 5 mg and 10 mg are shown in Figure 7.5. Four diffraction peaks centred at an angle, 2θ degree of $38.2°$, $44.36°$, $64.5°$ and $77.4°$ are obtained and that could be indexed to Bragg reflections of (111), (200), (220) and (311) crystallographic planes of FCC structure of Ag (JCPDS file no. 04-0783 for Ag) (Sharma et al. 2019a). Hydrogels embedded with Ag NWs show a characteristic peak of Ag and the peaks intensity increases with increasing concentration of Ag NWs. No diffraction peak was observed in case of PAsp/PVA/Collagen hydrogel which confirmed the absence of Ag NWs in hydrogel matrix (Li et al. 2020).
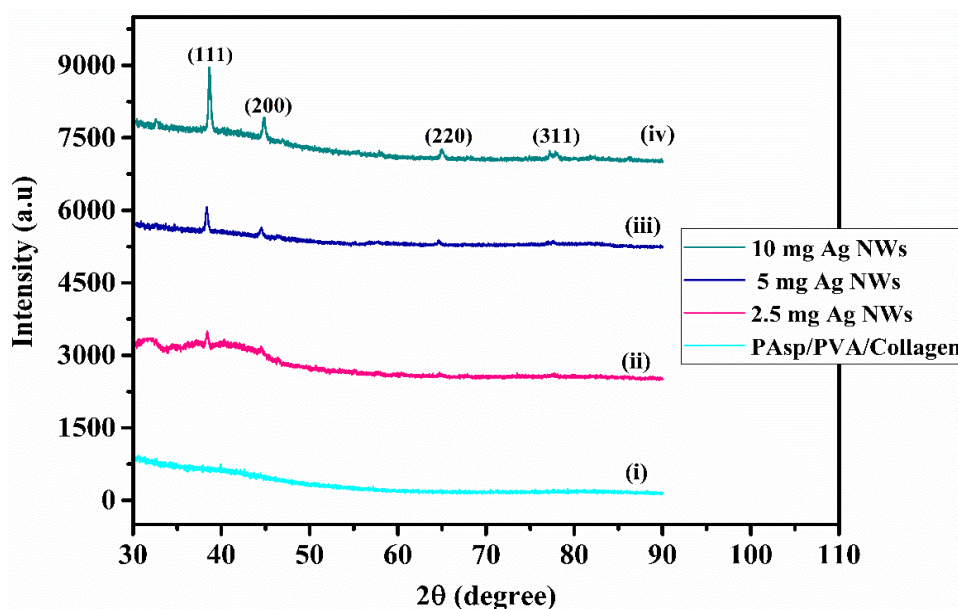
Figure 7.5 XRD pattern of (i) PAsp/PVA/Collagen hydrogel (ii) PAsp/PVA/Collagen hydrogel impregnated with 2.5 mg Ag NWs (iii) PAsp/PVA/Collagen hydrogel impregnated with 5 mg Ag NWs (iv) PAsp/PVA/Collagen hydrogel impregnated with 10 mg Ag NWs

7.4 Effect of Ag NWs on swelling ratio of hydrogel

The swelling behavior of PAsp/PVA/Collagen based hydrogel and hydrogel loaded with different amounts of Ag NWs such as 2.5 mg, 5 mg and 10 mg were studied at different pH (3-10) as shown in Figure 7.6. The results showed that swelling ratio of hydrogel gradually increases as the pH was increased. The increase in swelling ratio in

alkaline pH is due to ionization of carboxylic groups (COOH) present in collagen and PAsp polymer network. Under alkaline conditions, these COOH groups are deprotonated (COO⁻) and electrostatic repulsion generates between them, which leads to higher swelling ratio. The pH-responsive characteristics of hydrogel are helpful to use them as wound dressing material. Since, pH of the wound exudate is usually alkaline, this hydrogel can absorb exudate and can maintain moist environment on the wound bed. However, when PAsp/PVA/Collagen hydrogel impregnated with increasing concentration of Ag NWs, the swelling ratio slightly decreased. PAsp/PVA/Collagen based hydrogel having no Ag NWs achieved highest swelling ratio of 1511% at pH 10 as compared to Ag NWs impregnated hydrogels. Hydrogel impregnated with 2.5 mg Ag NWs has highest swelling ratio of 1460%, whereas hydrogel loaded with 5 mg and 10 mg Ag NWs have SR (%) of 1405% and 1332% respectively. This could be due to the fact that Ag NWs blocked the void spaces inside the hydrogel network during gel formation and should bind with carboxylate and hydroxyl groups of polymer chains that neutralizes the repulsion in hydrogel matrix (Basu et al. 2018; Bajpai et al. 2011). This resulted in the formation of highly crosslinked structure which in turn lowered swelling ratio of hydrogel loaded with Ag NWs. The antibacterial properties of Ag NWs can help the wound dressings to control bacterial infections (Ahmed and Aggor 2010).
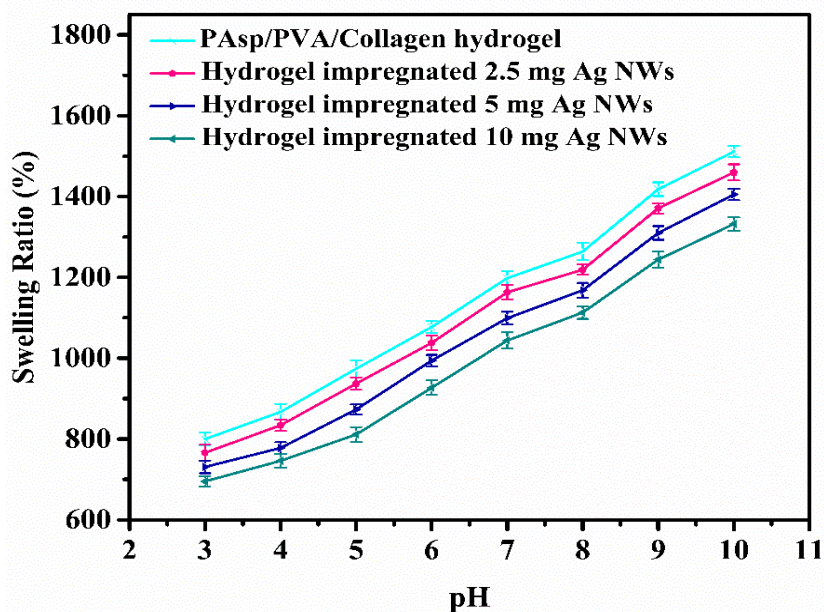
Figure 7.6 Effect of Ag NWs on swelling capacity of hydrogel in different pH

7.5 Release study of Ag NWs

The sustained release of silver ions from Ag NWs loaded hydrogel in distilled water was analysed by AAS as depicted in Figure 7.7. Analysis of results indicates that all the hydrogels followed same release profile i.e., very less amount of silver ions were released initially, but release rate increased gradually in a controlled manner over a period of 7 days or 168 hrs. The capability of Ag NWs to form percolated network within the hydrogel, owing to its large aspect ratio (Jiang and Teng 2017) has resulted in the phenomenon of suppressed release of Ag NWs with relatively less amount of silver ions, which supports the results obtained in the Figure 7.7. In case of hydrogel impregnated with 10 mg Ag NWs, more silver ions were released from hydrogel matrix as compared to hydrogel impregnated with 5 mg Ag NWs and hydrogel impregnated with 2.5 mg Ag NWs. This is due to repulsion between the neighbouring Ag NWs or ions in hydrogel matrix. If the silver concentration is more, release is more and if the silver concentration is less, release is less. Therefore, hydrogel loaded with 2.5 mg Ag NWs and 5 mg Ag NWs were considered for further animal studies as their released content of Ag ions is negligible. These wound dressing materials are safer to use for chronic wounds (Boonkaew et al. 2014; Jiang et al. 2020; Tao et al. 2019).
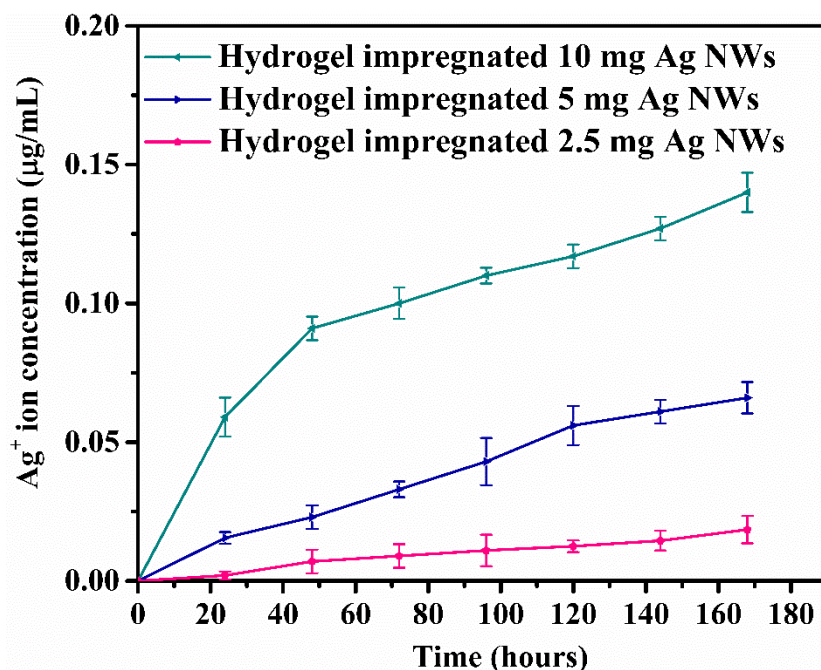
Figure 7.7 Release of silver ions from hydrogel impregnated with Ag NWs in distilled water

7.6 *In-vitro* assessment of antibacterial activity

For wound healing process, an ideal wound dressing material loaded with antibacterial agent should control bacterial infection. These Ag NWs should be entrapped or embedded in polymer matrix in order to control both the release of silver ions and bacterial growth. To assess the antibacterial activity of the synthesized PAsp/PVA/Collagen hydrogel loaded with different amounts of Ag NWs (2.5 mg, 5 mg and 10 mg) against *E. coli*, colony count method was used. The antibacterial effect of these hydrogels on the growth of *E. coli* was obtained by measuring initial (after 2 hrs) and final (after 15 hrs) OD at 600 nm. As the concentration of Ag NWs increased in the hydrogel matrix, the bacterial growth got decreased as demonstrated in Table 7.1. Further, colony forming unit analysis against *E. coli* was done to obtain the % reduction in viable *E. coli* count on LB plate before adding hydrogels and after adding hydrogels as shown in Table 7.1 and Figures 7.8 and 7.9 respectively.

Table 7.1 Quantitative data values of initial and final OD, CFU/mL and percentage reduction in *E. coli* CFU after incubating with hydrogel

S. No.	Initial O.D. (after 2 hrs)	Final O.D. (after 15 hrs)	Initial CFU/mL	Final CFU/mL	% CFU reduction
Control		1.247		Innumerable	-
PAsp/PVA/Collagen hydrogel (blank)		1.212		Innumerable	-
Hydrogel impregnated 2.5 mg Ag NWs	0.250	0.189	1.56×10^8	1.12×10^6	99.28
Hydrogel impregnated 5 mg Ag NWs		0.177		1.2×10^5	99.92
Hydrogel impregnated 10 mg Ag NWs		0.175		3.4×10^4	99.97
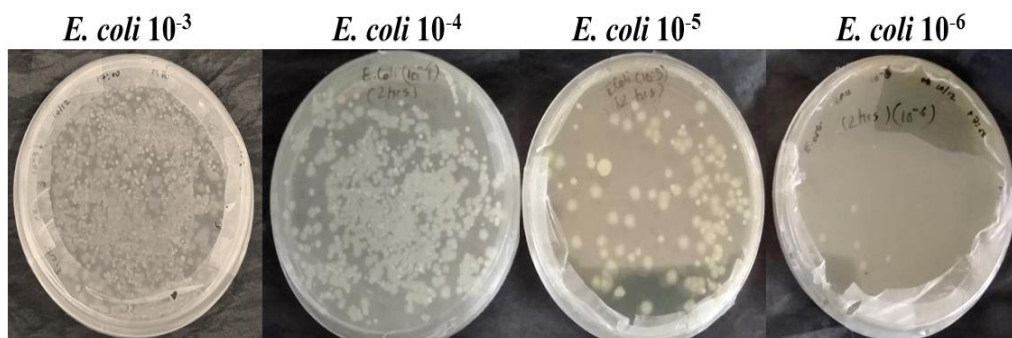
Figure 7.8 Serially diluted *E. coli* plates before adding hydrogel (after 2 hrs)
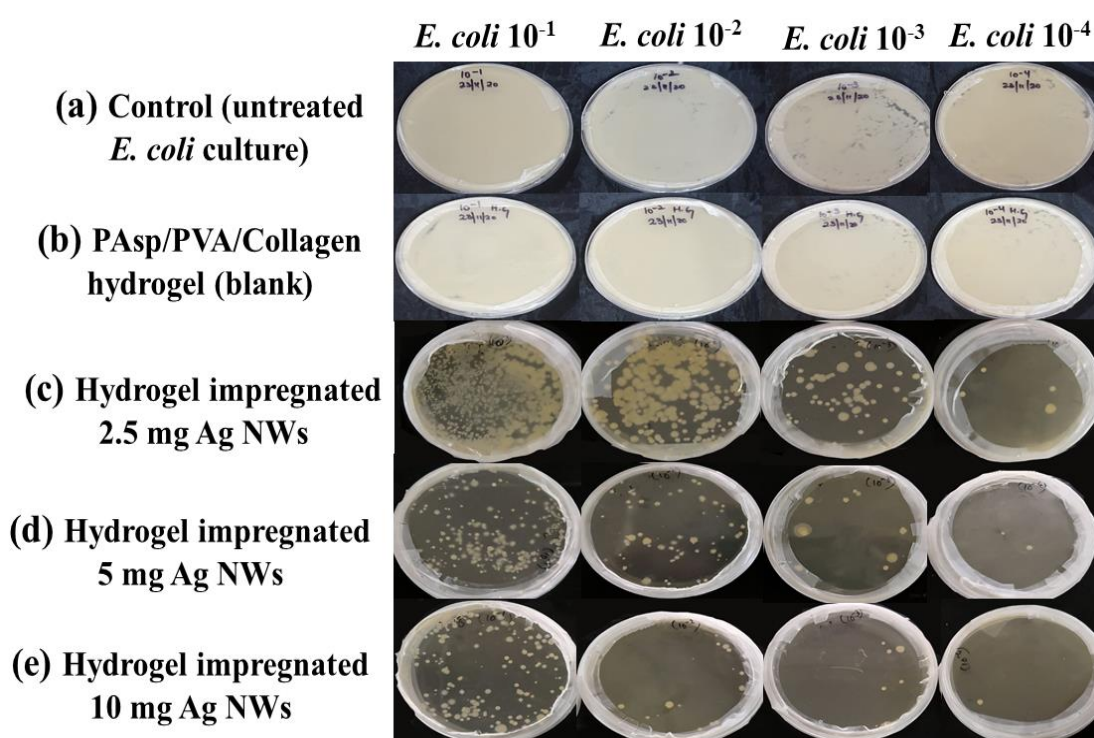
Figure 7.9 Serially diluted *E. coli* plates after incubated with hydrogel (after 15 hrs)

The results indicate that hydrogels impregnated with different amount of Ag NWs (2.5 mg, 5 mg, 10 mg) showed 99.28%, 99.92% and 99.97% reduction in viable *E. coli* colonies respectively after 15 hrs as compared to blank hydrogel (no Ag NWs) and control group as depicted in Figure 7.9. Innumerable colonies or formation of bacterial mats were observed on blank and control plate. This concludes that Ag NWs loaded hydrogel showed better antibacterial activity as compared to blank hydrogel and control group. The underlying reason is that silver ions released from hydrogel matrix interact with thiol group of bacterial respiratory enzyme leading to inhibition of bacterial growth (Li et al. 2020; Nguyen et al. 2019; Lustosa et al. 2017).

151

7.7 Degradation studies

Samples fabricated and being investigated in the present work were subjected to hydrolytic degradation studies in order to understand structural stability of hydrogel based wound dressing materials at the wound surface. As reported in Wang et al. (2012), polymers in general exhibit hydrolytic degradation behavior which mainly depends upon pH value, hydrophilicity, degree of crystallinity and the chemical composition. Figure 7.10 presents the results obtained from the degradation studies. It could be noticed from this figure that PAsp/PVA hydrogel exhibited a maximum degradation of 36.87% as compared to PAsp/PVA/Collagen hydrogel (29.77%), PAsp/PVA/Collagen hydrogel impregnated with 2.5 mg Ag NWs (22.68%), 5 mg Ag NWs (19.74%) and 10 mg Ag NWs (18.81%) on 35th day. In case of PAsp/PVA hydrogel, there is a gradual erosion of polymers from 7th day to 28th day. Maximum degradation was observed on 35th day and after that degradation rate became steady. PAsp/PVA/Collagen hydrogel showed a steady increment in the degradation rate from 7th day to 21st day and then sudden increase in degradation rate till 35th day. The increase in degradation rate could be due to breakdown of bonds in hydrolytic functional groups such as amide, ester, by the reaction of water that resulted in decrement of weight loss (Li et al. 2021).
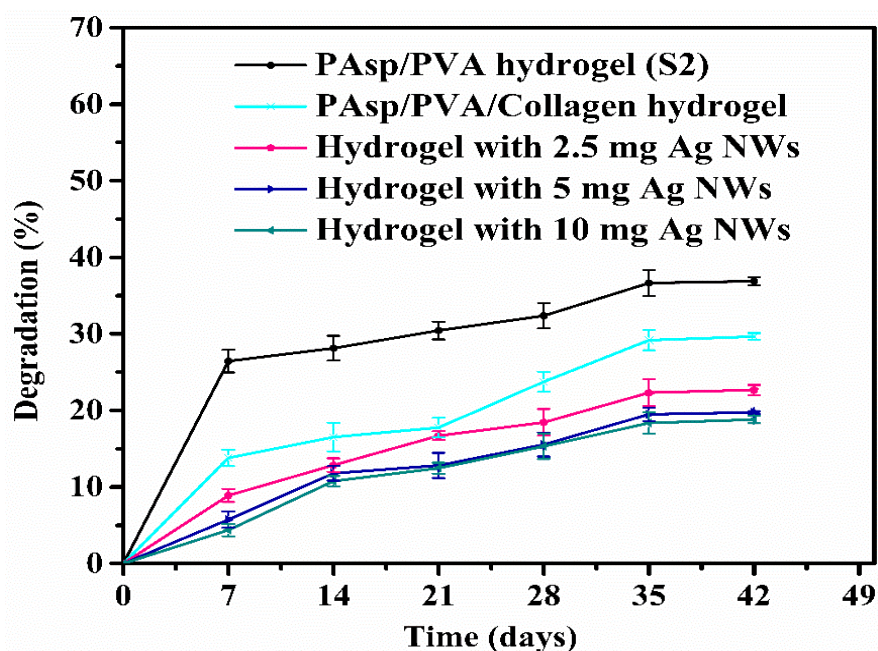
Figure 7.10 Degradation behavior of hydrogels in PBS buffer for a period of 42 days

Degradation rate was affected by the addition of Ag NWs in PAsp/PVA/Collagen hydrogel matrix. With increase in the content of Ag NWs, there was a decrease in the degradation rate. Reason behind this behavior is two folds i.e., microstructural strengthening due to the effect of entanglement in the presence of Ag NWs on hydrogel network boundaries and large cross linking leading to effective hindrance to the phenomenon of hydrolytic degradation. Consequently, the hydrogels impregnated with Ag NWs possessed high resistance to degradation. Henceforth, it was assumed that the PAsp/PVA/Collagen loaded with Ag NWs hydrogel based wound dressing materials would exist at the site of wound for a longer period of time to ensure fibroblast proliferation (Kandhasamy et al. 2017).

7.8 Cytotoxicity assay

The cytotoxic effect of synthesized smart hydrogel-based wound dressing materials such as PAsp/PVA hydrogel, PAsp/PVA/Collagen hydrogel, PAsp/PVA/Collagen hydrogel embedded with 2.5 mg Ag NWs, 5 mg Ag NWs and 10 mg Ag NWs on L929 fibroblast cells was evaluated by SRB assay. The cells were exposed to different concentrations of extraction media of hydrogel samples for 48 hrs. The cell viability of the hydrogel dressings with and without Ag NWs were compared with control (cells with no treatment) as shown in Figure 7.11a. It should be noticed from the figure that all hydrogel-based dressing materials exhibited cell viability greater than 95%, from which it is inferred that these dressings materials were not toxic to L929 cells. PAsp/PVA hydrogel had relatively less cell viability as compared to PAsp/PVA/Collagen hydrogel and PAsp/PVA/Collagen hydrogel embedded with 2.5 mg Ag NWs, 5 mg Ag NWs and 10 mg Ag NWs. This is due to the fact that with the addition of collagen in hydrogel matrix, cytocompatibility of the hydrogel is significantly improved as the collagen acts as natural substrate for promoting cell proliferation and adhesion (Bai et al. 2018; Xia et al. 2020). Therefore, the cell viabilities were increased and it is greater than 120% in case of PAsp/PVA/Collagen hydrogel and PAsp/PVA/Collagen hydrogel embedded with 2.5 mg Ag NWs, 5mg Ag NWs and 10 mg Ag NWs. Subsequently, hydrogels impregnated with 2.5 mg Ag NWs and 5 mg Ag NWs showed relatively greater cell viabilities than PAsp/PVA/Collagen embedded with 10 mg Ag NWs (Boonkaew et al. 2014). This could be inferred from

the results on release study of silver ions which confirmed that PAsp/PVA/Collagen hydrogel embedded with 10 mg Ag NWs releases comparatively more silver ions than hydrogels loaded with 2.5 mg Ag NWs and 5 mg Ag NWs. Thus, PAsp/PVA/Collagen hydrogel embedded with 2.5 mg Ag NWs and 5 mg Ag NWs were selected for *in-vivo* studies.
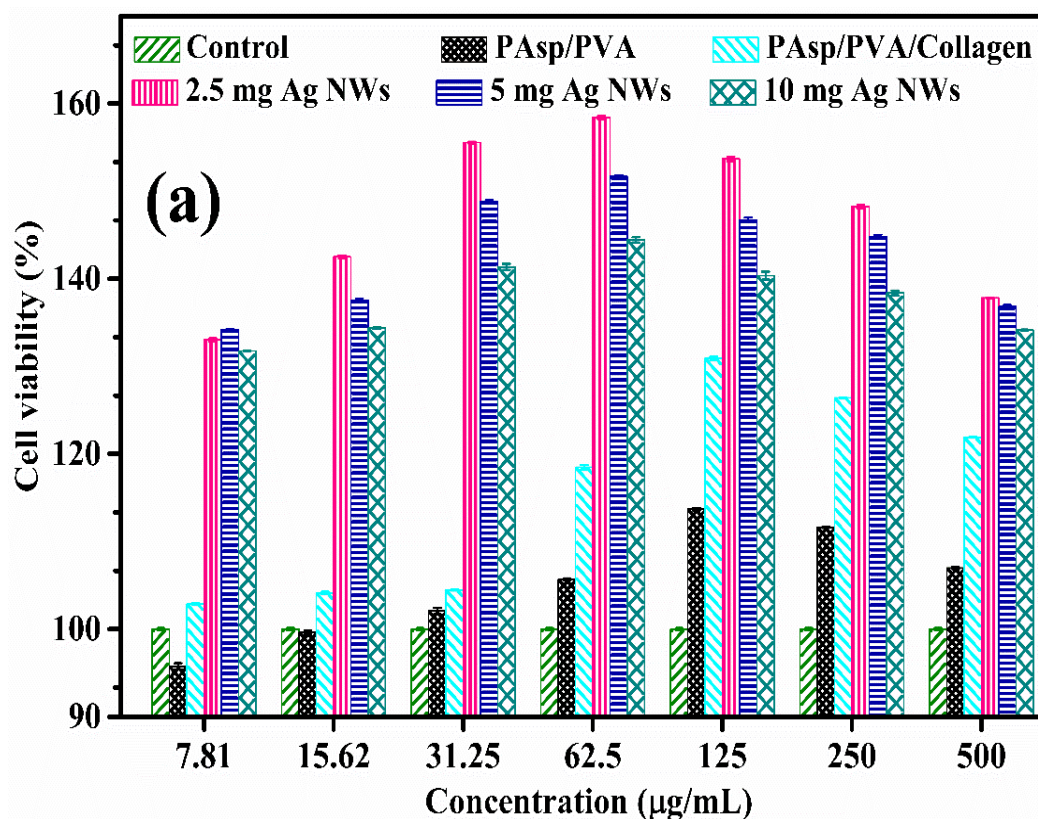
Figure 7.11 Cytotoxicity study of pH-sensitive hydrogel based wound dressing materials (a) Cell viability (%) of L929 cells treated exposed to different concentrations of hydrogel samples after 48 hrs incubation

The control and treated cells were also observed under phase contrast microscope (Labomeds, TCM 400) at 10X magnification after 48 hrs incubation (Figure 7.11b). The micrographs of control and extraction medium of hydrogel samples at low (7.81 µg/mL) and high concentration (500 µg/mL) has indicated that the cell viability was good. Henceforth, it can be concluded from the results that hydrogels loaded with Ag NWs had not shown toxicity, which makes them a suitable candidate for wound dressings promoting cell proliferation.

154

(b)

Concentration (µg/mL) ⟶

	Control	7.81	500

PAsp/PVA

PAsp/PVA/ Collagen

Hydrogel impregnated 2.5 mg Ag NWs

Hydrogel impregnated 5 mg Ag NWs

Hydrogel impregnated 10 mg Ag NWs
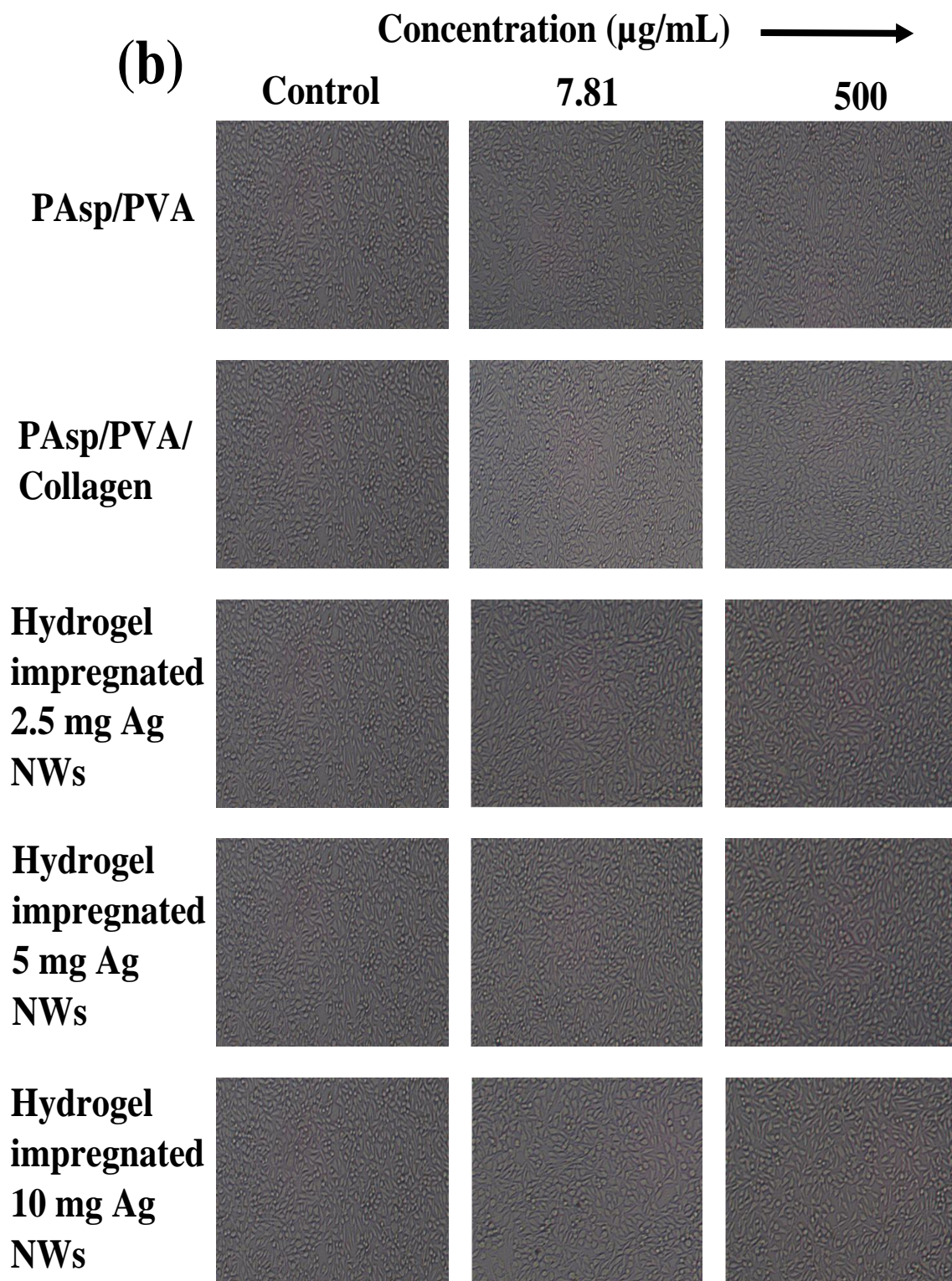
Figure 7.11 Cytotoxicity study of pH-sensitive hydrogel based wound dressing materials (b) Optical images of L929 cells treated at low (7.81 µg/mL) and high concentration (500 µg/mL) of hydrogel samples after 48 hrs incubation

7.9 *In-vivo* wound healing potential of pH-sensitive hydrogel-based dressing materials

Wound healing is a complex biological process that involves the repair of damaged epidermal and dermal tissues by the process of granulation tissue formation and wound contraction. The primary objective of *in-vivo* study was to examine the improvement in wound healing process due to pH-responsive behavior of developed dressing material, which results in absorption of excessive exudate, and maintain moist environment in the wound bed. Moreover, pH of the wound surface is reduced and inhibit microbial invasion, thus promoting epithelial cell migration and proliferation. Herein, wound healing efficacy of the prepared pH-sensitive hydrogel-based dressing material i.e., PAsp/PVA/Collagen impregnated with Ag NWs was assessed in full thickness excisional wound model in SD rats. The photographs of wound without any treatment (negative control, NC) and after treated with PAsp/PVA hydrogel, PAsp/PVA/Collagen hydrogel, PAsp/PVA/Collagen hydrogel loaded with 2.5 mg Ag NWs and 5 mg Ag NWs, commercially available silver nitrate gel (positive control, PC) were recorded on 0th day, 4th day, 8th day, 12th day and 16th day as shown in Figure 7.12a. The percentage of wound contraction of each animal group treated with dressings material at different time intervals and animal group without any treatment (negative control, NC) is presented in Figure 7.12b. It was noticed that all animals of group treated with PAsp/PVA/Collagen hydrogel loaded with 5 mg Ag NWs exhibited faster wound closure i.e., within four days as compared to animals of other treated groups and control groups. On day 4, animals treated with hydrogel loaded with 5 mg Ag NWs showed 58.46% wound closure, (49.30%) in negative control group, (54.45%) in positive control group, (53.84%) in PAsp/PVA hydrogel group, (54.91%) in PAsp/PVA/Collagen hydrogel group and (56.57%) in hydrogel loaded with 2.5 mg Ag NWs. However, statistically there was no significant difference in all groups treated with dressings when compared to negative control on 4th day.

In case of open wound or untreated wound, the healing rate was very slow because the surface of wound becomes dry, that led to the formation of scab/crust and impeded migration of epithelial cells towards the wound site. However, it was discerned that wound treated with dressing materials absorbed exudate as secreted on wound bed and

156
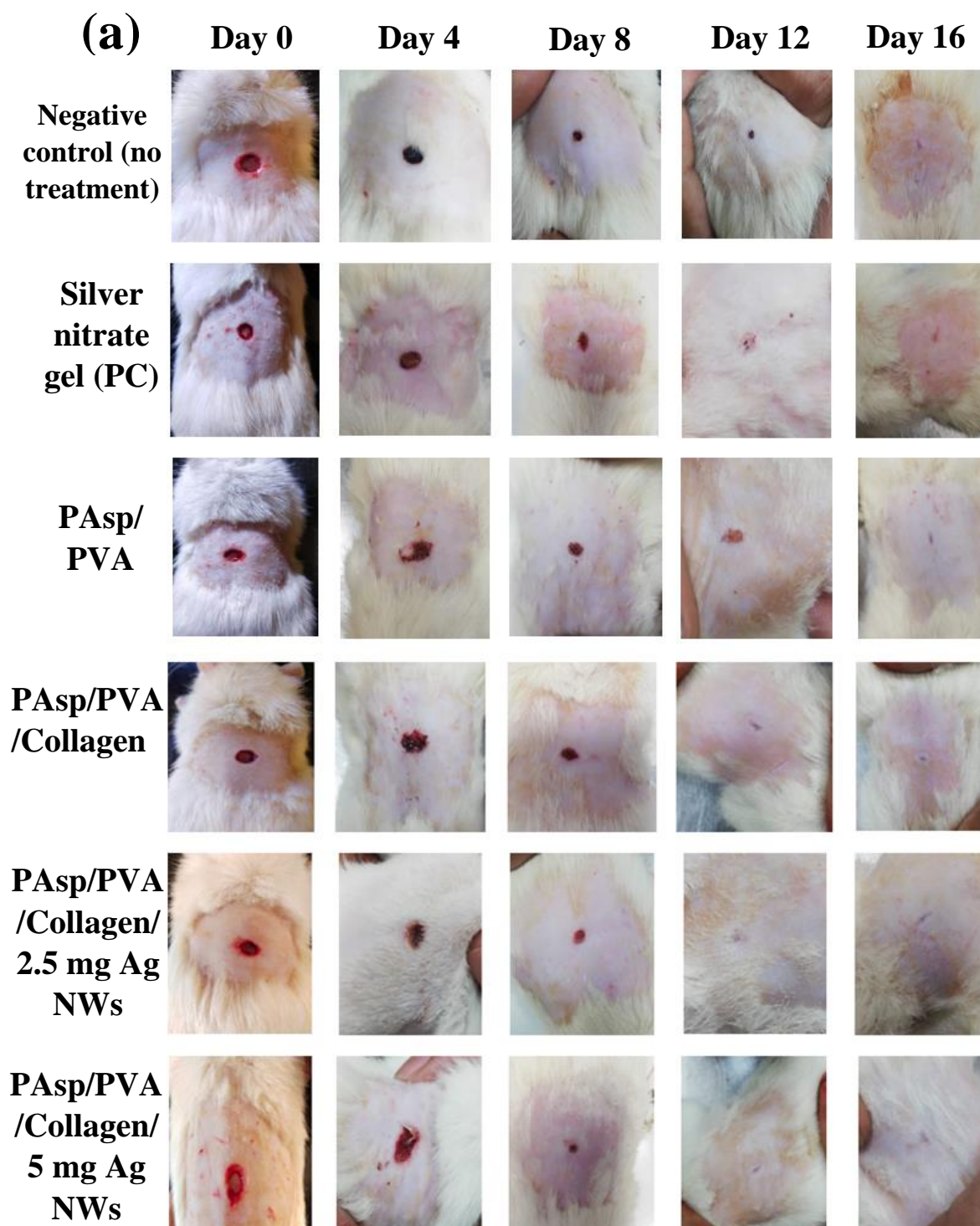
Figure 7.12 *In-vivo* wound healing efficacy of hydrogel-based dressing materials (a) Photographs of wounds without any treatment (negative control) and after treated with silver nitrate gel (positive control, PC), PAsp/PVA hydrogel, PAsp/PVA/Collagen hydrogel, hydrogel loaded with 2.5 mg Ag NWs and hydrogel loaded with 5 mg Ag NWs on days 0, 4, 8, 12 and 16

maintained moist wound environment that consequently resulted in migration of newly formed epithelial cells faster from wound edge to the injury site without any scab formation. Wounds covered with dressing materials showed faster healing rate as compared to standard silver nitrate gel because it was required to be applied once every day or otherwise wound dried up. However, these dressings were changed on every 4th day and they never adhered to wound area resulting in reduced damage to renewed epithelial cells. Similar trend of wound closure was observed on 8th day but statistically better results were obtained in case of animals group treated with PAsp/PVA/Collagen impregnated with 5 mg Ag NWs dressings as compared to negative control. This shows that hydrogel impregnated with 5 mg Ag NWs exhibited better healing rate as compared to other group animals.

PAsp/PVA hydrogels revealed better healing rate than control groups which was ascribed to pH-responsive behavior of hydrogel as they could absorb more exudate in alkaline pH and subsequently control the wound surface pH (Sharma et al. 2019b). The presence of collagen in PAsp/PVA hydrogel resulted in more improvement in the healing rate. This is because collagen in dressings acted as substrate for excessive levels of proteolytic enzymes such as MMPS present in chronic wounds responsible for its degradation and spared the ECM destruction (Chattopadhyay and Raines 2014). Hence, these collagen fragments are chemotactic for migration of fibroblasts and keratinocyte cells, which helps in the formation of granulation tissue and collagen synthesis. Moreover, collagen-based dressings, promote better cell adhesion and proliferation. In case of wounds treated with hydrogel loaded with Ag NWs showed faster wound healing as compared to other groups. This is attributed to the antimicrobial properties of Ag NWs which controls the infection on wound area (Rath et al. 2015). Further, Ag NWs tend to form percolated network (Jiang and Teng 2017) within hydrogel resulting in the phenomenon of suppressed release of Ag NWs on wound bed but acted as barrier inside the hydrogel matrix for the entry of microbes due to sustained release of silver ions in relatively lower amount. Therefore, animals treated with hydrogel loaded with 5 mg Ag NWs showed complete re-epithelization on 12th day i.e., 100% wound closure followed by 99.83% wound closure in hydrogel loaded with 2.5 mg Ag NWs group, 97.11% wound closure in PAsp//PVA/Collagen hydrogel group, 94.89% in PAsp/PVA hydrogel group, 90.06% in positive control group and 72.27% in negative control

group. Statistically, the difference was significant in groups treated with dressing materials w.r.t negative control except positive control on 12th day. All animals of other groups showed complete wound closure on 16th day with scar observed on skin and statistically no significant variations were observed. After 12th day, hair growth was observed, accompanied with no scar formation in case of wounds treated with hydrogel loaded with 5 mg Ag NWs. Henceforth, it is inferred that developed smart dressing material i.e., PAsp/PVA/Collagen hydrogel impregnated with 5 mg Ag NWs accelerated the healing process and showed complete wound closure within 12 days with scarless skin.
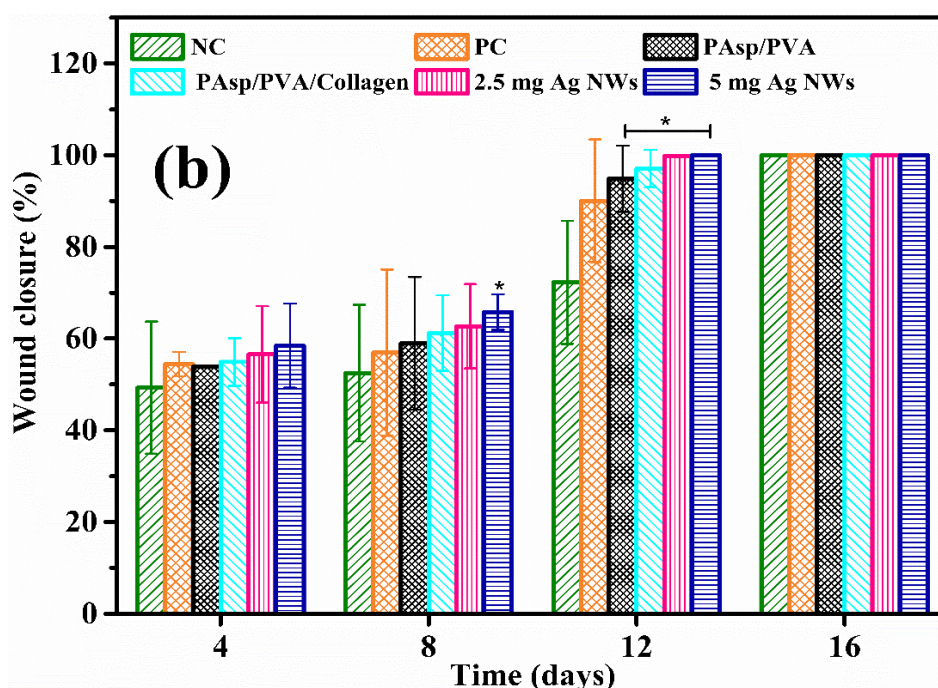
Figure 7.12 *In-vivo* wound healing efficacy of hydrogel-based dressing materials (b) Wound area closure (%) in animals after treatment with dressing materials and animals without treatment were used as negative control (NC). *P < 0.05, significant relative to negative control

7.10 Comparison of healing time of wound with other dressing materials

In Table 7.2, healing rate of wounds treated with developed pH-sensitive hydrogel-based dressing material i.e., PAsp/PVA/Collagen hydrogel loaded with 5 mg Ag NWs in animal model was compared with other wound dressing materials as reported in the literature. From the table, it is clear that the developed smart dressing material exhibits

better healing rate during all stages of wound healing when compared to other reported dressing materials and shows 100% wound closure within 12 days with scarless skin. This is due to the presence of collagen, which promotes cell proliferation while Ag NWs act as antimicrobial agent in dressing material.

Table 7.2 Comparison of PAsp/PVA/Collagen loaded with 5 mg Ag NWs hydrogel-based dressing material with other dressing materials in terms of healing time of wound

Wound dressing material	Antimicrobial agent	Wound healing time (days)	Reference
PNIPAM hydrogel (pH-sensitive)	Silk fibroin/alginate nanoparticles with vancomycin (antibiotics)	21 days with scar	Rezaei et al. 2021
Thiolated chitosan/silver nanowires composite	Silver nanowires	14 days with no scar	Li et al. 2020
Chitosan sponge	Quaternary ammonium chitosan nanoparticles (TMC NPs)	16 days with no scar	Xia et al. 2020
Chitosan/PEG hydrogel	Silver nanoparticles	12 days with no scar	Masood et al. 2019
Chitosan/poly(vinyl alcohol)	Silver nanoparticles	12 days with scar	Nguyen et al. 2019
Sericin/poly(vinyl alcohol) hydrogel	Silver nanoparticles	12 days with scar	Tao et al. 2019

Poly(aspartic and)/ polyacrylic acid with GHK-Cu peptide	GHK-Cu peptide	15 days with scar	Sharma et al. 2019b
PVP/CMC/Agar hydrogel	Silver nanoparticles	21 days with scar	Goetten de Lima et al. 2018
PVA/starch /chitosan hydrogel membranes	Nano zinc oxide	14 days with scar	Baghaie et al. 2017
Collagen-cellulose nanocrystal scaffolds	Curcumin/gelatin microspheres	21 days with scar	Guo et al. 2017
Collagen/chitosan scaffolds	Norfloxacin (antibiotics)	28 days with no scar	Mahmoud and Salama 2016
Collagen nanofiber	Silver nanoparticles	15 days with no scar	Rath et al. 2015
Acrylic acid with Ag/graphene hydrogel	Silver nanoparticles	15 days with no scar	Fan et al. 2014
PAsp/PVA/Collagen hydrogel impregnated with 5 mg Ag NWs (pH-sensitive hydrogel)	Silver nanowires	12 days with no scar	Present study

7.11 Histological examination of wounds

The results obtained during wound contraction were further confirmed by histological examination of collected wound samples on 4th day, 8th day and 16th day. The tissue sections were stained with H&E staining and examined microscopically to identify the changes in epidermis and dermis of skin tissue during healing process. The results are presented in Figure 7.13, Figure 7.14 and Figure 7.15.

7.11.1 Assessment of histological parameters on 4th day

It was noticed that on day 4, both groups i.e., animals treated with hydrogel loaded with 5 mg Ag NWs and 2.5 mg Ag NWs respectively had the highest healing score (13) as compared to other treated groups and control groups.
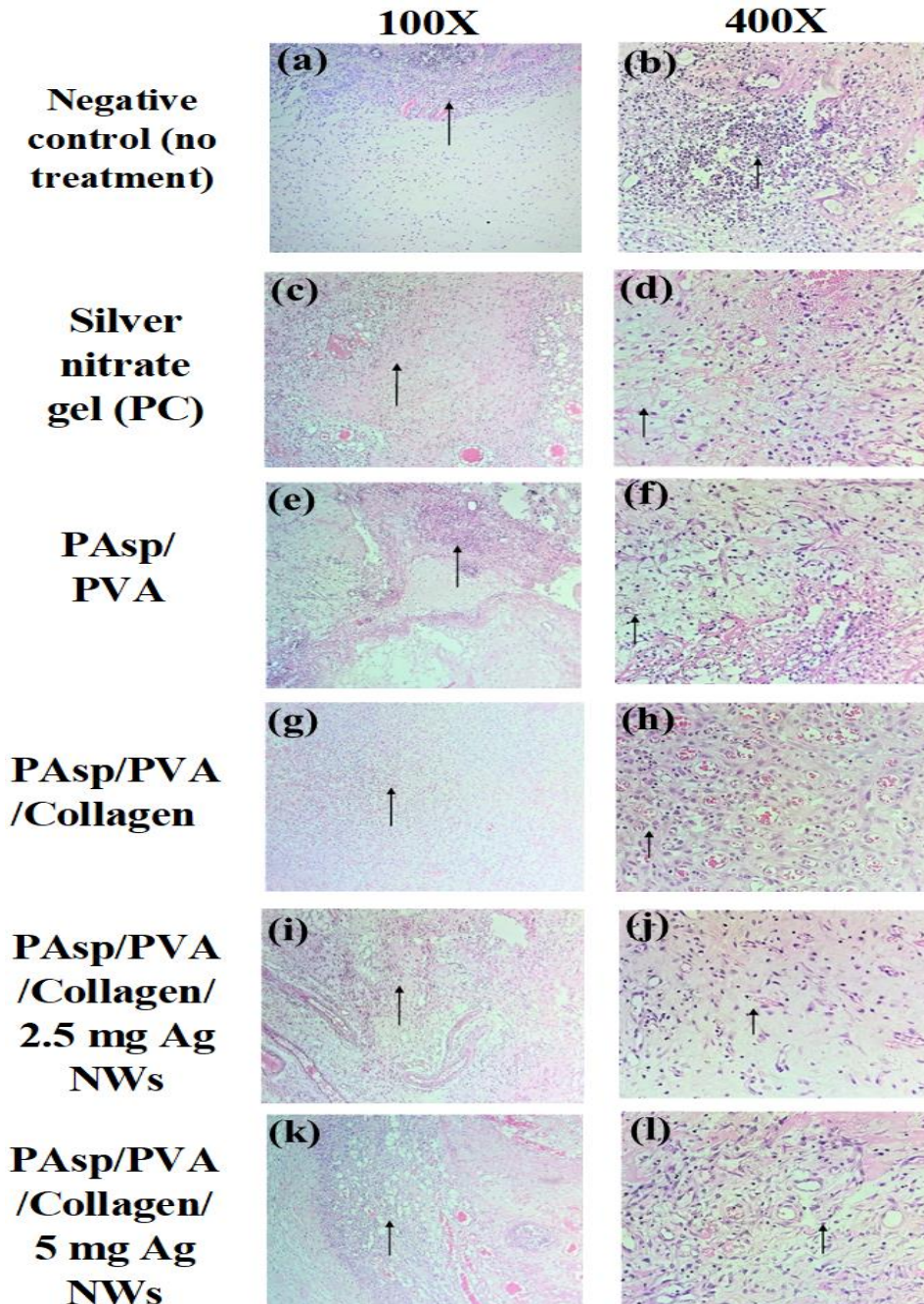
Figure 7.13 H&E-stained microscopic images of wound samples of different groups on 4th day

In these groups, moderate amount of granulation tissue (Figure 7.13, 100X and Figure 7.13, 100X; arrow), mixed collagen fibre orientation (Figure 7.13, 400X; arrow), mixed pattern of collagen and moderate amount of late collagen was observed. A few inflammatory infiltrates (Figure 7.13, 400X; arrow) and moderate amount of early collagen were present in group treated with hydrogel impregnated with 5 mg Ag NWs (Masood et al. 2019) while moderate inflammatory infiltrates (Figure 7.13j, arrow) and minimal amount of early collagen were observed in case of animals treated with 2.5 mg Ag NWs loaded hydrogel. Negative control group showed the lowest healing score (8) where moderate amount of granulation tissue (Figure 7.13a, arrow), profound amount of inflammatory infiltrates (Figure 7.13b, arrow), vertical collagen fibre orientation, reticular pattern of collagen, profound amount of early collagen and moderate amount of late collagen were observed. Animals treated with silver nitrate gel, PAsp/PVA hydrogel had same healing score (10) whereas PAsp/PVA/Collagen hydrogel group had healing score (11) with profound amount of granulation tissue, moderate inflammatory cells (Figure 7.13g, arrow), mixed collagen pattern and fibre orientation (Figure 7.13h, arrow), moderate amount of early and late collagen were present. Positive control group and PAsp/PVA hydrogel group showed moderate amount of granulation tissue, moderate inflammatory cells (Figure 7.13c and Figure 7.13e, arrow), vertical collagen fibre orientation, reticular pattern of collagen (Figure 7.13d and Figure 7.13f, arrow), profound amount of early and minimal amount of mature collagen.

7.11.2 Assessment of histological parameters on 8th day

On 8th day, 5 mg Ag NWs loaded hydrogel treated group exhibited the highest healing score (17) as compared to other treated groups and control groups. Scant amount of granulation tissue (Figure 7.14k, arrow), moderate inflammatory infiltrates (Figure 7.14l, arrow), horizontal collagen fibre orientation, fascicle pattern of collagen was observed whereas negative control group showed moderate granulation tissue, moderate inflammatory cells, mixed collagen fibres (Figure 7.14a, arrow) and reticular pattern of collagen (Figure 7.14b, arrow). Further, amount of early and mature collagen was minimal in hydrogel loaded with 5 mg Ag NWs treated group while minimal amount of early collagen and moderate amount of mature collagen were present in negative control group. Thus, it can be said that 5 mg Ag NWs loaded hydrogel group

had faster wound healing rate as compared to negative control group which had lowest healing score (11).
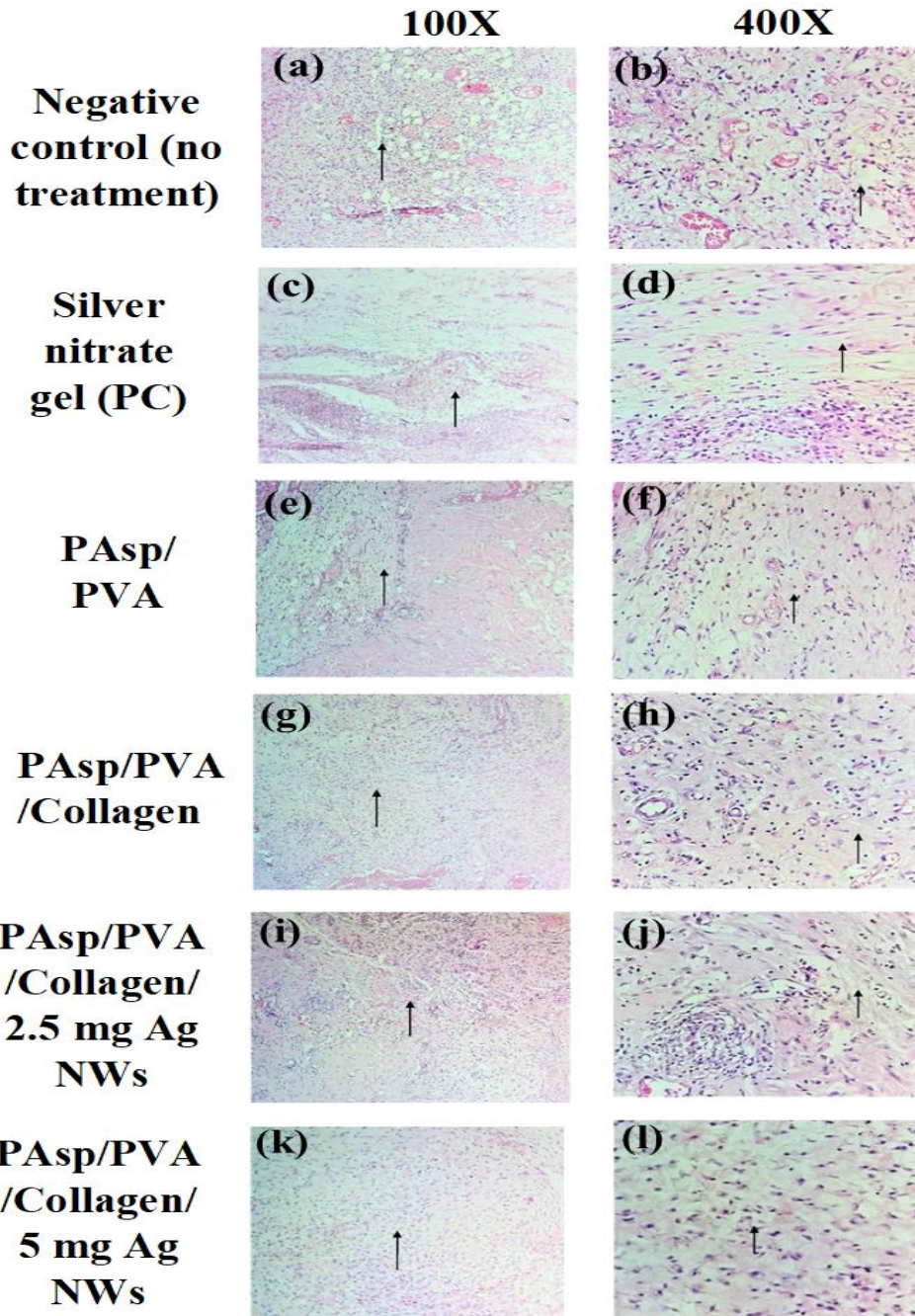
Figure 7.14 H&E-stained microscopic images of wound samples of different groups on 8th day

Animals of other treated groups also showed good healing score as compared to negative control. Both positive control and PAsp/PVA groups had same healing score

(14) with moderate amount of granulation tissue (Figure 7.14c and Figure 7.14e, arrow), moderate inflammatory infiltrates, horizontal collagen fibre orientation (Figure 7.14d and Figure 7.14e, arrow), mixed pattern of collagen (Figure 7.14f, arrow), minimal amount of early collagen and moderate amount of mature collagen were observed. Moderate granulation tissues were observed with moderate inflammatory infiltrates, horizontal collagen fibre orientation (Figure 7.14g, arrow), fascicle pattern of collagen (Figure 7.14h, arrow), minimal amount of early collagen and moderate amount of mature collagen in PAsp/PVA/Collagen treated group. 2.5 mg Ag NWs loaded hydrogel treated group showed moderate granulation tissue (Figure 7.14i, arrow), mild inflammatory infiltrates (Figure 7.14j, arrow), horizontal collagen orientation, fascicle collagen pattern, minimal amount of early collagen and moderate amount of mature collagen. Based on these histological parameters, healing score was obtained (15) in PAsp/PVA/Collagen group and (16) in hydrogel loaded with 2.5 mg Ag NWs group.

7.11.3 Assessment of histological parameters on 16th day

On day 16, it was observed that all groups had good healing score and showed complete re-epithelization. Animals treated with hydrogel impregnated with 5 mg Ag NWs and 2.5 mg Ag NWs showed healing score (19) and (18) respectively with scant amount of granulation tissue, mild inflammatory infiltrates, horizontal collagen orientation (Figure 7.15i and Figure 7.15k, arrow), fascicle collagen pattern (Figure 7.15j and Figure 7.15l, arrow). Minimal amount of mature collagen was present and early collagen was absent in 5 mg loaded hydrogel group whereas in 2.5 mg Ag NWs loaded hydrogel group minimal amount of early collagen was present (Sultana et al. 1970; Kandhasamy et al. 2017). The other treated groups positive control, PAsp/PVA, and PAsp/PVA/Collagen had same healing score (17) with scant granulation tissue, mild inflammatory cells, horizontal collagen fibre orientation (Figure 7.15c, Figure 7.15e and Figure 7.15g, arrow), fascicle pattern of collagen (Figure 7.15d, Figure 7.15f and Figure 7.15h, arrow), minimal early collagen and moderate amount of mature collagen. Negative control group also showed good healing score (16) on 16th day with moderate amount of granulation tissue, mild inflammatory cells, horizontal collagen orientation (Figure 7.15a, arrow) fascicle pattern of collagen (Figure 7.15b, arrow), minimal

amount of early collagen and moderate amount of mature collagen. Thus, it can be concluded that animals treated with PAsp/PVA/Collagen hydrogel loaded with 5 mg Ag NWs showed good wound healing score on each day as compared to other treated groups and control groups.
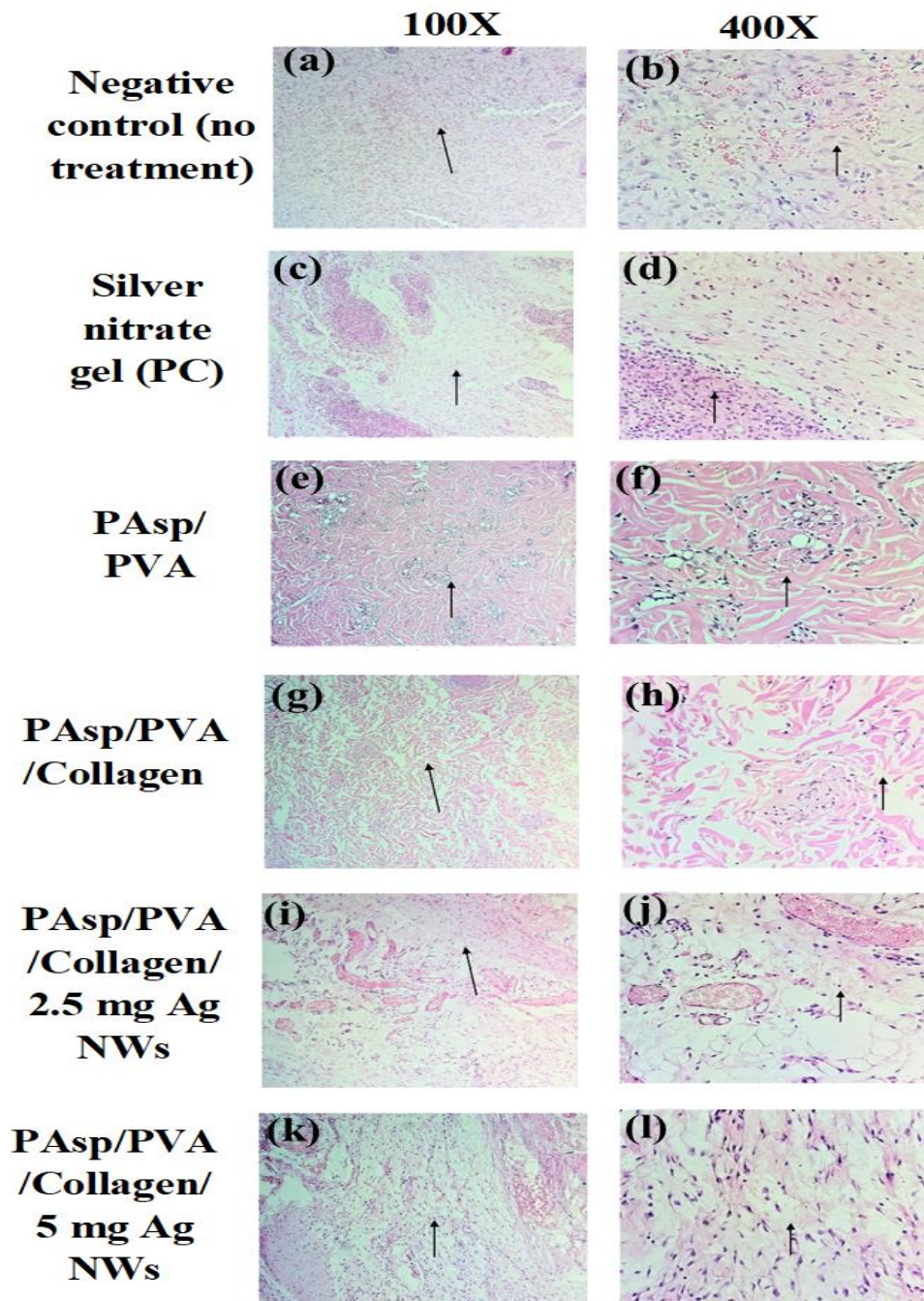
Figure 7.15 H&E-stained microscopic images of wound samples of different groups on 16th day

CHAPTER 8

SUMMARY AND CONCLUSIONS

8.1 Summary

The research work carried out in this dissertation and the conclusions obtained are summarized in this chapter. A comprehensive literature survey beginning from the development of traditional wound dressing materials was carried out in the present thesis work. Special attention was laid upon the critical review on the developed modern wound dressing materials essentially required for healing of chronic wounds; particularly in recent past years. Through this assessment, it was revealed that an urgent need exists for bringing new generation pH sensitive smart hydrogel based wound dressing materials. This is due to the fact that commercialized hydrogel dressing materials fail to retain optimal exudate of chronic wounds in response to wound pH and simultaneously to take control on bacterial infections thus leading to an impaired wound healing process. Accordingly, the present detailed research work endeavour was a step forward in this direction. The topic of this thesis comprehended the development and characterization of pH sensitive hydrogel based wound dressing material which maintains an optimum level of exudate in response to wound pH, through which MMPs activity can be controlled to attain better healing process. The synthesized smart pH-sensitive hydrogel is also capable of reducing bacterial infection because of Ag NWs incorporation.

In the present research work, smart wound dressing material i.e., PAsp/PVA/Collagen hydrogel impregnated with Ag NWs was successfully synthesized by free radical polymerization method and optimizing the process variables. In lieu of this achievement, this experimental research work was specifically addressed through five main objectives i.e., extraction of collagen from sole fish skin, synthesis of Ag NWs, synthesis of pH-sensitive hydrogel, synthesis of smart wound dressing material, and animal studies. The synthesized pH-sensitive hydrogel based wound dressing material was characterized using SEM-EDAX, FTIR, DSC, TGA, XRD while average diameter of Ag NWs was studied by particle size analysis and SDS-PAGE was carried out to

confirm collagen type. Antibacterial analysis of synthesized Ag NWs and developed pH-sensitive hydrogel based wound dressing material i.e., PAsp/PVA/Collagen impregnated with Ag NWs were evaluated against *E. coli* bacterium. The swelling behavior of hydrogel was studied in response to pH of medium and the cytotoxicity studies were also carried out to assess the biocompatibility. The results revealed that hydrogels are pH-sensitive and biocompatible. *In-vivo* studies were carried out to assess the wound healing potential of developed smart wound dressing material.

8.2 Conclusions

Following are some of the important conclusions from the current research work that are believed to address few knowledge gaps on the development of hydrogel-based pH-sensitive wound dressing material for accelerating healing process.

- Collagen was successfully extracted from Sole fish skin and the maximum collagen yield of 19.27 ± 0.05 mg/g of fish skin was achieved under the optimal conditions. This study has showed that improved yield of collagen was obtained when the concentration of acetic acid was 0.54 M, NaCl concentration of 1.90 M, solvent/solid ratio of 8.97 mL/g and time of 32.32 hrs.

- The response surface methodology with BBD was implemented and the optimal conditions (acetic acid, NaCl, solvent/solid ratio and time) to obtain the highest collagen yield (per gram of fish skin) were determined.

- It was found that each of the four variables showed a significant effect on the extraction of collagen from the Sole fish skin and a positive relation was observed between all these variables.

- The obtained mathematical model had an R^2 value of 0.9972 and a P-value of < 0.0001 which implied a good agreement between the predicted values and the experimental values of the yield of collagen from Sole fish skin and affirmed a good generalization of the mathematical model.

- Collagen extracted from Sole fish skin was found to be type I collagen, which consists of three α-chains and one β sheet ((α1)$_2$, α2, β). FTIR analysis indicated the presence of helical arrangement of collagen. SEM analysis of collagen confirms the presence and organization of collagen fibrils.

- Uniform and thin Ag NWs were synthesized by facile hydrothermal method using fructose as a reducing agent. SEM images showed that ultra-long, uniform and thin Ag NWs were obtained under optimal conditions with 0.02 M AgNO$_3$, 0.16 g/mL PVP concentration, 0.016 g/mL fructose concentration at 160 °C within 22 hrs.

- It was observed that less and high amounts of PVP, fructose and AgNO$_3$ formed undesired silver structures along with nanowires. Below the optimal temperature (160 °C), Ag NW formation was not observed and beyond that optimal temperature, micro-sized silver particles started growing dominantly which suppressed Ag NW formation.

- DLS analysis revealed that the Ag NWs obtained have an average diameter of 77 nm possessing high level of crystallinity with FCC phase that is evident from XRD peaks at (111), (200), (220), (311) and (222) planes. FTIR results suggested that there is adsorption of PVP molecules on the silver atoms.

- Antimicrobial activity was assayed against bacterium *E. coli* and the best inhibitory activity was observed at 80 μg/mL by measuring the O.D. at 600 nm. The synthesized Ag NWs exhibited better antioxidant activity of 67.22% (IC$_{50}$ =17.36 μg/mL).

- pH-sensitive hydrogel based on PAsp/PVA blended with and without collagen were prepared by free radical polymerization method. PAsp/PVA (S1) hydrogel showed highest swelling ratio of 1657% at pH 10 under the obtained optimized values as PAsp (100 mg), 2 mL of 8% PVA, 2 mL of 0.75 mM EGDMA and APS (125 mg). In spite of the highest swelling ratio, this hydrogel lost its stability on the addition of collagen (1 mg/mL).

- Hydrogel samples S2, S3 and S4 were further prepared by increasing the feed composition of S1 hydrogel. Among these, S2 showed the best physical strength and swelling ratio (1286%) as compared to other hydrogel samples with optimal conditions obtained as PAsp (150 mg), 8% PVA (3 mL), 0.75 mM EGDMA (3 mL) and APS (188 mg).

- The swelling ratio was increased from 1286% to 1511% upon addition of collagen (1 mg/mL) in the hydrogel (S2) at pH 10. This showed that the composite hydrogel had a good pH-sensitivity to alkaline environments and

attained a higher swelling degree when the PAsp/PVA/collagen hydrogel scaffold was immersed in buffer solution (pH = 10) as compared to pH 3.

- SEM analysis showed that the presence of open and porous network structure within the hydrogel and also the porosity of network increased with increase in pH.

- Thermal behavior of the synthesized hydrogel was determined using DSC and TGA, which concluded that the thermal stability of PAsp/PVA/Collagen hydrogel was greatly improved by the integration of collagen into the PAsp/PVA hydrogels.

- FTIR results of PAsp/PVA/Collagen and PAsp/PVA hydrogel showed the small displacement in peaks which confirmed the interaction between the polymers such as collagen, PAsp and PVA.

- A smart wound dressing material i.e., PAsp/PVA/Collagen hydrogel impregnated with Ag NWs was prepared by free radical polymerization.

- The swelling behavior of hydrogel impregnated with and without different amounts of Ag NWs (2.5 mg, 5 mg and 10 mg) was also studied. The swelling ratio of PAsp/PVA/Collagen hydrogel (1511%) slightly decreased with the addition of Ag NWs. Hydrogel impregnated with 2.5 mg Ag NWs has highest swelling ratio of 1460% whereas hydrogel loaded with 5 mg and 10 mg Ag NWs have SR (%) of 1405% and 1332% at pH 10 respectively. The prepared dressing material had good pH-sensitivity to alkaline environments and exhibited maximum swelling at pH 10 and minimum at pH 3.

- Furthermore, addition of Ag NWs in hydrogel matrix also affected the degradation rate. With increase in the content of Ag NWs, there was decrease in degradation rate. The existence of Ag NWs in hydrogel network was confirmed by EDAX and XRD. SEM results revealed that pore size of hydrogel reduced with increase in concentration of Ag NWs which is due to the fact that Ag NWs agglomerated within hydrogel matrix and block porous structure of hydrogel.

- The release profile of silver ions from PAsp/PVA/Collagen hydrogel loaded with 2.5 mg and 5 mg Ag NWs displayed very less amount of silver ions were released as compared to hydrogel impregnated with 10 mg Ag NWs.

- *In-vitro* cytotoxicity assay revealed that developed wound dressing materials had not shown any toxicity on L929 cells and promotes cell proliferation. Also, antibacterial activity of blank hydrogel and hydrogel loaded with Ag NWs was evaluated against *E. coli*. Hydrogel loaded with 2.5 mg Ag NWs, 5 mg Ag NWs and 10 mg Ag NWs exhibited 99.28%, 99.92% and 99.97% reduction in viable *E. coli* colonies respectively as compared to blank hydrogel.

- *In-vivo* wound healing studies showed that PAsp/PVA/Collagen impregnated with 5 mg Ag NWs accelerated the healing process and showed complete wound closure within 12 days with scarless skin which is also confirmed from assessment of histological parameters.

- Histological examination revealed that animals treated with PAsp/PVA/Collagen hydrogel loaded with 5 mg Ag NWs showed good wound healing score on each day as compared to other treated groups and control groups.

- Therefore, it can be concluded that PAsp/PVA/Collagen hydrogel impregnated with 5 mg Ag NWs can be a novel wound dressing material for chronic wounds.

8.3 Future Scope

- *In-vivo* studies using diabetic animal model.
- Embedment of pH sensor in wound dressing material to monitor wound surface pH.
- Incorporation of growth factors such as EGF (epidermal growth factor), FGF (fibroblast growth factor) and antibiotics such as painkiller in wound dressing material that promotes wound healing and relives pain.
- Compare wound healing test for male vs female rats.

REFERENCES

Abe, Y., and Krimm, S. (1972). "Normal vibrations of crystalline polyglycine I." *Biopolymers*, 11(9), 1817-1839.

Abraham, G. A., Queiroz, A. A. A. D., and Román, J. S. (2001). "Hydrophilic hybrid IPNs of segmented polyurethanes and copolymers of vinylpyrrolidone for applications in medicine." *Biomaterials*, 22(14), 1971-1985.

Abrigo, M., McArthur, S. L., and Kingshott, P. (2014). "Electrospun nanofibers as dressings for chronic wound care: Advances, challenges, and future prospects." *Macromol. Biosci.*, 14(6), 772-792.

Addad, S., Exposito, J. Y., Faye, C., Ricard-Blum, S., and Lethias, C. (2011). "Isolation, characterization and biological evaluation of jellyfish collagen for use in biomedical applications." *Mar. Drugs*, 9(6), 967-983.

Ahmed, E. M. (2015) "Hydrogel: Preparation, characterization, and applications: A review." *J. Adv. Res.*, 6(2), 105-121.

Ahmed, E. M., and Aggor, F. S. (2010). "Swelling kinetic study and characterization of crosslinked hydrogels containing silver nanoparticles." *J. Appl. Polym. Sci.*, 117(4), 2168-2174.

Ajayi, E., and Afolayan, A. (2017). "Green synthesis, characterization and biological activities of silver nanoparticles from alkalinized *Cymbopogon citratus* Stapf." *Adv. Nat. Sci.: Nanosci. Nanotechnol.*, 8, 1-8.

Alvarez-Lorenzo, C., Bromberg, L., and Concheiro, A. (2009). "Light-sensitive intelligent drug delivery systems." *Photochem. Photobiol.*, 85(4), 848-860.

Alvarez-Lorenzo, C., Concheiro, A., Dubovik, A. S., Grinberg, N. V., Burova, T. V., and Grinberg, V. Y. (2005). "Temperature-sensitive chitosan-poly(N-isopropylacrylamide) interpenetrated networks with enhanced loading capacity and controlled release properties." *J. Control. Release*, 102(3), 629-641.

Amal, B., Veena, B., Jayachandran, V. P., and Shilpa, J. (2015). "Preparation and characterisation of *Punica granatum* pericarp aqueous extract loaded chitosan-collagen-starch membrane: role in wound healing process." *J. Mater. Sci. Mater. Med.*, 26(5), 181.

Anisha, B. S., Biswas, R., Chennazhi, K. P., and Jayakumar, R. (2013). "Chitosan-hyaluronic acid/nano silver composite sponges for drug resistant bacteria infected diabetic wounds." *Int. J. Biol. Macromol.*, 62, 310-320.

Aswathy, S. H., Narendrakumar, U., and Manjubala, I. (2020). "Commercial hydrogels for biomedical applications." *Heliyon*, 6(4), e03719.

Baghaie, S., Khorasani, M. T., Zarrabi, A., and Moshtaghian, J. (2017). "Wound healing properties of PVA/starch/chitosan hydrogel membranes with nano zinc oxide as antibacterial wound dressing material." *J. Biomater. Sci. Polym. Ed.*, 28(18), 2220-2241.

Bai, Z., Dan, W., Yu, G., Wang, Y., Chen, Y., Huang, Y., Yang, C., and Dan, N. (2018). "Tough and tissue-adhesive polyacrylamide/collagen hydrogel with dopamine-grafted oxidized sodium alginate as crosslinker for cutaneous wound healing." *RSC Adv.*, 8(73), 42123-42132.

Bajpai, A. K., Sandeep, K. S., Smitha, B., and Sanjana, K. (2008). "Responsive polymers in controlled drug delivery." *Prog. Polym. Sci.*, 33, 1088-1118.

Bajpai, S. K., Bajpai, M., and Sharma, L. (2011). "*In situ* formation of silver nanoparticles in poly(N-isopropyl acrylamide) hydrogel for antibacterial applications." *Des. Monomers Polym.*, 14(4), 383-394.

Balaji, S., and Kumar, M. B. (2017). "Facile green synthesis of zinc oxide nanoparticles by *Eucalyptus globulus* and their photocatalytic and antioxidant activity." *Adv. Powder Technol.*, 28 (10), 785-797.

Banerjee, I., Mishra, D., Das, T., and Maiti, T. K. (2012). "Wound pH-responsive

sustained release of therapeutics from a poly(NIPAAm-co-AAc) hydrogel." *J. Biomater. Sci. Polym. Ed.*, 23(1-4), 111-132.

Bari, B., Lee, J., Jang, T., Won, P., Ko, S. H., Alamgir, K., Arshad, M., and Guo, L. J. (2016). "Simple hydrothermal synthesis of very-long and thin silver nanowires and their application in high quality transparent electrodes." *J. Mater. Chem. A*, 4(29), 11365-11371.

Basu, S., Samanta, H. S., and Ganguly, J. (2018). "Green synthesis and swelling behavior of Ag-nanocomposite semi-IPN hydrogels and their drug delivery using *Dolichos biflorus* Linn." *Soft Mater.*, 16(1), 7-19.

Bavaresco, V. P., Zavaglia, C. A. C., Reis, M. C., and Gomes, J. R. (2008). "Study on the tribological properties of pHEMA hydrogels for use in artificial articular cartilage." *Wear*, 265(3-4), 269-277.

Bektas, N., Şenel, B., Yenilmez, E., Özatik, O., and Arslan, R. (2020). "Evaluation of wound healing effect of chitosan-based gel formulation containing vitexin." *Saudi Pharm. J.*, 28(1), 87-94.

Bemmelen, J. M. V. (1894). "Der Hydrogel und das kristallinische Hydrat des kupferoxydes". *Z. Anorg. Chem.*, 5, 466-483.

Benamer, S., Mahlous, M., Boukrif, A., Mansouri, B., and Youcef, S. L. (2006). "Synthesis and characterisation of hydrogels based on poly(vinyl pyrrolidone)." *Nucl. Instrum. Meth. B*, 248(2), 284-290.

Bhishagratna, K. K. (1963). "The Sushruta Samhita." Chowkhamba Sanskrit Series Office, Varanasi, India.

Biswas, T. K., and Mukherjee, B. (2003). " Plant medicines of Indian origin for wound healing activity: A review." *Int. J. Low. Extrem. Wounds*, 2(1), 25-39.

Boateng, J., and Catanzano, O. (2015). "Advanced therapeutic dressings for effective wound healing - A review." *J. Pharm. Sci.*, 104(11), 3653-3680.

Boateng, J. S., Matthews, K. H., Stevens, H. N. E., and Eccleston, G. M. (2008). "Wound healing dressings and drug delivery systems: A review." *J. Pharm. Sci.*, 97(8), 2892-2923.

Boonkaew, B., Suwanpreuksa, P., Cuttle, L., Barber, P. M., and Supaphol, P. (2014). "Hydrogels containing silver nanoparticles for burn wounds show antimicrobial activity without cytotoxicity." *J. Appl. Polym. Sci.*, 131(9), 40215.

Bowler, P. G., Duerden, B. I., and Armstrong, D. G. (2001). "Wound microbiology and associated approaches to wound management." *Clin. Microbiol. Rev.*, 14(2), 244-269.

Braun, E., Eichen, Y., Sivan, U., and Ben-Yoseph, G. (1998). "DNA-templated assembly and electrode attachment of a conducting silver wire." *Nature*, 391(6669), 775-778.

Brett, D. (2008). "A review of collagen and collagen-based wound dressings." *Wounds*, 20(12), 347-356.

Bukhari, S. M. H., Khan, S., Rehanullah, M., and Ranjha, N. M. (2015). "Synthesis and characterization of chemically cross-linked acrylic acid/gelatin hydrogels: Effect of pH and composition on swelling and drug release." *Int. J. Polym. Sci.*, 2015, 1-15.

Buwalda, S. J., Boere, K. W. M., Dijkstra, P. J., Feijen, J., Vermonden, T., and Hennink, W. E. (2014). "Hydrogels in a historical perspective: From simple networks to smart materials." *J. Control. Release*, 190, 254-273.

Caló, E., and Khutoryanskiy, V. V. (2015). "Biomedical applications of hydrogels: A review of patents and commercial products." *Eur. Polym. J.*, 65, 252-267.

Cao, H., Zhu, J., Su, H., Fang, L., and Tan, T. (2009). "Preparation a novel pH-sensitive blend hydrogel based on polyaspartic acid and ethylcellulose for controlled release of naproxen sodium." *J. Appl. Polym. Sci.*, 113(1), 327-336.

Cardona, A. F., and Wilson, S. E. (2015). "Skin and soft-tissue infections: A critical review and the role of telavancin in their treatment." *Clin. Infect. Dis.*, 61(suppl_2),

S69-S78.

Cavendish, M. (2007). "Inventors and inventions." Marshall Cavendish Corporation, New York.

Chai, Q., Jiao, Y., and Yu, X. (2017). "Hydrogels for biomedical applications: Their characteristics and the mechanisms behind them." *Gels*, 3, 6-21.

Chattopadhyay, S., and Raines, R. T. (2014). "Review collagen-based biomaterials for wound healing." *Biopolymers*, 101(8), 821-833.

Chaudhari, A. A., Vig, K., Baganizi, D. R., Sahu, R., Dixit, S., Dennis, V., Singh, S. R., and Pillai, S. R. (2016). "Future prospects for scaffolding methods and biomaterials in skin tissue engineering: A review." *Int. J. Mol. Sci.*, 17(12), 1974.

Chavda, H., and Patel, C. (2011). "Effect of crosslinker concentration on characteristics of superporous hydrogel." *Int. J. Pharm. Investig.*, 1(1), 17.

Chen, J. K., and Chang, C. J. (2014). "Fabrications and applications of stimulus-responsive polymer films and patterns on surfaces: A review." *Materials*, 7(2), 805-875.

Chen, J., Li, L., Yi, R., Xu, N., Gao, R., and Hong, B. (2016a). "Extraction and characterization of acid-soluble collagen from scales and skin of tilapia (*Oreochromis niloticus*)." *LWT - Food Sci. Technol.*, 66, 453-459.

Chen, J. P., Chang, G. Y., and Chen, J. K. (2008). "Electrospun collagen/chitosan nanofibrous membrane as wound dressing." *Colloids Surfaces A Physicochem. Eng. Asp.*, 313, 183-188.

Chen, Y., Zhang, Y., Wang, F., Meng, W., Yang, X., Li, P., Jiang, J., Tan, H., and Zheng, Y. (2016b). "Preparation of porous carboxymethyl chitosan grafted poly(acrylic acid) superabsorbent by solvent precipitation and its application as a hemostatic wound dressing." *Mater. Sci. Eng. C*, 63, 18-29.

Chhatri, A., Bajpai, J., Bajpai, A. K., Sandhu, S. S., Jain, N., and Biswas, J. (2011). "Cryogenic fabrication of savlon loaded macroporous blends of alginate and polyvinyl alcohol (PVA). Swelling, deswelling and antibacterial behaviors." *Carbohydr. Polym.*, 83(2), 876-882.

Chou, W. L., Yu, D. G., and Yang, M. C. (2005). "The preparation and characterization of silver-loading cellulose acetate hollow fibre membrane for water treatment." *Polym. Adv. Technol.*, 16, 600-607.

Chowdhury, N. A., and Al-Jumaily, A. M. (2016). "Regenerated cellulose/polypyrrole/silver nanoparticles/ionic liquid composite films for potential wound healing applications." *Wound Med.*, 14, 16-18.

Cohen, I. K. (1998). "A brief history of wound healing." Oxford Clinical Communications, Inc., Yardley, PA, USA.

Colo, G. Di, Zaino, C., Zambito, Y., Mollica, G., Geppi, M., Serafini, M. F., and Carelli, V. (2007). "A novel polyelectrolyte complex (PEC) hydrogel for controlled drug delivery to the distal intestine." *Open Drug Deliv. J.*, 1(1), 68-75.

Coskun, S., Aksoy, B., and Unalan, H. E. (2011). "Polyol synthesis of silver nanowires: An extensive parametric study." *Cryst. Growth Des.*, 11(11), 4963-4969.

Coviello, T., Matricardi, P., Marianecci, C., and Alhaique, F. (2007). "Polysaccharide hydrogels for modified release formulations." *J. Control. Release*, 119(1), 5-24.

Croitoru, C., Pop, M. A., Bedo, T., Cosnita, M., Roata, I. C., and Hulka, I. (2020). "Physically crosslinked poly(vinyl alcohol)/kappa-carrageenan hydrogels: Structure and applications." *Polymers*, 12(3), 560.

Cumpstey, I. (2013). "Chemical modifications of polysaccharides." *ISRN Org. Chem.*, 2013, 417672.

Dang, Q., Liu, K., Zhang, Z., Liu, C., Liu, X., Xin, Y., Cheng, X., Xu, T., Cha, D., and Fan, B. (2017). "Fabrication and evaluation of thermosensitive chitosan/collagen/α, β-glycerophosphate hydrogels for tissue regeneration." *Carbohydr. Polym.*, 167(1), 145-

157.

Danno, A. (1958). "Gel formation of aqueous solution of polyvinyl alcohol irradiated by gamma rays from cobalt-60." *J. Phys. Soc. Japan*, 13(7), 722-727.

Das, N. (2013). "Preparation methods and properties of hydrogel: A review." *Int. J. Pharm. Pharm. Sci.*, 5(3), 112-117.

Degreef, H. J. (1998). "How to heal a wound fast." *Dermatol. Clin.*, 16(2), 365-375.

Dhivya, S., Padma, V. V., and Santhini, E. (2015). "Wound dressings - A review." *Biomed.*, 5(4), 24-28.

Ding, C., Tian, M., Feng, R., Dang, Y., and Zhang, M. (2020). "Novel self-healing hydrogel with injectable, pH-responsive, strain-sensitive, promoting wound-healing, and hemostatic properties based on collagen and chitosan." *ACS Biomater. Sci. Eng.*, 6(7), 3855-3867.

Diniz, F. R., Maia, R. C. A. P., Rannier, L., Andrade, L. N., Chaud, M. V., Silva, C. F. da, Corrêa, C. B., Albuquerque Junior, R. L. C. de, Costa, L. P. da, Shin, S. R., Hassan, S., Sanchez-Lopez, E., Souto, E. B., and Severino, P. (2020). "Silver nanoparticles-composing alginate/gelatine hydrogel improves wound healing *in vivo*." *Nanomaterials*, 10(2), 390.

Du, H., Liu, M., Yang, X., and Zhai, G. (2015). "The design of pH-sensitive chitosan-based formulations for gastrointestinal delivery." *Drug Discov. Today*, 20(8), 1004-1011.

Duan, R., Zhang, J., Du, X., Yao, X., and Konno, K. (2009). "Properties of collagen from skin, scale and bone of carp (*Cyprinus carpio*)." *Food Chem.*, 112(3), 702-706.

Duman, M., Şendemir Ürkmez, A., and Zeybek, B. (2014). "Electrospinning of nanofibrous polycaprolactone (PCL) and collagen-blended polycaprolactone for wound dressing and tissue engineering." *Usak Univ. J. Mater. Sci.*, 3(1), 121-121.

Dunnill, C., Patton, T., Brennan, J., Barrett, J., Dryden, M., Cooke, J., Leaper, D., and

Georgopoulos, N. T. (2017). "Reactive oxygen species (ROS) and wound healing: The functional role of ROS and emerging ROS-modulating technologies for augmentation of the healing process." *Int. Wound J.*, 14(1), 89-96.

Enoch, S., and Leaper, D. J. (2008). "Basic science of wound healing." *Surgery*, 26(2), 31-37.

Fan, Z., Liu, B., Wang, J., Zhang, S., Lin, Q., Gong, P., Ma, L., and Yang, S. (2014). "A novel wound dressing based on Ag/graphene polymer hydrogel: Effectively kill bacteria and accelerate wound healing." *Adv. Funct. Mater.*, 24(25), 3933-3943.

Fei, J., Zhang, Z., Zhong, L., and Gu, L. (2002). "PVA/PAA thermo-induced hydrogel fiber: Preparation and pH-sensitive behavior in electrolyte solution." *J. Appl. Polym. Sci.*, 85(11), 2423-2430.

Fellahi, O., Sarma, R. K., Das, M. R., Saikia, R., Marcon, L., Coffinier, Y., Hadjersi, T., Maamache, M., and Boukherroub, R. (2013). "The antimicrobial effect of silicon nanowires decorated with silver and copper nanoparticles." *Nanotechnology*, 24(49), 495101.

Fleck, C. A., and Simman, R. (2010). "Modern collagen wound dressings: Function and purpose." *J. Am. Col. Certif. Wound Spec.*, 2(3), 50-54.

Flores-Gonzalez, M., Talavera-Rojas, M., Soriano-Vargas, E., and Rodríguez-Gonzalez, V. (2018). "Practical mediated-assembly synthesis of silver nanowires using commercial *Camellia sinensis* extracts and their antibacterial properties." *New J. Chem.*, 42(3), 2133-2139.

Fonseca, E., Fábia, S., and Sander, H. (2006). "Synthesis and characterization of poly(vinyl alcohol) hydrogels and hybrids for rMPB70 protein adsorption." *Mater. Res.*, 9(2), 185-191.

Forrest, R. D. (1982). "Early history of wound treatment." *J. R. Soc. Med.*, 75(3), 198-205.

Fu, L. H., Qi, C., Ma, M. G., and Wan, P. (2019). "Multifunctional cellulose-based

hydrogels for biomedical applications." *J. Mater. Chem. B*, 7(10), 1541-1562.

Fu, X., Hosta-Rigau, L., Chandrawati, R., and Cui, J. (2018). "Multi-stimuli-responsive polymer particles, films, and hydrogels for drug delivery." *Chem*, 4(9), 2084-2107.

Gann, M. J. M., Higginbotham, C. L., Geever, L. M., and Nugent, M. J. D. (2009). "The synthesis of novel pH-sensitive poly(vinyl alcohol) composite hydrogels using a freeze/thaw process for biomedical applications." *Int. J. Pharm.*, 372(1-2), 154-161.

Gao, Y., Wang, Y., Liu, Z., and Li, H. (2010). "Synthesis, scale and corrosion inhibition of modified polyaspartic acid." *Asian J. Chem.*, 22(2), 1495-1502.

Ge, L., Xu, Y., Li, X., Yuan, L., Tan, H., Li, D., and Mu, C. (2018). "Fabrication of Antibacterial CollaGe, L., Xu, Y., Li, X., Yuan, L., Tan, H., Li, D., and Mu, C. (2018). 'Fabrication of antibacterial collagen-based composite wound dressing.' *ACS Sustain. Chem. Eng.*, 6(7), 9153-9166.

Gebeyehu, M. B., Chang, Y. H., Abay, A. K., Chang, S. Y., Lee, J. Y., Wu, C. M., Chiang, T.C. and Murakami, R. I. (2016). "Fabrication and characterization of continuous silver nanofiber/polyvinylpyrrolidone (AgNF/PVP) core-shell nanofibers using the coaxial electrospinning process." *RSC Adv.*, 6(59), 54162-54168.

Gelse, K., Pöschl, E., and Aigner, T. (2003). "Collagens-structure, function, and biosynthesis." *Adv. Drug Deliv. Rev.*, 55(12), 1531-1546.

Gethin, G. (2007). "The significance of surface pH in chronic wounds." *Wounds UK*, 3(3), 52-56.

Gethin, G. T., Cowman, S., and Conroy, R. M. (2008). "The impact of Manuka honey dressings on the surface pH of chronic wounds." *Int. Wound J.*, 5(2), 185-194.

Gibas, I., and Janik, H. (2010). "Review: Synthetic polymer hydrogels for biomedical applications." *Chem. Chem. Technol.*, 4(4), 297-304.

Gils, P. S., Ray, D., and Sahoo, P. K. (2010). "Designing of silver nanoparticles in gum arabic based semi-IPN hydrogel." *Int. J. Biol. Macromol.*, 46(2), 237-244.

Giusti, P., Lazzeri, L., Petris, S. De, Palla, M., and Cascone, M. G. (1994). "Collagen-based new bioartificial polymeric materials." *Biomaterials*, 15(15), 1229-1233.

Goetten de Lima, G., de Lima, D. W., de Oliveira, M. J., Lugão, A. B., Alcántara, M. S., Devine, D. M., & de Sá, M. J. (2018). Synthesis and *in vivo* behaviour of PVP/CMC/Agar hydrogel membranes impregnated with silver nanoparticles for wound healing applications. *ACS Appl. Bio Mater*, *1*, 1842-1852.

Gong, C. Y., Shi, S., Dong, P. W., Kan, B., Gou, M. L., Wang, X. H., Li, X. Y., Luo, F., Zhao, X., Wei, Y. Q., and Qian, Z. Y. (2009). "Synthesis and characterization of PEG-PCL-PEG thermosensitive hydrogel." *Int. J. Pharm.*, 365(1-2), 89-99.

Gorrasi, G., Bugatti, V., and Vittoria, V. (2012). "Pectins filled with LDH-antimicrobial molecules: Preparation, characterization and physical properties." *Carbohydr. Polym.*, 89(1), 132-137.

Gottrup, F., Melling, A., and Hollander, D. A. (2005). "An overview of surgical site infections: Aetiology, incidence and risk factors." *World Wide Wounds*, 5(2), 11-15.

Greene, A. F., Danielson, M. K., Delawder, A. O., Liles, K. P., Li, X., Natraj, A., Wellen, A., and Barnes, J. C. (2017). "Redox-responsive artificial molecular muscles: Reversible radical-based self-assembly for actuating hydrogels." *Chem. Mater.*, 29(21), 9498-9508.

Gunasekaran, T., Nigusse, T., and Dhanaraju, M. D. (2011). "Silver nanoparticles as real topical bullets for wound healing." *J. Am. Coll. Clin. Wound Spec.*, 3(4), 82-96.

Guo, R., Lan, Y., Xue, W., Cheng, B., Zhang, Y., Wang, C., and Ramakrishna, S. (2017). "Collagen-cellulose nanocrystal scaffolds containing curcumin-loaded microspheres on infected full-thickness burns repair." *J. Tissue Eng. Regen. Med.*, 11(12), 3544-3555.

Guo, S., and DiPietro, L. A. (2010). "Critical review in oral biology & medicine: Factors affecting wound healing." *J. Dent. Res.*, 89(3), 219-229.

Gupta, P., Vermani, K., and Garg, S. (2002). "Hydrogels: From controlled release to

pH-responsive drug delivery." *Drug Discov. Today*, 7(10), 569-579.

Hashmi, M. U., Khan, F., Khalid, N., Shahid, A. A., Javed, A., Alam, T., Jalal, N., Hayat, M. Q., Abbas, S. R., and Janjua, H. A. (2017). "Hydrogels incorporated with silver nanocolloids prepared from antioxidant rich *Aerva javanica* as disruptive agents against burn wound infections." *Colloids Surfaces A Physicochem. Eng. Asp.*, 529, 475-486.

Hassiba, A. J., Zowalaty, M. E. El, Nasrallah, G. K., Webster, T. J., Luyt, A. S., Abdullah, A. M., and Elzatahry, A. A. (2016). "Review of recent research on biomedical applications of electrospun polymer nanofibers for improved wound healing." *Nanomedicine*, 11(6), 715-737.

Havanur, S., and Farheenand, V. (2019). "Synthesis and optimization of poly(N,N-diethylacrylamide) hydrogel and evaluation of its anticancer drug doxorubicin's release behavior." *Iran. Polym. J.*, 28(2), 99-112.

Hennink, W. E., and Nostrum, C. F. Van. (2012). "Novel crosslinking methods to design hydrogels." *Adv. Drug Deliv. Rev.*, 64, 223-236.

Hezaveh, H., and Muhamad, I. I. (2012). "Controlled drug release via minimization of burst release in pH-response kappa-carrageenan/polyvinyl alcohol hydrogels." *Chem. Eng. Res. Des.*, 91(3), 508-519.

Hiep, N. T., Khon, H. C., Niem, V. V. T., Toi, V. Van, Ngoc Quyen, T., Hai, N. D., and Ngoc Tuan Anh, M. (2016). "Microwave-assisted synthesis of chitosan/polyvinyl alcohol silver nanoparticles gel for wound dressing applications." *Int. J. Polym. Sci.*, 2016, 1-11.

Hoare, T. R., and Kohane, D. S. (2008) "Hydrogels in drug delivery: Progress and challenges." *Polymer*, 49(8), 1993-2007.

Hoffman, A. S. (2012). "Hydrogels for biomedical applications." *Adv. Drug Deliv. Rev.*, 64, 18-23.

Hu, S., Bi, S., Yan, D., Zhou, Z., Sun, G., Cheng, X., and Chen, X. (2018). "Preparation of composite hydroxybutyl chitosan sponge and its role in promoting wound healing." *Carbohydr. Polym.*, 184, 154-163.

Hurd, T., Woodmansey, E. J., and Watkins, H. M. A. (2021). "A retrospective review of the use of a nanocrystalline silver dressing in the management of open chronic wounds in the community." *Int. Wound J.*, 1-10.

Jabbari, E., and Nozari, S. (1999). "Synthesis of acrylic acid hydrogel by γ-irradiation cross-linking of polyacrylic acid in aqueous solution." *Iran. Polym. J.*, 8(4), 263-270.

JagadeeshBabu, P. E., Suresh Kumar, R., and Maheswari, B. (2011). "Synthesis and characterization of temperature sensitive P-NIPAM macro/micro hydrogels." *Colloids Surf. A Physicochem. Eng. Asp.*, 384, 466-472.

Jamnongkan, T., and Kaewpirom, S. (2010). "Potassium release kinetics and water retention of controlled-release fertilizers based on chitosan hydrogels." *J. Polym. Environ.*, 18(3), 413-421.

Jayaramudu, T., Ko, H., Zhai, L., and Li, Y. (2017). "Preparation and characterization of hydrogels from polyvinyl alcohol and cellulose and their electroactive behavior." *Soft Mater.*, 15(1), 64-72.

Jen, A. C., Wake, M. C., and Mikos, A. G. (1996). "Review: Hydrogels for cell immobilization." *Biotechnol. Bioeng.*, 50(4), 357-364.

Jeong, B., and Gutowska, A. (2002). "Lessons from nature: Stimuli-responsive polymers and their biomedical applications." *Trends Biotechnol.*, 20(7), 305-311.

Jeong, S. H., Yeo, S. Y., and Yi, S. C. (2005). "The effect of filler particle size on the antibacterial properties of compounded polymer/silver fibres." *J. Mater. Sci.*, 40, 5407-5411.

Jiang, S., and Teng, C. P. (2017). "Fabrication of silver nanowires-loaded polydimethylsiloxane film with antimicrobial activities and cell compatibility." *Mater. Sci. Eng. C*, 70, 1011-1017.

Jiang, Y., Huang, J., Wu, X., Ren, Y., Li, Z., and Ren, J. (2020). "Controlled release of silver ions from Ag NPs using a hydrogel based on konjac glucomannan and chitosan for infected wounds." *Int. J. Biol. Macromol.*, 149, 148-157.

Ju, H. K., Kim, S. Y., Kim, S. J., and Lee, Y. M. (2002). "pH/temperature-responsive semi-IPN hydrogels composed of alginate and poly(N-isopropylacrylamide)." *J. Appl. Polym. Sci.*, 83(5), 1128-1139.

Kaewdang, O., Benjakul, S., Kaewmanee, T., and Kishimura, H. (2014). "Characteristics of collagens from the swim bladders of yellowfin tuna (Thunnus albacares)." *Food Chem.*, 155, 264-270.

Kaith, B. S., Jindal, R., Mittal, H., and Kiran, K. (2010). "Temperature, pH and electric stimulus responsive hydrogels from Gum ghatti and polyacrylamide-synthesis, characterization and swelling studies." *Der Chemica Sinica*, 1(2), 44-54.

Kamath, K. R., and Park, K. (1993). "Biodegradable hydrogels in drug delivery." *Adv. Drug Deliv. Rev.*, 11(1-2), 59-84.

Kamoun, E. A., Chen, X., Mohy Eldin, M. S., and Kenawy, E. R. S. (2015). "Crosslinked poly(vinyl alcohol) hydrogels for wound dressing applications: A review of remarkably blended polymers." *Arab. J. Chem.*, 8(1), 1-14.

Kamoun, E. A., Kenawy, E. R. S., and Chen, X. (2017). "A review on polymeric hydrogel membranes for wound dressing applications: PVA-based hydrogel dressings." *J. Adv. Res.*, 8(3), 217-233.

Kandhasamy, S., Perumal, S., Madhan, B., Umamaheswari, N., Banday, J. A., Perumal, P. T., and Santhanakrishnan, V. P. (2017). "Synthesis and fabrication of collagen-coated ostholamide electrospun nanofiber scaffold for wound healing." *ACS Appl. Mater. Interfaces*, 9(10), 8556-8568.

Kang, S. I., and Bae, Y. H. (2003). "A sulfonamide based glucose-responsive hydrogel with covalently immobilized glucose oxidase and catalase." *J. Control. Release*, 86(1), 115-121.

Kaufman, T., Eichenlaub, E. H., Angel, M. F., Levin, M., and Futrell, J. W. (1985). "Topical acidification promotes healing of experimental deep partial thickness skin burns: A randomized double-blind preliminary study." *Burns*, 12(2), 84-90.

Khan, S. B., Qian, Z. J., Ryu, B. M., and Kim, S. K. (2009). "Isolation and biochemical characterization of collagens from seaweed pipefish, *Syngnathus schlegeli*." *Biotechnol. Bioprocess Eng.*, 14(4), 436-442.

Kharat, S. N., and Mendhulkar, V. D., (2016). "Synthesis, characterization and studies on antioxidant activity of silver nanoparticles using *Elephantopus scaber* leaf extract." *Mater. Eng. Sci. C.*, 62, 719-724.

Khatuaa, C., Chinyaa, I., Sahab, D., Dasa, S., Sena, R., and Dhara, A. (2015). "Modified clad optical fibre coated with PVA/TiO$_2$ nano composite for humidity sensing application." *Int. J. Smart Sens. Intell. Syst.*, 8(3), 1424-1442.

Khong, N. M. ., Yusoff, F. M., Jamilah, B., Barsi, M., Maznah, I., Chan, K. W., Armania, N., and Nishikawa, J. (2017). "Improved collagen extraction from jellyfish (*Acromitus hardenbergi*) with increased physical-induced solubilization processes ." *Food Chem.*, 251, 41-50.

Kiew, P.L., Don, M.M., 2013. Modified Lowry's method for acid and pepsin soluble collagen measurement from *Clarias* species muscles. *Sci. Rep.*, 2 (3), 1-5.

Kim, B., and Peppas, N. A. (2003). "Poly(ethylene glycol)-containing hydrogels for oral protein delivery applications." *Biomed. Microdevices*, 5(4), 333-341.

Kim, I. S., and Oh, I. J. (2005). "Drug release from the enzyme-degradable and pH-sensitive hydrogel composed of glycidyl methacrylate dextran and poly(acrylic acid)." *Arch. Pharm. Res.*, 28(8), 983-987.

Kim, J. J., and Park, K. (1999). "Smart hydrogels for bioseparation." *Bioseparation,* 7(4), 177-184.

Kim, J. S., Kuk, E., Yu, K. N., Kim, J. H., Park, S. J., Lee, H. J., Kim, S. H., Park, Y. K., Park, Y. H., Hwang, C. Y., Kim, Y. K., Lee, Y. S., Jeong, D. H., and Cho, M. H. (2007). "Antimicrobial effects of silver nanoparticles." *Nanomedicine Nanotechnology, Biol. Med.*, 3(1), 950-101.

Kirschner, C. M., and Anseth, K. S. (2013). "Hydrogels in healthcare: From static to dynamic material microenvironments." *Acta Mater.*, 61(3), 931-944.

Kittiphattanabawon, P., Benjakul, S., and Visessanguan, W. (2010). "Isolation and Characterisation of collagen from the skin of brownbanded bamboo shark (*Chiloscyllium punctatum*)." *Food Chem.*, 119(4), 1519-1526.

Kittiphattanabawon, P., Benjakul, S., Visessanguan, W., Nagai, T., and Tanaka, M. (2005). "Characterisation of acid-soluble collagen from skin and bone of bigeye snapper (*Priacanthus tayenus*)." *Food Chem.*, 89(3), 363-372.

Kleinman, H. K., Murray, J. C., McGoodwin, E. B., and Martin, G. R. (1978). "Connective tissue structure: Cell binding to collagen." *J. Invest. Dermatol.*, 71(1), 9-11.

Koehler, J., Brandl, F. P., and Goepferich, A. M. (2018). "Hydrogel wound dressings for bioactive treatment of acute and chronic wounds." *Eur. Polym. J.*, 100, 1-11.

Koetting, M. C., Peters, J. T., Steichen, S. D., and Peppas, N. A. (2015). "Stimulus-responsive hydrogels: Theory, modern advances, and applications." *Mater. Sci. Eng. R Reports*, 93, 1-49.

Kołodziejska, I., Sikorski, Z. E., and Niecikowska, C. (1999). "Parameters affecting the isolation of collagen from squid (*Illex argentinus*) skins." *Food Chem.*, 66(2), 153-157.

Kondiah, P. J., Choonara, Y. E., Kondiah, P. P. D., Marimuthu, T., Kumar, P., Toit, L. C. Du, and Pillay, V. (2016). "A review of injectable polymeric hydrogel systems for application in bone tissue engineering." *Molecules*, 21(11), 1580.

Kong, L. B., Lu, M., Li, M. K., Li, H. L., and Guo, X. Y. (2003). "Branched silver

nanowires obtained in porous anodic aluminum oxide template." *J. Mater. Sci. Lett.*, 22(9), 701-702.

Kong, X. Bin, Tang, Q. Y., Chen, X. Y., Tu, Y., Sun, S. Z., and Sun, Z. L. (2017). "Polyethylene glycol as a promising synthetic material for repair of spinal cord injury." *Neural Regen. Res.*, 12(6), 1003-1008.

Kopecek, J. (2009). "Hydrogels: From soft contact lenses and implants to self-assembled nanomaterials." *J. Polym. Sci. Part A Polym. Chem.*, 47, 5929-5946.

Krishnamoorthi, J., Ramasamy, P., Shanmugam, V., and Shanmugam, A. (2017). "Isolation and partial characterization of collagen from outer skin of *Sepia pharaonis* (Ehrenberg, 1831) from Puducherry coast." *Biochem. Biophys. Reports*, 10, 39-45.

Krishnan, G., Arumugam, S., Sharma, D., and Balakrishnan, R. M. (2018). "Extraction, optimization and characterization of collagen from sole fish skin." *Sustain. Chem. Pharm.*, 9, 19-26.

Kubinová, Š., Horák, D., Kozubenko, N., Vaněček, V., Proks, V., Price, J., Cocks, G., and Syková, E. (2010). "The use of superporous Ac-CGGASIKVAVS-OH-modified PHEMA scaffolds to promote cell adhesion and the differentiation of human fetal neural precursors." *Biomaterials*, 31(23), 5966-5975.

Kumar, D., Singh, K., Verma, V., and Bhatti, H. S. (2015). "Microwave-assisted synthesis and characterization of silver nanowires by polyol process." *Appl. Nanosci.*, 5(7), 881-890.

Kumar, N. M., Varaprasad, K., Rao, K. M., Babu, A. S., Srinivasulu, M., and Naidu, S. V. (2012). "A novel biodegradable green poly(L-aspartic acid-citric acid) copolymer for antimicrobial applications." *J. Polym. Environ.*, 20, 17-22.

Kumar, S., and Leaper, D. J. (2008). "Classification and management of acute wounds." *Surgery*, 26(2), 43-47.

Larouche, J., Sheoran, S., Maruyama, K., and Martino, M. M. (2018). "Immune regulation of skin wound healing: Mechanisms and novel therapeutic targets." *Adv.*

Wound Care, 7(7), 209-231.

Lee, H. Y., Park, H. K., Lee, Y. M., Kim, K., and Park, S. B. (2007). "A practical procedure for producing silver nanocoated fabric and its antibacterial evaluation for biomedical applications." *Chem. Commun.*, 28, 2959-2961.

Lee, J. S., Park, H. S., Kim, Y. J., and Kim, J. H. (2017). "Hybrid double-network hydrogel based on poly(aspartic acid) and poly(acryl amide) with improved mechanical properties." *J. Appl. Polym. Sci.*, 135(9), 45925.

Lee, Y. H., Hong, Y. L., and Wu, T. L. (2021). "Novel silver and nanoparticle-encapsulated growth factor co-loaded chitosan composite hydrogel with sustained antimicrobility and promoted biological properties for diabetic wound healing." *Mater. Sci. Eng. C*, 118, 111385.

Lei, B., Wang, J., Du, Y., and Zhang, K. (2017). "Controlling the size of silver nanowires through one-pot polyol method with trace halide and its effect on kinetic process." *Mater. Res. Express*, 4(7), 075052.

Leitinger, B., and Hohenester, E. (2007). "Mammalian collagen receptors." *Matrix Biol.*, 26(3), 146-155.

Levine, N. S., Lindberg, R. B., Mason, A. D., and Pruitt, B. A. (1976). "The quantitative swab culture and smear: A quick, simple method for determining the number of viable aerobic bacteria on open wounds." *J. Trauma* , 16(2), 89-94.

Li, H., Cheng, F., Wei, X., Yi, X., Tang, S., Wang, Z., Zhang, Y. S., He, J., and Huang, Y. (2021). "Injectable, self-healing, antibacterial, and hemostatic N,O-carboxymethyl chitosan/oxidized chondroitin sulfate composite hydrogel for wound dressing." *Mater. Sci. Eng. C*, 118, 111324.

Li, H., Liu, B. L., Gao, L. Z., and Chen, H. L. (2004). "Studies on bullfrog skin collagen." *Food Chem.* 84 (1), 65-69.

Li, J., Li, L., Lv, J., Wang, C., and Liu, Y. (2020). "Preparation of thiolated chitosan/silver nanowire composite hydrogels with antimicrobial activity for obstetric

wound care." *Mater. Lett.*, 280, 128497.

Liang, Q., Wang, L., Sun, W., Wang, Z., Xu, J., and Ma, H. (2014). "Isolation and characterization of collagen from the cartilage of amur sturgeon (*Acipenser schrenckii*)." *Process Biochem.*, 49(2), 318-323.

Lim, F., and Sun, A. M. (1980). "Microencapsulated islets as bioartificial endocrine pancreas." *Science*, 210(4472), 908-910.

Lim, S. L., Ngee, W., Tang, H., Ooi, C. W., Chan, E., and Tey, T. (2016). "Rapid swelling and deswelling of semi-interpenetrating network poly(acrylic acid)/poly(aspartic acid) hydrogels prepared by freezing polymerization." *J. Appl. Polym. Sci.*, 133(24), 43515.

Lima, G. G. De, Lima, D. W. F. De, Oliveira, M. J. A. De, Lugaõ, A. B., Alcântara, M. T. S., Devine, D. M., and Sá, M. J. C. De. (2018). "Synthesis and *in vivo* behavior of PVP/CMC/Agar hydrogel membranes impregnated with silver nanoparticles for wound healing applications." *ACS Appl. Bio Mater.*, 1(6), 1842-1852.

Lin, Y. H., Hsu, W. S., Chung, W. Y., Ko, T. H., and Lin, J. H. (2016). "Silver-based wound dressings reduce bacterial burden and promote wound healing." *Int. Wound J.*, 13(4), 505-511.

Lipsky, B. A., and Hoey, C. (2009). "Topical antimicrobial therapy for treating chronic wounds." *Clin. Infect. Dis.*, 49(10), 1541-1549.

Liu, C., Chen, Y., and Chen, J. (2009). "Synthesis and characteristics of pH-sensitive semi-interpenetrating polymer network hydrogels based on konjac glucomannan and poly(aspartic acid) for *in vitro* drug delivery." *Carbohydr. Polym.*, 79(3), 500-506.

Liu, F., Tao, G. L., and Zhuo, R. X. (1993). "Synthesis of thermal phase-separating reactive polymers and their applications in immobilized enzymes." *Polym. J.*, 25, 561-567.

Liu, H., Li, D., and Guo, S. (2007). "Studies on collagen from the skin of channel catfish (*Ictalurus punctaus*)." *Food Chem.*, 101(2), 621-625.

Liu, L., Wen, H., Rao, Z., Zhu, C., Liu, M., Min, L., Fan, L., and Tao, S. (2018). "Preparation and characterization of chitosan-collagen peptide/oxidized konjac glucomannan hydrogel." *Int. J. Biol. Macromol.*, 108, 376-382.

Liu, M., Su, H., and Tan, T. (2012). "Synthesis and properties of thermo and pH-sensitive poly (N-isopropylacrylamide)/polyaspartic acid IPN hydrogels." *Carbohydr. Polym.*, 87(4), 2425-2431.

Liu, M., Wang, L., Su, H., Cao, H., and Tan, T. (2013). "pH-sensitive IPN hydrogel based on poly(aspartic acid) and poly(vinyl alcohol) for controlled release." *Polym. Bull.*, 70(10), 2815-2827.

Liu, W., Li, G., Miao, Y., and Wu, X. (2009). "Preparation and characterization of pepsin-solu- bilized type I collagen from the scales of snakehead (*Ophiocephalus argus*)." *J. Food Biochem.*, 33, 20-37.

Liu, Y., and Chan-Park, M. B. (2009). "Hydrogel based on interpenetrating polymer networks of dextran and gelatin for vascular tissue engineering." *Biomaterials*, 30(2), 196-207.

Lu, S., Liu, M., Ni, B., and Gao, C. (2010). "A novel pH and thermo-sensitive PVP/CMC semi-IPN hydrogel: Swelling, phase behavior, and drug release study." *J. Polym. Sci. Part B Polym. Phys.*, 48, 1749-1756.

Lugão, A. B., Rogero, S. O., and Malmonge, S. M. (2002). "Rheological behavior of irradiated wound dressing poly(vinyl pyrrolidone) hydrogels." *Radiat. Phys. Chem.*, 63(3-6), 543-546.

Lukáč, P., Hartinger, J. M., Mlček, M., Popková, M., Suchý, T., Šupová, M., Závora, J., Adámková, V., Benáková, H., Slanař, O., Bartoš, M., Chlup, H., Lambert, L., and Grus, T. (2019). "A novel gentamicin-releasing wound dressing prepared from freshwater fish *Cyprinus carpio* collagen cross-linked with carbodiimide." *J. Bioact. Compat. Polym.*, 34(3), 246-262.

Lustosa, A. K. M. F., Jesus Oliveira, A. C. De, Quelemes, P. V., Plácido, A., Silva, F.

V. Da, Oliveira, I. S., Almeida, M. P. De, Amorim, A. das G. N., Delerue-Matos, C., Oliveira, R. de C. M. de, Silva, D. A. da, Eaton, P., and Souza de Almeida Leite, J. R. de. (2017). "*In situ* synthesis of silver nanoparticles in a hydrogel of carboxymethyl cellulose with phthalated-cashew gum as a promising antibacterial and healing agent." *Int. J. Mol. Sci.*, 18(11), 2399.

Ma, M., Zhong, Y., and Jiang, X. (2020). "Thermosensitive and pH-responsive tannin-containing hydroxypropyl chitin hydrogel with long-lasting antibacterial activity for wound healing." *Carbohydr. Polym.*, 236, 116096.

Madaghiele, M., Sannino, A., Ambrosio, L., and Demitri, C. (2014). "Polymeric hydrogels for burn wound care: Advanced skin wound dressings and regenerative templates." *Burns Trauma*, 2(4), 2321-3868.

Madhumathi, K., Sudheesh Kumar, P. T., Abhilash, S., Sreeja, V., Tamura, H., Manzoor, K., Nair, S. V., and Jayakumar, R. (2010). "Development of novel chitin/nanosilver composite scaffolds for wound dressing applications." *J. Mater. Sci. Mater. Med.*, 21(2), 807-813.

Mah, E., and Ghosh, R. (2013). "Thermo-responsive hydrogels for stimuli membranes." *Processes*, 1, 238-262.

Maheswari, B., Babu, P. E. J., and Agarwal, M. (2014). "Role of N-vinyl-2-pyrrolidinone on the thermoresponsive behavior of PNIPAm hydrogel and its release kinetics using dye and vitamin-B12 as model drug." *J. Biomat. Sci.*, 25(3), 37-41.

Mahmoud, A. A., and Salama, A. H. (2016). "Norfloxacin-loaded collagen/chitosan scaffolds for skin reconstruction: Preparation, evaluation and *in-vivo* wound healing assessment." *Eur. J. Pharm. Sci.*, 83, 155-165.

Maiti, S., Krishnan, D., Barman, G., Ghosh, S. K., and Laha, J. K. (2014). "Antimicrobial activities of silver nanoparticles synthesized from *Lycopersicon esculentum* extract." *J. Anal. Sci. Technol.*, 5, 1-7.

Maitra, J., and Shukla, V. K. (2014). "Cross-linking in hydrogels - A review." *Am. J.*

Polym. Sci., 4, 25-31.

Mallikarjun, P. N., Anusha, S., Sai Nandini, V., Rama Rao, B., Kamala Kumari, P. V., and Srinivasa Rao, Y. (2021). "Hydrogel: Responsive structures for drug delivery." *Int. J. Appl. Pharm.*, 13(1), 65-76.

Marin, S., Kaya, M. G. A., Ghica, M. V., Dinu-pirvu, C., Popa, L., Udeanu, D. I., Mihai, G., and Enachescu, M. (2018). "Collagen-polyvinyl alcohol-indomethacin biohybrid matrices as wound dressings." *Pharmaceutics*, 10(4), 224.

Marousek, J., Marouskova, A., Myskova, K., Vachal, J., Vochozka, M., and Zak, J. (2015). "Techno-economic assessment of collagen casings waste management." *Int. J. Environ. Sci. Technol.*, 12(10), 3385-3390.

Martins, A. F., Facchi, S. P., Monteiro, J. P., Nocchi, S. R., Silva, C. T. P., Nakamura, C. V., Girotto, E. M., Rubira, A. F., and Muniz, E. C. (2015). "Preparation and cytotoxicity of N,N,N-trimethyl chitosan/alginate beads containing gold nanoparticles." *Int. J. Biol. Macromol.*, 72, 466-471.

Masood, N., Ahmed, R., Tariq, M., and Ahmed, Z. (2019). "Silver nanoparticle impregnated chitosan-PEG hydrogel enhances wound healing in diabetes induced rabbits." *Int. J. Pharm.*, 559, 23-36.

Matsumoto, A., Kurata, T., Shiino, D., and Kataoka, K. (2004). "Swelling and shrinking kinetics of totally synthetic, glucose-responsive polymer gel bearing phenylborate derivative as a glucose-sensing moiety." *Macromolecules*, 37(4), 1502-1510.

Mazur, M. (2004). "Electrochemically prepared silver nanoflakes and nanowires." *Electrochem. Commun.*, 6(4), 400-403.

Mekkawy, A. I., El-Mokhtar, M. A., Nafady, N. A., Yousef, N., Hamad, M., El-Shanawany, S. M., Ibrahim, E. H., and Elsabahy, M. (2017). "*In vitro* and *in vivo* evaluation of biologically synthesized silver nanoparticles for topical applications: Effect of surface coating and loading into hydrogels." *Int. J. Nanomedicine*, 12, 759-

777.

Milner, S. M. (1992). "Acetic acid to treat *Pseudomonas aeruginosa* in superficial wounds and burns." *Lancet*, 340(8810), 61.

Mir, M., Ali, M. N., Barakullah, A., Gulzar, A., Arshad, M., Fatima, S., and Asad, M. (2018). "Synthetic polymeric biomaterials for wound healing: A review." *Prog. Biomater.*, 7(1), 1-21.

Miyata, T., Uragami, T., and Nakamae, K. (2002). "Biomolecule-sensitive hydrogels." *Adv. Drug Deliv. Rev.*, 54(1), 79-98.

Mohanta, Y. K., Panda, S. K., Jayabalan, R., Sharma, N., Bastial, A. K., and Mohanta, T. K., (2017). "Antimicrobial, antioxidant and cytotoxic activity of silver nanoparticles synthesized by leaf extract of *Erythrina suberosa* (Roxb.)**.**" *Front. Mol. Biosci.*, 4, 1-9.

Mohsin, M., Hossin, A., and Haik, Y. (2011). "Thermal and mechanical properties of poly(vinyl alcohol) plasticized with glycerol." *J. Appl. Polym. Sci.*, 112, 3102-3109.

Montesano, F. F., Parente, A., Santamaria, P., Sannino, A., and Serio, F. (2015). "Biodegradable superabsorbent hydrogel increases water retention properties of growing media and plant growth." *Agric. Agric. Sci. Procedia*, 4, 451-458.

Morones, J. R., Elechiguerra, J. L., Camacho, A., Holt, K., Kouri, J. T., and Ramirez, J. T. (2005). "The bactericidal effect of silver nanoparticles." *Nanotechnol.*, 16, 2346-2353.

Moura, L. I. F., Dias, A. M. A., Carvalho, E., and Sousa, H. C. De. (2013). "Recent advances on the development of wound dressings for diabetic foot ulcer treatment - A review." *Acta Biomater.*, 9(7), 7093-7114.

Muhammed, A., Ali, M., Kishimura, H., and Benjakul, S. (2018). "Extraction efficiency and characteristics of acid and pepsin soluble collagens from the skin of golden carp (*Probarbus jullieni*) as affected by ultrasonication." *Process Biochem.*, 66, 237-244.

Murakami, Y., and Maeda, M. (2005). "DNA-responsive hydrogels that can shrink or swell." *Biomacromolecules*, 6(6), 2927-2929.

Murali, M., Mahendra, C., Rajashekar, N., Sudarshana, M. S., Raveesha, K. A., and Amruthesh, K. N. (2017). "Antibacterial and antioxidant properties of biosynthesized zinc oxide nanoparticles from *Ceropegia candelabrum* L. - An endemic species." *Spectrochim. Acta A Mol. Biomol. Spectrosc.*, 179, 104-109.

Muyonga, J. H., Cole, C. G. B. B., and Duodu, K. G. (2004). "Characterisation of acid soluble collagen from skins of young and adult Nile perch (*Lates niloticus*)." *Food Chem.*, 85(1), 81-89.

Nagai, T., Araki, Y., and Suzuki, N. (2002). "Collagen of the skin of ocellate puffer fish (*Takifugu rubripes*)." *Food Chem.*, 78(2), 173-177.

Nagai, T., and Suzuki, N. (2000). "Isolation of collagen from fish waste material - Skin, bone and fins." *Food Chem.*, 68(3), 277-281.

Nagai, T., and Suzuki, N. (2002). "Preparation and partial characterization of collagen from paper nautilus (*Argonauta argo*, Linnaeus) outer skin." *Food Chem.*, 76(2), 149-153.

Nagai, T., Yamashita, E., Taniguchi, K., Kanamori, N., and Suzuki, N. (2001). "Isolation and characterisation of collagen from the outer skin waste material of cuttlefish (*Sepia lycidas*)." *Food Chem.*, 72(4), 425-429.

Namdeo, M., Bajpai, S. K., and Kakkar, S. (2009). "Preparation of a magnetic-field-sensitive hydrogel and preliminary study of its drug release behavior." *J. Biomater. Sci. Polym. Ed.*, 20(12), 1747-1761.

Netti, P. A., Shelton, J. C., Revell, P. A., Pirie, G., Smith, S., Ambrosio, L., Nicolais, L., and Bonfield, W. (1993). "Hydrogels as an interface between bone and an implant." *Biomaterials*, 14(14), 1098-1104.

Ngadaonye, J. I., Geever, L. M., Killion, J., and Higginbotham, C. L. (2013). "Development of novel chitosan-poly(N,N-diethylacrylamide) IPN films for potential

wound dressing and biomedical applications." *J. Polym. Res.*, 20(7), 161-173.

Nguyen, T. D., Nguyen, T. T., Ly, K. L., Tran, A. H., Nguyen, T. T. N., Vo, M. T., Ho, H. M., Dang, N. T. N., Vo, V. T., Nguyen, D. H., Nguyen, T. T. H., and Nguyen, T. H. (2019). "*In vivo* study of the antibacterial chitosan/polyvinyl alcohol loaded with silver nanoparticle hydrogel for wound healing applications." *Int. J. Polym. Sci.*, 2019, 1-10.

Ninan, N., Forget, A., Shastri, V. P., Voelcker, N. H., and Blencowe, A. (2016). "Antibacterial and anti-inflammatory pH-responsive tannic acid-carboxylated agarose composite hydrogels for wound healing." *ACS Appl. Mater. Interfaces*, 8(42), 28511-28521.

Nistor, M. T., Chiriac, A. P., Nita, L. E., Neamtu, I., and Vasile, C. (2013). "Semi-interpenetrated network with improved sensitivity based on poly(N-isopropylacrylamide) and poly(aspartic acid)." *Polym. Eng. Sci.*, 53(11), 2345-2352.

Normah, I., and Nur-Hani Suryati, M. Z. (2015). "Isolation of threadfin bream (*Nemipterus japonicus*) waste collagen using natural acid from calamansi (*Citrofortunella microcarpa)* juice." *Int. Food Res. J.*, 22(6), 2294-2301.

Nurilmala, M., Pertiwi, R. M., Nurhayati, T., Fauzi, S., Batubara, I., and Ochiai, Y. (2019). "Characterization of collagen and its hydrolysate from yellowfin tuna *Thunnus albacares* skin and their potencies as antioxidant and antiglycation agents." *Fish. Sci.*, 85(3), 591-599.

Okay, O. (2009). "General properties of hydrogels." *Hydrogel sensors and actuators*, Springer, Berlin, Heidelberg, 1-14.

Okay, O. (2018). "Semicrystalline physical hydrogels with shape-memory and self-healing properties." *J. Mater. Chem. B*, 7(10), 1581-1596.

Omidi, M., Yadegari, A., and Tayebi, L. (2017). "Wound dressing application of pH-sensitive carbon dots/chitosan hydrogel." *RSC Adv.*, 7(18), 10638-10649.

Onyekwelu, I., Yakkanti, R., Protzer, L., Pinkston, C. M., Tucker, C., and Seligson, D. (2017). "Surgical wound classification and surgical site infections in the orthopaedic

patient." *J. Am.Acad. Ortho. Surg. Glob. Res. Rev.*, 1(3), e022.

Osada, Y., and Gong, J. (1993). "Stimuli-responsive polymer gels and their application to chemomechanical systems." *Prog. Polym. Sci.*, 18(2), 187-226.

Pal, K., Banthia, A. K., and Majumdar, D. K. (2007). "Preparation and characterization of polyvinyl alcohol-gelatin hydrogel membranes for biomedical applications." *AAPS Pharm. Sci. Tech.*, 8(1), 142-146.

Pal, P., Srivas, P. K., Dadhich, P., Das, B., Maity, P. P., Moulik, D., and Dhara, S. (2016). "Accelerating full thickness wound healing using collagen sponge of mrigal fish (*Cirrhinus cirrhosus*) scale origin." *Int. J. Biol. Macromol.*, 93, 1507-1518.

Pamfil, D., Vasile, C., Tarţâu, L., Vereştiuc, L., and Poiatâ, A. (2017). "pH-responsive 2-hydroxyethyl methacrylate/citraconic anhydride-modified collagen hydrogels as ciprofloxacin carriers for wound dressings." *J. Bioact. Compat. Polym.*, 32(4), 355-381.

Pan, L., Chortos, A., Yu, G., Wang, Y., Isaacson, S., Allen, R., Shi, Y., Dauskardt, R., and Bao, Z. (2014). "An ultra-sensitive resistive pressure sensor based on hollow-sphere microstructure induced elasticity in conducting polymer film." *Nat. Commun.*, 5(1), 1-8.

Pandey, M., Mohamad, N., and Low, W. (2017). "Microwaved bacterial cellulose-based hydrogel microparticles for the healing of partial thickness burn wounds." *Drug Deliv. Transl. Res.*, 7(1), 89-99.

Parikh, D. V., Fink, T., Rajasekharan, K., Sachinvala, N. D., Sawhney, A. P. S., Calamari, T. A., and Parikh, A. D. (2005). "Antimicrobial silver/sodium carboxymethyl cotton dressings for burn wounds." *Text. Res. J.*, 75, 134-138.

Park, S., Nho, Y., Lim, Y., and Kim, H. (2003). "Preparation of pH-sensitive poly(vinyl alcohol-g-methacrylic acid) and poly(vinyl alcohol-g-acrylic acid) hydrogels by gamma ray irradiation and their insulin release behavior." *J. Appl. Polym. Sci.*, 91(1), 636-643.

Pathan, I. B., Munde, S. J., Shelke, S., Ambekar, W., and Mallikarjuna Setty, C. (2019).

"Curcumin loaded fish scale collagen-HPMC nanogel for wound healing application: *Ex-vivo* and *in-vivo* evaluation." *Int. J. Polym. Mater. Polym. Biomater.*, 68(4), 165-174.

Pati, F., Adhikari, B., and Dhara, S. (2010). "Isolation and characterization of fish scale collagen of higher thermal stability." *Bioresour. Technol.*, 101(10), 3737-3742.

Patravale, V. B., and Mandawgade, S. D. (2008). "Novel cosmetic delivery systems: An application update." *Int. J. Cosmet. Sci.*, 30(1), 19-33.

Patwadkar, M. V., Gopinath, C. S., and Badiger, M. V. (2015). "An efficient Ag-nanoparticle embedded semi-IPN hydrogel for catalytic applications." *RSC Adv.*, 5(10), 7567-7574.

Paul, W., and Sharma, C. P. (2004). "Chitosan and alginate wound dressings: A short review." *Trends Biometerials Artif. Organs*, 18(1), 18-23.

Pawar, H. V., Tetteh, J., and Boateng, J. S. (2013). "Preparation, optimisation and characterisation of novel wound healing film dressings loaded with streptomycin and diclofenac." *Colloids Surfaces B Biointerfaces*, 102, 102-110.

Peng, Z., Li, Z., Zhang, F., and Peng, X. (2012). "Preparation and properties of polyvinyl alcohol/collagen hydrogel." *J. Macromol. Sci. Part B*, 51(10), 1934-1941.

Peppas, N. A., Keys, K. B., Torres-Lugo, M., and Lowman, A. M. (1999). "Poly(ethylene glycol)-containing hydrogels in drug delivery." *J. Control. Release*, 62(1-2), 81-87.

Peppas, N. A., and Langer, R. (1994). "New challenges in biomaterials." *Science*, 263(5154), 1715-1720.

Percival, N. J. (2002). "Classification of wounds and their management." *Surgery*, 20(5), 114-117.

Pescosolido, L., Vermonden, T., Malda, J., Censi, R., Dhert, W. J. A., Alhaique, F., Hennink, W. E., and Matricardi, P. (2011). "*In situ* forming IPN hydrogels of calcium

alginate and dextran-HEMA for biomedical applications." *Acta Biomater.*, 7(4), 1627-1633.

Pinar, I., and Ozgur, O. (2017). "Novel stimuli-responsive hydrogels derived from morpholine: synthesis, characterization and absorption uptake of textile azo dye." *Iran. Polym. J.*, 26(6), 391-404.

Pinto, A. M., Cerqueira, M. A., Bañobre-Lópes, M., Pastrana, L. M., and Sillankorva, S. (2020). "Bacteriophages for chronic wound treatment: From traditional to novel delivery systems." *Viruses*, 12(2), 1-29.

Postlethwaite, A. E., Seyer, J. M., and Kang, A. H. (1978). "Chemotactic attraction of human fibroblasts to type I, II and III collagens and collagen-derived peptides." *Proc. Natl. Acad. Sci.*, 75(2), 871-875.

Pourjavadi, A., Barzegar, S., and Mahdavinia, G. R. (2006). "MBA-crosslinked Na-Alg/CMC as a smart full-polysaccharide superabsorbent hydrogelsccharide superabsorbent hydrogels." *Carbohydr. Polym.*, 66(2), 386-395.

Pourjavadi, A., Kurdtabar, M., and Ghasemzadeh, H. (2008). "Salt and pH-resisting collagen-based highly porous hydrogel." *Polym. J.*, 40(2), 94-103.

Powers, J. G., Higham, C., Broussard, K., and Phillips, T. J. (2016). "Wound healing and treating wounds chronic wound care and management." *J. Am. Acad. Dermatol.*, 74(4), 607-625.

Prabhu, S., and Poulose, E. K. (2012). "Silver nanoparticles: Mechanism of antimicrobial." *Int. Nano Lett.*, 2, 32-41.

Qiao, M., Chen, D., Ma, X., and Liu, Y. (2005). "Injectable biodegradable temperature-responsive PLGA-PEG-PLGA copolymers: Synthesis and effect of copolymer composition on the drug release from the copolymer-based hydrogels." *Int. J. Pharm.*, 294(1-2), 103-112.

Qiu, Y., and Park, K. (2001). "Environment-sensitive hydrogels for drug delivery."

Adv. Drug Deliv. Rev., 53, 321-339.

Qu, J., Zhao, X., Liang, Y., Zhang, T., Ma, P. X., and Guo, B. (2018). "Biomaterials Antibacterial adhesive injectable hydrogels with rapid self-healing, extensibility and compressibility as wound dressing for joints skin wound healing." *Biomaterials*, 183, 185-199.

Ramanathan, G., Singaravelu, S., Raja, M. D., Liji Sobhana, S. S., and Sivagnanam, U. T. (2014). "Extraction and characterization of collagen from the skin of arothron stellatus fish-a novel source of collagen for tissue engineering." *J. Biomater. Tissue Eng.*, 4(3), 203-209.

Rana, M., Rahman, S., Ullah, A., and Siddika, A. (2020). "Amnion and collagen-based blended hydrogel improves burn healing efficacy on rat skin wound model in presence of wound dressing biomembrane." *Biomed. Mater. Eng.*, 31(1), 1-17.

Rasool, A., Ata, S., and Islam, A. (2019). "Stimuli responsive biopolymer (chitosan) based blend hydrogels for wound healing application." *Carbohydr. Polym.*, 203, 423-429.

Rasool, N., Yasin, T., Heng, J. Y. Y., and Akhter, Z. (2010). "Synthesis and characterization of novel pH, ionic strength and temperature- sensitive hydrogel for insulin delivery." *Polymer*, 51(8), 1687-1693.

Rath, G., Hussain, T., Chauhan, G., Garg, T., and Goyal, A. K. (2015). "Collagen nanofiber containing silver nanoparticles for improved wound-healing applications." *J. Drug Target.*, 24(6), 520-529.

Ravichandran, V., Vasanthi, S., Shalini, S., Shah, S. A., and Harish, R., (2016). "Green synthesis of silver nanoparticles using *Atrocarpus altilis* leaf extract and the study of their antimicrobial and antioxidant activity." *Mater. Lett.*, 180, 264-267.

Rehana, D., Mahendiran, D., Kumar, R. S., and Rahiman, A. K. (2017). "Evaluation of antioxidant and anticancer activity of copper oxide nanoparticles synthesized using medicinally important plant extracts." *Biomed. Pharmacother.*, 89, 1067-1077.

Ren, Y., Yu, X., Li, Z., Liu, D., and Xue, X. (2020). "Fabrication of pH-responsive TA-keratin bio-composited hydrogels encapsulated with photoluminescent GO quantum dots for improved bacterial inhibition and healing efficacy in wound care management: *In-vivo* wound evaluations." *J. Photochem. Photobiol. B Biol.*, 202, 111676.

Rezaei, F., Damoogh, S., Reis, R. L., Kundu, S. C., and Mottaghitalab, F. (2021). "Dual drug delivery system based on pH-sensitive silk fibroin/alginate nanoparticles entrapped in PNIPAM hydrogel for treating severe infected burn wound." *Biofabrication*, 13(1), 015005.

Rezvani Ghomi, E., Khalili, S., Nouri Khorasani, S., Esmaeely Neisiany, R., and Ramakrishna, S. (2019). "Wound dressings: Current advances and future directions." *J. Appl. Polym. Sci.*, 136(27), 1-12.

Rieger, K. A., Birch, N. P., and Schiffman, J. D. (2013). "Designing electrospun nanofiber mats to promote wound healing - A review." *J. Mater. Chem. B*, 1(36), 4531.

Rizwan, M., Yahya, R., Hassan, A., Yar, M., Azzahari, A. D., Selvanathan, V., Sonsudin, F., and Abouloula, C. N. (2017). "pH-sensitive hydrogels in drug delivery: Brief history, properties, swelling, and release mechanism, material selection and applications." *Polymer*, 9(4), 137.

Roberts, G., Hammad, L., Creevy, J., Shearman, C., and Mani, R. (1997). "Physical changes in dermal tissues around chronic venous ulcers." E*uropean Conf. on Advances in Wound Managemen*t, EWMA, Harrogate, UK, 104-5.

Rodríguez, F., Morán, L., González, G., Troncoso, E., and Zúñiga, R. N. (2017). "Collagen extraction from mussel byssus: A new marine collagen source with physicochemical properties of industrial interest." *J. Food Sci. Technol.*, 54(5), 1228-1238.

Russell, A. D., and Hugo, W. B. (1994). "Antimicrobial activity and action of silver." *Prog. Med. Chem.*, 31, 351-370.

Sadowska, M., and Turk, M. (2010). "Isolation and some properties of collagen from

the backbone of baltic cod (*Gadus morhua*)." *Food Hydrocoll.*, 24, 325-329.

Sahiner, N., Sagbas, S., Sahiner, M., Silan, C., Aktas, N., and Turk, M. (2016). "Biocompatible and biodegradable poly(tannic acid) hydrogel with antimicrobial and antioxidant properties." *Int. J. Biol. Macromol.*, 82, 150-159.

Samuel, U., and Guggenbichler, J. P. (2004). "Prevention of catheter-related infections: The potential of a new nanosilver impregnated catheter." *Int. J. Antimicrob. Agents*, 23, 75-78.

Sankar, S., Sekar, S., Mohan, R., Rani, S., Sundaraseelan, J., and Sastry, T. P. (2008). "Preparation and partial characterization of collagen sheet from fish (*Lates calcarifer*) scales." *Int. J. Biol. Macromol.*, 42(1), 6-9.

Schmaljohann, D. (2006). "Thermo and pH-responsive polymers in drug delivery." *Adv. Drug Deliv. Rev.*, 58(15), 1655-1670.

Schmidt, M. M., Dornelles, R. C. P., Mello, R. O., Kubota, E. H., Mazutti, M. A., Kempka, A. P., and Demiate, I. M. (2016). "Collagen extraction process." *Int. Food Res. J.*, 23(3), 913-922.

Schneider, L. A., Korber, A., Grabbe, S., and Dissemond, J. (2007). "Influence of pH on wound-healing: A new perspective for wound-therapy?" *Arch. Dermatol. Res.*, 298(9), 413-420.

Sen, C. K. (2019). "Human wounds and its burden: An updated compendium of estimates." *Adv. Wound Care*, 8(2), 39-48.

Shah, J. B. (2011). "The history of wound care." *J. Am. Col. Certif. Wound Spec.*, 3(3), 65-66.

Shanmugam, V. (2012). "Extraction, structural and physical characterization of type I collagen from the outer skin of *Sepiella inermis* (Orbigny, 1848)." *African J. Biotechnol.*, 11(78), 14326-14337.

Sharma, D., Rakshana, D. A., Balakrishnan, R. M., and JagadeeshBabu, P. E. (2019a).

"One step synthesis of silver nanowires using fructose as a reducing agent and its antibacterial and antioxidant analysis." *Mater. Res. Express*, 6, 075050.

Sharma, R., Kaith, B. S., Kalia, S., Pathania, D., Kumar, A., Sharma, N., Street, R. M., and Schauer, C. (2015). "Biodegradable and conducting hydrogels based on Guar gum polysaccharide for antibacterial and dye removal applications." *J. Environ. Manage.*, 162, 37-45.

Sharma, S., Anwar, M. F., Dinda, A., Singhal, M., and Malik, A. (2019b). "*In-vitro* and *in-vivo* studies of pH-sensitive GHK-Cu-incorporated polyaspartic and polyacrylic acid superabsorbent polymer." *ACS Omega*, 4(23), 20118-20128.

Sharma, S., Dua, A., and Malik, A. (2016). "Superabsorbent polymer gels based on polyaspartic acid and polyacrylic acid." *J. Mater. Sci. Eng.*, 5(3), 235.

Sharma, S., Dua, A., and Malik, A. (2017). "Biocompatible stimuli responsive superabsorbent polymer for controlled release of GHK-Cu peptide for wound dressing application." *J. Polym. Res.*, 24, 104.

Shevchenko, R. V, James, S. L., and James, S. E. (2009). "A review of tissue-engineered skin bioconstructs available for skin reconstruction." *J. R. Soc. Interface*, 7(43), 229-258.

Shi, L., Yang, N., Zhang, H., Chen, L., Tao, L., Wei, Y., Liu, H., and Luo, Y. (2015). "A novel poly(γ-glutamic acid)/silk-sericin hydrogel for wound dressing: Synthesis, characterization and biological evaluation." *Mater. Sci. Eng. C*, 48, 533-540.

Shi, M., Zhang, H., Song, T., Liu, X., Gao, Y., and Zhou, J. (2019). "Sustainable dual release of antibiotic and growth factor from pH-responsive uniform alginate composite microparticles to enhance wound healing." *ACS Appl. Mater. Interfaces*, 11, 22730-22744.

Silva, T. H., Moreira-Silva, J., Marques, A. L. P., Domingues, A., Bayon, Y., and Reis, R. L. (2014). "Marine origin collagens and its potential applications." *Mar. Drugs*, 12(12), 5881-5901.

Silvipriya, K. S., Krishna Kumar, K., Bhat, A. R., Dinesh Kumar, B., John, A., and Lakshmanan, P. (2015). "Collagen: Animal sources and biomedical application." *J. Appl. Pharm. Sci.*, 5(3), 123-127.

Simões, D., Miguel, S. P., Ribeiro, M. P., Coutinho, P., Mendonça, A. G., and Correia, I. J. (2018). "Recent advances on antimicrobial wound dressing: A review." *Eur. J. Pharm. Biopharm.*, 127, 130-141.

Singh, P., Benjakul, S., Maqsood, S., and Kishimura, H. (2011). "Isolation and characterisation of collagen extracted from the skin of striped catfish (*Pangasianodon hypophthalmus*)." *Food Chem.*, 124(1), 97-105.

Sinha, M., Banik, R. M., Haldar, C., and Maiti, P. (2013). "Development of ciprofloxacin hydrochloride loaded poly(ethylene glycol)/chitosan scaffold as wound dressing." *J. Porous Mater.*, 20(4), 799-807.

Sionkowska, A., Kozłowska, J., Skorupska, M., and Michalska, M. (2015). "Isolation and characterization of collagen from the skin of Brama australis." *Int. J. Biol. Macromol.*, 80, 605–609.

Skierka, E., and Sadowska, M. (2007). "The influence of different acids and pepsin on the extractability of collagen from the skin of baltic cod (*Gadus morhua*)." *Food Chem.*, 105(3), 1302-1306.

Slistan-Grijalva, A., Herrera-Urbina, R., Rivas-Silva, J. F., Avalos-Borja, M., Castillon-Barraza, F. F., and Posada-Amarillas, A. (2005). "Assessment of growth of silver nanoparticles synthesized from an ethylene glycol-silver nitrate-polyvinylpyrrolidone solution." *Physica E: Low Dimens. Syst. Nanostruct.*, 25(4), 438-448.

Sondi, I., and Salopek-Sondi, B. (2004). "Silver nanoparticles as antimicrobial agent: A case study on *E. coli* as a model for gram-negative bacteria." *J. Colloid Interface Sci.*, 275(1), 177-182.

Song, J., Zhang, P., Cheng, L., Liao, Y., Xu, B., Bao, R., Wang, W., and Liu, W. (2015).

"Nano-silver *in situ* hybridized collagen scaffolds for regeneration of infected full-thickness burn skin." *J. Mater. Chem. B*, 3(20), 4231-4241.

Sood, A., Granick, M. S., and Tomaselli, N. L. (2014). "Wound dressings and comparative effectiveness data." *Adv. Wound Care*, 3(8), 511-529.

Sood, N., Bhardwaj, A., Mehta, S., and Mehta, A. (2016). "Stimuli-responsive hydrogels in drug delivery and tissue engineering." *Drug Deliv.*, 23(3), 748-770.

Sosnik, A., and Seremeta, K. (2017). "Polymeric hydrogels as technology platform for drug delivery applications." *Gels*, 3(3), 25.

Sripriya, R., and Kumar, R. (2016). "A novel enzymatic method for preparation and characterization of collagen film from swim bladder of fish rohu (*Labeo rohita*)." *Food Sci. Nutr.*, 6(15), 1468-1478..

Stashak, T. S., Farstvedt, E., and Othic, A. (2004). "Update on wound dressings: Indications and best use." *Clin. Tech. Equine Pract.*, 3(2), 148-163.

Steichen, S., O'Connor, C., and Peppas, N. A. (2016). "Development of a P((MAA-co-NVP)-g-EG)) hydrogel platform for oral protein delivery: Effects of hydrogel composition on environmental response and protein partitioning." *Macromol. Biosci.*, 17(1), 1600266.

Subhan, F., Ikram, M., Shehzad, A., and Ghafoor, A. (2015). "Marine collagen: An emerging player in biomedical applications." *J. Food Sci. Technol.*, 52(8), 4703-4707.

Sujithra, S., Kiruthiga, N., Prabhu, M. J., and Kumeresan, R. (2013). "Isolation and determination of type I collagen from tilapia (*Oreochromis niloticus*) waste." *Int. J. Eng. Technol.*, 5(3), 2181-2185.

Sultana, J., Molla, M. R., Kamal, M., Shahidullah, M., Begum, F., and Bashar, M. A. (1970). "Histological differences in wound healing in Maxillofacial region in patients with or without risk factors." *Bangladesh J. Pathol.*, 24(1), 3-8.

Sundaramurthi, D., Krishnan, U. M., and Sethuraman, S. (2014). "Electrospun

nanofibers as scaffolds for skin tissue engineering." *Polym. Rev.*, 54(2), 348-376.

Supp, D. M., and Boyce, S. T. (2005). "Engineered skin substitutes: Practices and potentials." *Clin. Dermatol.*, 23(4), 403-412.

Suresh, D., Nethravathi, P. C., Rajanaika, H., Nagabhushana, H., and Sharma, S. C. (2015). "Green synthesis of multifunctional zinc oxide (ZnO) nanoparticles using *Cassia fistula* plant extract and their photodegradative, antioxidant and antibacterial activities." *Mater. Sci. Semicond. Process*, 31, 446-454.

Susana, S., Ana, F., and Francisco, V. (2012). "Modular hydrogels for drug delivery." *J. Biomater. Nanobiotechnol.*, 3, 185-199.

Sweeney, I. R., Miraftab, M., and Collyer, G. (2012). "A critical review of modern and emerging absorbent dressings used to treat exuding wounds." *Int. Wound J.*, 9(6), 601-612.

Sweeney, S. M., DiLullo, G., Slater, S. J., Martinez, J., Iozzo, R. V., Lauer-Fields, J. L., Fields, G. B., and San Antonio, J. D. (2003). "Angiogenesis in collagen I requires α2β1 ligation of a GFP*GER sequence and possibly p38 MAPK activation and focal adhesion disassembly." *J. Biol. Chem.*, 278(33), 30516-30524.

Syková, E., Jendelová, P., Urdzíková, L., Lesný, P., and Hejčl, A. (2006). "Bone marrow stem cells and polymer hydrogels - two strategies for spinal cord injury repair." *Cell. Mol. Neurobiol.*, 26(7-8), 1113-1129.

Takeda, K., Kitagawa, H., Tsuboi, R., Kiba, W., Sasaki, J. I., Hayashi, M., and Imazato, S. (2015). "Effectiveness of non-biodegradable poly(2-hydroxyethyl methacrylate) based hydrogel particles as a fibroblast growth factor-2 releasing carrier." *Dent. Mater.*, 31(11), 1406-1414.

Tanaka, T., Takahashi, K., Tsubaki, K., Hirata, M., Yamamoto, K., and Biswas, A. (2018). "Isolation and characterization of acid-soluble bluefin tuna (*Thunnus orientalis*) skin collagen." *Fish. Aquatic Sci.*, 21(1), 7.

Tao, G., Cai, R., Wang, Y., Liu, L., Zuo, H., Zhao, P., Umar, A., Mao, C., Xia, Q., and He, H. (2019). "Bioinspired design of Ag NPs embedded silk sericin-based sponges for efficiently combating bacteria and promoting wound healing." *Mater. Des.*, 180, 107940.

Tomic, S. L., Micic, M. M., Dobic, S. N., Filipovic, J. M., and Suljovrujic, E. H. (2010). "Smart poly (2-hydroxyethyl methacrylate/itaconic acid) hydrogels for biomedical application." *Radiat. Phys. Chem.*, 79, 643-649.

Torres, F. G., Commeaux, S., and Troncoso, O. P. (2013). "Starch-based biomaterials for wound-dressing applications." *Starke*, 65(7-8), 543-551.

Tsao, C. T., Chang, C. H., Lin, Y. Y., Wu, M. F., Wang, J. L., Young, T. H., Han, J. L., and Hsieh, K. H. (2011). "Evaluation of chitosan/γ-poly(glutamic acid) polyelectrolyte complex for wound dressing materials." *Carbohydr. Polym.*, 84(2), 812-819.

Tylingo, R., Mania, S., Panek, A., Piątek, R., and Pawłowicz, R. (2016). "Isolation and characterization of acid soluble collagen from the skin of African catfish (*Clarias gariepinus*), salmon (*Salmo salar*) and baltic cod (*Gadus morhua*)." *J. Biotechnol. Biomater.*, 6, 234.

Uddandarao, P., and Balakrishnan, R. M. (2016). "ZnS semiconductor quantum dots production by an endophytic fungus *Aspergillus flavus*." *Mater. Sci. Eng. B*, 207, 26-32.

Ueno, H. (2001). "Topical findings of healing with chitosan at early phase of experimental open skin wound." *Adv. Drug Deliv. Rev.*, 52, 105-115.

Ulkur, E., Oncul, O., Karagoz, H., Yeniz, E., and Celikoz, B. (2005). "Comparison of silver-coated dressing (Acticoat[TM]), chlorhexidine acetate 0.5% (Bactigrass[®]), and fusidic acid 2% (Fucidin[®]) for topical antibacterial effect in methicillin-resistant Staphylococci-contaminated, full-skin thickness rat burn wounds." *Burns*, 31, 874-877.

Ullah, F., Bisyrul, M., Javed, F., and Akil, H. (2015). "Classification, processing and application of hydrogels: A review." *Mater. Sci. Eng. C*, 57, 414-433.

Uzun, M. (2018). "A review of wound management materials." *J. Text. Eng. Fash. Technol.*, 4(1), 53-59.

Valderruten, N. E., Valverde, J. D., Zuluaga, F., and Ruiz-Durántez, E. (2014). "Synthesis and characterization of chitosan hydrogels cross-linked with dicarboxylic acids." *React. Funct. Polym.*, 84, 21-28.

Vallejos, N., González, G., Troncoso, E., and Zúñiga, R. N. (2014). "Acid and enzyme-aided collagen extraction from the byssus of chilean mussels (*Mytilus chilensis*): Effect of process parameters on extraction performance." *Food Biophys.*, 9(4), 322-331.

Varaprasad, K., Raghavendra, G. M., Jayaramudu, T., Yallapu, M. M., and Sadiku, R. (2017). "A mini review on hydrogels classification and recent developments in miscellaneous applications." *Matr. Sci. Eng. C*, 79, 958-971.

Varvarenko, S., Voronov, A., Samaryk, V., Tarnavchyk, I., Nosova, N., Kohut, A., and Voronov, S. (2010). "Covalent grafting of polyacrylamide-based hydrogels to a polypropylene surface activated with functional polyperoxide." *React. Funct. Polym.*, 70(9), 647-655.

Veeruraj, A., Arumugam, M., and Balasubramanian, T. (2013). "Isolation and characterization of thermostable collagen from the marine eel-fish (*Evenchelys macrura*)." *Process Biochem.*, 48(10), 1592-1602.

Velnar, T., Bailey, T., and Smrkolj, V. (2009). "The wound healing process: An overview of the cellular and molecular mechanisms." *J. Int. Med. Res.*, 37(5), 1528-1542.

Vermylen, J., Verstraete, M., and Fuster, V. (1986). "Role of platelet activation and fibrin formation in thrombogenesis." *J. Am. Coll. Cardiol.*, 8(6), 2B-9B.

Verné, E., Bruno, M., Miola, M., Maina, G., Bianco, C., Cochis, A., and Rimondini, L. (2015). "Composite bone cements loaded with a bioactive and ferrimagnetic glass-ceramic: Leaching, bioactivity and cytocompatibility." *Mater. Sci. Eng. C*, 53, 95-103.

Vichai, V., and Kirtikara, K. (2006). "Sulforhodamine B colorimetric assay for cytotoxicity screening." *Nat. Protoc.*, 1(3), 1112-1116.

Vijayakumar, V., Samal, S. K., Mohanty, S., and Nayak, S. K. (2019). "Recent advancements in biopolymer and metal nanoparticle-based materials in diabetic wound healing management." *Int. J. Biol. Macromol.*, 122, 137-148.

Vuković, J. S., Babić, M. M., Antić, K. M., Miljković, M. G., Perić-Grujić, A. A., Filipović, J. M., and Tomić, S. L. (2015). "A high efficacy antimicrobial acrylate based hydrogels with incorporated copper for wound healing application." *Mater. Chem. Phys.*, 164, 51-62.

Wang, J., Jiu, J., Araki, T., Nogi, M., Sugahara, T., Nagao, S., Koga, H., He, P., and Suganuma, K. (2015). "Silver nanowire electrodes: Conductivity improvement without post-treatment and application in capacitive pressure sensors." *Nano-Micro Lett.*, 7(1), 51-58.

Wang, K., Fu, Q., Chen, X., Gao, Y., and Dong, K. (2012). "Preparation and characterization of pH-sensitive hydrogel for drug delivery system." *RSC Adv.*, 2(20), 7772.

Wang, L., An, X., Yang, F., Xin, Z., Zhao, L., and Hu, Q. (2008a). "Isolation and characterisation of collagens from the skin, scale and bone of deep-sea redfish (*Sebastes mentella*)." *Food Chem.*, 108(2), 616-623.

Wang, L., Hu, C., and Shao, L. (2017). "The antimicrobial activity of nanoparticles: Present situation and prospects for the future." *Int. J. Nanomedicine*, 12, 1227-1249.

Wang, L., Liang, Q., Wang, Z., Xu, J., Liu, Y., and Ma, H. (2014a). "Preparation and characterisation of type I and V collagens from the skin of amur sturgeon (*Acipenser schrenckii*)." *Food Chem.*, 148, 410-414.

Wang, L., Yang, B., Du, X., Yang, Y., and Liu, J. (2008b). "Optimization of conditions for extraction of acid-soluble collagen from grass carp (*Ctenopharyngodon idella*) by response surface methodology." *Innov. Food Sci. Emerg. Technol.*, 9(4), 604-607.

Wang, M., Xu, L., Hu, H., Zhai, M., Peng, J., Nho, Y., Li, J., and Wei, G. (2007). "Radiation synthesis of PVP/CMC hydrogels as wound dressing." *Nucl. Instrum. Meth. B*, 265(1), 385-389.

Wang, W., and Wang, A. (2010). "Synthesis and swelling properties of pH-sensitive semi-IPN superabsorbent hydrogels based on sodium alginate-g-poly(sodium acrylate) and polyvinylpyrrolidone." *Carbohydr. Polym.*, 80(4), 1028-1036.

Wang, Y., Armato, U., and Wu, J. (2020). "Targeting tunable physical properties of materials for chronic wound care." *Front. Bioeng. Biotechnol.*, 8, 584.

Wang, Z., Wang, L., Lin, S., Liang, Q., Shi, Z., Xu, J., and Ma, H. (2014b). "Isolation and characterization of collagen from the muscle of amur sturgeon (*Acipenser schrenckii*)." *Biotechnol. Bioprocess Eng.*, 19(5), 935-941.

White, R. J., Cooper, R., and Kingsley, A. (2001). "Wound colonization and infection: The role of topical antimicrobials." *Br. J. Nurs.*, 10(9), 563-578.

White, R. J., Cutting, K., and Kingsley, A. (2006). "Topical antimicrobials in the control of wound bioburden." *Ostomy Wound Manag.*, 52(8), 26-58.

Wichterle, O., and Lim, D. (1960). "Hydrophilic gels for biological use." *Nature*,185, 117-118.

Winter, G. D. (1962). "Formation of the scab and the rate of epithelization of superficial wounds in the skin of the young domestic pig." *Nature*, 193(4812), 293-294.

Winter, G. D., and Scales, J. T. (1963). "Effect of air drying and dressings on the surface of a wound." *Nature*, 197(4862), 91-92.

Wu, G. P., Wang, X. M., Lin, L. P., Chen, S. H., and Wu, Q. Q. (2014). "Isolation and characterization of pepsin-solubilized collagen from the skin of black carp (*Mylopharyngdon piceus*)." *Adv. Biosci. Biotechnol.*, 5(7), 642-650.

Xia, G., Zhai, D., Sun, Y., Hou, L., Guo, X., Wang, L., Li, Z., and Wang, F. (2020).

"Preparation of a novel asymmetric wettable chitosan-based sponge and its role in promoting chronic wound healing." *Carbohydr. Polym.*, 227(7166), 115296.

Xu, J., Hu, J., Peng, C., Liu, H., and Hu, Y. (2006). "A simple approach to the synthesis of silver nanowires by hydrothermal process in the presence of gemini surfactant." *J. Colloid Interface Sci.*, 298(2), 689-693.

Yan, M., Li, B., Zhao, X., Ren, G., Zhuang, Y., Hou, H., Zhang, X., Chen, L., and Fan, Y. (2008). "Characterization of acid-soluble collagen from the skin of walleye pollock (*Theragra chalcogramma*)." *Food Chem.*, 107, 1581-1586.

Yannas, I. V., Gordon, P. L., Huang, C., Silver, F. H., and Burke, J. F. (1981). "Crosslinked collagen-mucopolysaccharide composite materials." U.S. Patent No. 4, 280, 954.

Yang, N., Wang, Y., Zhang, Q., Chen, L., and Zhao, Y. (2017). "γ-polyglutamic acid mediated crosslinking PNIPAAm-based thermo/pH-responsive hydrogels for controlled drug release." *Polym. Degrad. Stab.*, 144, 53-61.

Yang, Y. J., Jung, D., Yang, B., Hwang, B. H., and Cha, H. J. (2014). "Aquatic proteins with repetitive motifs provide insights to bioengineering of novel biomaterials." *Biotechnol. J.*, 9(12), 1493-1502.

Yang, Z., Qian, H., Chen, H., and Anker, J. N. (2010). "One-pot hydrothermal synthesis of silver nanowires via citrate reduction." *J. Colloid Interface Sci.*, 352(2), 285-291.

Yegappan, R., Selvaprithiviraj, V., Amirthalingam, S., and Jayakumar, R. (2018). "Carrageenan based hydrogels for drug delivery, tissue engineering and wound healing." *Carbohydr. Polym.*, 198, 385-400.

Yoshida, T., Lai, T. C., Kwon, G. S., and Sako, K. (2013). "pH and ion-sensitive polymers for drug delivery." E*xpert Opin. Drug Deliv.*, 10(11), 1497-1513.

Zahedi, P., Rezaeian, I., and Ranaei-siadat, S. (2010). "A review on wound dressings with an emphasis on electrospun nanofibrous polymeric bandages." *Polym. Adv. Technol.*, 21(2), 77-95.

Zhang, H., Peng, M., Cheng, T., and Qiu, L. (2018a). "Biomaterials silver nanoparticles-doped collagen-alginate antimicrobial biocomposite as potential wound dressing." *J. Mater. Sci.*, 53(21), 14944-14952.

Zhang, L., Ma, Y., Pan, X., Chen, S., Zhuang, H., and Wang, S. (2018b). "A composite hydrogel of chitosan/heparin/poly(γ-glutamic acid) loaded with superoxide dismutase for wound healing." *Carbohydr. Polym.*, 180, 168-174.

Zhang, M., Liu, W., and Li, G. (2009). "Isolation and characterisation of collagens from the skin of largefin longbarbel catfish (*Mystus macropterus*)." *Food Chem.*, 115(3), 826-831.

Zhang, M., and Zhao, X. (2020). "Alginate hydrogel dressings for advanced wound management." *Int. J. Biol. Macromol.*, 162, 1414-1428.

Zhang, P., Wyman, I., Hu, J., Lin, S., Zhong, Z., and Tu, Y. (2017). "Silver nanowires: Synthesis technologies , growth mechanism and multifunctional applications." *Mater. Sci. Eng. B*, 223, 1-23.

Zhang, Y. L., Zhao, C. X., Liu, X. D., Li, W., Wang, J. L., and Hu, Z. G.. (2016). "Application of poly(aspartic acid-citric acid) copolymer compound inhibitor as an effective and environmental agent against calcium phosphate in cooling water systems." *J. Appl. Res. Technol.*, 14(6), 425-433.

Zhang, Y., Wu, F., Li, M., and Wang, E. (2005). "pH switching on-off semi-IPN hydrogel based on cross-linked poly(acrylamide-co-acrylic acid) and linear polyallyamine." *Polymer*, 46(18), 7695-7700.

Zhang, Y., Yin, H., Zhang, Q., Li, Y., Yao, P., and Huo, H. (2018c). "A novel polyaspartic acid derivative with multifunctional groups for scale inhibition application." *Environ. Technol.*, 39(7), 843-850.

Zhao, Y. H., and Chi, Y.J. (2009). "Charaterization of collagen from eggshell membrane." *Biotechnology*, 8(2), 254-258.

Zhao, Y., Kang, J., and Tan, T. (2006). "Salt, pH and temperature-responsive semi-

interpenetrating polymer network hydrogel based on poly(aspartic acid) and poly(acrylic acid)." *Polymer*, 47, 7702-7710.

Zhao, Y., Su, H., Fang, L., and Tan, T. (2005). "Superabsorbent hydrogels from poly(aspartic acid) with salt, temperature and pH-responsiveness properties." *Polymer*, 46, 5368-5376.

Zhou, T., Sui, B., Mo, X., and Sun, J. (2017). "Multifunctional and biomimetic fish collagen/bioactive glass nanofibers: Fabrication, antibacterial activity and inducing skin regeneration *in vitro* and *in vivo*." *Int. J. Nanomedicine*, 12, 3495-3507.

Zhou, T., Wang, N., Xue, Y., Ding, T., Liu, X., Mo, X., and Sun, J. (2016). "Electrospun tilapia collagen nanofibers accelerating wound healing via inducing keratinocytes proliferation and differentiation." *Colloids Surfaces B Biointerfaces*, 143, 415-422.

Zhou, Y., Yu, S. H., Wang, C. Y., Li, X. G., Zhu, Y. R., and Chen, Z. Y. (1999). "A novel ultraviolet irradiation photoreduction technique for the preparation of single-crystal Ag nanorods and Ag dendrites." *Adv. Mater.*, 11(10), 850-852.

Zine, R., and Sinha, M. (2017). "Nanofibrous poly(3-hydroxybutyrate-co-3-hydroxyvalerate)/collagen/graphene oxide scaffolds for wound coverage." *Mater. Sci. Eng. C*, 80, 129-134.

Zou, K., Zhang, X. H., Duan, X. F., Meng, X. M., and Wu, S. K. (2004). "Seed-mediated synthesis of silver nanostructures and polymer/silver nanocables by UV irradiation." *J. Cryst. Growth*, 27*3*(1-2), 285-291.

Zewde, B., Ambaye, A., Stubbs III, J., and Raghavan, D. (2016). "A review of stabilized silver nanoparticles – synthesis, biological properties, characterization, and potential areas of applications." *JSM Nanotechnol. Nanomed.*, 4(2), 1043.

APPENDIX I

AI.1 Effect of Acetic acid on collagen extraction

Acetic acid (M)	NaCl (M)	Solvent/solid ratio (mL/mg)	Time (hrs)	Collagen yield (mg/g)
0.2	0.5	12	24	10.59
0.4	0	12	24	13.37
0.6	0.5	12	24	15.97
0.8	0.5	12	24	13.81
1.0	0.5	12	24	12.62

AI.2 Effect of NaCl on collagen extraction

Acetic acid (M)	NaCl (M)	Solvent/solid ratio (mL/mg)	Time (hrs)	Collagen yield (mg/g)
0.6	0.5	12	24	14.50
0.6	1.0	12	24	15.44
0.6	1.5	12	24	16.08
0.6	2.0	12	24	17.68
0.6	2.5	12	24	16.58

AI.3 Effect of Solvent/solid ratio on collagen extraction

Acetic acid (M)	NaCl (M)	Solvent/solid ratio (mL/mg)	Time (hrs)	Collagen yield (mg/g)
0.6	2.0	8	24	16.24
0.6	2.0	10	24	18.36
0.6	2.0	12	24	17.78
0.6	2.0	14	24	15.70
0.6	2.0	16	24	10.57

AI.4 Effect of extraction time on collagen extraction

Acetic acid (M)	NaCl (M)	Solvent/solid ratio (mL/mg)	Time (hrs)	Collagen yield (mg/g)
0.6	2.0	10	12	12.59
0.6	2.0	10	24	17.93
0.6	2.0	10	36	19.18
0.6	2.0	10	48	18.30
0.6	2.0	10	60	12.58

AI.5 Effect of reaction parameters on silver nanowires synthesis

Sample	AgNO₃ (M)	Fructose (g/mL)	PVP (g/mL)	Temperature (° C)
1	0.01	0.008	0.08	120 ° C
2	0.02	0.016	0.12	140 ° C
3	0.03	0.024	0.16	160 ° C
4	0.04	0.032	0.2	170 ° C

AI.6 Feed composition of PAsp/PVA hydrogel

Sample	PAsp (mg)	PVA (%)	EGDMA (mM)	APS (mg)
1	50	4	0.25	100
2	100	6	0.50	125
3	150	8	0.75	150
4	200	10	1	175

AI.7 Feed composition of collagen-based hydrogel

Sample	PAsp (mg)	PVA (8%) (mL)	EGDMA (0.75mM) (mL)	Collagen (mg/mL)	APS (mg)
1	150	3	3	0.5	188
2	150	3	3	1	188
3	150	3	3	2	188
4	150	3	3	3	188

AII.1 Calibration curve for Collagen

$y = 0.474x$
$R^2 = 0.9989$

AII.2 Calibration curve of AgNO$_3$ solution

The calibration curve shows Absorbance (y-axis, 0 to 0.2) versus Concentration (µg/mL) (x-axis, 0 to 12), with:

$$y = 0.019x$$
$$R^2 = 0.9992$$
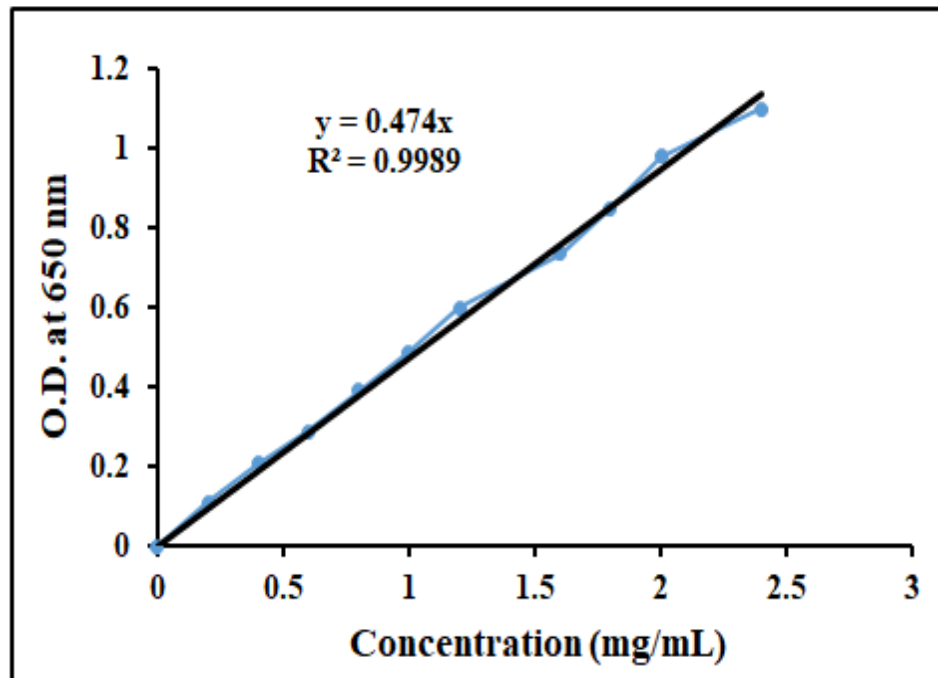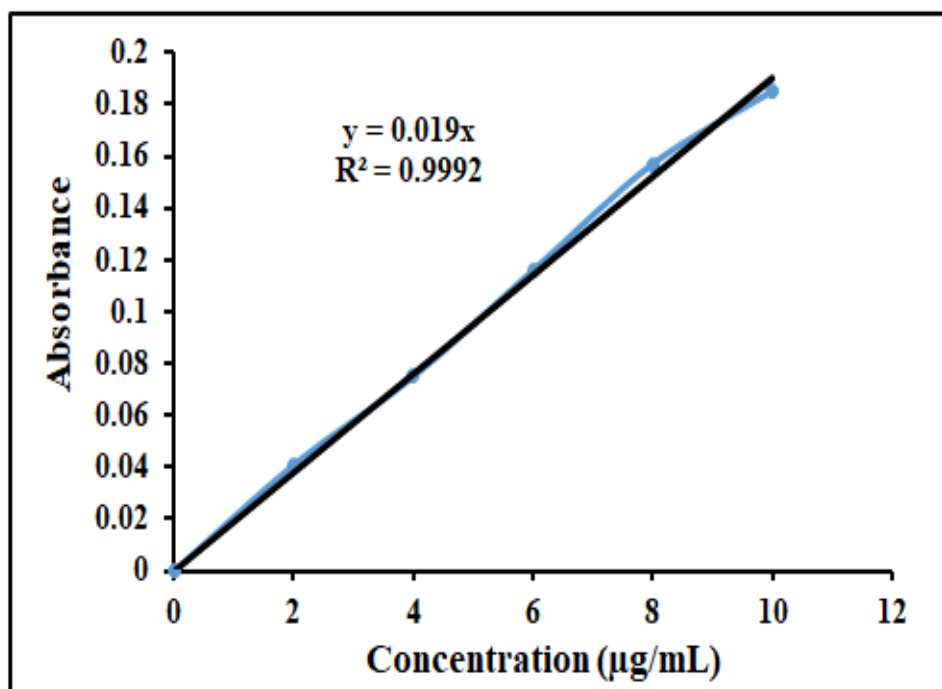
LIST OF PUBLICATIONS FROM THIS RESEARCH WORK

Patent Filed

1. Title: A pH-sensitive topical wound healing hydrogel.

   Inventors: P.E. JagadeeshBabu, Diksha Sharma, Raj Mohan Balakrishnan

   Application number: 202141035520

Research Articles

1. Arumugam, G. K. S., **Sharma, D.,** Balakrishnan, R. M., and Ettiyappan, J. B. P. (2018). "Extraction, optimization and characterization of collagen from Sole fish skin." *Sustain. Chem. Pharm.*, Elsevier, 9, pp.19-26.
2. **Sharma, D.,** Rakshana D. A., Balakrishnan, R. M., and Ettiyappan, J. B. P. (2019). "One step synthesis of silver nanowires using fructose as a reducing agent and its antibacterial and antioxidant analysis." Mater. Res. Express, IOPScience, 6, pp.075050.

BIO-DATA

DIKSHA SHARMA

Email ID: diksha.sharma18@gmail.com

Contact no: +91-6005602886

Personal Details:

Name: Diksha Sharma

Father's name: Rajinder Sharma

Date of birth: 14 November, 1989

Gender: Female

Permanent address: Diksha Sharma, W/O Dr. Akhil Khajuria, 490/4, Gangyal Garden, Jammu, Jammu & Kashmir, India, 180010.

Educational qualification

➤ Ph.D. (Pursuing) in Chemical Engineering (CGPA-9.33), 2016-2021, Department of Chemical Engineering, NITK Surathkal, Karnataka.

➤ M. Tech in Nanoscience and Technology (79.55%), 2012-2014, Department of Nanoscience & Technology, KUVEMPU University, Karnataka.

➤ B. Tech in Biotechnology (CGPA-7.76), 2008-2012, Department of Biotechnology, Lovely Professional University, Punjab.

Google scholar citations

No. of patents filed: 1

No. of publications: 2

Total citations: 65

Declaration:

I hereby declare that the above written particulars are true to the best of my knowledge.

Place: Surathkal, India

Date: 23-12-2021

DIKSHA SHARMA